Universidad de Valladolid

PhD PROGRAMME IN PHYSICS

DOCTORAL THESIS:

EXTENDED OBJECTS IN QUANTUM FIELD THEORY IN THREE DIMENSIONS AND APPLICATIONS

Thesis submitted by:

LUCÍA SANTAMARÍA SANZ

as part of the requirements for the degree of

Doctor by the University of Valladolid

Supervised by:

Dr. LUIS MIGUEL NIETO CALZADA

Dr. JOSÉ MARÍA MUÑOZ CASTAÑEDA

Universidad de Valladolid

Escuela de Doctorado Universidad de Valladolid

PROGRAMA DE DOCTORADO EN FÍSICA

TESIS DOCTORAL:

OBJETOS EXTENSOS EN TEORÍAS DE CAMPOS CUÁNTICOS EN TRES DIMENSIONES Y APLICACIONES

Presentada por:

LUCÍA SANTAMARÍA SANZ

Para optar al grado de Doctora por la

Universidad de Valladolid

Dirigida por:

Dr. LUIS MIGUEL NIETO CALZADA

Dr. JOSÉ MARÍA MUÑOZ CASTAÑEDA

Declaration of Authorship

I, Lucía SANTAMARÍA SANZ, declare that this thesis entitled, «EXTENDED OBJECTS IN QUANTUM FIELD THEORY IN THREE DIMENSIONS AND APPLICATIONS» and the work presented in it are my own. I confirm that:

- This work was done wholly while in candidature for a doctoral degree at this University.
- Where any part of this thesis has previously been submitted for a degree or any other qualification at this University or any other institution, this has been clearly stated.
- Where I have consulted the published work of others, this is always clearly attributed.
- Where I have quoted from the work of others, the source is always given. With the exception of such quotations, this thesis is entirely my own work.
- I have acknowledged all main sources of help.

Signed: LUCÍA SANTAMARÍA SANZ

Date: February 4, 2023

Acknowledgements

First of all, I thank my supervisors Dr. Luis Miguel Nieto Calzada and Dr. José María Muñoz Castañeda for the means made available to me, the time they have devoted to this work and the interesting discussions held over the years.

Likewise I would like to express my sincere thanks to all the people from the Department of Theoretical Physics of the University of Valladolid for the respect always shown for my ideas since I came to this research group and the affection with which they have treated me over the years. I would also like to thank the collaborators with whom I have been fortunate to work, especially Dr. Juan Mateos Guilarte, Dr. Michael Bordag, Dr. Inés Cavero Pélaez and Dr. Irina Pirozhenko, because a research work is always built from previous ideas and efforts of other people. I thank all of them for their kindness in providing me with their time and knowledge. I wish to extend my special thanks to César Romaniega Sancho for the support, valuable comments and insights that he has offered me this last year, even when he was busy finishing his own thesis.

Moreover, I would like to acknowledge Dr. Olalla Castro Alvaredo and her scientific group at City University of London for the valuable support and dedication they gave me during either my stay there and my last year of the thesis. Thank you for introducing me to the interesting field of research which is the entanglement entropy.

The work done in this thesis has been financially supported by the Spanish Government (FPU-fellowships programme FPU18/00957 and the Mobility Subprogramme EST19/00616) and the University of Valladolid (PhD fellowships programme "Contratos predoctorales de la UVa"). It has been also supported by the Spanish Government projects (MTM2014-57129-C2-1-P and PID2020-113406GB-I00), the Spanish Junta de Castilla y León and FEDER projects (BU229P18, VA137G18 and VA057U16), the German Research Foundation (DFG) and Universität Leipzig (programme of Open Access Publishing). I am very grateful for all the financial support received.

But a research work is also nourished by the support of the people who appreciate us, thanks to which we have the motivation to improve in all aspects of life, including the professional. For this I want to thank my friends for their great trust in me. But above all, I must thank my parents and my sister for the unconditional support as well as their infinite patience and understanding all these years. Without your help I would not be here today and, therefore, this work is also yours.

To all of you, thank you very much.

«How can it be that mathematics, being after all a product of human thought which is independent of experience, is so admirably appropriate to the objects of reality?»

ALBERT EINSTEIN

UNIVERSITY OF VALLADOLID

Abstract

Faculty of Sciences

DEPARTMENT OF THEORETICAL PHYSICS, ATOMIC PHYSICS AND OPTICS

Doctor of Philosophy

EXTENDED OBJECTS IN QUANTUM FIELD THEORY IN THREE DIMENSIONS AND APPLICATIONS

by Lucía SANTAMARÍA SANZ

In this thesis the systematic study of Quantum Field Theories (QFT) in various dimensions is proposed from the point of view of mathematical and theoretical physics, paying special attention to systems of one and three spatial dimensions (in addition to the temporal dimension in both cases) under the influence of some particular external conditions. These conditions vary from local interactions with other external classical fields to ideal boundary conditions in confining geometries. More specifically, the **main objective** of this work is the study of the spectrum of quantum fluctuations of the fields in the vacuum state subject to the external conditions already indicated. This study will be applied to the calculation of several relevant parameters in three-dimensional and one-dimensional extended structures. These systems have recently received increasing interest in material physics (in micro-electromechanical devices based on the Casimir effect or topological defects in meta materials and nano tubes) and in fundamental physics (quantum effects in modern cosmology and topological defects such as domain walls, monopoles and skyrmions).

Different configurations of quantum fields, both in compact domains and in open ones with boundaries, will be studied:

- A scalar field confined between plates mimicked by the most general type of lossless and frequently independent boundary conditions.
- Scalar fields propagating at finite temperature under the influence of Dirac δ-δ' lattices and Pöschl-Teller combs.
- Scalar fields between two parallel plates mimicked by Dirac δ potentials in a curved background of a topological Pöschl-Teller kink.
- Relativistic fermionic particles propagating in the real space under the influence of either a single and a double Dirac δ potential.

Only effective theories will be considered. Here effective means that the microscopic degrees of freedom relative to the atoms and quarks of the matter composing the plates or objects between which the vacuum quantum interaction energy will be studied are not going to be taken into account.

The **methodology** developed for the project is the following. Firstly, the spectrum of the non-relativistic Schrödinger operator or the relativistic Dirac one that will give rise to the set of one-particle states of the corresponding QFT will be characterised. Secondly, analytical and numerical results of the vacuum interaction energy between extended objects at zero temperature will be obtained. Finally, the study will be generalised to other thermodynamic magnitudes of interest such as the one loop quantum corrections to the Helmholtz free energy, the entropy and the Casimir force between objects at finite non zero temperature. Furthermore, graphical representations obtained numerically with the software *Mathematica* will be added. The thesis is **structured** in such a way that Chapter 1 gives an introduction to the work as a whole and the following chapters present the concrete results of each of the systems listed above. Finally, Chapter 6 summarises the main conclusions to give an overall view of the work carried out.

UNIVERSITY OF VALLADOLID

Resumen

Faculty of Sciences

DEPARTMENT OF THEORETICAL PHYSICS, ATOMIC PHYSICS AND OPTICS

Doctor of Philosophy

EXTENDED OBJECTS IN QUANTUM FIELD THEORY IN THREE DIMENSIONS AND APPLICATIONS

by Lucía SANTAMARÍA SANZ

El **objetivo** de esta tesis es el estudio, bajo el punto de vista de la física matemática, de teorías cuánticas de campos en una y en tres dimensiones espaciales (aparte de la temporal) bajo la influencia de diversas condiciones externas. Estas condiciones comprenden tanto la interacción con otros campos clásicos externos así como condiciones de borde en geometrías confinantes. En particular, el principal interés de este trabajo es el estudio del espectro de las fluctuaciones cuánticas de los campos en el estado de vacío sujeto a las condiciones externas anteriormente indicadas. Este estudio permitirá obtener parámetros relevantes en algunas estructuras extensas en una y tres dimensiones. Este tipo de sistemas han suscitado recientemente un gran interés en la física de materiales (por ejemplo en dispositivos microelectromecánicos basados en el efecto Casimir, nanotubos y defectos topológicos en metamateriales) y en física fundamental (defectos topológicos como paredes de dominio, cuerdas cósmicas, monopolos y skyrmiones).

Uno de los conceptos nucleares en la teoría cuántica de campos es el **estado de vacío**, ya que sus propiedades así como las de las funciones de correlación caracterizan completamente la teoría. El estado de vacío, tanto en una teoría clásica como en una cuántica, es el estado fundamental. Es decir, es el estado de mínima energía del funcional energía. Para una teoría clásica de campos escalares libres descrita por la densidad lagrangiana en $D+1$ dimensiones

$$\mathcal{L} = \frac{1}{2}(\partial_\mu\phi)(\partial^\mu\phi) - U(\phi), \qquad [\phi]^2 = ML^{4-D}T^{-2}, \qquad [U(\phi)] = ML^{2-D}T^{-2},$$

donde $U(\phi)$ incluye los términos de autointeracción y los posibles términos de masa (por ejemplo, el usual término $c^2m^2\phi^2/(2\hbar^2)$ que aparece en teorías cuadráticas en el campo), el estado de vacío ϕ_{cl} es el mínimo del funcional:

$$E[\phi] = \int d^Dx \left(\frac{1}{2}\left[\frac{1}{c^2}(\partial_t\phi)^2 + \sum_i(\partial_i\phi)^2\right] + U(\phi)\right), \qquad i = 1,\dots,D,$$

donde $\partial_i = \partial/\partial x^i$. Una vez conocido ϕ_{cl} se puede estudiar la dinámica de las pequeñas fluctuaciones o perturbaciones $\eta(t,\vec{x})$ hasta segundo orden alrededor de este estado fundamental clásico. Si se estudia la acción de $\phi(t,\vec{x}) = \phi_{cl}(\vec{x}) + \eta(t,\vec{x})$, la contribución de las fluctuaciones es

$$S[\eta] = \frac{1}{2}\int d^{D+1}x \left[\partial_\mu\eta\partial^\mu\eta - U''(\phi_{cl})\eta^2\right] + o(\eta^3).$$

Las correspondientes ecuaciones de campos

$$-\frac{1}{c^2}\partial_0^2\eta = \hat{K}(\eta), \qquad \text{con} \quad \hat{K} = -\Delta + U''(\phi_{cl}(\vec{x})) = -(\sum_i \partial_i^2) + U''(\phi_{cl}(\vec{x})),$$

son cuadráticas, por lo que se pueden expresar las fluctuaciones como una superposición de modos normales:

$$\eta(x) = \mathrm{Re}\sum_n a_n e^{i\omega_n t/\hbar}\varphi_n(\vec{x}), \qquad \text{donde se cumple que} \qquad \hat{K}\varphi_n(\vec{x}) = \frac{\omega^2}{c^2\hbar^2}\varphi_n(\vec{x}).$$

Los coeficientes a_n serán los operadores de creación y aniquilación de partículas cuando se lleve a cabo el proceso de segunda cuantización. Para teorías cuadráticas y dado que η no autointeracciona, en este punto se puede entender el campo cuántico η como una colectividad macrocanónica de estados, es decir, como una colección infinita de osciladores armónicos que no interaccionan entre sí. La frecuencia $\omega/\hbar$ de cada oscilador representa a un conjunto de partículas con energía ω. Estas frecuencias se obtienen a partir de las raíces cuadradas de los autovalores de $c^2\hat{K}$ siendo $\hat{K}$ el operador de Schrödinger no relativista a partir del cual se construye el conjunto de estados de una partícula en la teoría cuántica de campos. El hamiltoniano de la teoría cuántica de campos resultante es

$$\hat{H} = \sum_{\omega^2\in\sigma^*(\hat{K})}\left(\hat{N}(\omega) + \frac{1}{2}\right)\omega, \qquad \text{siendo} \qquad \sigma^*(\hat{K}) = \{\omega^2 \in \mathbb{R} - \{0\} | \hat{K}\varphi_n = \frac{\omega^2}{c^2\hbar^2}\varphi_n\},$$

y donde $N(\omega) = \mathfrak{a}^\dagger(\omega)\,\mathfrak{a}(\omega)$ es el operador que determina el número de partículas con energía ω en cada oscilador. El estado de vacío para las fluctuaciones es aquel que tiene cero partículas reales en cada frecuencia de cada oscilador. Pero el concepto de *vacío* en una teoría clásica y en una cuántica es diferente. El estado cuántico de vacío contiene ondas electromagnéticas e infinitos pares de partículas y antipartículas virtuales de vida corta que generalmente se aniquilan rápidamente siguiendo el principio de incertidumbre de Heisenberg $\Delta E\Delta t \geq \hbar/2$. Sin embargo, cuando se introducen placas u objetos en el vacío y las partículas virtuales se crean muy cerca de ellos, a veces pueden rebotar contra esas paredes y ser reflejadas de forma que no se aniquilen con su antipartícula [1, 2]. Entonces estas partículas pasan a ser reales y generan fuerzas de vacío entre los objetos [3-5]. Además, la energía de todas las partículas en el vacío se puede sumar, dando lugar a una energía de vacío infinita[1] (divergente en el límite ultravioleta):

$$E_0 = \frac{1}{2}\sum_{w^2\in\sigma^*(\hat{K})}\omega. \tag{1}$$

[1] La densidad lagrangiana en una teoría de campos libres complejos es $\mathcal{L} = \partial_\mu\phi^*\partial^\mu\phi - U(\phi,\phi^*)$ y por tanto la energía de vacío en ese caso se escribiría como $E_0 = \sum_{w^2}\omega$.

En este trabajo se pretende calcular la energía cuántica de interacción entre diversos objetos. Esta energía es un resultado finito. El punto crucial para calcularla es desarrollar la dinámica de las fluctuaciones alrededor del vacío clásico sólo hasta segundo orden para que la teoría resultante sea cuadrática en la fluctuación. Entonces, la aproximación perturbativa semiclásica de Wentzel-Kramers-Brillouin (WKB) es exacta [6-9] y la corrección cuántica a un lazo de la energía de vacío $\langle 0|\,\hat{H}\,|0\rangle$ será un resultado exacto. La aproximación WKB se basa en que en el límite en el que $\hbar$ tiende a un número pequeño no nulo, la fase de la función de partición cambia rápidamente, incluso para cambios pequeños en la configuración de los campos. Por tanto sólo hay interferencias constructivas entre las configuraciones de campos que estén próximos a la clásica o estacionaria. En consecuencia, se pueden despreciar los términos de orden cúbico o superior cuando se desarrolla la acción respecto a la solución del campo clásico. La función de partición en el formalismo de integral de camino se reescribiría como

$$Z = e^{\frac{i}{\hbar}S[\phi_{cl}]}\int [d\eta]\, e^{\frac{i}{2\hbar}\eta\,\frac{\delta^2 S}{\delta\phi^2}\Big|_{\phi_{cl}}\eta}, \qquad \text{con} \qquad \phi = \phi_{cl} + \eta \qquad \text{y} \qquad \frac{\delta S}{\delta\phi}\Big|_{\phi_{cl}} = 0.$$

La fuerza de Casimir que se calcule a partir de este punto será el diagrama de Feynman a un lazo con dos líneas externas en el desarrollo que se muestra en la FIGURA 1, o, equivalentemente, el término lineal cuando se expanda la integral de camino en términos de $\hbar$.

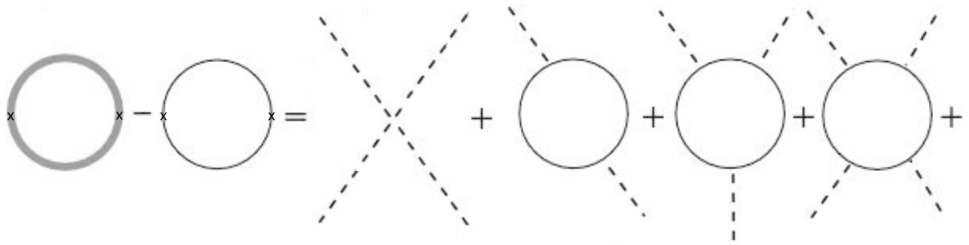

FIGURA 1: Expansión diagramática de la fuerza de Casimir [10]. La línea gruesa (delgada) denota la función de Green completa (libre). El diagrama sin bucle (diagrama árbol) corresponde a la acción clásica y los diagramas con un bucle representan la contribución cuántica dominante debida a las fluctuaciones alrededor del estado de vacío clásico.

La energía del punto cero fue sugerida por primera vez en 1911 por Max Planck [11] cuando estudiaba la absorción y emisión de energía de radiación. En 1925, Heisenberg demostró teoréticamente la existencia de esta energía de punto cero para sistemas oscilantes [12] y en 1948, Hendrik B.G. Casimir predijo el efecto Casimir [13]: la fuerza atractiva que surge entre dos placas conductoras neutras paralelas debido a las fluctuaciones electromagnéticas del vacío entre ellas. Casimir consiguió sustraer la energía cuántica de vacío de un campo escalar en el espacio libre de Minkowski de la energía cuántica de vacío para el mismo campo pero en presencia de las placas. Aunque ambas cantidades por separado son infinitas, al sustraerlas el resultado es una presión finita entre las placas dada por

$$\frac{F}{A} = -\frac{\pi^2\hbar c}{240 d^4} = -\frac{1{,}30\cdot 10^{-27}}{d^4} Nm^2,$$

donde A es el área de cada placa, d la distancia entre ellas, $\hbar$ la constante de Planck y c la velocidad

de la luz. La magnitud de esta fueza pone de manifiesto que es necesario colocar las placas paralelas a distancia de al menos micrómetros para poder ser medida, y esta es la principal dificultad desde un punto de vista experimental. Por ello, no fue hasta 1985 cuando Spaarnay midió por primera vez en un laboratorio la fuerza de Casimir entre placas metálicas [14]. Desde entonces, se han realizado numerosas medidas de este fuerza para otro tipo de materiales y diferentes geometrías [15, 16]. Hay que tener en cuenta que cuando hay un material entre las placas o cuando los objetos entre los que se mide la fuerza de Casimir están sumergidos en un medio, la fuerza entre cuerpos debe ser estudiada mediante la teoría de Lifshitz de las fuerzas de van der Waals [17, 18]. Esto se debe a que aunque los métodos para calcular la fuerza de Casimir entre objetos en el vacío y la fuerza de van der Waals entre moléculas en presencia de materia son esencialmente análogos, la interpretación física es diferente.

Por otro lado, aunque al principio se pensó que la fuerza de Casimir entre objetos era siempre atractiva, también pueden encontrarse configuraciones en las que es repulsiva [19-23]. A pesar de que hasta ahora no es posible deducir el signo de la fuerza de Casimir de interacción entre objetos antes de hacer el cálculo, se ha comprobado que este signo está fuertemente ligado a las dimensiones y a las condiciones de contorno de los sistemas considerados. Cabe destacar que hoy en día el efecto Casimir tiene aplicaciones en muchas áreas [5, 15, 24] como en física de la materia condensada (fuerzas de atracción y repulsión en sistemas con capas [25]), física atómica (fenómenos de absorción en nanotubos de carbono [26, 27]), astrofísica (inflación [28], polarización del vacío producida por defectos topológicos [29]) o nanociencia (fabricación de dispositivos nanométricos MEMS [30-33]), por citar algunos ejemplos.

La polarización del vacío que se produce debido a la presencia de bordes o de regiones del espacio con diferentes topologías demuestra que las propiedades del estado de vacío y de su energía dependen fuertemente del tipo de fronteras o bordes presentes en la teoría. A lo largo de esta tesis se van a estudiar distintas configuraciones de campos cuánticos tanto en dominios compactos como en dominios no acotados con bordes. Para extraer la energía cuántica de vacío de interacción entre objetos de la energía total de vacío hay que llevar a cabo un proceso de regularización y renormalización:

$$E_{Cas} = \int d\bar{x}\, \langle 0|\, T_{00}(\bar{x})\, |0\rangle - \int d\bar{x}\, \langle 0_M|\, T_{00}(\bar{x})\, |0_M\rangle - (\text{autointeracciones de los objetos}),$$

donde el campo cuántico ϕ satisface ciertas condiciones de contorno debido a la presencia de fronteras en la teoría. En la expresión anterior $|0_M\rangle$ es el vacío de la teoría en el espacio de Minkowski libre sin cuerpos mientras que $|0\rangle$ representa el estado de vacío de la teoría con los objetos. T_{00} es la componente 00 del tensor energía momento:

$$T_{\mu\nu} = \frac{\partial \mathcal{L}}{\partial(\partial^\mu \phi)} \partial_\nu \phi - g_{\mu\nu}\mathcal{L}.$$

En el proceso de regularización y renormalización se sustrae la divergencia dominante asociada a la energía de vacío en el espacio de Minkowski o en el background libre, sin objetos. Además también se elimina la divergencia subdominante que está relacionada con la autoenergía de cada placa u objeto.

Este término sólo es divergente si el área de los objetos es infinita. Con divergencia dominante o subdominante se hace referencia al grado de divergencia ultravioleta que presentan los dos términos. En [34] se demuestra que para el sistema de un campo escalar confinado entre dos placas, la divergencia dominante es un término proporcional a la energía elevada a la potencia $(D+1)/2$ siendo D la dimensión espacial de la teoría, y la subdominante como la energía elevada a $D/2$. Ambos términos son divergentes en el régimen ultravioleta.

En dominios no acotados con bordes existe un formalismo extremadamente útil para calcular la energía de vacío y otras magnitudes termodinámicas haciendo uso de la teoría de scattering [15, 35]. A la hora de efectuar la suma a modos (1) y regularizar y renormalizar el resultado para obtener una energía de interacción finita, se pueden aplicar varias técnicas:

1. Relacionar la componente del tensor energía momento con las funciones de Green y usar técnicas de scattering para el cálculo de estas funciones [36].

2. Calcular el operador de transición de Lippmann-Schwinger T mediante la matriz de scattering y hacer uso del formalismo $TGTG$ desarrollado por Kenneth y Klich [37, 38].

3. Usar regularización zeta [39-42].

Por otro lado, para teorías en dominios acotados con bordes (dominios compactos) el espectro es discreto y no siempre ocurren procesos de scattering, por lo que es necesario generalizar las técnicas usadas en dominios no acotados con bordes. La teoría de extensiones autoadjuntas del operador $\hat{K}$, desarrollado por Asorey, Muñoz-Castañeda y sus colaboradores, ha demostrado ser muy útil para trabajar en dominios compactos [34, 43, 44]. Esta teoría se basa en que la presencia de bordes en el sistema es un obstáculo para preservar la unitariedad requerida por la teoría cuántica de campos. Sin embargo, hay una colección infinita de extensiones autoadjuntas no negativas del hamiltoniano de la teoría que están en correspondencia uno a uno con las matrices de condiciones de contorno que representan las placas u objetos que consituyen los bordes del sistema. Estudiar el espectro de estas extensiones permite calcular la energía cuántica de vacío de interacción entre las placas u objetos en este tipo de teorías en las que el campo está confinado en un dominio acotado con fronteras.

Es importante destacar que en esta tesis se van a considerar únicamente teorías "efectivas", en el sentido de que no se van a tener en cuenta los grados de libertad microscópicos relativos a los átomos y los quarks de la materia que compone las placas o objetos entre los cuales se va a estudiar la energía de interacción cuántica de vacío.

Hasta ahora se ha considerado la teoría de campos cuánticos escalares en espacio-tiempos planos (con métrica $g_{\mu\nu} = (+1, -1, -1 \dots)$). Ese será el caso tratado en los capítulos 2 y 3 de la tesis donde se estudiarán campos escalares confinados entre placas y campos escalares propagándose en cristales, respectivamente. No obstante, en el capítulo 4 se trabajará con campos escalares confinados entre placas pero en un potencial de fondo curvo (consitutido por un potencial de tipo kink de sine-Gordon). Finalmente, en el capítulo 5 se estudiarán campos fermiónicos confinados entre placas (representadas por un potencial tipo δ de Dirac) en un espacio-tiempo plano .

La **metodología** general empleada para la obtención de estos objetivos es la siguiente: primero se caracterizará el espectro del operador de Schrödinger no relativista que dará lugar al conjunto de estados de una partícula de la teoría cuántica de campos correspondiente, después se obtendrán fórmulas analíticas para el cálculo de la energía de vacío de interacción entre los objetos extensos considerados a temperatura cero y finalmente se generalizará el estudio a otras magnitudes termodinámicas de interés como las correcciones cuánticas a un lazo de la energía libre de Helmholtz, la entropía y la fuerza de Casimir entre los objetos a temperatura finita no nula. Se obtendrán resultados analíticos cuando sea posible y además, todo ello irá acompañado de representaciones gráficas obtenidas numéricamente con ayuda del software *Mathematica*.

Los **resultados** más relevantes de la tesis son los siguientes:

- Se ha derivado una fórmula nueva para la energía cuántica de vacío para un sistema de un campo escalar complejo sin masa confinado entre placas paralelas, homogéneas e isótropas de dimensión D a temperatura nula. Las novedades de este resultado son que es independiente de la longitud de regularización del sistema y que permite clasificar las divergencias subdominantes de la teoría en términos de los invariantes algebraicos de la matriz unitaria de condiciones de contorno asociada a la extensión autoadjunta a tratar. Las placas se han caracterizado mediante las condiciones de borde independientes de la frecuencia de los modos más generales permitidas por la unitariedad de la teoría cuántica de campos. Con ayuda de técnicas de análisis complejo, se han obtenido fórmulas para las correcciones cuánticas a un lazo de la energía libre de Helmholtz, la entropía y la fuerza de Casimir para el mismo sistema en equilibrio térmico a temperatura no nula. Dichas fórmulas se han deducido empleando la teoría de extensiones autoadjuntas del operador de Laplace-Beltrami en dominios acotados con borde. A pesar de que las fórmulas usadas para analizar las magnitudes termodinámicas anteriormente citadas son válidas para toda temperatura, se han estudiado los límites de baja y alta temperatura para llegar a aproximaciones más simplificadas.
- Se ha avanzado en el estudio de campos escalares que se propagan a temperatura no nula bajo la influencia de potenciales periódicos tanto en una como en tres dimensiones espaciales. Estas redes se han construido como una cadena infinita de potenciales idénticos δ-δ' de Dirac ó de potenciales con soporte compacto tipo Pöschl-Teller, centrados en los nodos de la red. Se ha caracterizado la estructura de bandas de las redes a través de los ceros de las funciones espectrales. También se ha desarrollado un nuevo procedimiento basado en análisis complejo que facilita el cálculo numérico de la corrección térmica a la energía cuántica de vacío y la corrección cuántica a un lazo de la entropía a temperatura no nula. Es importante señalar que la energía cuántica de vacío a temperatura nula en este sistema se interpreta como las correcciones cuánticas a un lazo de las frecuencias de los fonones debido a las vibraciones de la red cristalina.
- Se ha usado el sistema de un campo cuántico escalar confinado entre dos placas paralelas, isótropas y homogéneas (representadas esta vez por un potencial delta de Dirac) a temperatura nula en un background topológico formado por el potencial curvo de un kink de tipo sine-Gordon para modelizar las fluctuaciones cuánticas de vacío de un campo escalar en el espacio

tiempo de una pared de dominio. Se ha calculado la energía cuántica de interacción de vacío como función de los parámetros que describen los potenciales y de la distancia de las placas al centro del kink mediante el formalismo *TGTG*. Para ello, ha sido necesario obtener las funciones de Green a partir de los coeficientes de scattering asociados al problema.

- Se ha determinado el espectro de estados ligados y de scattering de una partícula fermiónica relativista tanto en un potencial de una como de dos δ de Dirac en 1+1 dimensiones. Los fermiones propagándose en una recta se han interpretado como cuantos que emergen de los campos espinoriales y de este modo, se ha entendido cómo son distorsionadas las fluctuaciones de los campos espinoriales por un background estático formado por potenciales δ de Dirac. Para estudiar las fluctuaciones de los campos espinoriales se han resuelto al mismo tiempo los problemas espectrales del hamiltoniano de Dirac $\boldsymbol{H}_D$ así como de su conjugado $\overline{\boldsymbol{H}}_D$. Los estados propios de ambos hamiltonianos se interpretan como los estados de una partícula con energía positiva que serán ocupados por los electrones y positrones después del proceso de cuantización.

A continuación se enumeran, siguiendo el orden de los capítulos, las principales **conclusiones** extraídas a partir de los resultados de este trabajo:

- Se ha comprobado que la energía libre de Helmholtz de un sistema cuántico de un campo escalar confinado entre placas homogéneas e isótropas, representadas por condiciones de contorno suficientemente generales, presenta un cambio de signo para temperaturas inferiores a una temperatura crítica. Este valor separa los dos regímenes en los cuales dominan las fluctuaciones cuánticas de vacío o las fluctuaciones térmicas. También se ha demostrado la existencia de una temperatura crítica (que no coincide con la temperatura crítica hallada en el estudio de la energía libre) para la cual la presión entre placas pasa de ser repulsiva, atractiva o nula en función de la condición de contorno, a repulsiva para toda temperatura y condición de contorno. Por tanto, el teorema de Kenneth y Klich de "los opuestos se atraen" [37, 38] sólo se cumple para las condiciones de contorno que preservan la simetría $\mathbb{Z}_2$ para temperaturas inferiores a la temperatura crítica, es decir, en el régimen dominado por las fluctuaciones cuánticas de vacío.

  Además, la corrección cuántica a un lazo de la entropía es definida positiva para toda temperatura y condición de contorno estudiada, por lo que el sistema es termodinámicamente estable. Se llega a la conclusión de que el sistema cuántico es más estable que su análogo clásico.

  Respecto al límite de bajas temperaturas se ha visto que, si a una temperatura finita dada, las condiciones de contorno están "muy cerca" de aquellas relacionadas con extensiones autoadjuntas con cero modos, la aproximación bibliográfica estándar para la energía libre de Helmholtz necesita ser refinada. Este hecho justifica la necesidad de introducir una nueva escala $k_0/T \ll 1$, no considerada antes en las referencias especializadas, relacionada con la frecuencia más baja de los modos del campo. Esta escala es la que permite determinar cómo de baja es la temperatura a una distancia fija entre placas y cuánto se acerca el espectro al característico de las extensiones con cero modos.

Por el contrario, a altas temperaturas, únicamente la parte más energética del espectro de estados de una partícula es relevante en la expansión de la energía libre de Helmholtz. Además, se ha comprobado que esta magnitud se puede aproximar como un producto de los coeficientes del núcleo del calor asociados al operador de Laplace en el espacio $\mathbb{R}^2$ sin bordes, por los coeficientes del núcleo del calor asociados al operador laplaciano en el intervalo $[0, L] \in \mathbb{R}$ sujeto a condiciones de contorno en los puntos extremos del citado intervalo.

- Se ha conseguido caracterizar con total generalidad el espectro de modos de los fonones interaccionando con diferentes tipos de redes. El potencial individual que forma las redes está centrado en el punto medio de la celda primitiva. Así, se ha interpretado la red como un conjunto de pistones cuya membrana intermedia es ese potencial individual y cuyas paredes externas corresponden a una familia uniparamétrica de extensiones autoadjuntas del operador de Laplace. Esta familia está en correspondencia uno a uno con la familia de condiciones de contorno quasiperiódicas de Bloch aplicadas a los puntos extremos de la celda primitiva. De esta forma se han determinado las bandas de energía permitidas y prohibidas de las redes. Para la red formada como repetición de potenciales δ de Dirac y su primera derivada, el valor de los coeficientes de los potenciales determina la existencia o no de bandas con energías negativas. Sin embargo, en la red formada por potenciales Pöschl-Teller siempre hay una banda de energía negativa para ciertos valores del cuasi momento de la primera zona de Brillouin, independientemente del valor del soporte compacto del potencial y el espaciado de la red. En ambos tipos de redes, siempre hay bandas de energías positivas. Determinar si hay o no estados con energía negativa es fundamental cuando se promocione la teoría de mecánica cuántica no relativista a teoría cuántica de campos, ya que para aquellas redes con bandas de energía negativa, hay que introducir una masa para asegurar la unitariedad en la teoría cuántica de campos asociada.

  Se ha calculado la energía cuántica de vacío de la red usando el método de regularización zeta. Para ello se ha visto que la función zeta de la red es la suma continua, sobre los quasimomentos de Bloch en la celda dual primitiva, de funciones zeta individuales de cada celda. Es decir, cuando se calcule (1) primero se debe efectuar la suma sobre el espectro discreto de modos que surgen al considerar el campo confinado en la celda primitiva, y posteriormente se suma sobre los espectros discretos que conforman todas las bandas cuando el quasimomento recorre todos los valores posibles en la primera zona de Brilluoin. De esta manera se entiende la energía cuántica de vacío como las correcciones cuánticas a un lazo de las fuerzas elásticas producidas por el campo cuántico escalar de los fonones. Para los dos tipos de redes estudiadas la fuerza clásica entre los nodos de la red es repulsiva. Sin embargo, se ha comprobado que a temperatura nula la energía cuántica de vacío producida por el campo de los fonones, y en consecuencia la fuerza cuántica de vacío, toma valores positivos, negativos o nulos en función de los parámetros que caracterizan la red de Dirac. Esto hace que el espaciado de la red pueda aumentar, verse inalterado o disminuir con respecto a su análogo clásico a consecuencia de esta interacción cuántica. Contrariamente, en la red formada por potenciales de Pöschl-Teller, la energía cuántica de vacío toma siempre valores positivos, lo cual incrementa la fuerza de repulsión entre nodos de la red.

Bajo esta interpretación novedosa de las redes, se ve que los fonones propagándose en una red cuadrada en dos dimensiones con periodicidad de Bloch en los bordes y un campo escalar moviéndose sobre la superficie de un toro atravesado por un flujo magnético (efecto Aharonov-Bohm) son el mismo problema.

Finalmente se ha calculado la corrección térmica a la energía cuántica de vacío, a la entropía y a la fuerza de Casimir mediante un nuevo método basado en el análisis complejo no contemplado anteriormente en la literatura. Este nuevo formalismo es distinto de la representación más usual en términos de frecuencias reales y de la de frecuencias de Matsubara. Se ha visto que cuando se considera el sistema en equilibrio térmico a una temperatura distinta de cero, las correcciones cuánticas al orden de un lazo de la entropía son siempre positivas en el caso de la red de Dirac generalizada y en el cristal de potenciales Pöschl-Teller, lo cual indica que el sistema clásico del cristal es más estable que el análogo cuántico. Por otro lado, la fuerza de Casimir entre los nodos es siempre repulsiva en ambas redes. Ello implica que, al considerar temperaturas no triviales, la celda primitiva siempre aumenta de tamaño debido a la interacción cuántica del campo de los fonones. Se han generalizado estos resultados a redes tridimensionales y se han obtenido cualitativamente los mismos resultados.

- En el sistema del campo escalar confinado entre placas bidimensionales en presencia de un potencial curvo de tipo kink hay una ruptura de la simetría de traslaciones dado que el espacio es anisótropo. Esto se traduce en que los coeficientes de scattering, así como las funciones de Green, dependen de la posición de forma no trivial. A pesar de ello se ha conseguido caracterizar el espectro continuo de estados con energía positiva. Sus funciones de onda se han descrito mediante los coeficientes de scattering calculados. Además, se ha estudiado el conjunto de estados ligados, obteniendo una cota inferior para el valor mínimo de la energía negativa del sistema. La unitariedad de la teoría cuántica de campos obliga a introducir una masa de las fluctuaciones en el sistema que sea igual a ese valor mínimo de la energía. De esa manera se garantiza que el valor más bajo de energía de los estados del espectro sea igual a cero y no ocurran fenómenos de absorción de fluctuaciones que rompan la unitariedad de la teoría.

  El resultado más importante de este capítulo ha sido la generalización de la fórmula *TGTG* para objetos separados en espacio-tiempos curvos débiles y transparentes. Cuando se trabaja con espacio-tiempos curvos que no son globalmente hiperbólicos con un vector de Killing bien definido, no se puede definir una coordenada temporal global ni se puede foliar el espacio-tiempo en superficies de Cauchy espaciales para cada valor de la coordenada temporal. Por tanto, la noción de espectro de partículas independientemente del observador no existe y el tensor energía momento y la matriz de transferencia con los que se calcula la energía cuántica de vacío de interacción no son resultados universales. La única forma de calcular la energía en un espacio-tiempo curvo general sería usando regularización zeta. Sin embargo, si el campo gravitatorio es suficientemente débil como para no necesitar una cuantización propia pero sí causar efectos gravitatorios en la materia, se puede usar la teoría de perturbaciones y considerar el potencial de fondo curvo como se hace con los potenciales de interacción clásicos en espacio-tiempos

planos. Además, como el potencial Pöschl-Teller es transparente, existe la noción de partícula entrante y saliente desde un punto de vista asintótico y la matriz de scattering se calcularía de forma análoga a los casos considerados en el resto de capítulos con espacio-tiempos planos. Desde esta perspectiva, se ha calculado una fórmula *TGTG* para estos espacio-tiempos curvos, que sólo depende de los coeficientes de reflexión del problema de scattering entre placas y de las ondas planas características del potencial de fondo curvo, por lo que es fácilmente generalizable a otras configuraciones.

Para las dos placas bidimensionales representadas por potenciales delta introducidas en el potencial de Pöschl-Teller, se ha comprobado que la energía es siempre negativa, independientemente del valor de los coeficientes de los potenciales y de la distancia relativa de las placas respecto al centro del kink. Esto implica que la fuerza de Casimir entre placas siempre es atractiva en este sistema a temperatura nula. También se ha descubierto que incluso cuando una de las placas es retirada del sistema, la otra sigue sintiendo una energía cuántica de interacción no nula. Por otra parte, no se han calculado otras magnitudes termodinámicas a temperatura no nula porque al tratarse de un campo gravitatorio débil, en cuanto se toma una temperatura diferente de cero, las fluctuaciones térmicas se vuelven dominantes borrando cualquier rastro o influencia del potencial curvo. Por ello, se obtendrían los mismos resultados que en el sistema de dos placas en un espacio-tiempo plano, caso ya estudiado en el segundo capítulo de la tesis.

- Respecto al estudio de los campos de Dirac en interacción con potenciales soportados en puntos, se ha demostrado que para la representación del álgebra de Clifford descrita mediante $\{\gamma^0 = \sigma_3, \gamma^1 = i\sigma_2, \gamma^2 = \sigma_1\}$, la matriz de condiciones de borde que define el potencial δ es invariante bajo transformaciones de paridad e inversión temporal, pero no lo es bajo conjugación de carga.

  Se han construido las matrices de scattering para el potencial unidimensional descrito por $V(z) = (q\mathbb{1} + \lambda\sigma_3)\delta(z)$. Se llama z a la coordenada espacial de esta teoría y t a la temporal, de forma que $x = (t, z)$. Se ha comprobado que los coeficientes de transmisión zurdo y diestro son iguales entre sí tanto en el caso de electrones como para positrones. Esto indica que el sistema es invariante ante inversión temporal. Además, los coeficientes de reflexión zurdo y diestro también son iguales entre sí, lo que garantiza que el potencial es invariante bajo paridad. También se han calculado los momentos $k = i\kappa(q, \lambda, m)$ con $\kappa > 0$ que caracterizan los estados ligados en el gap $[0, m]$. Como ejemplos, se han estudiado los potenciales formados por una delta puramente eléctrica $V(z) = q\mathbb{1}\delta(z)$ y una delta únicamente masiva $V(z) = \lambda\sigma_3\delta(z)$. En el primer caso, debido a la periodicidad angular característica del sistema, hay un estado ligado de electrón en el segundo y cuarto cuadrantes y uno de positrón en los otros dos cuadrantes restantes. En el caso del potencial formado por una delta masiva, sólo hay un estado ligado de electrón si $\kappa = -m\tanh\lambda$ con $\lambda < 0$ y uno para positrones siempre que $\kappa = m\tanh\lambda$, donde $\lambda > 0$. Tanto para el caso eléctrico como el masivo, los coeficientes de transmisión y reflexión de electrones (σ, ρ) y los de positrones $(\tilde{\sigma}, \tilde{\rho})$ se relacionan mediante $\sigma = \tilde{\sigma}^*$ y $\rho = -\tilde{\rho}^*$. Además, en ambos casos se han calculado explícitamente las funciones de onda de los espinores y se ha

estudiado la densidad de carga de los estados. Cabe destacar que al ser la densidad de carga una función continua, se garantiza que en el sistema se cumple la ecuación de continuidad y se conserva la amplitud de probabilidad.

También se ha resuelto el problema espectral para un potencial doble delta eléctrica descrito por $V(z) = q_1\mathbb{1}\delta(z-a) + q_2\mathbb{1}\delta(z+a)$ y para la doble delta masiva caracterizada mediante la expresión $V(z) = \lambda_1\sigma_3\delta(z-a) + \lambda_2\sigma_3\delta(z+a)$. En el caso eléctrico, se han obtenido ecuaciones trascendentes para calcular los momentos de los estados ligados. Se ha representado gráficamente las zonas del espacio de los parámetros de la teoría en los que hay cero, uno o dos estados ligados así como cero modos. Estos mapas son imprescindibles para saber las zonas en las que se pueden construir teorías cuánticas de campos. Se ha visto que la familia biparamétrica de teorías indexadas por los coeficientes de las deltas eléctricas está en correspondencia uno a uno con un subconjunto del moduli de toros complejos. La topología de los toros queda determinada por las dos variables angulares q_1, q_2 y su estructura compleja por la masa de las partículas de la teoría y la distancia entre los dos potenciales delta eléctricos. En el caso de dos deltas masivas, también se ha elaborado el mapa de estados ligados en el espacio de parámetros de la teoría pero en este caso no hay cero modos. Cabe señalar que tanto en el caso eléctrico como en el masivo se han calculado las matrices de scattering. En el caso masivo se ha comprobado que el proceso de scattering solo es invariante bajo paridad si $\lambda_1 = \lambda_2$.

Por último se ha entendido que la matriz de condiciones de contorno $T_\delta(q,\lambda)$ que define la extensión autoadjunta de los hamiltonianos de Dirac sólo es unitaria en los casos en los que $\lambda = 0, q \neq 0$ ó $q_r = \sqrt{\lambda^2 + \pi^2 r^2}$ siendo $r \in \mathbb{Z} - \{0\}$. Para estos casos, que representan placas totalmente opacas, se puede aplicar el formalismo explicado en [45] para calcular las funciones espectrales y la energía cuántica de vacío de interacción para fermiones confinados en un intervalo finito.

Durante la tesis han surgido preguntas que por ahora han quedado sin contestar y darán lugar a **futuras líneas de investigación**:

- Respecto a los campos escalares confinados entre placas representadas por condiciones de contorno generales, sería interesante encontrar una explicación al hecho de que los valores máximos (mínimos) de la corrección cuántica a un lazo de la entropía se alcanzan en los puntos fijos más inestables (estables) del flujo del grupo de renormalización de borde (es decir, condiciones de contorno Dirichlet y Neumann, respectivamente).

  Otra pregunta abierta es si existe o no una relación entre la corrección cuántica a un lazo de la entropía debida a las fluctuaciones del vacío y la entropía de entrelazamiento. Durante mi estancia predoctoral en la City University de Londres bajo la supervisión de la Dra. Olalla Castro Alvaredo, estudié el exceso de entropía resultante de excitar un número finito de cuasipartículas por encima del estado fundamental de una teoría cuántica de campos integrable con una simetría interna $U(1)$, tanto en el caso de bosones como fermiones [46, 47]. Dada la enorme relevancia de la teoría de entrelazamiento en la computación cuántica, en sistemas de muchos

cuerpos fuera del equilibrio o teorías integrables de campos en interacción, esta pregunta podría abrir fructíferas líneas de investigación.

Además, hasta ahora no ha sido posible averiguar el signo de la presión de Casimir entre placas de antemano antes de realizar el cálculo. Este signo varía según las condiciones de contorno y la temperatura. Lograr este objetivo sería un gran avance.

Hay otro aspecto de este tipo de sistemas que aún está pendiente: el estudio de extensiones autoadjuntas con estados de energía negativa en función del valor de la distancia entre placas. El cómo se construiría la teoría cuántica de campos en estos casos podría ser considerado en un trabajo futuro.

- Respecto al estudio de los campos escalares cuánticos que se propagan en cristales, el cálculo de la función de Green del sistema se deja para posteriores investigaciones. A partir de ella se puede obtener el valor esperado de vacío de T_{00}, que proporciona mucha más información sobre cómo se distribuye la energía que la energía cuántica de vacío de interacción total.

  También sería interesante considerar algún tipo de interacción débil entre fonones y electrones en las redes, ya que un material realista está hecho de electrones. En este caso, se debe tener en cuenta la conexión spin-estadística.

  Una vez más, no existe una regla general para adivinar el signo de las correcciones cuánticas a un lazo de la entropía en teorías cuántica de campos con potenciales de fondo clásicos. Además, continuar la línea de investigación para averiguar si hay algún tipo de cristal construido a partir de potenciales de soporte compacto para el cual las correcciones cuánticas a la entropía clásica sean negativas podría ser prometedor.

  Finalmente, es relevante constatar que el estudio de las correcciones cuánticas a un lazo a las frecuencias de los fonones que se propagan en las redes cristalinas se puede utilizar para discernir la estabilidad de algunas soluciones hipotéticas del estado de vacío en la cromodinámica cuántica (QCD). Siempre que se puedan encontrar teorías que describan de una forma suficientemente rigurosa el acoplamiento entre las fluctuaciones de los axiones y el estado de vacío QCD, los métodos proporcionados en este capítulo pueden ser de ayuda.

- Una vez calculada la energía cuántica de vacío de interacción entre placas en el potencial de fondo de un kink mediante la fórmula *TGTG*, sería de gran relevancia estudiar esta misma cantidad a través de la integral de la componente 00 del tensor energía momento, para caracterizar la distribución de la densidad de energía en el espacio.

  Por otro lado, sería interesante obtener la forma de la métrica para un espacio-tiempo curvo tal que la ecuación que describe la dinámica de las fluctuaciones alrededor de la solución del kink sea la ecuación de movimiento de un campo escalar acoplado a un potencial de fondo gravitatorio que represente a una pared de dominio.

  Además, la generalización de la fórmula *TGTG* presentada en esta tesis a otro tipo de configuraciones, ya sea para otro potencial de fondo curvo o para otros potenciales que puedan

modelizar adecuadamente las placas, es sencilla. Por ejemplo, el estudio de si el signo de la interacción de Casimir entre las placas cambia al introducir dos placas representadas por potenciales delta de Dirac y su primera derivada en el potencial de fondo del kink Pöschl-Teller es un proyecto prometedor actualmente en progreso.

- La generalización del cálculo de la energía cuántica de vacío y las fuerzas de Casimir para campos fermiónicos confinados entre placas representadas por potenciales tipo δ de Dirac y fermiones propagándose en redes cristalinas de Dirac no se ha estudiado hasta ahora. Con ayuda de la caracterización del espectro de modos de los campos fermiónicos entre placas de esta tesis y el estudio de las extensiones autoadjuntas del operador de Dirac dado en la referencia [45], se puede continuar con el estudio de campos de Dirac en redes cristalinas. Este tema suscita un gran interés en física de la materia condensada debido a los estados de borde presentes en metamateriales que se pueden modelizar con este tipo de teorías. También sería interesante ampliar el estudio al potencial $V(z) = (q_1\delta(z-a) + q_2\delta(z-b))\mathbb{1} + (\lambda_1\delta(z-a) + \lambda_2\delta(z-b))\sigma_3$ donde $a, b \in \mathbb{R}$ para comprobar si hay cambios en los resultados de la energía de vacío en este caso en el que las deltas no son totalmente eléctricas ni totalmente masivas ni están situadas de forma simétrica respecto al origen. También se podría calcular la función de Green para los fermiones entre placas modelizadas por potenciales delta e intentar rehacer los resultados para dimensiones espaciales más altas.

- Sería de gran interés estudiar la interacción cuántica de vacío entre otros tipos de objetos extensos como monopolos y skyrmiones en el límite diluido (*límite BPS*). En este límite los objetos están suficientemente separados y la contribución dominante de las fluctuaciones cuánticas debidas a la interacción entre objetos son ondas de muy baja frecuencia, es decir, ondas cuyas longitudes son del orden de la distancia entre los objetos. Si los cuerpos están muy separados la longitud de ondas de las fluctuaciones es mayor que la dimensión de los objetos y estos se pueden considerar como puntuales, facilitando su estudio.

- Finalmente, algunos de los problemas abiertos mencionados anteriormente podrían estudiarse también en sistemas con dos dimensiones espaciales aparte de la temporal. De esta forma, podrían modelizarse sistemas bidimensionales como el grafeno, cuyo tratamiento desempeña un papel importante hoy en día en física de materiales. Además, la simetría conforme presente en ciertas teorías con dos dimensiones podría jugar un papel relevante, dando lugar a resultados novedosos y diferentes de los obtenidos en QFTs en una y tres dimensiones espaciales.

Contents

List of Figures

List of Tables

Chapter 1

INTRODUCTION

The overall aim of this thesis is the analysis of the spectrum of the quantum fluctuations of the fields in the vacuum state under the influence of some boundary conditions and local interactions with other classical external fields. Some Quantum Field Theories (QFT) in one and three spatial dimensions, apart from the temporal one, will be discussed.

Quantum Field Theory is definitely one of the most successful theories in theoretical physics. It has turned out to be an extremely fruitful research area in the last decades. Accordingly, it seems necessary to provide in this chapter a brief bibliographic review of the concepts which are going to be relevant along the whole work. Natural units $\hbar = c = k_B = 1$ for the reduced Planck constant, the speed of light and the Boltzmann constant will be used throughout the thesis.

1.1. Vacuum energy and Quantum Field Theory

Quantum Field Theory successfully combines both special relativity and quantum mechanics. Neither the non-relativistic quantum mechanics nor the relativistic one can describe processes in which the number of particles changes. Other problems such that the appearance of negative density probabilities, the existence of negative energy solutions and the causality violation can only be explained in the QFT formalism. Inside it, one can manage Fock spaces and infinite Grassmanians with an arbitrary number of integer or half integer spin particles respectively, solutions with negative energy (antiparticles) and all the aforementioned problems. Furthermore, different measurements of observables have been precisely computed in accordance with the experimental results. For instance, the anomalous magnetic moment[1] is the most accurate theoretical prediction which has ever been made by QFT. It agrees with the experimental value to more than ten significant figures.

Another core concept in QFT is the vacuum state and the vacuum energy. The properties of the vacuum state, and the n-point correlation function obtained from it, completely characterise the theory. In general, the vacuum state of an arbitrary either classical or Quantum Field Theory is the fundamental one (i.e. the state of minimum energy of the Hamiltonian). A free real scalar classical

[1] According to the Dirac equation, a $1/2$ spin particle with magnetic moment $-e/(2m)$ has a gyromagnetic ratio $g = 2$. The anomalous magnetic moment is the quantum correction to the classical value (or tree-level Feynman diagram) of the g-factor. It was firstly derived by Schwinger in 1948.

field theory is described by the Lagrangian density

$$\mathcal{L} = \frac{1}{2}(\partial_\mu \phi)(\partial^\mu \phi) - U(\phi), \tag{1.1}$$

where $\partial_\mu = \partial/\partial x^\mu$ and $U(\phi)$ includes the mass and the interaction terms. The Einstein Summation Convention in which repeated indices are implicitly summed over has been used. From (1.1) one can obtain the fundamental classical state of the lowest energy as a minimum of the energy functional:

$$E[\phi] = \int d^D \boldsymbol{x} \left(\frac{1}{2} \left[(\partial_0 \phi)^2 + \sum_{i=1}^{D} (\partial_i \phi)^2 \right] + U(\phi) \right),$$

It is clear that the fundamental state ϕ must be a minimum of the potential $U(\phi)$. The vacuum or fundamental state exists when the energy functional, and consequently $U(\phi)$, is bounded from below.

Sometimes the theory has an internal symmetry that can be spontaneously broken if the minimum of the potential is degenerated. One well-known example is the $\lambda\phi^4$ theory. In this type of theories, the configurational space is splitted into different connected sectors which in general cannot be connected by means of the temporal evolution operator. There is a minimum of the potential in each one of these sectors and hence, one can build a different theory when studying small oscillations around the corresponding minimum on each sector. For this reason, as soon as one chooses one specific minimum of the potential to build a field theory, its ground state would not longer be invariant under the symmetry group of the Hamiltonian and the symmetry becomes broken. In terms of groups, consider a theory invariant under the action of a symmetry group G with a representation given by

$$\begin{aligned} \rho \colon G &\to \mathrm{GL}(E) \\ g &\mapsto \rho(g), \end{aligned}$$

being E a vector space. The action of the elements of G on $p \in E$ is $\mathrm{orb}(p) = \{\rho(g(p)), \forall g \in G\}$. Consider the subgroup $S_p = \{g \in G \,|\, \rho(g(p)) = p\}$. The action of the quotient G/S_p on a vacuum point yields the vacuum manifold or orbit. When the vacuum is degenerated and one chooses a specific value of the vacuum state, the original symmetry becomes broken. Now the theory is no longer invariant under G but it is still invariant under the symmetries of the subgroup S_p. A well known example of $S_p \neq \{\emptyset, \mathbb{1}\}$ is the Kaluza Klein model in $\mathbb{R}^{3,1} \times S^1$. Here the general coordinate transformations symmetry in five dimensions is spontaneously broken into the product of the general coordinate transformations symmetry in four dimension times a local $U(1)$ gauge symmetry. There are generalisations of this problem to higher dimensional compact manifolds $\mathcal{B}$ instead of S^1 [48–50]. In them, the election of a vacuum state[2] determines the group S_p following the diagram shown in (1.2). In it, the global symmetries of the first column are related to the gauge ones in the last column via the Einstein Equivalence Principle (EEP). Yet, the determination of which non trivial group S_p the

[2]The spontaneous breaking of the vacuum symmetry in these works is also called spontaneous compactification of the extra dimensions.

original group must be quotient by to obtain the desired symmetry in G/S_p is still an open question.

$$\begin{array}{ccc} G \in \mathbb{R}^{3,1} \times \mathcal{B} & & \text{Diff}\,(\mathbb{R}^{3,1} \times \mathcal{B}) \\ \Big\downarrow S_p? & \xrightarrow{\text{EEP}} & \Big\downarrow \\ G/S_p \equiv SU(3) \times SU(2) \times U(1) & & \text{Standard Model} \end{array} \tag{1.2}$$

In other cases, such as the $\lambda\phi^4$ theory, $S_p = \mathbb{1}$ and consequently, after the spontaneous breaking of the global $\mathbb{Z}_2$ symmetry, the theory is no longer invariant under any non trivial symmetry. When the broken symmetry is continuous, Goldstone bosons appear. If the theory is enlarged and extra degrees of freedom (gauge fields) are introduced, the internal global symmetry group is promoted to a gauge or local symmetry group according to the Equivalence Principle. Before the promotion to a gauge group, at every point of the Minkowski spacetime there is a reference frame which is static or moves at constant velocity from one point to another thus defining a global basis of the vector space E. After the promotion, the spacetime $\mathbb{R}^{D+1} \times E$ is a vector bundle such that the reference frame could undergo acceleration when moving from one point to another and hence, at each point of the spacetime there exists a local basis of E for the representation of the group [51]. However, it is always possible to choose the gauge such that the degrees of freedom that would become Goldstone bosons disappear and the gauge fields associated with the spontaneous broken symmetries acquire masses [52].

Either for degenerated and non degenerated potentials, it is possible to study small fluctuations around the classical fundamental state, i.e. $\phi(t,\vec{x}) = \phi_{cl}(\vec{x}) + \eta(t,\vec{x})$, up to second order. The equation which describes the dynamics of the fluctuations/small perturbations around a classical ground state is quadratic

$$-\partial_0^2\eta = \hat{K}(\eta) = [-\Delta + U''(\phi_{cl}(\vec{x}))]\eta = \left[-(\sum_i \partial_i^2) + U''(\phi_{cl}(\vec{x}))\right]\eta,$$

as it will be proved in the following section. Thus, the fluctuations can be expressed as a superposition of normal modes:

$$\eta(x) = \text{Re}\sum_n a_n e^{i\omega_n t}\varphi_n(\vec{x}), \qquad \text{which satisfy} \qquad \hat{K}\varphi_n(\vec{x}) = \omega_n^2\varphi_n(\vec{x}).$$

The coefficients a_n will be promoted to operators of creation an annihilation of particles when the second quantisation is applied. At this point and for quadratic field theories, one can understand the quantum field as a grand canonical ensemble of particles. More specifically, the quantum field can be interpreted as an infinite collection of non interacting harmonic oscillators, where each oscillator of frequency ω represents an ensemble of particles with energy given by ω. The corresponding number operator $\hat{N}(\omega) = \mathfrak{a}^\dagger(\omega)\,\mathfrak{a}(\omega)$ determines the number of particles of energy ω in each ensemble. The Hamiltonian of this quadratic scalar QFT would be

$$\hat{H} = \sum_{\omega^2 \in \sigma^*(\hat{K})} \left(\hat{N}(\omega) + \frac{1}{2}\right)\omega, \qquad \text{with} \qquad \sigma^*(\hat{K}) = \{\omega^2 \in \mathbb{R}^* / \hat{K}\varphi_n = \omega^2\varphi_n\}. \tag{1.3}$$

Notice that the frequencies of the infinite set of non interacting harmonic oscillators are given by the squared root of the eigenvalues of the corresponding non relativistic Schrödinger operator[3].

Consider the operators of particle creation $\mathfrak{a}^\dagger$ and annihilation $\mathfrak{a}$ defined in the Hilbert space of quantised field states (the Fock representation of canonical commutation relations in the quantised quadratic theory). The vacuum state in the Fock space is hence defined as

$$\mathfrak{a}(\omega)\,|0\rangle = 0, \qquad \forall\omega. \tag{1.4}$$

This state is the eigenstate of the number of real particles operator with eigenvalue zero. Consequently, the quantum vacuum state corresponds to the state with zero real particles in each frequency or each harmonic oscillator. But the concept of *emptiness* in classical physics is quite different from the *vacuum* concept in quantum physics. The quantum vacuum state is not empty but instead contains electromagnetic waves and infinite pairs of virtual short-lived particles/antiparticles or vacuum bubbles. Virtual particles appear in the perturbative study of QFT to explain the interaction of forces between real particles. In general, the virtual particles/antiparticles annihilate each other very quickly in accordance with the Heisenberg energy-time uncertainty principle: $\Delta E \Delta t \geq \hbar/2$. Nevertheless, when some objects or plates are introduced in the space, if the virtual particles and antiparticles are close to the plates, sometimes one of them collides with the plate and gets reflected in a way that it does not combine again with its antipaticle. Hence, they become real particles which give rise to vacuum forces in the system [3–5]. The energy of all of these particles in the vacuum can be added together. In fact it is easy to see in (1.3) that each oscillator mode contributes to the vacuum energy with a $\omega/2$ term and consequently the vacuum energy of the theory

$$E_0 = \frac{1}{2}\sum_{w^2\in\sigma^*(\hat{K})} \omega$$

is infinite (ultraviolet divergent). Notice that the Lagrangian density of a free complex scalar field theory is $\mathcal{L} = \partial_\mu\phi^*\partial^\mu\phi - U(\phi,\phi^*)$ and the associated quantum vacuum energy reads $E_0 = \sum_{w^2}\omega$, twice the value of the vacuum energy of a real scalar field theory.

Setting the vacuum state and the zero-point energy in a field theory has two crucial obstacles:

1. On the one hand, the energy is not relativistic invariant. As a component of the four-vector $(E,\vec{p})$, the energy is frame dependent. Consequently, the spectrum of the one-particle states for an observer in one inertial reference frame could be different from the one observed in another frame. What is more, for some curved spacetime configurations in QFT, there is not a correspondence between a set of states and the one-particle spectrum. This is due to the fact that one could not always interpret a quantum field as a collection of particles. So whenever the spectrum changes with observers, the space of states in the theory is no longer an infinite

[3] In QFT, the energies of the set of one-particle states are given by the squared root of the eigenvalues of the non relativistic Schrödinger operator $\hat{K}$ whereas in quantum mechanics the frequencies of the harmonic oscillators are given by the eigenvalues of $\hat{K}$. Most references tend to mix both notations. Moreover, for $D+1$ dimensional massive QFT the frequency of modes is such that $\omega^2 = \vec{k}^2 + m^2$. In 1+1 dimensional QFT, $\omega^2 = k^2 + m^2$ (for massless theories $m = 0$). Throughout the introduction, the appropriate dispersion relation will be used automatically, depending on the situation.

tensor product of the unique irreducible unitary representation of the Heisenberg group [53].

For quadratic scalar theories in flat spacetime, the Fock space is the tensor product of infinite copies of this unitary representation. Since the quantum Hamiltonian of the theory commutes with the group operators[4] $\{\exp(\Pi_\hbar(A))\}$, being

$$\Pi_\hbar(A)f(z) = e^{-i\hbar b}e^{i\hbar cz}f(z-a), \quad \forall \hbar \in \mathbb{R}-\{0\}, \quad f \in L^2(\mathbb{R}),$$

it is possible to simultaneously diagonalise $\{\hat{H}, \exp(\Pi_\hbar(A))\}$. Thus, one can perform the decomposition of this reducible representation. Each eigenspace of the diagonalised Hamiltonian will be an irreducible representation corresponding to a canonical set of particles. Consequently, one could build the whole state space by defining the states of n-particles acting with the creation operators over the fundamental state. Notice that now the space of states of the theory will be the same as the one of the free particle because the unitary irreducible representation of the Heisenberg group is unique.

The vacuum state is the field theoretical wave function of the fundamental state. This state, defined in this way is relativistic invariant. Nevertheless, it is not always possible to associate to the vacuum state a frame invariant one-particle spectrum.

2. On the other hand, it is not possible to measure absolute energies but energy variations. The only way to perform a measurement is by fixing a zero point energy as part of the renormalisation process[5] and comparing energies of other systems or bodies with respect to this reference point. At this stage it is still unclear if this benchmark can be universal. In fact, since for massless theories the renormalisation criteria by which the infinite mass fluctuations corresponds to zero energy[6] does not apply, the self-energy of several systems is not uniquely defined. An example is the vacuum self-energy of a plate mimicked by a Dirac δ potential [54]. The universality of the zero-point energy is already an open question. However, the part of the quantum vacuum energy which depends on the distance between objects is related to a physical universal finite force which can be measured. Only this quantum vacuum interaction energy between objects is the focus of this thesis. Thus, the problem of the universality of the whole zero-point energy is not going to be the focus of the work in the following chapters.

The zero-point energy was firstly suggested in 1911 by Max Planck [11] when he assumed continuous absorbtion of the radiation energy but quantised emission. Consequently, the energy of the harmonic oscillator became $h\nu/2$ instead of zero at zero temperature. This finite *residual energy* or zero-point energy established some controversy among the scientific community. In 1925 there was a quantum mechanical revolution and Heisenberg theoretically proved the finite zero-point energy for

[4] See Appendix A for the definition of the irreducible representation and the group operators of the Heisenberg group.

[5] For the system of a scalar field confined between two infinite parallel plates, one fixes a reference point in the renormalisation process by removing the infinite contribution of the density energy in the bulk. But in this case it is also necessary to eliminate another divergence related to the infinite area of the plates. For compact objects such as kinks or skyrmions, this term is no longer divergent but finite and it has a physical interpretation as the one loop quantum correction to the mass of these objects.

[6] If the masses go to infinity the fluctuations are freezing and the related terms in the quantum vacuum energy are exponentially suppressed (terms of the form $e^{-(mL)^2}$).

oscillating systems [12]. And in 1948 Hendrik B.G. Casimir predicted what was named in his honour the Casimir effect [13]: the attractive force that appears between two conducting neutral parallel plates due to the electromagnetic vacuum fluctuations between them. The value of this pressure, once one recovers the system of units $\hbar \neq 1, c \neq 1$, is

$$\frac{F}{A} = -\frac{\pi^2 \hbar c}{240 d^4} = -\frac{1.30 \cdot 10^{-27}}{d^4} N m^2, \tag{1.5}$$

being A the area of the plates and d the distance between them. This electromagnetic force results from the computation of the one loop quantum correction to the vacuum polarisation in QED. Nevertheless, it does not depend on the coupling constant of the theory, and for that reason the force is relevant at the nanometre scale. The fact that the force does not depend on the fine structure constant is a consequence of taking a quadratic approximation for the action. The action in QED in the absence of external sources is given by

$$S_{QED} = \int d^4x \left[-\frac{1}{4} F^{\mu\nu} F_{\mu\nu} + \bar{\psi}(i\gamma^\mu D_\mu - m)\psi \right],$$

with $D_\mu = \partial_\mu + ieA_\mu$ the covariant derivative and $F_{\mu\nu} = \partial_\mu A_\nu - \partial_\nu A_\mu$ the electromagnetic field tensor. When studying the action up to quadratic order in the fluctuations around a classical solution for the fields A_μ and ψ, the only term that depends on the coupling of the theory, i.e. $e\bar{\psi}\gamma^\mu \delta A_\mu \psi$, is neglected because it represents a cubic interaction in the fields. Therefore, when calculating the operator $\hat{K}$ associated to the fluctuations and obtaining the spectrum in order to sum all the squared roots of its eigenvalues (and hence computing the Casimir force), the coupling constant will not appear in any term. Moreover, in the vacuum expectation value of the quadratic action, the fermionic fluctuations are disregarded because, being massive fermions, they are exponentially supressed compared to those of the photon. By the same argument, if instead of computing corrections to the photon propagator, one loop quantum corrections to the graviton propagator were calculated, the coupling constant of the gravitational theory would not appear either. And therefore, since the graviton has zero mass (just like the photon) one could think of studying the quantum interacting force between gravitational objects described by sufficiently strong fields separated by a small distance, using the same quadratic approximation reasoning. This force caused by non massive quantum vacuum fluctuations around a classical solution for gravitons coupled to no matter which other massive field would constitute an example of quantum corrections to the gravitational field theory. The difficulty lies in finding a material that is opaque to the gravitational waves [55].

The basic idea behind the Casimir effect is the creation of pairs of particle/antiparticle from the vacuum [56]. This process does not break the principles of QFT. The polarization of the vacuum and the pairs creation were also proposed by Heisenberg [1], Schwinger and Euler [2]. Around mid 40s Clausius and many others published experimental confirmations [57]. It was not until 1970s when cosmologist started to study the Casimir effect within the general relativity framework [58].

H. B. G. Casimir succeeded in subtracting from the infinite vacuum energy of the quantised electromagnetic field in the presence of ideal metal planes, the infinite vacuum energy of the same field

in free Minkowski spacetime, leaving a finite pressure between plates. There are some methods to regularise the Casimir force between parallel, uncharged and conducting plates. Divergences arise in QFT when computing some observables such as the vacuum energy. For obtaining a finite result, an auxiliary suitable parameter or regulator must be introduced. The correct physical result will be obtained when performing the limit in which the regulator vanishes. However, when introducing the regulator, the resulting expression for the observable may include terms that are not well-defined in the physical limit. For this reason, a renormalisation procedure follows the regularisation one. The renormalisation consists on cancelling out these ill-defined regulator-dependent terms with counter-terms. Finally, the physical limit is performed obtaining the finite result.

A first simplified attempt to extract the finite result for the Casimir energy based on dimensional regularisation is well explained in [36]. In summarised form, consider for simplicity a massless complex scalar field ϕ confined between two parallel $(D-1)$-dimensional plates separated by a distance d in the axis orthogonal to the plates, i.e. the z axis. The Schrödinger operator reduces to the Laplace Beltrami one, whose eigenstates are plane waves. Splitting the spatial coordinate $x = (\vec{y}_{\parallel}, z)$ with $\vec{y}_{\parallel} \in \mathbb{R}^{D-1}$ and taking into account that the plates are isotropic and homogeneous[7], the equation for the modes of the scalar field is given by the non relativistic Schrödinger separable eigenvalue problem

$$-\Delta\phi_\omega(x) = \omega^2\phi_\omega(x) \qquad \begin{cases} \Delta = \Delta_{\parallel} + \partial_z^2 \\ \omega^2 = \vec{k}_{\parallel}^2 + k^2 \end{cases}, \tag{1.6}$$

being k the transverse momentum of the normal modes and $\vec{k}_{\parallel}$ the D-1 momenta of the modes parallel to the plates. Assuming that the fields satisfy Dirichlet boundary conditions[8] on the plates and setting again $\hbar = c = 1$, the Casimir energy per unit area of the plates is given by

$$\frac{E_0}{A} = \sum_{\omega^2 \in \sigma^*(-\triangle)} \omega = \sum_{n=1}^{\infty} \int \frac{d^{D-1}k_{\parallel}}{(2\pi)^{D-1}} \sqrt{k_{\parallel}^2 + \frac{n^2\pi^2}{d^2}}.$$

Using the Schwinger proper-time representation for the square root[9], the Euler integral representation of the gamma function and the reflection property for gamma and zeta functions[10] one gets

$$\frac{E_0}{A} = -\frac{1}{2\sqrt{\pi}} \frac{1}{(4\pi)^{D/2}} \sum_{n=1}^{\infty} \int_0^{\infty} \frac{dt}{t} t^{-1/2-D/2} e^{-tn^2\pi^2/d^2} = -\frac{1}{2^{D+1}\pi^{D/2+1}} \Gamma\left[1+\frac{D}{2}\right] \zeta(D+2) \frac{1}{d^{D+1}}.$$

[7] Because of the isotropy and the homogeneity of the plates there exists a translational symmetry along the surface of the plates. Consequently, the theory of free fields without boundaries is recovered for the parallel direction coordinates $y_{\parallel} \in \mathbb{R}^{D-1}$. Hence, the problem can be focused in solving the field equations only in the direction orthogonal to the surfaces of the plates.

[8] The Dirichlet boundary conditions (representing conducting plates) means that the plates are totally impermeable to the field, that is, the expression $\phi(x=0) = \phi(x=d) = 0$ holds.

[9] Schwinger proper-time representation: $(k^2+\rho^2)^{\sigma} = 1/\Gamma(\sigma) \int_0^{\infty} dt\ t^{\sigma-1} e^{-t(k^2+\rho^2)}$ being t a parameter called the proper time.

[10] The reflection property is given by $\Gamma(z/2)\zeta(z)\pi^{-z/2} = \Gamma((1-z)/2)\zeta(1-z)\pi^{(z-1)/2}$. Notice that by definition of the Euler representation of the Gamma function $\Gamma(z) = \int_0^{\infty} dt\ t^{z-1}e^{-t}$, the value of $z \in \mathbb{C}$ should verify $\mathrm{Re}(z) > 0$. And by definition of the zeta function $\zeta(s) = \sum_{n=1}^{\infty} n^{-s}$, the value of $s \in \mathbb{C}$ should verify $\mathrm{Re}(s) > 1$.

One obtains the result stated in (1.5) by performing $-\partial_d E_0$ and evaluating the resulting formula for $D = 2$.

Until the prediction of the Casimir force by mid-twentieth century, it had often been stated that the zero point energy in QFT was not observable and for that reason the theory should be normal ordered[11]. In fact, the numerical result for the Casimir force is quite small and any attemp to experimentally measure it must be performed at the μm scale. However, the attractive Casimir force is a finite quantity which was experimentally measured for the first time in 1958 by Spaarnay [14] for flat metallic parallel plates.

Concerning the quantum vacuum energy of fields in presence of real materials, going from simpler models as media with frequency-independent permitivities to more complicated theories as the hydrodinamical Barton model [59–61], some further caveats are worth stressing (see [15, 24, 36]). On balance, when there is a material between the objects or even in the case that the objects are embedded in a media, the force between these objects must be studied within the Lifshitz theory [17, 18] of van der Waals forces[12] . It is true that the methods for computing the Casimir force between objects in the vacuum and for calculating the van der Waals force between molecules in the presence of matter are esentially analogous, but the physical interpretation in both systems is quite different. In 1873 van der Waals included the finite size of molecules and weak forces between them [62] while studying the kinetic theory of noninteracting point molecules. In 1930 London developed the quantum theory for these forces [63] taking into account the interaction of a dipole operator with a fluctuating electric field[13] and he obtained an interaction potential energy that behaves with the distance between molecules r as

$$U(r) = -\frac{A}{r^6}, \qquad A = \frac{3\hbar}{2\pi}\int_{-\infty}^{\infty} \alpha^{(1)}(i\omega)\alpha^{(2)}(i\omega)d\omega, \qquad \text{if} \qquad \frac{w_0 r}{c} \ll 1,$$

being α the electrical polarisability of the atoms in the ground state, ω_0 the frequencies of transitions between the ground and excited states and c the speed of light. It was only in 1947 that another meaningful improvement was apparent when Casimir and Polder found that the interaction potential energy at large distances between molecules with electric dipole moments and separated by a distance r behaves as

$$U(r) = -\frac{23}{4\pi}\hbar c\frac{\alpha^{(1)}(0)\alpha^{(2)}(0)}{r^7}, \qquad \text{if} \qquad \frac{w_0 r}{c} \gg 1.$$

It was called *retarded van der Waals force* [64] because it is a quantum effect but also a relativistic one

[11] Since the energy of all the field theories except from the gravitational one is defined up to an additive constant, the zero-point oscillations energy in the free space was generally preassigned to be zero. This was incorrect taking into account that in the presence of material plates, the separation distance between them induces different frequencies of the oscillators of the quantised theory with respect to those in the real Minkowski space without plates.

[12] In the van der Waals interaction between neutral atoms or condensed bodies separated by a distance r greater than the atomic dimension d, forces that decay as a power of d/r are neglected. The potential interaction energy $U(r)$ gives the same scattering amplitudes between atoms as the real interaction $V = -\hat{E}(r_1)\hat{\mathcal{D}}^{(1)} - \hat{E}(r_2)\hat{\mathcal{D}}^{(2)}$, being $\hat{\mathcal{D}}$ the dipole moments for the atoms and $\hat{E}$ the electric field at the positions of the atoms $r_{1,2}$.

[13] A fluctuating electromagnetic field induces instantaneous dipole moments in atoms and molecules and consequently the expectation values of the operator of the dipole moment are no longer zero for non-polar molecules.

due to its dependence on the speed of light c. In this same year, Bohr commented that the van der Wals force must have something to do with zero point energy. Finally, one year later, H. B.G. Casimir changed from action at a distance between molecules to local action of fluctuating electric fields. Notice that in the Casimir effect, the quantum field is confined to a finite region of the space because of the boundaries. Casimir explained that there is a pressure on the boundary surfaces[14] because, since the spectrum of the vacuum fluctuations are not the same inside and outside the plates, these fluctuations produce different pressures on each side of the plate which do not cancel each other, giving rise to a measurable force.

Since the first measurements of the Casimir force by Spaarnay, it has rapidly received increasing attention. It is important to mention that the major difficulty in the Casimir setup was dealing with exactly parallel plates. Since it was not possible to ensure parallel plates in the laboratory, a plane and a sphere with a large radius were used instead as an approximation of *parallel plates*. Since then, several measurements have been performed for other real materials, at nonzero temperature and for bodies of various geometrical shapes (see [15] and [16] for an in-depth review).

At the beginning, the Casimir pressure between objects was thought to be always attractive. It was in part enhanced by the experimental measurements performed ([65] and references quoted in Chapter 18 of [15]). Nevertheless, repulsive Casimir forces can be found for a scalar field confined between two plates with Dirichlet boundary conditions in one plate and Neumann ones in the other [19], or with non-local boundary conditions [20]. The Casimir pressure between thick plates with a liquid layer between them [21, 22], or between an ideal metal plate[15] and a plane with infinitely large magnetic permeability [23], can be repulsive too. Furthermore, the Casimir pressure for a single body instead of two can take a positive value (for instance, for an ideal metal conducting spherical shell [66]). Obtaining an attractive or repulsive Casimir effect has been shown to be strongly dependent on the dimension and boundary conditions of the configuration studied. Indeed, the deduction of the sign of the Casimir effect before performing the computation is still an open question.

The quantum vacuum produces important physical effects [5] which can be described by the QFT formalism. For instance, the creation of particles from the vacuum by an external electromagnetic field [67] (or by nonstationary boundaries in the so called dynamical Casimir effect [68, 69]). Other examples are the initial evaporation of black holes with small masses due to the vacuum polarization and the creation of particles and antiparticles caused by strong gravitational fields in the early stages of the universe [70]. Another related phenomenon in quantum electrodynamic (QED) is the Schwinger effect [2], where electron/positron pairs are created from the decay of the vacuum in the background of strong electric fields. In the Schwinger effect one has to sum all the diagrams with one electron loop and any number of external photon legs, as shown in Figure 1.1. Consequently, the techniques presented in following chapters to compute the Casimir energy between objects could be also applied here.

[14] The boundaries could be described by real materials with electromagnetic properties but they could also represent the topology of the space or the interface between different phases of the vacuum.

[15] An ideal metal plate is made of a material with infinitely large dielectric permittivity.

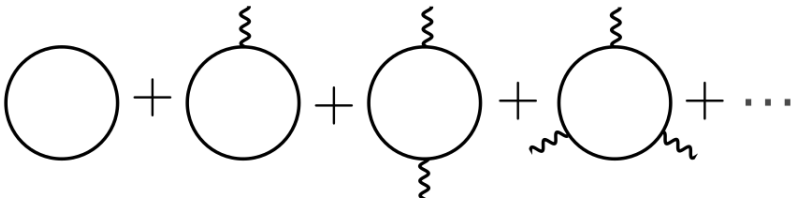

FIGURE 1.1: One loop quantum corrections Feynman diagrams for the polarization of the vacuum because of the creation of electron and positron pairs in the Schwinger effect.

In fact, the imaginary part of the zero-point energy will be related to the vacuum decay rate. Schwinger derived that if the electric field $\vec{E}$ is constant, the pair production takes place at the constant rate per unit volume

$$\Gamma = \frac{(eE)^2}{4\pi^3 c\hbar^2} \sum_{n=1}^{\infty} \frac{1}{n^2} e^{-\frac{\pi m^2 c^3 n}{eE\hbar}},$$

being m the electron mass, e its charge and E the strenght of the electric field. In order for this effect to be measurable, extremely strong electric-field strengths of order $10^8 V/m$ are needed. This is the major difficulty in the laboratory setups. Recently, high energy lasers and shaped laser pulses have been proposed to achieve strong enough electric fields [56, 71]. It is also being studied the characteristic diffraction pattern produced by the polarization of vacuum's virtual pairs during the collision of two counterpropagating optical lasers of ultra-high intensity [72]. Furthermore, it has been observed that particle creation is enhanced when combining different time-dependent electric fields [73]. Although much work has been developed since its theoretical prediction (it is worth mentioning the references [3, 74–76]), the Schwinger effect has not been observed in a laboratory yet. The pair production can be also increased by the presence of a gravitational field [77]. In the Kaluza-Klein theory [78–80], the Universe is considered to have a high number of dimensions: four of them are observable and the remaining ones form a compact manifold which induce physical effects in the observable four-dimensional space. A possible measurement of the decay rate different from the one computed for four dimensions would be an evidence of the existence and the geometry of these extra dimensions.

The Casimir effect has applications in many areas of physics [5, 15, 24]: condensed matter physics (attractive and repulsive forces in layered systems [25]), atomic physics (absorption phenomena in carbon nanotubes [26, 27]), astrophysics (inflation process [28], Casimir-type polarization of the vacuum produced by topological defects [29]) or nano-science (fabrication of nanometric devices MEMS [30–33] where it is possible to control the sign of the force and its magnitude by optical modification of the charge carrier density with laser light), to name but a few of them.

1.2. QFT of scalar fields

Consider a real massless scalar field ϕ with action functional involving the Lagrangian density in equation (1.1):

$$S[\phi] = \int d^{D+1}x \left(\frac{1}{2}\partial_\mu \phi \partial^\mu \phi - U(\phi) \right), \tag{1.7}$$

where $U(\phi)$ is a potential describing the self-autointeraction of the field (for instance, in the Higgs model $U(\phi) = \lambda/8(\phi^2 - v^2)^2$). Notice that this action could be non quadratic in general. The field equations are

$$\partial_\mu \partial^\mu \phi + U'(\phi) = 0.$$

Let ϕ_{cl} be a classical static solution of these field equations. If one studies small fluctuations η around ϕ_{cl} up to second order, it is easy to reach

$$S[\phi_{cl} + \eta] = S[\phi_{cl}] + \frac{1}{2}\int d^{D+1}x \left[\partial_u \eta \partial^\mu \eta - U''(\phi_{cl})\eta^2 \right] + o(\eta^3).$$

Notice that $S[\phi_{cl}]$ is a constant independent of η that should not be consider when studying the dynamics of small fluctuations around ϕ_{cl}. When considering $\phi = \phi_{cl} + \eta$ only paths which are very close to the classical one contribute to the path integral $S[\phi]$. The dynamics of the small fluctuations will be described by the action

$$S[\eta] = \frac{1}{2}\int d^{D+1}x \left[\partial_u \eta \partial^\mu \eta - U''(\phi_{cl})\eta^2 \right] + o(\eta^3),$$

whose related field equation is:

$$\partial_\mu \partial^\mu \eta + U''(\phi_{cl})\eta = 0.$$

Taking the metric $g_{\mu\nu} = (+ - - - \dots)$ one can rewrite the last equation as

$$-\partial_0^2 \eta = \hat{K}(\eta), \qquad \hat{K} = -\Delta + U''(\phi_{cl}(\vec{x})),$$

where $\hat{K}$ is now a Schrödinger operator. Since the potential has been expanded up to second order, the Wentzel–Kramers–Brillouin approximation[16] could be used to find $\eta(x)$ as will be explained later. Treating η as a quantum scalar field, one could expand it as

$$\eta(x) = \sum\!\!\!\!\!\!\int_{\omega_k^2 \in \sigma(\hat{K})} \left(a_k e^{i\omega_k t} f_k(\vec{x}) + a_k^\dagger e^{-i\omega_k t} f_k^*(\vec{x}) \right),$$

where instead of over Fourier modes, the summation is over the spectrum of $\hat{K}$. Now, promoting the Fourier modes to creation and annihilation operators to quantise the fluctuations one arrives to the Hamiltonian

$$\hat{H}_\eta = \sum\!\!\!\!\!\!\int_{\omega_k^2 \in \sigma(\hat{K})} \omega_k \left(N_k + \frac{1}{2} \right).$$

[16] The WKB approximation, typically used for a semi-classical calculation in quantum mechanics, allows to find approximate solutions to linear differential equations with spatially varying coefficients.

As the action of the fluctuation fields is quadratic, there is no interaction between fields beyond the mass term (for free theories) or beyond the quadratic interaction of the field due to the background potential (for general theories), i.e. there are no more vertices in the theory. Consequently, the Hamiltonian represents a grand canonical ensemble of particles with frequencies ω_k that do not interact with each other, as it was introduced in the previous section.

The crucial point is that, since the dynamics of the fluctuations have only been considered up to second order, the action of the resulting theory is quadratic in η. In order to compute the quantum vacuum energy $\langle 0|\,\hat{H}\,|0\rangle$ from here, two approximations will be used: the WKB semiclassical approximation and the calculation of $\langle 0|\,\hat{H}\,|0\rangle$ up to the first order loop. The WKB approximation would be exact so the one loop quantum corrections to the vacuum energy is an exact result. This is the starting point in the computation of the quantum vacuum energy $\langle 0|\,\hat{H}\,|0\rangle$ in the seminal paper [37].

When evaluating path integrals in quantum theories [81], the partition function of the system is a functional determinant if the action is quadratic in the field, i.e.

$$Z = \int [d\phi] e^{iS[\phi]} = [\det \hat{O}]^{1/2} \qquad \text{if} \qquad S[\phi] = \int dx\, \phi\, \hat{O}\, \phi. \tag{1.8}$$

But for general actions without an exact solution it is common to perturb the theory with respect to a dimensionless, small parameter. The perturbative expansion of the partition function with respect to the potential V of the Lagrangian gives the Born series, which can also be expressed in terms of Feynman diagrams. The number of vertex in the diagram expansion determines the order of the perturbation theory because each vertex basically contributes as $-iV$. Another way to solve the path integral makes use of the WKB approximation [6–9], which is a generalisation for infinite degrees of freedom of the stationary phase approximation in quantum mechanics [82]. This method is based on the fact that in the semi-classical limit in which $\hbar$ takes small but no zero value, the phase in Z changes quickly even for small changes in the field configuration. Hence, interferences between similar field configurations are only constructive for those near the classical or stationary one. Consequently, one can neglect cubic and greater order terms when performing an expansion of the action with respect to this classical field[17] and thus, Z can be rewritten as

$$Z = e^{iS[\phi_{cl}]} \int [d\eta]\, e^{\frac{i}{2}\eta \left.\frac{\delta^2 S}{\delta \phi^2}\right|_{\phi_{cl}} \eta}, \qquad \text{if} \qquad \phi = \phi_{cl} + \eta \qquad \text{and} \qquad \left.\frac{\delta S}{\delta \phi}\right|_{\phi_{cl}} = 0.$$

This is equivalent to an expansion of the path integral with respect to $\hbar$. In terms of diagrams, it is an expansion with respect to the number of loops: the zero loop approximation or tree diagrams gives a phase equal to the classical action and the first loop diagram represents the leading order in the

[17] This is nothing but the *weak-coupling* approximation. Notice that the Lagrangian of a field theory can be splitted as $\mathcal{L} = T(\phi) + V(g, \phi)$. In general, $V(g, \phi)$ contains cubic or greater degree terms of the fields whereas the kinetic part involves only quadratic contributions. The coupling constant g gives information about the magnitude of the kinetic part with respect to the potential part. In the weak-coupling approximation, $g \ll 1$, the perturbation theory can be applied and the theory can be renormalised. Although in the explanation of the WKB approximation, the coupling constant does not appear, it is implicit. The reason is that most of the potentials can be rewritten as $U(g, \phi) = \overline{U}(\overline{\phi})/\Sigma(q)^2$ where $\overline{\phi} = \Sigma(g)\phi$. Here, $\overline{U}$ does not depend on any coupling constant. The WKB approximation explained in this section works directly with $\overline{U}(\overline{\phi})$.

integral over the quantum fluctuations. Consequently, when the Casimir force between objects will be computed in following chapters, the result would be just the one-loop Feynman diagram with two external legs in the expansion of Figure 1.2.

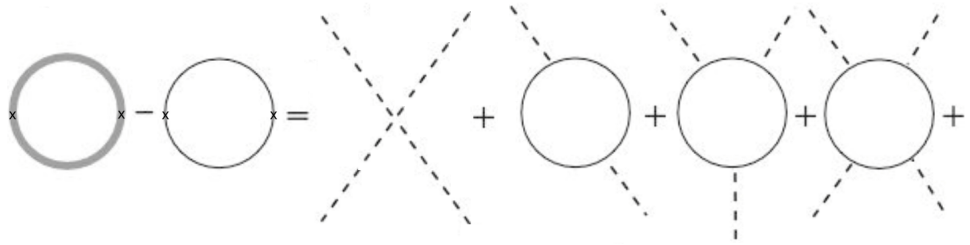

FIGURE 1.2: Expansion of the Casimir force with Feynman diagrams. The thick (thin) line denotes the full (free) Green's function [10].

This Feynman diagram associated to the Casimir energy is similar to the one for the Schwinger effect that appears in Figure 1.1.

Notice that if the action has several stationary points or classical paths widely separated from each other, the WKB approximation still holds and each stationary configuration is an additive contribution to the final result. Out of curiosity, this method is considered by some authors as slightly different from a perturbation theory because the expansion parameter $\hbar$ is not dimensionless. Anyway, this semi-classical expansion can also be seen as the expansion in powers of $\hbar$ of the effective generating functional [83–86] for the one-particle irreducible graphs[18] in the diagrammatic scheme. From the classical action in the presence of an arbitrary source $J(x)$:

$$S[\phi, J] = \int d^{D+1}x \, [\mathcal{L} + J(x)\phi(x)],$$

and the generating functional for full Green's functions

$$Z[J] = e^{iW[J]} \propto \int [d\phi] e^{iS[\phi,J]},$$

one could define the effective action $\Gamma[\bar{\phi}]$ as the Legendre transformation

$$\Gamma[\bar{\phi}] = W[J] - \int d^{D+1}x \, \bar{\phi}(x) J(x), \qquad \text{with} \qquad \bar{\phi}(x) = \frac{\delta W[J]}{\delta J(x)} = \frac{{}^{-\infty}_{J}\langle 0| \, \phi(x) \, |0\rangle^{\infty}_{J}}{{}^{-\infty}_{J}\langle 0| \, |0\rangle^{\infty}_{J}},$$

if J is independent of time. In this sense, in the perturbative study of the quantum theory one could write

$$\Gamma[\bar{\phi}] = S[\bar{\phi}] + \hbar \text{ (one loop)} + o(\hbar^2). \tag{1.9}$$

Consequently, in this context, the ground state is found through the stationary point of the effective action and the one-particle irreducible diagrams for Green's functions can be obtained from its expansion around its minima. At tree approximation, the effective potential is nothing but the classical

[18] A one-particle irreducible Feynman diagram is a connected one that cannot be disconnected by cutting a single internal line.

action. It is important to note that when studying the action of the fluctuations around a classical field solution up to second order (1.8), one is really studying the one loop term of (1.9). This result is again diagrammatically represented as the second term of the right hand side in Figure 1.2.

It is worth noticing that in the following chapters only effective theories [83, 84] are going to be considered. When computing the Casimir force between plates or objects, one should also take into account the microscopic details of the material that the object is built of. The QED Lagrangian should also be introduced to add the contribution of the atoms of the objects. However, this is not what happens. In fact, if one were to do it, the theory would become as complicated that it probably could not be solved. Consequently, one traces over the microscopic degrees of freedom concerning the fermions in the plates to work with an effective theory which analytically describes the system properly enough.

1.3. QFT in domains with boundaries

The physical properties of the vacuum state and the vacuum energy show a strong dependence on the type of boundaries. The effects of the boundaries or the non-trivial topology of the space are more relevant for determining the vacuum spectrum in the low energy or infrared behavior of the quantum field theories than in the high energy or ultraviolet one[19]. As previously introduced, one of the most important boundary phenomenon is the Casimir effect, in which such external conditions restric the modes of the field giving rise to the vacuum polarization. Besides this, the properties that boundaries introduce in the systems need to be deeply studied in other physical phenomena like the spontaneous symmetry breaking and anomalies [87], the quantum Hall effect [88], black holes [70] and in other areas such as string theory [89], quantum gravity [90] and solid state physics [91].

An extremely useful formalism has been developed so far to make calculations regarding the vacuum energy and the thermodynamics of fields in open domains with boundaries by using the huge amount of powerful tools provided by scattering theory [15, 35]. The essential elements of this formalism will be introduced in the remaining part of this section. But first of all, it will be explained how field theory varies in presence of boundaries.

Consider a quantum scalar field[20] in a manifold $\mathcal{M}$ with boundaries $\partial\mathcal{M}$. Notice that when integrating by parts the action (1.7) in a theory without external sources (which is the case for scalar zero-point oscillations) an extra integration over the boundaries arises:

$$S[\phi] = -\frac{1}{2}\int_{\mathcal{M}} d^{D+1}x\,\phi\left(\partial^{\mu}\partial_{\mu} + m^2\right)\phi + \frac{1}{2}\int_{\partial\mathcal{M}} d^{D}x\,\phi\partial_{n}\phi.$$

The second integral in the previous expression relates values of the field in the bulk with its values at

[19] Notice that the high energetic modes of the spectrum do not feel the background and they pass through the system without being scattered.

[20] Although the effects of the boundaries are more significant for massless field theories due to the characteristic long distance correlations which allow these effects to be filtered in the whole interior region, the action of a general massive theory is going to be treated here for completeness.

the boundary. This means that the equations of motion derived from this action functional are non-local. In such a a theory, boundary conditions are imposed over the frontiers in order for the integral over $\partial\mathcal{M}$ to vanish. In this way, the corresponding Hamiltonian could be quantised following the usual commutation relations of the second quantisation and one recovers the interpretation of the system as an infinite collection of non-interacting harmonic oscillators. To obtain local equations of motion it is necessary to consider

$$S[\phi] = \int d^{D+1}x \left(\frac{1}{2}\partial_\mu\phi\partial^\mu\phi + m^2\phi^2\right) - \frac{1}{2}\int_{\partial\mathcal{M}} d^D x\, \phi\partial_n\phi. \tag{1.10}$$

as the starting action. For a free scalar field propagating in a more general $D+1$ dimensional manifold $(\mathcal{M}, g)$ with boundaries $\partial\mathcal{M}$, the action should be written as

$$S[\phi] = \frac{1}{2}\int_{\mathcal{M}} d^{D+1}x\,\sqrt{-g}\left[g_{\mu\nu}D_\mu\phi D_\nu\phi - m^2|\phi|^2 - \xi R|\phi|^2\right] - \frac{1}{2}\int_{\partial M} d^D x\,\sqrt{-g_{\partial\mathcal{M}}}\;\left[\phi\partial_n\phi\right]|_{\partial\mathcal{M}}\,, \tag{1.11}$$

being g the determinant of the metric tensor with pseudo-Riemannian signature $(+---\cdots-)$, D_μ the covariant derivative obtained from the Levi-Civita connection, R the Ricci scalar curvature and ξ the coupling to the gravitational field.

From (1.10) one could rewrite the action as

$$S[\phi(x)] = -\frac{1}{2}\int d^{D+1}x\;\phi(x)\hat{K}\phi(x),$$

being the operator $\hat{K} = \partial^\nu\partial_\nu + m^2$ the kernel of the action.

Considering smooth stationary[21] boundaries of any geometrical shape, one can obtain the normalised positive and negative frequency solutions of the Klein Gordon equation of motion:

$$\phi_J^+(x) = \frac{1}{\sqrt{2\omega_J}}e^{-i\omega_J t}\varphi_J(\bar{x}), \qquad \phi_J^-(x) = \frac{1}{\sqrt{2\omega_J}}e^{i\omega_J t}\varphi_J^*(\bar{x}),$$

being $\varphi_J(\bar{x})$ the solutions[22] of $(-\partial^i\partial_i + m^2)\varphi_J(\bar{x}) = \lambda_J^2\,\varphi_J(\bar{x})$ with the dispersion relation given by $\lambda_J^2 = \omega_J^2 - m^2$. J is a collective index for the generalised wave vector, following the notation given in [15]. The novelty is that now the eigenstates of the kernel operator verify the boundary condition $f(\varphi(\bar{x}), \partial\varphi(\bar{x})) = 0$ on the boundary surface S. Once quantised, the field can be written as the sum of all the modes[23]

$$\phi(x) = \sum\!\!\!\!\!\!\int \left(\phi_J^+(x)\mathfrak{a}_J + \phi_J^-(x)\mathfrak{a}_J^\dagger\right),$$

where $\mathfrak{a}_J, \mathfrak{a}_J^\dagger$ are the annihilation and creation operators of a particle (characterised by quantum numbers indexed by J). Both operators satisfy the usual commutation relations. By applying the creation

[21] One consider smooth stationary boundaries in order for the separation of the temporal variable to be applicable.

[22] Notice that when considering the free Minkowski space, φ_J are simply the normalised plane waves and $\lambda_J^2 = k^2$ is the wave vector.

[23] In massive QFT there could be a summation over the discrete states of positive energy lying in the gap and an integral over the continuous ones.

operators to the vacuum state $|0\rangle$, the Fock space of particles is built.

Concerning the energy density operator of the scalar field it is necessary to study the 00-component of the energy–momentum tensor. From the Lagrangian of the theory one can construct it for fields of spin zero as

$$T^{(0)}_{\mu\nu} = \partial_\mu\phi\partial_\nu\phi - g_{\mu\nu}\mathcal{L}.$$

The total vacuum energy of the scalar field in the volume V with boundaries is

$$E_0 = \frac{1}{2}\sum_J \omega_J = \int d\bar{x}\, \langle 0|\, T^{(0)}_{00}(\bar{x})\, |0\rangle\,,$$

taking into account that the functions ϕ satisfy some boundary condition on the boundary surface S. For obtaining a finite result, it is necessary to subtract the contribution of the total vacuum energy in the same volume in the free Minkowski space without boundaries:

$$E_{0,M} = \int d\bar{x}\, \langle 0_M|\, T^{(0)}_{00}(\bar{x})\, |0_M\rangle\,.$$

There are several approaches to tackle the problem of computing the summation over modes and regularising and renormalising the quantum vacuum energy. Most of them involve scattering theory. Those procedures that will be covered during the thesis will be listed hereafter according to the basic tools or principles on which they are based:

- **In terms of Green's functions**.

  The Green's function of a system of a scalar field in a domain with boundaries is defined as the time-ordered product of two fields as[24]

  $$G(x,x') = i\,\langle 0|\,\mathcal{T}\phi(x)\phi(x')\,|0\rangle = \int \frac{d\omega}{2\pi} e^{-i\omega(t-t')} \sum_{n=0}^{\infty} \frac{\varphi_n(\bar{x})\varphi_n^*(\bar{x}')}{-w^2+\lambda_n^2}$$
  $$\text{such that} \qquad \hat{K}\cdot G(x,x') = \delta(x-x').$$

  The Green's function can be expressed as a series expansion depending on the associated free Green's function and the coupling with the frontiers by using the Lippmann-Schwinger equation. Hence, the Casimir energy can be computed as the summation of all the Feynman diagrams with external legs or in other words, in terms of the scattering matrix elements.

  If the boundaries are two $(D-1)$-dimensional flat plates placed in the z-direction (which is orthogonal to the plates), one easy way to view this relation between the reduced Green's function $G_k(z,z')$ defined as

  $$G(x,x') = \int \frac{d^{D-1}k_\parallel}{(2\pi)^{D-1}} e^{i\vec{k}_\parallel(\vec{x}_\parallel - \vec{x}'_\parallel)} \int \frac{d\omega}{2\pi} e^{-i\omega(t-t')} G_k(z,z'), \qquad x = (\vec{x}_\parallel, z) \in \mathbb{R}^D, \tag{1.12}$$

[24] Notice that $\mathcal{T}\varphi(x)\varphi(x') = \Theta(t-t')\varphi(x)\varphi(x') + \Theta(t'-t)\varphi(x')\varphi(x)$ being Θ the Heaviside step function.

and the scattering eigenfunctions ψ_k^R, ψ_k^L is found in [92]

$$G_k(z,z') = \frac{1}{W[\psi_k^R, \psi_k^L]} \left(\Theta(z-z')\psi_k^R(z)\psi_k^L(z') + \Theta(z'-z)\psi_k^R(z')\psi_k^L(z) \right), \tag{1.13}$$

being $W[\dots]$ the Wronskian. The asymptotic behaviour of the scattering eigenfunction is determined by the scattering coefficients:

$$\psi_k^R(z) \approx \begin{cases} e^{ikz} + r_R(k)e^{-ikz}, & z \to -\infty \\ t(k)e^{ikz}, & z \to \infty \end{cases}, \qquad \psi_k^L(z) \approx \begin{cases} t(k)e^{-ikz}, & z \to -\infty \\ e^{-ikz} + r_L(k)e^{ikz}, & z \to \infty \end{cases}.$$

R. Balian and B. Duplantier gave another approach [93, 94] by expressing the Casimir energy of electromagnetic fields bounded by arbitrary smooth-shaped perfect conductors by using a convergent multiple reflection expansion and derived explicit results to leading order at asymptotically large separation.

Either way, the 00-component of the energy momentum tensor can be related to the Green's functions by means of:

$$\langle 0| \, T_{00}^{(0)}(x) \, |0\rangle = \frac{1}{2i} \left(\partial_{x^\mu} \partial_{x'^\mu} + m^2 \right) G(x,x') \big|_{x=x'}. \tag{1.14}$$

Once $\langle 0| \, T_{00}^{(0)}(x) \, |0\rangle$ is computed[25] the divergent contributions must be subtracted by means of a regularisation and renormalisation procedure. One well-known example in which this method has been used appears in [95]. In this work, the 00-component of the energy momentum tensor of a fluctuating quantum field coupled to a classical background is computed by relating the matrix elements of T_{00} to the scattering Green's function at coincident points with appropriate boundary conditions. They regularised its divergent behaviour at large wave moment k by subtracting the first few terms in its Born expansion and adding back the contribution of the associated low–order Feynman diagram. These diagrams are then regularised and renormalised in ordinary Feynman perturbation theory. As a result, the quantum vacuum energy of a field in the presence of boundaries can be finally computed.

- **In terms of transfer matrices**.

  In [37, 38] Kenneth and Klich developed another formalism based on transition operators (more precisely the so called Lippmann-Schwinger T operator) to compute the quantum vacuum energy between dielectric bodies of arbitrary shapes. The method is also valid for both scalar and electromagnetic fields.

  When using the scattering formalism to solve the quantum vacuum energy between several objects it is necessary to characterise the whole sprectrum in the background of these two objects, which can frequently be rather difficult. By contrast, the $TGTG$ formula only requires

[25] If there is a background potential $V(x)$ in the system, the equation (1.14) should be modified accordingly, that is, it should be replaced by $\langle 0| \, T_{00}^{(0)}(x) \, |0\rangle = \frac{1}{2i} \left(\partial_{x^\mu} \partial_{x'^\mu} + m^2 + V(x) \right) G(x,x') \big|_{x=x'}$.

knowing the spectrum of a single object and hence, the computational effort is much smaller. The *TGTG* formula has been used for instance in [92, 96] to compute the vacuum interaction energy of non compact disjoint objects represented by a smooth classical background of two sine Gordon kinks and by two $\delta\delta'$ potentials mimicking two plates, respectively. Since in both cases the potentials representing the two objects do not overlap (i.e. they are potentials with disjoint compact supports), the *TGTG* formula provides exact results in these cases. In the references [35, 37, 38, 96–98] one could find all the intermediate steps to reach the final *TGTG* formula. Nevertheless, only the main results which are required in next chapters will be stated here below.

The transfer matrix or T operator can be defined in an integral kernel form by using the Green's functions[26] and the Lippmann-Schwinger equation of quantum mechanical 1D scattering theory as:

$$G_\omega(z_1,z_2) = G^{(0)}_\omega(z_1,z_2) - \int dz_3\, dz_4\, G^{(0)}_\omega(z_1,z_3) T_\omega(z_3,z_4) G^{(0)}_\omega(z_4,z_2), \tag{1.15}$$

being $G^{(0)}_\omega$ the reduced Green's function corresponding to a particle in the free spacetime. Remember that for a 1+1 dimensional massless theory, $\omega = k$. Hence, $G^{(0)}_\omega$ is the solution of the differential equation $-\partial_z^2 \cdot G(z,z') = \delta(z-z')$ for the Laplace Beltrami operator in 1D. Consider a background potential composed by the sum of two non-intersecting compact supported[27] potentials, i.e. $V(z) = V_1(z) + V_2(z)$ such that $V(z)$ do not allow bound states[28]. The quantum vacuum energy before regularisation reads

$$E_0 = -\frac{i}{2}\int_0^\infty \frac{dk}{\pi}\left[-\mathrm{Tr}\,\log\, \boldsymbol{G^{(0)}_k} + \mathrm{Tr}\,\log\left(\frac{\boldsymbol{G^{(0)}_k}}{1+\boldsymbol{G^{(0)}_k V_1}}\right) + \mathrm{Tr}\,\log\left(\frac{\boldsymbol{G^{(0)}_k}}{1+\boldsymbol{G^{(0)}_k V_2}}\right) - \mathrm{Tr}\,\log(1-\boldsymbol{M_k})\right], \tag{1.16}$$

being the $\mathbf{M}_k$ operator expressed in terms of the integral kernel as:

$$M_k(z_1,z_2) = \int dz_3\, dz_4\, dz_5\, G^{(0)}_k(z_1,z_3) T^{(1)}_k(z_3,z_4) G^{(0)}_k(z_4,z_5) T^{(2)}_k(z_5,z_2).$$

$T^{(i)}$ with $i = 1,2$ refers to the T operator of the object represented by V_i with $i = 1,2$. The smoothness of $G^{(0)}(z_1,z_2)$ for $z_1 \neq z_2$ guarantees that for any two compact bodies separated by a finite distance, the operator $G^{(0)}$ between them is a trace class operator[29]. Since $T^{(i)}$ are bounded then M_k is a trace class operator. Moreover the modulus of the eigenvalues of M_k is less than one and the integrand is well defined. A rigorous proof of this statement is given in [38].

The integrand in (1.16) involves three types of different behaviour terms:

[26] Note that the Lippmann-Schwinger operator $\mathbf{T}$ is related to the $\mathbf{S}$ matrix by $\boldsymbol{S} = \mathbb{1} - 2\pi i\delta(\omega^2 - \omega'^2)\boldsymbol{T_\omega}$ so the *TGTG* formula is directly connected to scattering data.

[27] If the potentials do overlap the results reached by using this method would still be a good approximation if the individual potentials approach their asymptotic values exponentially fast (specifically, as soon as the separation between objects becomes larger than their size).

[28] If the non relativistic Schrödinger operator which defines the set of one particle states admits states with negative energy (bound states), it would be indispensable to introduce a mass in the theory acting as an infrared cut off. In such a way, the whole spectrum becomes a set of discrete and continuous states with positive energy. Then all the operators G, T, K act in the same Hilbert space and fluctuation absorption becomes impossible.

[29] An operator is trace class if the summation of the modulus of its eigenvalues is finite.

- The first term is the divergent zero point energy of the free background.
- The next two terms are the self-energies of each of the objects. They represent a divergent contribution if the area of the objects is infinite.
- The last term is the only one that depends on the distance between plates so it is the only one necessary to obtain the quantum vacuum interaction energy formula. It is noteworthy that in 1D this term can be given only in terms of the reflection scattering coefficientes [99]. However, in higher dimensional spacetimes, partial wave expansions of scattering states must be considered. Regarding this term, some caveats are worth stressing. The dominant quantum fluctuations due to the interaction of the volumes are waves of very low frequency. Consequently, their wavelengths are of the order of the distance between plates. Since the wavelength of the fluctuations is greater than the typical magnitude of the objects, they can be considered as pointlike. There is another special case when the objects have spherical symmetry. Then, the leading term in the interaction between them comes from s-wave scattering contributions, whenever they exist in the theory.

Scattering would be the base of some methods discussed at length in sections 1.5 and 4.4, where the *TGTG* formula is used. Moreover, in section 4.3 the Green's functions of the corresponding problem will be explicitely computed from the scattering data.

It is worth stressing that although in the explanation of this method the focus of attention has been put in separated interacting bodies (one outside the other one), the *TGTG* formalism also applies for other geometries as a body inside another one [100–102]. It is also relevant to highlight that apart from Kenneth and Klich, other authors have computed the Casimir energy by means of the transition matrices of the scattered waves and the propagator between objects [103–105]. Kenneth and Klich identified $G^{-1}(z_1, z_2)$ in the functional determinant as a T-matrix and derived a formal result for the Casimir interaction for scalar fields in a medium with a space-and frequency-dependent speed of light. Jaffe *et al.* described a method based on a multipole expansion of fluctuating charges, characterising each object by its on-shell electromagnetic scattering amplitudes. Their derivation allows for an extension to gauge fields in the presence of objects with general dielectric and magnetic properties.

- **In terms of complex integrals, heat trace and zeta function.**

For systems with boundaries described by the most completely general conditions, the summation over the frequencies of the modes of the quantum field should best be performed by using the Cauchy theorem and the integration in the complex frequency plane. This formalism provides a solution to the lack of an universal mathematical prescription for the subtraction of the divergences in the problem. For instance, in [106] the authors calculate the Casimir energy for a massless scalar field obeying the Dirichlet and Neumann boundary conditions on a spherical shell. For a spherical boundary with radius a the authors state that the Casimir energy is given by:

$$E_0 = \frac{1}{2}\sum\omega = \sum_{\ell=1}^{\infty}\frac{\ell+1/2}{2\pi i}\oint_C dk\,k\frac{d}{dk}\log f(k,a),$$

being $f(k,a)$ the function defining the frequency equation $f(k,a)=0$. Notice that $f(k,a)$ is related to the Jost function[30] [97, 98, 107, 108]. The contour C will consist on the segment $[-ib,ib]$ of the imaginary axis and a semicircle of radius b in the right half complex plane (the limit $b\to\infty$ will be considered). Then they subtract the contribution of the Minkowski space corresponding to the limit of the radius of the sphere going to infinity. In such a way and by using the techniques of complex contour integration, they obtain that the regularised and partially renormalised desired quantity is given by

$$E_0=\sum_{\ell=1}^{\infty}\frac{\ell+1/2}{\pi}\int_0^{\infty}d\xi\log\frac{f(i\xi,a)}{f(i\xi,a\to\infty)}. \tag{1.17}$$

The essential advantage of this approach is that once the renormalisation of the dominant divergence has been performed, there are no more constant terms (contact terms) in the integrand leading to divergences. On the other hand, the divergences which appear when summing over ℓ are removed by means of the Hurwitz ζ-function giving rise to a highly precise numerical asymptotic result for the renormalised Casimir energy in this configuration.

This is just one example but the idea behind is based on how to make the sum $\sum_{\omega^2\in\sigma(\hat{K})}\omega$ convergent to compute the Casimir energy between objects. To obtain this goal one could use the heat equation kernel method [39] and add a regularisation parameter $\epsilon\in\mathbb{R}^+$ with units of inverse energy squared to compute

$$\sum_{\omega^2\in\sigma(\hat{K})}\omega e^{-\epsilon\omega^2}. \tag{1.18}$$

If, as in the previous example, the spectrum of frequencies can be determined as the zeroes of a secular function, one could express this summation as a complex contour integral similar to (1.17). An asymptotic expansion in the distance between objects is then performed and the terms that would be divergent when $\epsilon\to 0$ must be subtracted. Once the result of the summation is obtained, the physical limit $\epsilon\to 0$ is taken. Another way of making the summation $\sum_{\omega^2\in\sigma(\hat{K})}\omega$ convergent is using zeta regularisation to study

$$\sum_{\omega^2\in\sigma(\hat{K})}\omega^{-2s},\quad s\in\mathbb{C}, \tag{1.19}$$

which converges providing $\mathrm{Re}\,s>D/2$, being D the dimension of the space under consideration. Again, when there exists a secular function whose zeroes completely characterise the spectrum of the related Schrödinger operator, this last summation can be written in terms of

[30] The Jost function $j(k)$ is defined in scattering theory as the Wronskian between a regular solution and an irregular one of the radial Schrödinger equation. The regular solution satisfies the conditions $\varphi(k,r=0)=0$ and $\varphi'(k,r=0)=1$. On the other hand, the irregular Jost solutions are two linearly independent functions such that $\lim_{r\to\infty}f_{\pm}(k,r)=e^{\pm ikr}+o(r)$. The Jost function is related to the S-matrix by $\det S=t^2(k)-r_R(k)r_L(k)=e^{i2\delta(k)}=j^*(k)/j(k)$ being $j^*(k)=j(-k)$. Any scattering solution of the Schrödinger equation can be expressed as a linear combination of $f_{\pm}(k,r)$. It should be noted that the phase shift in the scattering problem is just minus the phase of the Jost function. Furthermore, the zeroes of the Jost functions providing $\mathrm{Im}\,k>0$ are the bound states of the theory. Consequently, the Jost function determines both the spectrum and the phase shift of the scattering problem.

a complex integral. In the zeta function method, calculating the finite part of the vacuum interaction energy is linked to computing some residues, as it will be explained a bit further on. The Casimir energy will arise finally when considering the physical limit $s \to -1/2$. The zeta function is the Mellin transform of the heat trace so both methods are somehow closely related but there is an important difference. Whilst the zeta regularisation is more effective, being applicable even for curved spacetime, the heat kernel method has a more obvious physical interpretation because the terms that one must subtract in the asymptotic expansion have the physical interpretation of the ultraviolet divergent terms associated to the energy density of the theory in the bulk and the self-interaction energy of the objects, if applicable. In contrast, these physically divergent contributions are not so evident when the residues and the heat kernel coefficients are calculated in the zeta regularisation procedure.

Now, due to its relevance, a more in-depth study of the zeta regularisation method is to be carried out. The physical properties of the system of a non self-interacting field under external conditions in 1+1 dimensions (for simplicity) can be described by means of the Euclidean path-integral functional

$$Z[V] = \int D\phi\, e^{-iS[\phi]},$$

where $V(z)$ is the background potential. The Gaussian integration of $Z[V]$ is given by

$$\Gamma[V] = -\log Z[V] = \frac{1}{2}\log\det[(-\Delta + V(z))/\nu^2] = \frac{1}{2}\log\det[\hat{K}/\nu^2],$$

being ν an arbitrary parameter with dimension of mass introduced to adjust the dimension of the argument of the logarithm. Possible zero modes are excluded in order for the determinant not to vanish. $\hat{K}$ is a formally self-adjoint elliptic second-order differential Laplace-type operator on a smooth compact Riemannian D-dimensional manifold $\mathcal{M}$ with a smooth boundary $\partial\mathcal{M}$ and local boundary conditions $\mathcal{B}$.

The summation over the frequencies of the field modes can be performed by using the zeta regularisation method [39–42] in which:

$$\log\det\left[\hat{K}/\nu^2\right] = \sum_{n=1}^{N}\log\,\lambda_n = -\frac{d}{ds}\sum_{n=1}^{N}\lambda_n^{-s}\big|_{s=0} = -\frac{d}{ds}\,\zeta_{\hat{K}/\nu^2}(s)\big|_{s=0}, \tag{1.20}$$

where the sum is convergent for $\mathrm{Re}\, s > D/2$. The analytical structure of the zeta function of $\hat{K}$ is better studied when using the Gamma representation

$$\zeta_{\hat{K}/\nu^2}(s) = \frac{\nu^s}{\Gamma(s)}\int_0^\infty t^{s-1}K(t)dt, \qquad K(t) = \sum_{n=1}^{\infty} e^{-\nu\lambda_n t}.$$

$K(t)$ is the global heat kernel and t has been considered as a temporal coordinate. The local version $K(t,z,z') = \sum_{n=1}^{\infty} e^{-\nu\lambda_n t}\phi_n(z)\phi_n^*(z')\nu^{2-D}$ is the solution of the heat equation

$$(\partial_t + \hat{K}/\nu)K(t,z,z') = 0, \qquad \text{with boundary conditions} \qquad \mathcal{B}K(t,z,z')|_{\partial\mathcal{M}} = 0.$$

Notice that $K(t) = \int_{\mathcal{M}} dz\, K(t,z,z)$. If $\lambda_n > 0$ the definition in (1.20) is well defined because of the convergent exponential function. The possible residues only arise in the limit $t \to 0$, where $K(t)$ can be expanded in terms of the heat kernel coefficients $a_\ell(\hat{K}, \mathcal{B})$ as:

$$K(t) \sim \sum_{\ell=0,1/2,1\ldots}^{\infty} a_\ell(\hat{K}/\nu^2, \mathcal{B})\, t^{\ell - D/2} \nu^{\ell - D/2}.$$

In this way, in the zeta function regularisation technique, divergences up to one-loop order are completely described by the leading heat kernel coefficients of the associated field equations. $\zeta_{\hat{K}}(s)$ has poles at the points $D/2, (D-1)/2, \ldots, 1/2, -(2n+1)/2$ but it is analytic at $s = 0$ so $\zeta'_{\hat{K}}(0)$ in (1.20) is well defined.

Sometimes, the spectrum of $\hat{K}$ can be characterised by means of a spectral function $f_{\hat{K}}(k)$ [43]. Consider a holomorphic function $f_{\hat{K}}(k)$ on $\mathbb{C}$ such that $\lim_{k\to 0} f_{\hat{K}}(k) \neq 0, \infty$. In this way, the formal definition of the spectral zeta function associated to $\hat{K}$ is

$$\zeta_{\hat{K}/\nu^2}(s) = \sum_{\tilde{\sigma}(\hat{K}/\nu^2)} (\nu^{2s} k^{-2s}) = \oint_C dk\, \nu^{2s} k^{-2s} \frac{d}{dk} \log f_{\hat{K}}(k) \qquad \text{for Re(s)} > s_0 \in \mathbb{R}^+. \tag{1.21}$$

Note that $Z(f_{\hat{K}}) \equiv \{k_n \in \mathbb{R} / f_{\hat{K}}(k_n) = 0\}$ is the set of zeroes of the spectral function and $\tilde{\sigma}(\hat{K}/\nu^2) \equiv \{\lambda_n \in \mathbb{R}^+ / (\hat{K}/\nu^2)\psi_n = \lambda_n \psi_n\}$ the set of eigenvalues of the operator $\hat{K}/\nu^2$. In this way $\forall k_n \in Z(f_{\hat{K}})$, $k_n^2 = \nu^2 \lambda_n \in \tilde{\sigma}(\hat{K}/\nu^2)$, the multiplicity of k_n is the degeneracy of λ_n and summing over λ_n is equivalent to the summation over k_n. Since $Z(f_{\hat{K}}) \in \mathbb{R}$, the complex contour C can be chosen to be the semicircle $[-iR, iR] \cup \{z \in \mathbb{C} / \ |z| = R, \text{ and } \arg(z) \in [-\pi, \pi]\}$. Then the contour will be deformed by taking the limit $R \to \infty$. After the limit is done an expression for the spectral zeta function is obtained:

$$\zeta_{\hat{K}/\nu^2}(s) = \frac{\sin(\pi s)}{\pi} \int_0^\infty dk\, \nu^{2s} k^{-2s} \partial_k \log[f_{\hat{K}}(ik)]. \tag{1.22}$$

In this representation the information about the poles of $\zeta_{\hat{K}}(s)$ and the values at $s \in \mathbb{Z}$ is contained in

$$\frac{\sin(\pi s)}{\pi} \int_1^\infty dk\, \nu^{2s} k^{-2s}\, \partial_k \log[f_{\hat{K}}(ik)]. \tag{1.23}$$

Hence, it all reduces to study (1.23) in order to obtain the pole structure (Res) and $\zeta_{\hat{K}/\nu^2}(s \in \mathbb{Z})$. It is relevant to highlight that one needs to evaluate the zeta function at $s = -1/2$ to compute the Casimir energy from (1.21). The analytic continuation of the representation of the zeta function given in (1.22) to the left of the convergence abscissa $Re(s) < 1/2$ is achieved by subtracting an appropiate number of terms in the asymptotic expansion of the integrand, as can be seen in Section 3.1 of [39].

Notice that even for higher spatial dimensions, in many cases the Schrödinger operator is such that $\hat{K} = -\partial_\tau^2 + \hat{K}_s$, where $\hat{K}_s$ is a Laplace-type operator which does not depend on the temporal coordinate τ. When imposing periodic boundary conditions on τ, the temperature appears on

the manifold $\mathcal{M} = S^1 \times M_s$. Thus the eigenstates of $\hat{K}$ can be written as

$$\phi_{(\ell,J)}(\tau, \vec{x}) = \frac{e^{-i\xi_\ell \tau}}{\sqrt{2\pi}} \phi_J(\vec{x})$$

with $\xi_\ell = 2\pi T\ell$, $\ell \in \mathbb{Z}$ the Matsubara frequencies. Furthermore, $\beta = 1/T$ is the perimeter of the circle S^1. The one-particle frequencies of the harmonic oscillators in the associated QFT will be given by $\sqrt{\xi_\ell^2 + k_J^2 + m^2}$ being $\hat{K}_s \phi_J(\vec{x}) = k_J^2 \phi_J(\vec{x})$. Consequently, one could write the total Helmholtz free energy of the system at finite non trivial temperature as

$$\mathcal{F} = -\frac{1}{\beta} \log Z = -\frac{1}{2\beta} \zeta'_{\hat{K}/\nu^2}(0).$$

The Casimir energy at $T = 0$ will be

$$E_{Cas} = \lim_{\beta \to \infty} \mathcal{F} = \frac{\nu}{2} FP \left[\zeta_{\hat{K}_s} \left(-\frac{1}{2} \right) \right] - \frac{\nu}{4\sqrt{\pi}} a_{\frac{D}{2}}(\hat{K}_s, \mathcal{B}) \log \left(\frac{\nu e}{2} \right)^2$$

being FP the finite part of the zeta function and e the electron charge. This expression still presents divergences that have to be removed as will be explained in detail in the following chapters.

The summation over the frequency modes by using a complex contour integral would be the main result of Chapters 2 and 3.

1.4. Quantum vacuum energy in compact spaces

It is necessary to distinguish between QFT in domains with boundaries and in compact spaces, because the corresponding former spaces do not necessarily need to be compact (for instance the real line without a point is a domain with boundaries but not a compact space). Open domains with boundaries always present a continuous spectrum whereas in compact spaces there is a discrete one. In this last case, scattering processes could not always happen[31]. Thus, it would be useful to generalise the mathematical methods explained in the previous section. The self-adjoint extensions formalism makes it possible to unify both theories and to profit from the widely variety of scattering tools in theories with boundaries, without making a distinction between compact or open spaces.

For either classical and quantum theories with boundaries it is necessary to specify the behaviour of the particles or the fields in these frontiers for being able to solve the system and make physical predictions about it. There exists a crucial difference between the requirements imposed in classical mechanics, quantum mechanics and QFT with boundaries. In classical mechanics, when a free

[31] For a compact configuration of a scalar field confined between two plates mimicked by periodic or antiperiodic boundary conditions there exist two degenerated states of the same energy. An incoming dextro state in a scattering process in such a compact space could become a combination of dextro and levo wave functions. Another example of scattering in the compact space of a circle crossed by a flux is the Aharonov-Bohm effect. In this example of transparent scattering, the incoming and outgoing state is the same but the global phase acquired has a physical non trivial interpretation.

particle interacts with a plate there could be an elastic collision or the particle could be trapped by the plate. These two situations would be characterised by means of boundary conditions that inform about the physical properties of the frontiers and the way the particle interacts with them. Newton's laws and the determinism of the theory ensures the uniqueness of the solution of the equations of motion for the system once these boundary conditions are added. On the other hand, the formulations in non-relativistic quantum mechanics states that observables are given by self-adjoint operators. Furthermore, particles are interpreted as waves, enabling more complicated intermediate interactions between them and the plate or frontier. For instance, if the spectrum of the quantum Hamiltonian associated to the system has bound states, a wave packet could collide with the plate in such a way that the reflected wave's amplitude is smaller than the original one. Again, this wider range of possibilities for the interaction with the frontier is characterized by boundary conditions. Thus in quantum mechanics the preservation of unitarity implies that the Hamiltonian operator for this system with boundaries must be a self-adjoint operator. Otherwise, there will exist a non trivial probability flow $\vec{J}$ across the boundary. This can be easily seen for the simplest case of a massless particle confined between two plates (∂M) placed at $z = 0, L$. In this example, the Hamiltonian in nothing but the Laplace operator $-\partial_z^2$. One can see that if $-\partial_z^2$ is not a self-adjoint operator $\forall \psi_1, \psi_2 \in L^2_{\mathbb{C}}(\mathcal{M})$, then

$$\langle \psi_1, -\partial_z^2 \psi_2 \rangle - \langle -\partial_z^2 \psi_1, \psi_2 \rangle = -\int_0^L \psi_1^* \, \partial_z^2 \psi_2 + \int_0^L \psi_2 \, \partial_z^2 \psi_1^* = [-\psi_1^* \, \partial_z \psi_2 + \psi_2 \, \partial_z \psi_1^*]_0^L = -i \, \vec{J}\Big|_0^L ,$$
$$\int_{\partial \mathcal{M}} \vec{J} dS \neq 0. \tag{1.24}$$

Finally, as explained in previous sections, in QFT one treats with a grand canonical ensemble of particles. Preservation of unitarity in QFT implies that the Hamiltonian operator must be a non-negative self-adjoint operator. It must be self-adjoint in order for the eigenvalues to be real numbers and hence measureables. Furthermore, despite the case of quantum mechanics, in QFT the Hamiltonian must be non-negative. This is due to the fact that the presence of negative energy states in the Schrödinger problem that gives the one particle states of QFT results in an imaginary quantum vacuum energy caused by the absorption and emission of the scalar field fluctuations by the plates. This effect is the bosonic version of the Schwinger effect. In general, the presence of boundaries in a system defined in a compact space is an obstacle to the self-adjointness of the Hamiltonian operator. This motivates the study of the self-adjoint extensions of the Hamiltonian. In [34, 43, 44] a detailed explanation of this problem is presented. The main ideas are assembled hereafter.

Consider again a free massless complex scalar field ϕ (it can be easily generalised to massless fermions and gauge theories) confined in a domain $\Omega \in R^{D+1}$ bounded by two D-dimensional, parallel, isotropic and homogeneous plates orthogonal to the z axis and placed at $z = 0, L$. Following the Asorey-Ibort-Marmo formalism [109], the properties of the plates can be characterised through 2×2 unitary matrices $U \subset U(2)$ parametrised in the usual way as:

$$U(\alpha, \theta, \vec{n}) = e^{i\alpha}[\mathbb{1}_2 \cos\theta + i(\vec{n}\,\vec{\sigma}) \sin\theta], \qquad \begin{cases} \alpha \in [0, \pi] \\ \theta \in [-\pi/2, \pi/2] \end{cases}, \tag{1.25}$$

where $\vec{n}$ is a 3-dimensional unit vector and $\vec{\sigma}$ the Pauli matrices. As previously mentioned, the equation of the modes of the quantum scalar field is given by (1.6) and the Hamiltonian describes an infinite collection of non-interacting harmonic oscillators whose frequencies are given by the Fourier modes of the Laplace Beltrami operator. In order to preserve the unitarity of the QFT, the Laplace Beltrami operator must be self-adjoint and non-negative[32]. Due to the homogeneity and isotropy of the plates the Laplacian over the dimensions parallel to the plates, $-\triangle_{\parallel}$ is self-adjoint but $-\partial_z^2$ in the finite interval $[0, L]$ is not essentially self-adjoint in the domain $L^2_{\mathbb{C}}([0, L])$ due to the existence of a non zero probability flow $\vec{J}$ across the boundaries. By defining two vectors in $\mathbb{C}^2$ associated to the restrictions that the boundaries impose over the wave functions:

$$\Phi_{\pm}(\varphi) = \begin{pmatrix} \varphi(0) \mp ia\varphi'(0) \\ \varphi(L) \pm ia\varphi'(L) \end{pmatrix}, \qquad \varphi \in L^2_{\mathbb{C}}([0, L])$$

(where a is a length parameter related to the electromagnetic properties of the plates), and by considering the usual scalar product, it is possible to rewrite the non trivial flow in (1.24) as the following degenerate quadratic form

$$\vec{J} = \frac{1}{2}[\Phi^{\dagger}_{-}(\phi_1)\Phi_{-}(\phi_2) - \Phi^{\dagger}_{+}(\phi_1)\Phi_{+}(\phi_2)]. \tag{1.26}$$

Notice that if $\Phi_{\pm}$ are isotropic with respect to this bilineal form, there exists $U \in U(2)$ relating both vectors enabling to cancel $\vec{J}$. So although whenever $\vec{J} \neq 0$ the Hamiltonian is not essentially self-adjoint in $L^2_{\mathbb{C}}([0, L])$, there exists an infinite collection of non negative self-adjoint extensions (i.e. an infinite set of QFTs that describe the behaviour of this field). They are in one-to-one correspondence with the unitary matrices of boundary conditions U that mimic the plates. The domain of fields that cancels the probability flow across the boundaries and characterises the self-adjoint extensions of the Laplacian operator is given by:

$$\mathcal{D}_U = \{\phi \in W^2_2([0, L], \mathbb{C}) \quad | \quad \Phi_{-}(\phi) = U\Phi_{+}(\phi)\}, \tag{1.27}$$

being $W^2_2([0, L], \mathbb{C})$ the Sobolev space of functions over the finite interval that are L^2 together with their derivatives up to second order. From the geometrical point of view which relates the flow with a degenerate form, the self-adjoint extensions are the subspaces of isotropy of (1.26). Consequently, this point of view allows to interpret the self-adjoint extensions in terms of quantities (boundary values) with physical meaning. This is not the case when using the standard formalism of deficiency indices and subspaces [110].

Moreover, apart from the self-adjointness previously explained, non-negativity of the Laplace-Beltrami operator in the domain Ω is also required[33], giving rise to a relation between some of the

[32] For the temporal evolution operator $e^{it\hat{H}}$ to be unitary and for the amplitude of probability of a process to be preserved, $\hat{H} = \hat{H}^{\dagger}$ must be fulfilled and hence $\langle \psi_1, -\partial_z^2\psi_2\rangle = \langle -\partial_z^2\psi_1, \psi_2\rangle$ for all $\psi \in W^2_2([0, L], \mathbb{C})$.

[33] Notice that those boundary conditions for which bounded states arise in the quantum mechanics theory associated to the QFT must be forbidden. Otherwise, the vacuum energy becomes imaginary, representing an instability in the theory related to the production of particle-antiparticle pairs.

parameters of the boundary conditions. In this way, the space of boundary conditions giving rise to non-negative self-adjoint extensions $-\Delta_U$ of the $-\partial_z^2$ operator in the finite interval $[0, L]$ for any finite value of the distance between plates L, and the subspace of non-negative self-adjoint extensions with a constant zero-mode can be defined respectively as

$$\mathcal{M}_F \equiv \{U(\alpha,\theta,\vec{n}) \in U(2) \quad | \quad 0 \leq \alpha \pm \theta \leq \pi\},$$
$$\mathcal{M}_F^{(0)} \equiv \{U(\alpha,\theta,\vec{n}) \in \mathcal{M}_F \quad | \quad n_1 = \pm 1,\ \theta = -n_1\alpha\}.$$

A plot of these spaces in the boundary condition parameters plane is shown in Figure 1.3.

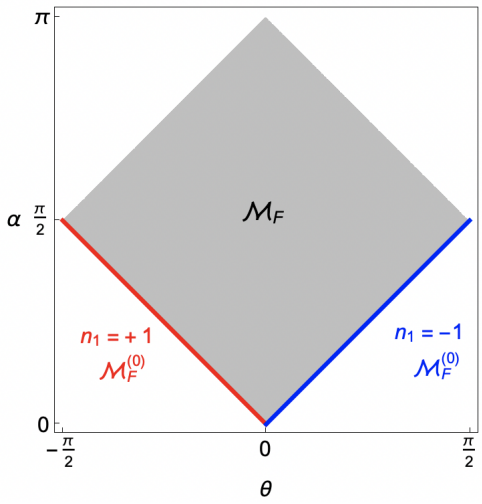

FIGURE 1.3: $\mathcal{M}_F$ and $\mathcal{M}_F^{(0)}$ in the α-θ plane [43]. The most common boundary conditions are Dirichlet (top corner of the rhombus), Neumann (bottom corner of the rhombus), periodic (left corner for $n_1 = 1$ and right corner for $n_1 = -1$) and antiperiodic ones (left corner for $n_1 = -1$ and right corner for $n_1 = 1$). Notice that since $U(\alpha,\theta,n) = U(\alpha,-\theta,-n)$, the two edges of the rhombus that constitute $\mathcal{M}_F^{(0)}$ represent the same self-adjoint extensions.

The boundary conditions such that $\alpha + \theta = 0$ contain topology changes and variations in the properties of the plates. One can go from a theory of two separated plates ($\alpha = \theta = 0$) to only one circular single plate ($\alpha = -\theta = \pi/2$), passing through intermediate situations similar to what happens in a Josephson junction. This effect occurs when two superconductors are placed very close to each other but with some barrier or insulator between them. In spite of this barrier, a current continuously flows between the superconductors although any voltage is applied. Returning to the present case of a scalar field confined in the interval $[0, L]$, the two plates placed at the extremal points of the interval $[0, L]$ for $\alpha = \theta = 0$ flows as $\alpha = -\theta \to \pi/2$ to a single quasi cylindrical surface in which the ends of the circle in the base of the cylinder are almost joined (the base of the cylinder is a horseshoe-shaped). Here, a non trivial probability current flows across these two edges.

Finally, it is interesting to study what happens outside the rhombus. Moving from boundary conditions outside the rhombus (i.e. those with negative energy states for some value of L) to $\mathcal{M}_F^{(0)}$ requires a finite amount of energy. The negative energy states transform into the zero mode making it to be degenerated. On the contrary, moving from boundary conditions outside the rhombus to its

edges without zero modes requires an infinite amount of energy. The corresponding work presented in this thesis will be focused only on boundary conditions in $\mathcal{M}_F$ and $\mathcal{M}_F^{(0)}$.

Computing the Casimir energy goes through the summation of the spectrum of the self-adjoint extension $-\Delta_U \in \mathcal{M}_F$. Since $[0, L]$ is a compact domain, the spectrum of $-\Delta_U$ is discrete. It takes real values. This spectrum can be studied through the zeroes of the following secular equation:

$$h_U(k) = 2ie^{i\alpha}[-2ka\cos(kL)\sin\alpha - 2ka\, n_1 \sin\theta + \sin(kL)[(k^2a^2-1)\cos\theta + (k^2a^2+1)\cos\alpha]] = i[(k^2a^2+1)(1+\det U) + (k^2a^2-1)\mathrm{tr}\, U]\sin(kL) - 2ka(U_{12}+U_{21}) - 2ka(-1+\det U)\cos(kL). \quad (1.28)$$

Since $\lim_{k\to 0} h_U(k) = 0$, this function does not inform about the contribution of the zero-modes. Hence, it is better to substitute it by the following ones [43]

- If $-\Delta_U \in \mathcal{M}_F$ then $h_U(k)$ should be replaced by $f_U(k) = \frac{h_U(k)}{k}$,
- If $-\Delta_U \in \mathcal{M}_F^{(0)}$ then $h_U(k)$ should be replaced by $f_U^{(0)}(k) = \frac{h_U(k)}{k^3}$,

which only have zeroes in $\mathbb{R} - \{0\}$ and then introduce the contribution of the zero modes independently *ad hoc*. The summation over zeros can be rewritten in terms of an contour integral enclosing all the zeros of h_U by using the Cauchy's theorem in a similar way that the one introduced in the previous section. Again, the leading divergence of the vacuum energy induced from fluctuations of the fields in the bulk and the subleading divergent contribution associated with the self-energy of the infinitely large plates must be subtracted to obtain the finite result. This would be longer explained in the following chapter but it is worth mentioning that, according to [34], the finite Casimir energy (once regularised the ultraviolet divergences) for spaces of D dimensions apart from the temporal one is proportional to:

$$\frac{E_U^L}{S} \propto \frac{L_0^D}{L^D - L_0^D}\int_0^\infty dk\, k^D \left[L - L_0 - \frac{d}{dk}\log\left(\frac{h_U^{(L)}(ik)}{h_U^{(L_0)}(ik)}\right)\right], \quad (1.29)$$

being S the infinite volume of the plates and L_0 a fixed regularisation length such that $L_0 < L$.

Aditionally, in [43] all the coefficients in the asymptotic expansion of the heat kernel corresponding to any self-adjoint extension $-\Delta_U \in \mathcal{M}_F$ are computed analytically and compared with the known results for the most common boundary conditions (periodic, Dirichlet, Robin and Neumann). Furthermore, in [34] the authors analyse with complete generality which boundary conditions give rise to attractive, repulsive and null Casimir forces in the system for various dimensions. In three spatial dimensions, apart from the most common boundary conditions aforementioned, the authors also study in detail anti periodic, Zaremba, quasi-periodic and pseudo-periodic boundary conditions.

1.5. Quantum vacuum interactions between kinks

Apart from plates, other types of extended objects like lattices or domain walls will appear through this thesis[34]. This section will introduce one kind of extended object that will play a central role further on: the so called kink, or more generally, soliton. Firstly, a discussion concerning the differences between solitary waves, solitons and topological solitons is going to be presented.

There are several seminal references about classical solitons and solitary waves [8, 111–113]. Historically, the first mention of classical solitary waves travelling without changing its size, shape or speed dates back to 1834 thanks to the observation of such a wave in a channel of Edinburgh by S. Russell [114]. Around 1900, D. Korteweg and H. de Vries introduced a non-linear partial differential equation in which the non linearity balances the dispersive character of the equation [115]. Their equation

$$\partial_t \varphi(t,z) + \partial_z^3 \varphi(t,z) - 6\varphi(t,z)\partial_z \varphi(t,z) = 0,$$

has a solitary wave as a solution. It was not until 1965 that N. Zabusky and M. Kruskal, besides others, completely solved the KdV-equation [116]. From then on, solitary waves have been proved to be solutions of the nonlinear Schrödinger equations for several solvable models in non linear optics [117] or solutions of the Gross–Pitaevskii equation in Bose-Einstein condensates [118], to cite just a couple of examples.

An unexpected property of solitons is that they survive collisions without being affected[35]. The addition of this new property regarding collisions to the one related to the shape and velocity conservation of the wave packet, allows to distinguish between solitons (when the two properties are present) and solitary waves (when only the second one appears). In [52] both non dissipative solutions are called energy lumps. Some of the most relevant examples of solitons are: the sine-Gordon *kink* in 1+1 dimensions, the characteristic *vortices* in the Abelian Higgs model in 2+1 dimensions and the t'Hooft-Polyakov *monopole* in non abelian gauge theories in 3+1 dimensions. Anyway, one could completely define a soliton as a finite-energy propagating solution[36] of a non linear theory of fields, with an energy density $\epsilon(t,\vec{x}) = \epsilon(\vec{x} - \vec{u}t)$ localised in space for finite times. This means that the energy density is not distorted while moving in the space with speed $\vec{u}$. Furthermore, the asymptotical values of $\epsilon(t,\vec{x})$ must be the same as the initial ones even after collisions of several solitary waves. If the soliton is a solution of nonlinear field equations in 1+1 dimensions (only for simplicity), the requirement of localised finite energy for the field implies that

$$\lim_{z\to\pm\infty} \phi(t,z) = \phi(t,\pm\infty) = \phi^{\pm}, \qquad \text{and} \qquad \lim_{z\to\pm\infty} \partial_\mu \phi(t,z) = 0,$$

[34] An extended object $\mathcal{N}$ embedded in a manifold $\mathcal{M}$ is a sub variety with co-dimension different from the dimension of the manifold, i.e. $\dim(\mathcal{M}) - \dim(\mathcal{N}) \neq \dim(\mathcal{M})$.

[35] Note that the phase shift in the relative position of the two waves that appears as the sole residual effect of the interaction is not possible for waves satisfying linear equations.

[36] A localised solution is the one whose energy density is finite in any finite region of the space and that vanishes fast enough in the limit $x \to \infty$ so as to be integrable.

with $\phi^{\pm}$ the configurations in which there is an absolute minimum of the potential in the theory. An example of soliton is the Q-ball[37] [119] arising in bosonic theories.

Topological solitons are another special type of solitary waves. They are solutions of the classical equations of fields that spontaneously break the translational symmetry in QFTs whose configurational spaces are the sum of several topologically disconnected subspaces. For instance, spontaneous symmetry breaking causes the appearance of non trivial topological sectors but it is not the only possible scenario. Anyway, field configurations in different topological sectors cannot evolve into each other without violating the finite energy condition. In 1+1 dimensional theories, since $\phi^{\pm}$ define a set of topological stationary indices for classifying the topological sectors[38], one could define a topological charge as $Q \propto \phi^{+} - \phi^{-}$. For higher dimensional spaces there exist other topological quantities such as the winding number defining topological charges but a more detailed discussion of the issue is not necessary here in order to understand the idea to be conveyed. The important thing is that once defined the topological charge, if $Q \neq 0$ the solitary wave is topological, otherwise non-topological. If the potential has only one minimum, the field asymptotically converges to the same value and hence $Q = 0$. But if the potential is degenerated, i.e. it has several minima, it is also possible to have different asymptotic values as happens for the kink in the $\lambda(\phi^2 - \mu^2/\lambda)^2$ theory. Topological solitons asymptotically connect states of different topological sectors.

Topological defects are classical solutions and it is also possible to study small fluctuations around the absolute minima of the energy in each topological sector [113], in a similar way to the one explained in previous sections. The spacetime in which topological defects live determines when a given topological defect is a domain wall (surface defect), string (line defect), particle (point defect) or texture (instanton). Several physical models have topological defects as their main solution to describe the fundamental particle interactions. For instance, the Skyrme model describes baryons as quantum solitons (called skyrmions) whose classical limit are topological defects of the associated field theories, whereas mesons are the fluctuations of the field around these solitons. Some well-known equations as the non-linear Schrödinger equation (present in non-linear optics) and the sine-Gordon equation (relevant for instance in the Josephson effect in semiconductors) have topological solitons in their space of solutions.

Because of its importance in several chapters of this thesis, a little more will be said below about sine-Gordon's kink. The action of the sine-Gordon 1+1 dimensional classical theory of fields in terms of non-dimensional fields and coordinate variables takes the form

$$S[\phi] = \frac{m^2}{\lambda} \int dt\, dz \left(\frac{1}{2} \partial_\mu \phi \partial^\mu \phi + (-1 + \cos\phi) \right).$$

The Lagrangian is invariant under the discrete transformations $\phi \to -\phi$ and $\phi \to \phi + 2\pi n$, $n \in \mathbb{R}$. Both of them are spontaneously broken when choosing a specific minimum of the vacua orbit. The

[37] A Q-ball is a finite-sized, drop-like cluster of bosonic particles which is stable against fission into smaller drops and against evaporation into individual particles. This object is stable because due to the attraction between particles, it is the lowest energy configuration of that number of particles. This number would be a conserved charge.

[38] It is important to note that the conserved topological indices in the theory come from the finite energy condition and not from a continuous symmetry.

infinite set of minima of the potential is $\phi_n = 2\pi n$, $n \in \mathbb{Z}$. Apart from $\{\phi_n\}$ there is another type of solutions of the corresponding equation of motion which are called static kink $\phi_{kink}(z)$ and antikink $\phi_{\overline{kink}}(z)$:

$$\partial_\mu \partial^\mu \phi + \sin\phi = 0, \qquad \rightarrow \qquad \phi_{kink}(z) = 4\arctan e^z, \qquad \phi_{\overline{kink}}(z) = 4\arctan e^{-z}.$$

They are homotopically different from the trivial vacua solutions $\{\phi_n\}$. It is worth noting that since $\phi(z \to \pm\infty) = 2\pi n_\pm$, these two numbers $\{n_+, n_-\}$ are the characteristic topological indices of each topological sector. The sine-Gordon kink and antikink connect different neighbouring minima ϕ_n and their topological charge is $Q = \pm 1$ respectively. Performing the usual Lorentz-boost by means of $z \to (z - vt)/\sqrt{1 - v^2}$ yields the moving solitons with speed v.

The behaviour of classical topological solitons and its quantisation in QFT have intensively taken place during the last decades [120, 121]. For the sine-Gordon theory there are some relevant differences when studying small fluctuations $\eta(t, z)$ around a classical solution either in the trivial vacuum sector and in the kink one [122]. They are summarised in Table 1.1:

	TRIVIAL SECTOR	**KINK SECTOR**
Vacuum state	ϕ_n Translational invariant	$\phi_{kink}(z)$ No translational invariant
Classical energy of the vacuum state	$E[\phi_n] = 0$	$E[\phi_{kink}] = 8m^3/\lambda \neq 0$
E.o.m. for the fluctuations up to second order	$[\partial_\mu\partial^\mu + 1]\eta(x^\mu) = 0$	$[\partial_\mu\partial^\mu + 1 - \frac{2}{\cosh^2(z)}]\eta(x^\mu) = 0$
Canonical commutation relations at $t = t'$	$[\eta(x), \dot\eta(x')] = i\frac{\lambda}{m^2}\delta(x - x')$, $[\eta(x), \eta(x')] = 0$, $[\dot\eta(x), \dot\eta(x')] = 0$	
Schrödinger problem for the fluctuations	$\hat K_0\, h_n(z) = \omega^2(k_n) h_n(z)$	$\hat K f_k(z) = \omega^2(k) f_k(z)$
Fluctuations field $\eta(t, z)$	$h_n(z)$ are plane waves	$f_k(z)$ are Pöschl-Teller waves
Canonical quantisation relations	$[a(k_n), a^\dagger(k_m)] = \delta_{mn}$ $[a(k_n), a(k_m)] = 0$ $[a^\dagger(k_n), a^\dagger(k_m)] = 0$	$[A(\tilde k_n), A^\dagger(\tilde k_m)] = \delta_{mn}$ $[A(\tilde k_n), A(\tilde k_m)] = 0$ $[A^\dagger(\tilde k_n), A^\dagger(\tilde k_m)] = 0$
Hamiltonian	$\sum_{k_n} \omega(k_n) \left[a^\dagger(k_n) a(k_n) + \frac{1}{2}\right]$	$\sum_{\tilde k_n} \omega(\tilde k_n) \left[A^\dagger(\tilde k_n) A(\tilde k_n) + \frac{1}{2}\right]$

TABLE 1.1: Differences between working on the trivial and the kink sector in the sine-Gordon theory in 1+1 dimensional theories. Notice that in the canonical commutations relations, the notation $x \equiv x^\mu = (t, z)$ has been used just for simplifying the equations.

On the one hand, the fluctuation field in the trivial vacuum sector can be written as a superposition of plane waves as

$$\eta(t,z)=\sum_{k_n}\frac{1}{\sqrt{w(k_n)}}\left[a(k_n)e^{-ik_\mu x^\mu}+a^\dagger(k_n)e^{ik_\mu x^\mu}\right],\qquad k_n\in\sigma^*(\hat{K}_0=-\partial_z^2+1).$$

On the other hand, the fluctuation field in the kink sector can be written as a superposition of plane waves as

$$\eta(t,z)=\sum_{\tilde{k}_n}\frac{1}{\sqrt{w(\tilde{k}_n)}}\left[A(\tilde{k}_n)e^{-i\omega(\tilde{k}_n)t}f_{\tilde{k}_n}(z)+A^\dagger(\tilde{k}_n)e^{i\omega(\tilde{k}_n)t}f^*_{\tilde{k}_n}(z)\right],\qquad \tilde{k}_n\in\sigma^*(\hat{K}=-\partial_z^2+1-2\,\mathrm{sech}^2(z)).$$

Just as there exists a Casimir effect between conducting plates, there is also a quantum vacuum effect due to the vacuum fluctuations of quantum fields when they are coupled to the background of a single topological soliton. In fact, there is a quantum correction to its rest mass or total energy, which was firstly calculated in 1974 up to one-loop order by Dashen-Hasslacher-Neveu [123, 124]. The authors claimed that the static soliton behaves as a particle with mass

$$M_{kink}=\frac{8m^3}{\lambda}-\frac{m}{\pi},$$

where the first term is the classical mass and the second term is the contribution of the small fluctuations developed up to second order around the classical solution. For several kinks, their common mass receives similar corrections [120]. In these multikinks systems, the vacuum interaction energy between them is still divergent due to the dominant contribution of the density energy of the theory in the bulk. However, since the surface of the kink is finite, there is no subdominant divergence in this case. In fact, this term is the quantum correction to the mass above mentioned. Dominant or subdominant divergence refers to the degree of ultraviolet divergence of the two terms[39]. In Chapter 4 the vacuum energy of a scalar field confined between two plates mimicked by δ-δ' potentials in the smooth curved background of a sine-Gordon kink will be computed.

Notice that similarly to the Casimir effect for conductors, where there is no classical force between the objects, there is neither a classical force between several kinks in the Bogomol'nyi-Prasad-Sommerfield (BPS) limit[40]. In this situation there are two kinks with different centres of mass separated by a large distance in such a way that there is a negligible coupling between them. This means that both kinks can be represented by two potentials with non intersecting compact support. Hence, the solution of the whole system, which is rather complicated to solved analytically, can be well approximated by the summation of the solutions for each soliton separately. This method facilitates the

[39] In [34] it is shown that for the system of a scalar field confined between two plates, the dominant divergence is a term proportional to the energy raised to the power $(D+1)/2$ with D being the spatial dimension of the theory, and the subdominant as the energy raised to $D/2$. Both terms are divergent in the ultraviolet regime. Whilst the former is associated to the density energy of the free theory in the bulk, the latter is due to the self-energy of infinite area plates.

[40] In [96] it has been stated that the classical force between two kinks represented by potentials which do overlap behaves as $E_{classical}(\phi_{kink},\phi_{kink})\propto 32\,e^{-d}$ being d the distance between kinks. Hence, whenever d becomes larger that the size of the kinks and the potentials reach their asymptotic values exponentially so fast that the overlap becomes really small, the classical force could be taken as zero.

computation of the distance-dependent terms of the one loop quantum correction to the energy between two kinks and consequently, the quantum force between them. The non-existence of a classical force between kinks in the BPS limit is the reason that there have not been empirical observations of such extended objects in nature. Accordingly, the computation of the quantum force is relevant as a way to study the stability of these systems. For instance, if the quantum force between some solitons is repulsive, they will not come close to annihilate each other and subsequently decay to the trivial vacuum in their topological sector, so they could finally been observed.

Before finishing this section it is worth mentioning that multikinks theory is essential to deal with the multiple instantons' solutions which describe the vacuum state of quantum chromodynamics. QCD is a relativistic QFT which describes the strong interaction in the Standard Model. The interest here is that the action contains a special theta term of the form $S_\theta = \theta \cdot Q$, where the integer Q represents a topological charge and θ is a constant bounded by the value $1.97 \cdot 10^{-10}$. This term theoretically breaks the $\mathcal{CP}$ symmetry although this fact has never been observed for strong interactions in nature. This apparent contradiction is still unsolved ($\mathcal{CP}$ problem). A way to solve it would be the introduction of an additional global $U(1)$ symmetry in the theory that would eventually be spontaneously broken by a scalar field [125]. The particle playing the role of the Nambu-Goldstone boson of the theory would be the axion [126] but it has never been detected so far. The theta term arises as a consequence of the complex topological structure of the vacuum in the theory [127, 128]. In fact it can be thought as a superposition of an infinite number of topologically different classical vacua classified by a winding number often referred as *Chern-Simons characteristic*. The different vacua are connected via quantum tunneling by fields with non trivial topological charge called instantons [129] at zero temperature and calorons at finite one. The instantons are solutions of the equations of motion $D_\mu F_{\mu\nu} = 0$ and they constitute topological fluctuations of the gauge fields of the model. Hence, one could perturbatively analyse the fluctuations around the classical local minima in a similar way as the one explained in Section 1.2 and study the BPS limit or semiclassical approximation of the QCD vacuum. In this specific limit, the approximate ground state of the theory is a dilute non-interacting instantons' gas [130, 131] although to date it is not known how these instantons are distributed (as an irregular or regular lattice or in another completely different way). But what is known is that they are instantonic solutions (i.e. Wick rotated topological solitons) so that it is another interesting reason for studying the theory of topological solitons.

1.6. Thesis structure

Having presented the main ideas which motivate this thesis, the original content of each of the subsequent chapters is the following one:

- In Chapter 2 the study of the quantum vacuum energy of a scalar massless quantum field confined between two parallel, isotropic, two dimensional and homogeneous plates will be carried out. Such plates will be represented by the most general kind of boundary conditions allowed by the requirement of unitarity in Quantum Field Theory. Firstly, the Casimir energy

of the aforementioned 3+1 dimensional system at zero temperature will be computed. This quantity was already studied in [34] but the novelty presenting in this thesis is the derivation of a more general formula independent of regularisation lengths. Then a new method based on complex analysis for computing thermodynamic quantities such as the one loop quantum corrections to the Helmholtz free energy, the entropy and the Casimir pressure between plates at finite non zero temperature will be advanced.

- In Chapter 3 the new method presented in the previous one will be applied to treat the system of a non interacting scalar field propagating in a one-dimensional lattice. This structure will be mimicked by a periodic potential built from an infinite array of identical individual potentials with compact support. In particular, two examples of crystals will be presented: one built from the repetition of Pöschl-Teller truncated potentials and the other one will be a chain of Dirac delta functions. The new method presented in this chapter enables to interpret the quantum vacuum energy at zero temperature as the one loop quantum corrections to the frequencies of the phonons due to the vibrations of the crystal lattice. This innovative interpretation makes it possible to see that phonons propagating in one squared lattice in two dimensions with Bloch periodicity in its edges and a scalar field moving on the surface of a torus traversed by a magnetic flux (in a similar way that the one present in the Aharonov-Bohm effect) are essentially the same. The band structure of the lattices will be fully established. Moreover, the main thermodynamics of these systems at finite non zero temperature will be analysed. Finally, a generalisation of this study to three spatial dimensional lattices will be provided. All the aforementioned computations are original work.

  This problem is also intriguing for another reason. The study of the one loop quantum corrections to the frequencies of the phonons propagating in crystal lattices can be used to discern the stability of some hypothetical solutions for the vacuum state in quantum chromodynamics. Whenever one could find theories in which the coupling between the fluctuations of the axions and the QCD vacuum state be enough properly analytically mimicked, the methods provided in this chapter could help.

- In Chapter 4 the main focus of attention is the study of the quantum vacuum interaction between objects described by singular potentials with compact support in three spatial dimensions in interaction with classical curved backgrounds. More concretely, the Casimir effect between two semitransparent plates represented by Dirac δ potentials in the topological background of a sine-Gordon kink will be treated. The quantum vacuum oscillations around the sine-Gordon kink solution could be interpreted as a scalar QFT in the spacetime of a domain wall. The Green's function and the Lippmann-Schwinger operator will be computed both analytically and numerically to obtain the generalisation of the *TGTG* formula for curved backgrounds. All the results presented in this chapter are original work, not previously published in the literature on this subject.

- In Chapter 5 the bound and scattering states that form the one-particle spectrum for fermions moving in the one dimensional real line in the presence of impurities that disrupt their free

propagation will be analysed. The impurities will be implemented by means of δ-function potentials. This problem has not been solved so far in the literature. The interest lies in the future generalisation of this calculations to an infinity array of δ-impurities (often called δ-comb potential) since this periodic potential arises in several material models. The novelty in this chapter is that the problem of determining the spinor field fluctuations in the static δ background is going to be adressed by solving at the same time the spectral problem of either the Dirac Hamiltonian and its conjugate in one-dimensional relativistic quantum mechanics. The eigenspinors of both Hamiltonians are going to be thus interpreted as the one particle states to be occupied by electrons and positrons respectively after the fermionic second quantisation procedure be implemented. The spectrum of the fluctuations is going to be analysed for a generic single and double δ-potential and it is going to be particularised to a pure electric δ-potential and a pure mass-like one. This study will lead to the novel conclusion that the biparametric family of double δ-potential theories in the electric case is related to a subset of the moduli of complex tori. Since a complex torus is homeomorphic to $\mathbb{C}/L(a_1, a_2)$ being $L(a_1, a_2)$ a squared lattice generated by $a_1, a_2 \in \mathbb{R}$ one could apply the innovative interpretation given in Chapter 3 and relate fermions propagating in one squared lattice in two dimensions with the Aharonov-Bohm effect present when a field moves on the surface of a torus traversed by a magnetic flux. Original work will also be carried out to study which boundary condition matrices given by the definition of the δ potential are unitary and therefore amenable to the procedure presented in [45] for calculating the spectral function and vacuum energy of the corresponding problem of fermions confined in a finite interval.

- In Chapter 6 the central conclusions of the work carried out in this thesis will be summarised and some open problems which are left for further future investigation will be stated.

Chapter 2

SCALAR FIELDS BETWEEN PLATES

Most of the results concerning the dynamic properties of quantum scalar fields follow a semi-classical approach and they do not take into account expansions up to one-loop order of the related Quantum Field Theory. The main objective of this chapter is to study the one-loop quantum corrections for the system of a scalar field confined between a pair of two-dimensional plates due to the quantum fluctuations of the scalar field. Hence, a 3+1 dimensional QFT is the focus of the following sections. A semi-analytical method will be developed to calculate the quantum vacuum energy of the scalar field at zero temperature as well as other thermodynamic quantities of great interest at finite temperature (Helmholtz free energy, entropy and Casimir force).

As previously explained in the last chapter, the Casimir force between plates is due to the coupling between the quantum vacuum fluctuations of the electromagnetic field with the charged current fluctuations of the plates [17]. For distances between plates rather larger than any other lenght scale concerning the electric response of the plates, only the long wavelenght transverse modes of the electromagnetic field are relevant to the interaction. They can be mimicked by the normal modes of a scalar field as stated in (1.6) following [36].

In this chapter the plates that confine the scalar field are mimicked by the most general dispersionless and frequency-independent boundary condictions mimicking constant permitivities and permeabilities of lossless plates. For an ideal conductor (the permittivity tends to infinity) the transverse electric and magnetic modes satisfy Dirichlet $U = -\mathbb{1}_2$ and Neumann boundary conditions $U = \mathbb{1}_2$, respectively. In the case where the permeability tends to infinity, the transverse electric modes satisfy Neumann boundary condition meanwhile the transverse magnetic modes verify Dirichlet boundary condition. Generally, in realistic materials the response of the plates depend on the frequency as well as on the parallel components of the momentum of the field modes (one example is given in [132] for the case in which the effective coupling between the plates and the electromagnetic field involves the integration of the electron Dirac field in the graphene plates), but in this chapter only isotropic and homogeneous plates will be studied.

2.1. Vacuum energy at zero temperature

The quantum vacuum energy per unit area between two parallel, isotropic and homogenous plates mimicked by the most general lossless and frequency independent boundary conditions allowed by the unitarity of the QFT was studied by Asorey and Muñoz Castañeda in [34] and it is given by equation (1.29). The intermediate steps that yield this closed formula can be found in [34] but the idea can be easily explained in a summarised form. Firstly, the heat equation kernel method is used to regularise the summation over the eigenvalues of the self-adjoint extension related to the boundary conditions given by the U matrix. Hence, the regularised vacuum energy takes the form

$$E_U^\epsilon = \operatorname{tr} \sqrt{-\triangle_U}\, e^{-\epsilon \triangle_U},$$

being ϵ the ultraviolet regularisation parameter (at the end the limit $\epsilon \to 0$ must be considered to obtain the vacuum energy). Then, by using generalised spherical coordinates, the confluent hypergeometric function $\mathcal{U}(a, b, \mathrm{z})$ and the Cauchy's residues theorem, the authors write the regularised vacuum energy as

$$E_U^\epsilon = \frac{1}{2\pi i} \oint_\Gamma dk\, k\, e^{-\epsilon k^2}\, \mathcal{U}\left(\frac{D-1}{2}, \frac{D}{2}+1, \epsilon k^2\right) \frac{d}{dk} \log h_U(k),$$

with Γ a contour enclosing a thin strip around all the positive real axis which includes all the zeroes of the spectral function (1.28). Since in the limit $\epsilon \to 0$ the expression diverges the authors need to subtract the ultraviolet divergences. They finally use the different asymptotic behaviours of the confluent hypergeometric function in the integrand when considering an odd or even dimension D for the spaces to obtain formula (1.29).

Subtracting the ultraviolet divergences requires some clarity on a couple of points. The summation over the spectrum of modes

$$\sum_{\omega^2 \in \sigma(-\Delta_U)} \omega = \sum_{\sigma(-\Delta_U)} \sqrt{\vec{k}_\parallel^2 + k^2} \;\propto\; -\frac{1}{A} \int_0^\infty dk\, k^D\, \partial_k \log h_U(ik, L) \tag{2.1}$$

has several different divergences. The dominant one is the contribution of the energy density of the field theory in the bulk (in this case the space between plates, which is proportional to $L \times A$ being A the area of the plates), which does not depend on the boundary conditions. Hence, first of all it is necessary to subtract it. But the arising result involving the integration of $L - \partial_k \log h_U(ik, L)$ is still divergent due to the surface density energy associated to the plates. Consequently, one should use a regularisation length L_0 to subtract the subdominant divergence which does depend on the boundary conditions. The resulting integral of $L - \partial_k \log h_U(ik, L) - L_0 + \partial_k \log h_U(ik, L_0)$ is finite. Notice that L_0 must be subtracted in the previous expression in order to remove the dominant contribution that one introduces when adding $\partial_k \log h_U(ik, L_0)$.

Nevertheless, equation (1.29) is restricted to cases in which there are no background potentials between plates. A significant headway would be to extend this formula to cases in which there is a

potential of compact support between plates because this situation applies to a large number of situations as the ones studied in Chapters 3 and 4. In this kind of physical situations, the operator of the action that characterises the normal modes of the quantum scalar field between $(D-1)$-dimensional plates (splitting the spatial coordinates[1] as $\boldsymbol{x}=(\boldsymbol{y}_{\parallel},z)$ with $y_{\parallel}\in\mathbb{R}^{D-1}$ and $z\in[0,L]$), placed generically at $z=0,L$, is given by:

$$\hat{K}=-\frac{d^2}{dz^2}+V(z),\qquad z\in[0,L],$$

provided that the potential $V(z)$ does not have bound states.

To achieve the aforementioned goal of obtaining a more simplified expresion of the quantum vacuum energy, the regularisation length is going to be removed by taking the limit $L_0\to\infty$ in (1.29) or, what is the same, by studying the asymptotics of $-L_0+\partial_k\log h_U(ik,L_0)$ as $L_0\to\infty$. Before doing that it is useful to rewrite $h_U(ik,L_0)$ in a more convenient form[2]

$$h_U(ik,L_0)=-2ik[-1+\det(U)]\frac{e^{-kL_0}+e^{kL_0}}{2}+i\frac{e^{-kL_0}-e^{kL_0}}{2i}[(1-k^2)\det(U)-(k^2+1)\mathrm{tr}(U)]$$
$$-2ik(U_{12}+U_{21})=\frac{1}{2}e^{kL_0}(k-i)^2\left[\left(\frac{k+i}{k-i}\right)^2+\left(\frac{k+i}{k-i}\right)\mathrm{tr}(U)+\det(U)\right]+\mathcal{O}(e^{-kL_0}).$$

The aforementioned desired limit is

$$\lim_{L_0\to\infty}\left(-L_0+\frac{d}{dk}\log h_U(ik,L_0)\right)=\lim_{L_0\to\infty}\left(-L_0+\frac{d}{dk}\log e^{kL_0}+\frac{d}{dk}\log\left(\frac{1}{2}(k-i)^2c_U\left(-\frac{k+i}{k-i}\right)\right)\right.$$
$$\left.+\frac{d}{dk}\log\mathcal{O}(e^{-kL_0})\right)=\frac{d}{dk}\log\left(\frac{1}{2}(k-i)^2c_U\left(-\frac{k+i}{k-i}\right)\right)=\frac{d}{dk}\log h_U^{\infty}(ik),$$

where $c_U(\mathrm{z})\equiv\det(U)-\mathrm{tr(U)z}+\mathrm{z}^2=\det(\mathrm{z}-U)$ is the characteristic polynomial of the boundary condition matrix that mimics the plates. It is worth stressing that the asymptotics of the spectral function as the regularisation length goes to infinity only depend on algebraic invariants of the boundary condition matrix. Thus, the boundary conditions vary under changes of basis whereas the subdominant divergences remain unaffected. Since the subdominant divergences only depends on algebraic invariants of the U matrix, all the theories in which the corresponding U matrices have the same characteristic polynomial are going to present the same subdominant divergences.

Taking into account the previous results, the regularised Casimir energy per unit area A of the plates can be rewritten as follows:

$$\frac{E^{(D)}(U)}{A}=-w(D)\int_0^{\infty}dk\,k^D\left[L-\frac{d}{dk}\log\left(\frac{h_U(ik,L)}{h_U^{\infty}(ik)}\right)\right],\tag{2.2}$$

being $w(D)$ a constant which only depends on the dimension of the space and that was previously studied in [34]. This constant can be written as

[1] All along the chapter, z is going to describe the spatial coordinate orthogonal to the surface of the plates and z is used to refer to any general complex number.

[2] At this stage it is necessary to point out that hereafter, only the case $a=1$ in (1.28) and the rest of formulae in Section 1.4 is going to be studied just for simplicity, unless otherwise indicated. Consequently, the distance between plates L and the transversal momentum k will be rescaled in units of a as $L=\tilde{L}a$ and $k=\tilde{k}/a$. But in order not to complicate the notation unnecessarily, after this rescaling of the parameters, they will be still designated by L,k.

$$w(D) = \begin{cases} \frac{4(-1)^{\frac{D-1}{2}}\Gamma\left(-\frac{D}{2}\right)}{(4\pi)^{\frac{D}{2}+1}} & D \quad \text{odd}, \\ \frac{(4\pi)^{-\frac{D}{2}}}{\Gamma\left(\frac{D}{2}+1\right)} & D \quad \text{even}. \end{cases}$$

This new formula for the Casimir energy with general boundary conditions is independent of the regularisation lenght and consequently this original important result enables to extend the one given in [34] to much general situations in which there is a potential of compact support between plates that depends only in z. This result has been recently published in [133].

2.2. Free energy and Casimir pressure at finite temperature

When considering thermal excitations of an ensemble of particles, the statistical behaviour of the ensemble is characterised by a temperature T and a probability distribution once the equilibrium is reached. As it has been explained in sections 1.1 and 1.2 of the first chapter, the quantum system of a massless scalar field can be treated as a grand canonical ensemble of particles that exchanges thermal energy and particles with a background external field acting as a reservoir. In the thermal equilibrium the chemical potential μ, the volume V and the temperature T ($\beta = T^{-1}$) of such an ensemble are fixed. Its grand canonical partition function can be written as

$$\mathcal{Z} = \prod_{i=1}^{s} \sum_{N_i=0}^{\infty} \prod_{k} e^{-\beta(n_k\varepsilon_k - \mu_i n_{k,i})},$$

being N_i the total number of particles of each one of the s possible types, $\prod_k$ the product over each microstate for the macrostate with N_i particles, n_k the number of particles occupying the microstate k so that $\sum_k n_{k,i} = N_i$ and ε_k the energy of the particle in this microstate k. From this partition function one can derive the expected values of other thermodynamic state functions such as the occupation number, the internal energy or the pressure.

2.2.1. Helmholtz free energy

It has just been established in the first chapter the picture in which the Hamiltonian of a massless complex QFT can be understood as an infinite collection of non interacting harmonic oscillators with frequencies given by the squared root of the eigenvalues of the self-adjoint extensions of the Laplacian operator with boundary conditions given by matrices of the $U(2)$ group. Since the oscillators do not interact, the grand canonical partition function of the system can be written as an infinite product of harmonic oscillator's canonical partition functions

$$\mathcal{Z} = \prod_{\omega^2 \in \sigma(-\Delta_U)} \operatorname{Tr} e^{-\beta \hat{H}_{os}} = \prod_{\omega^2 \in \sigma(-\Delta_U)} \sum_{n=0}^{\infty} \langle \psi_n | \, e^{-\beta \hat{H}_{os}} \, | \psi_n \rangle = \prod_{\omega^2 \in \sigma(-\Delta_U)} \sum_{n=0}^{\infty} e^{-\frac{\omega}{T}(n+\frac{1}{2})} = \prod_{\omega^2 \in \sigma(-\Delta_U)} \frac{e^{-\omega/2T}}{1 - e^{-\omega/T}}.$$

Consequently, the corresponding Helmholtz free energy takes the form

$$\mathcal{F}(T) = -T\log\mathcal{Z} = -T\sum_{\omega^2\in\sigma(-\Delta_U)}\log\left(\frac{e^{-\omega/2T}}{1-e^{-\omega/T}}\right) = \sum_{\omega^2\in\sigma(-\Delta_U)}\left[\frac{\omega}{2}+T\log\left(1-e^{-\omega/T}\right)\right] \tag{2.3}$$

This expression can be splitted in two terms: the one corresponding to the divergent vacuum energy E_0 that needs to be regularised and renormalised as explained in the previous section (it is the only term in this expression that was previously studied in [34]) and the one related to the thermal quantum corrections to E_0, which is not divergent and which will be the focus of this section. Consequently,

$$\frac{\mathcal{F}(T)}{A} = \frac{E_0}{A} + \frac{\triangle_T\mathcal{F}}{A}. \tag{2.4}$$

In equation (2.3) the summation over the field modes ω such that $\omega^2 = \vec{k_\parallel}^{\,2} + k^2$ involves an integral over the parallel momenta $\vec{k_\parallel}$ and a discrete summation over the transverse momenta k (which can be obtained from the zeroes of the spectral function, i.e., $Z(f_U)$). In other words, the summation over the whole spectrum $\sigma(-\Delta_U)$ transforms into

$$\triangle_T\mathcal{F} = \sum_{\omega^2\in\sigma(-\Delta_U)} T\log\left(1-e^{-\frac{\omega}{T}}\right) = A\int_{\mathbb{R}^2}\frac{d^2\vec{k_\parallel}}{(2\pi)^2}\sum_{k\in Z(f_U)} B(\omega,T),$$

being $B(\omega,T) = T\log\left(1-e^{-\frac{\omega}{T}}\right)$ the Boltzmann factor. At this point it is necessary to consider two possible different cases:

- If $U \in \mathcal{M}_F^{(0)}$ the whole spectrum of transverse momenta is $\sigma(-\Delta_U) = \{0\}\cup Z(f_U^{(0)})$, where $f_U^{(0)} = k^{-3}h_U(k)$. So in this case the summation over the spectrum $\sigma(-\Delta_U)$ splits into two terms:

$$\frac{\Delta_T^{(0)}\mathcal{F}}{A} = \int\frac{d^2\vec{k_\parallel}}{(2\pi)^2}\left[B(k_\parallel,T) + \sum_{k\in Z(f_U^{(0)})} B(\omega,T)\right],$$

  where the integration of the first term in the parenthesis accounts for all the zero modes of the field characterised by frequencies $\omega = \sqrt{k_\parallel^2+0^2}$, that are not included when performing the summation over the zeroes of $f_U^{(0)}(k)$. Notice that there is at most one[3] zero mode for the case considered. This term can be computed analytically to obtain:

$$\begin{aligned}\frac{\Delta_T^{(0)}\mathcal{F}}{A} &= \frac{T}{2\pi}\int_0^\infty k_\parallel\,\log\left(1-e^{-k_\parallel/T}\right)dk_\parallel + \int\frac{d^2\vec{k_\parallel}}{(2\pi)^2}\sum_{k\in Z(f_U^{(0)})} B(\omega,T)\\ &= -\frac{\zeta_R(3)}{2\pi}T^3 + \int\frac{d^2\vec{k_\parallel}}{(2\pi)^2}\sum_{k\in Z(f_U^{(0)})} B(\omega,T).\end{aligned}$$

[3] But for other cases, if there were more, the Boltzmann factor should be multiplied by the dimension of the zero mode space.

Notice that the contribution of the zero mode gives the dominant term at high temperatures since it behaves as T^3:

$$-\frac{T^3\zeta_R(3)}{2\pi} \simeq -0.191313\, T^3.$$

- If $U \in \mathcal{M}_F - \mathcal{M}_F^{(0)}$ the whole spectrum of transverse momenta is $\sigma(-\Delta_U) = Z(f_U)$, being the spectral function $f_U = k^{-1}h_U(k)$, so in this case the summation over the spectrum can be computed as

$$\frac{\Delta_T\mathcal{F}}{A} = \int \frac{d^2\vec{k}_\parallel}{(2\pi)^2} \sum_{k\in Z(f_U)} B(\omega, T).$$

Both cases could be written simultaneously in a more compact form as:

$$\frac{\Delta_T\mathcal{F}}{A} = q_0 + \int \frac{d^2\vec{k}_\parallel}{(2\pi)^2} \sum_{k\in Z(f_U^{(J)})} B(\omega, T), \tag{2.5}$$

being

$$q_0 = \begin{cases} 0, & \text{if } U \in \mathcal{M}_F - \mathcal{M}_F^{(0)} \\ -\frac{\zeta_R(3)}{2\pi}T^3, & \text{if } U \in \mathcal{M}_F^{(0)} \end{cases} \quad \text{and} \quad f_U^{(J)} = \begin{cases} f_U, & \text{if } U \in \mathcal{M}_F - \mathcal{M}_F^{(0)} \\ f_U^{(0)}, & \text{if } U \in \mathcal{M}_F^{(0)} \end{cases}.$$

The integration over the parallel momenta of (2.5) can be commuted with the summation over the discrete transverse momenta in order to perform the integral first by using *Mathematica* and obtain

$$\begin{aligned} I_3(k,T) &= T\int_{\mathbb{R}^2} \frac{d^2\vec{k}_\parallel}{(2\pi)^2} \log\left(1 - e^{-\frac{\sqrt{k_\parallel^2+k^2}}{T}}\right) = \frac{Tk}{2\pi}\int_0^\infty dk_\parallel \frac{k_\parallel}{k} \log\left(1 - e^{-\frac{k}{T}\sqrt{\frac{k_\parallel^2}{k^2}+1}}\right) \\ &= -\frac{T^3}{2\pi}\left(\frac{k}{T}\mathrm{Li}_2\left(e^{-\frac{k}{T}}\right) + \mathrm{Li}_3\left(e^{-\frac{k}{T}}\right)\right), \end{aligned} \tag{2.6}$$

being $\mathrm{Li}_s(z)$ the polylogarithmic function of order s [134]. Finally, one can rewrite $\triangle_T\mathcal{F}/A$ in equation (2.5) as a complex contour integral by using Cauchy's residue theorem

$$\frac{\triangle_T\mathcal{F}}{A} = q_0 + \sum_{k\in Z(f_U^J)} I_3(k,T) = q_0 + \lim_{R\to\infty}\oint_\Gamma \frac{dk}{2\pi i} I_3(k,T)\partial_k \log f_U^{(J)}(k), \tag{2.7}$$

where Γ is the complex contour described in Figure 2.1. Notice that since the spectral function $f_U^{(J)}$ does not decay to zero as the transversal momenta does, the contour integral avoids the problems at $k = 0$.

Regarding the integration over the non-zero part of the spectrum, the secular function $f_U^{(J)}(k)$ in the integrand is a holomorphic function on k and its logarithmic derivative has poles at its zeroes,

i.e. on the real axis[4]. On the other hand, $I_3(k,T)$ in equation (2.6) does not have singular points and it tends to zero as k increases. Notice that the integral over the circumference arc in Figure 2.1 parametrised as $\Gamma_3 \equiv \{z \in \mathbb{C} \,|\, z = Re^{i\nu},\, \nu \in [-\gamma,\gamma]\}$ when $R \to \infty$ is:

$$\lim_{R\to\infty} \left| \int_{\Gamma_3} \frac{dk}{2\pi i} I_3(k,T) \partial_k \log f_U(k) \right| \leq \lim_{R\to\infty} \int_{-\gamma}^{\gamma} \frac{d\nu}{2\pi} |I_3(Re^{i\nu},T)||\partial_\nu \log f_U(Re^{i\nu})|.$$

But the combination of poly-logarithms I_3 decays faster than e^{-R} and the logarithmic derivative of the spectral function behaves as RL when $R \to \infty$. Hence, the integral is exponentially suppressed due to the dominant contribution of I_3 and the integration over the circumference arc Γ_3 is zero.

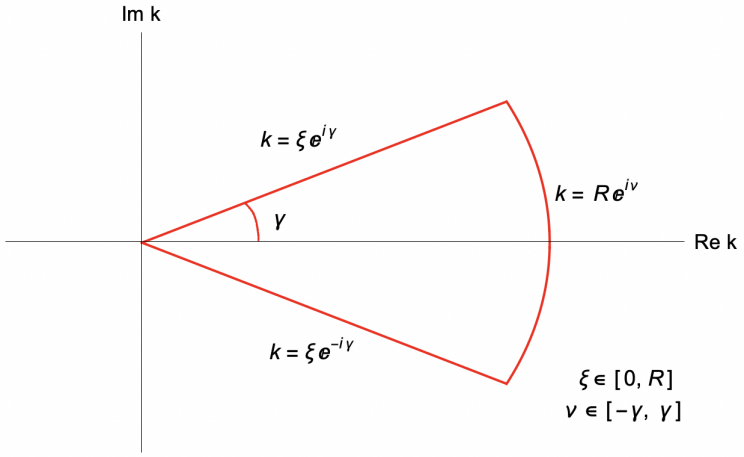

FIGURE 2.1: Complex contour Γ that encloses all the zeroes of $f_U^{(J)}(k)$ as $R \to \infty$. Notice that $R > 0$ and $0 < \gamma < \pi/2$ are constants.

The integration over the whole contour Γ in this limit reduces to the integration over the two straight lines $z = \xi e^{\pm i\gamma}$ being γ a constant angle and $\xi \in [0,\infty)$:

$$\frac{\triangle_T \mathcal{F}}{A} = q_0 + \int_0^\infty \frac{d\xi}{2\pi i} \left[-I_3(\xi e^{i\gamma},T) \partial_\xi \log f_U^{(J)}(\xi e^{i\gamma}) + I_3(\xi e^{-i\gamma},T) \partial_\xi \log f_U^{(J)}(\xi e^{-i\gamma}) \right]. \tag{2.8}$$

When integrating (2.8) over the Γ contour, the axis of frequency is turned towards the imaginary axis by a finite angle lower than $\pi/2$ in order to ease the numerical evaluation and to avoid possible oscillations of the integrand caused by the secular function $f_U^{(J)}$ on the real axis. The residue theorem ensures that the result of this integration does not depend on the angle γ taken in the contour. If $\gamma = \pi/2$ and one considers Cauchy Principal Values in the integral (2.7), the Matsubara formula arises after integrating by parts [15, 36].

This integral can be computed numerically by using *Mathematica* for any finite temperature T and any unitary matrix $U \in \mathcal{M}_F$. The results for low temperatures and boundary conditions without zero modes $U \in \mathcal{M}_F - \mathcal{M}_F^{(0)}$ are shown in Figures 2.2, 2.3 and 2.4.

[4]Since the Hamiltonian $-\Delta_U$ is a self-adjoint second order elliptic operator, its spectrum is real. It is also positive since only non negative self-adjoint extensions have been considered. Moreover, since the spectral function $f_U^{(J)}(k)$ is even in k, its zeroes appear both in the positive and the negative real axis. Consequently, there will be two plane waves with wave vector k and $-k$ but same energy $E = k^2$ travelling to the right and to the left, respectively.

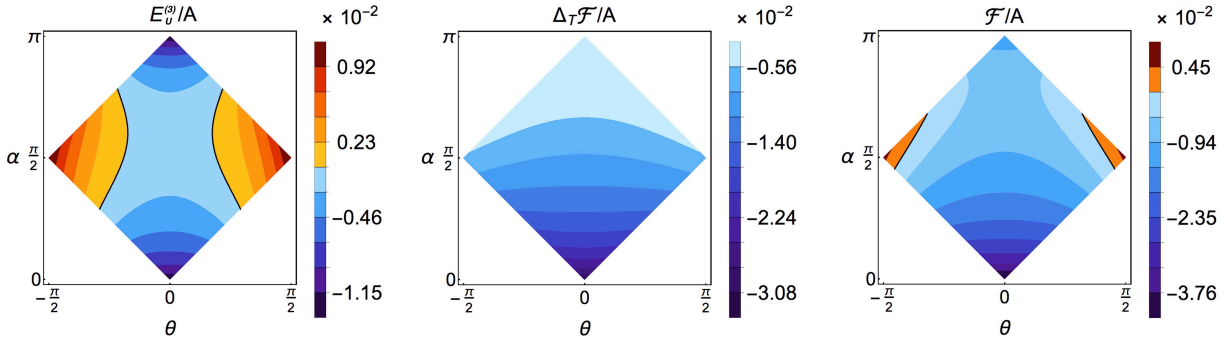

FIGURE 2.2: Quantum vacuum energy per unit area for $U \in \mathcal{M}_F - \mathcal{M}_F^{(0)}$ at $T = 0$ (left), thermal correction $\Delta_T\mathcal{F}/A$ (center) and total Helmholtz free energy per unit area (right) as functions of the parameters α and θ. In these plots, $T = 0.55, n_1 = 0$ and $L = 1$.

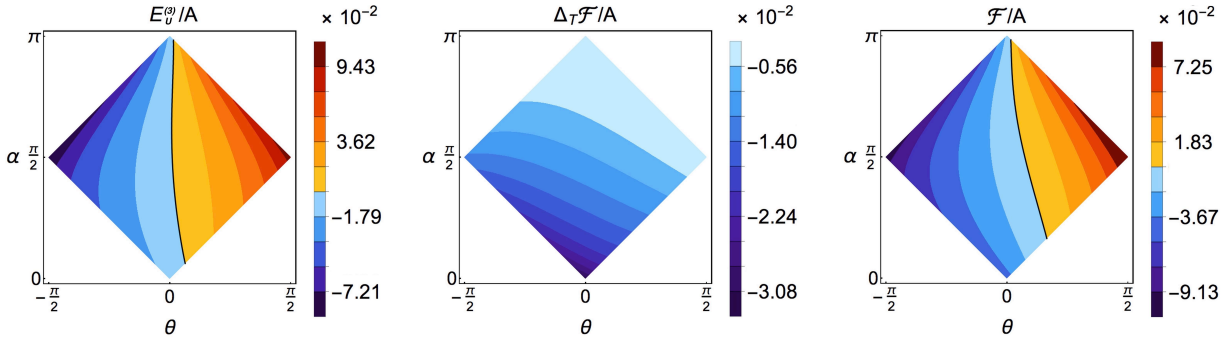

FIGURE 2.3: Quantum vacuum energy per unit area for $U \in \mathcal{M}_F - \mathcal{M}_F^{(0)}$ at $T = 0$ (left), thermal correction $\Delta_T\mathcal{F}/A$ (center) and total Helmholtz free energy per unit area (right) as functions of the parameters α and θ. In these plots, $T = 0.55, n_1 = 0.5$ and $L = 1$.

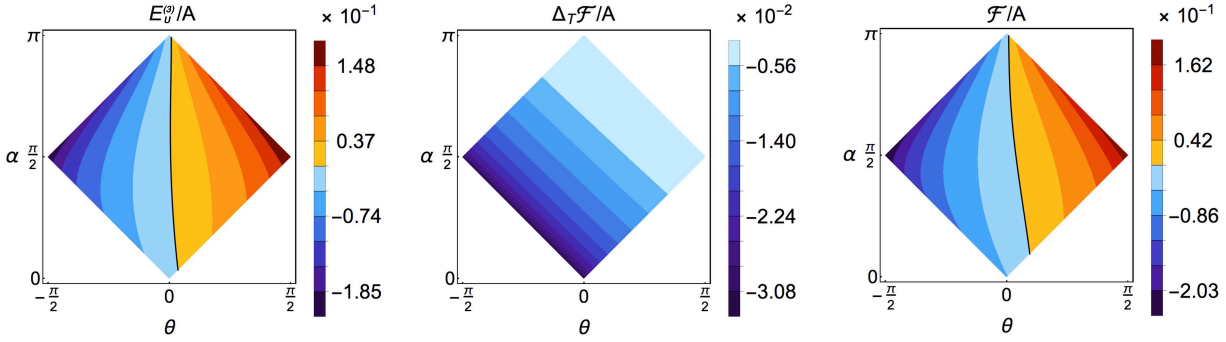

FIGURE 2.4: Quantum vacuum energy per unit area for $U \in \mathcal{M}_F - \mathcal{M}_F^{(0)}$ at $T = 0$ (left), thermal correction $\Delta_T\mathcal{F}/A$ (center) and total Helmholtz free energy per unit area (right) as functions of the parameters α and θ. In these plots, $T = 0.55, n_1 = 1$ and $L = 1$.

Each figure shows the quantum vacuum energy E_0/A at $T = 0$ (left plots[5]) computed with formula (2.2), the thermal correction $\Delta_T\mathcal{F}/A$ given by (2.8) (central plots) and the total free energy $\mathcal{F}/A$ in (2.4) (right plots) as functions of the parameters $\{\alpha, \theta, n_1\}$ defining the boundary condition. On the other hand in Figure 2.5 the high temperature behaviour of the free energy for $U \in \mathcal{M}_F - \mathcal{M}_F^{(0)}$ is plotted.

[5]These plots for E_0 were first obtained in [34] but now, they are reproduced here with the new formula (2.2), which converges faster than the method used in the aforementioned paper.

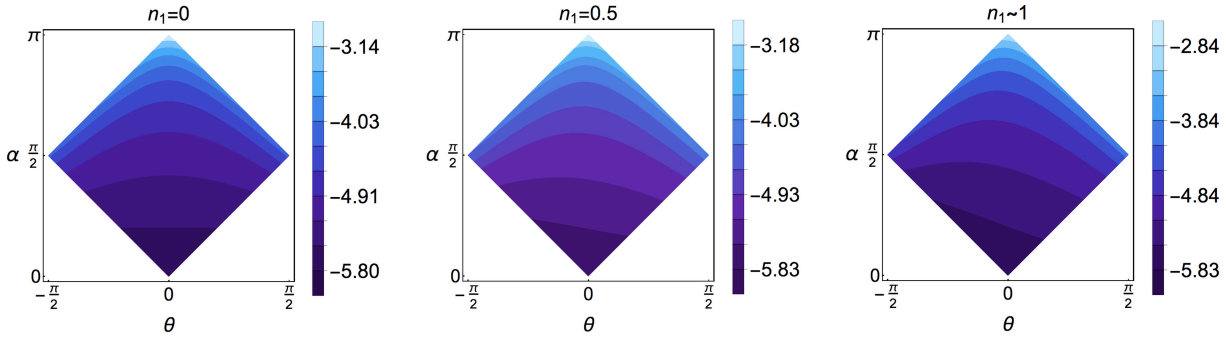

FIGURE 2.5: $\Delta_T\mathcal{F}/A$ for $U \in \mathcal{M}_F - \mathcal{M}_F^{(0)}$ for high temperature (T=2.5) as a function of the parameters α, θ and n_1. In these plots $L = 1$ is fixed.

The figures show that the thermal correction $\Delta_T\mathcal{F}/A$ to the quantum vacuum energy is definite negative for any boundary condition. However, if the temperature is low enough, the total Helmholtz free energy can be positive, negative or zero as happens for the quantum vacuum energy at zero temperature [34]. If the temperature increases, since $\Delta_T\mathcal{F}/A$ is a monotonically decreasing function of T (as can be seen in Figure 2.5), the thermal fluctuations dominate the total Helmholtz free energy giving rise to only negative values. This is the reason that at low temperatures the maximum and minimum of the energy take place at anti-periodic and periodic boundary conditions (respectively), whereas at high temperatures they occur at Dirichlet and Neumann boundary conditions.

It is also possible to evaluate $\mathcal{F}/A$ for boundary conditions with a constant zero mode $U \in \mathcal{M}_F^{(0)}$ for different values of the temperature as a function of the single free parameter α (the zero mode line is characterised by $n_1 = \pm 1, \alpha \pm \theta = 0$). The result can be seen in Figure 2.6.

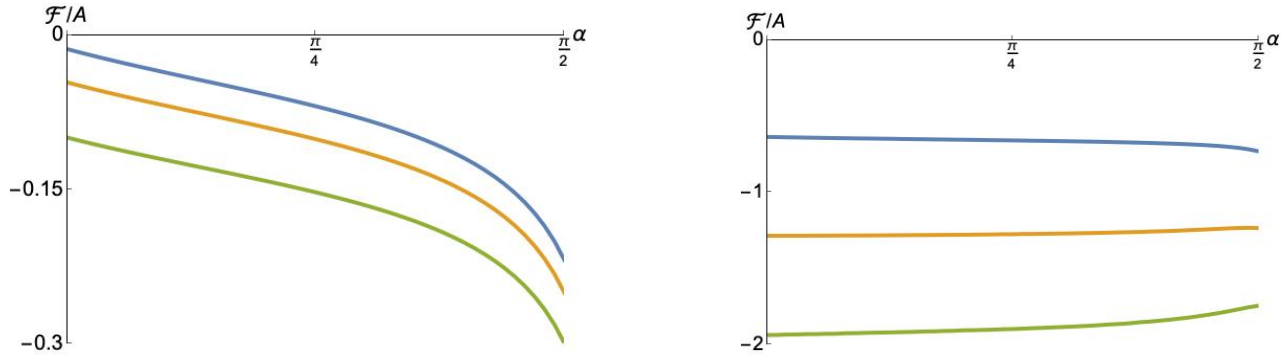

FIGURE 2.6: Left: $\mathcal{F}/A$ for $U \in \mathcal{M}_F^{(0)}$ at low temperatures: $T = 0$ (blue line), $T = 0.55$ (yellow line), and $T = 0.75$ (green line). Right: $\mathcal{F}/A$ for $U \in \mathcal{M}_F^{(0)}$ at high temperatures: $T = 1.35$ (blue line), $T = 1.65$ (yellow line), and $T = 1.85$ (green line).

At low temperatures $TL < 1$, the minimum of $\mathcal{F}/A$ occurs at periodic boundary conditions (i.e. $\alpha = \pi/2$) as can be seen in Figure 2.6 (left). In contrast, when the temperature is sufficiently high, $\mathcal{F}/A$ becomes a monotonically increasing function of α, so the minimum is reached at Neumann boundary condition ($\alpha = 0$) as shown in Figure 2.6 (right).

Other boundary conditions outside the space $\mathcal{M}_F$ could be also studied even though their spectra may include some states with negative energy [109] depending on the value of the distance between

plates L. However, if the subdominant divergences for these cases were different, the formulae presented in this section could not be used. Since these boundary conditions outside the rhombus in Figure 1.3 do not define unitary quantum field theories with non-negative self-adjoint Hamiltonians for any value of the distance between plates, they are all beyond the scope of this work.

The expression (2.7) can be generalised for arbitrary higher dimensions $[0, L] \times \mathbb{R}^{D-1}$ of the physical space with boundaries in which the quantum field is confined. Either the formulas on this section and those of the following two sections are valid but replacing $I_3(k, T)$ in equation (2.6) by the integral

$$I_D(k, T) = T \int_{\mathbb{R}^{D-1}} \frac{d^{D-1}\vec{k}_{\|}}{(2\pi)^{D-1}} \log\left(1 - e^{-\frac{\sqrt{\vec{k}_{\|}^{\,2} + k^2}}{T}}\right),$$

whose solution involves more complicated combinations of poly-logarithms of higher order but with the same arguments $e^{-k/T}$. This fact ensures no problems while summing over the transversal momenta in (2.7).

2.2.2. Casimir force between plates

It is possible to obtain the Casimir force per unit area of the plates at a given temperature by computing the opposite sign derivative of the total Helmholtz free energy with respect to the distance between plates[6]:

$$P = -\frac{1}{A}\left(\frac{\partial \mathcal{F}}{\partial L}\right)\Big|_T = -\frac{1}{A}\left(\frac{\partial E_0}{\partial L}\right)\Big|_T - \frac{1}{A}\left(\frac{\partial \triangle_T \mathcal{F}}{\partial L}\right)\Big|_T = P(T=0) + \Delta_T P.$$

On the one hand, since in three spatial dimensions $E_0 \propto L^{-3}$ for any $U \in \mathcal{M}_F$ (as can be seen in [34]), the zero temperature quantum vacuum pressure can be computed from (2.2) and takes the form

$$P(T=0) = \frac{1}{A}\frac{3E_0}{L} = \frac{3}{L}\frac{1}{6\pi^2}\int_0^\infty dk\, k^3 \left[L - \partial_k \log\left(\frac{f_U(ik, L)}{f_U^\infty(ik)}\right)\right]. \tag{2.9}$$

On the other hand, taking into account (2.8), the quantum correction to the pressure of the plates can be written as

$$\Delta_T P = \int_0^\infty \frac{d\xi}{2\pi i}\left[I_3(\xi e^{i\gamma}, T)\partial_L \partial_\xi \log f_U(\xi e^{i\gamma}) - I_3(\xi e^{-i\gamma}, T)\partial_L \partial_\xi \log f_U(\xi e^{-i\gamma})\right]. \tag{2.10}$$

The numerical results of the total Casimir pressure between plates in the space of boundary conditions parameters are collected in Figure 2.7 for low temperatures.

[6]For this reason, there is no distinction between boundary conditions with zero mode, i.e. $U \in \mathcal{M}_F^{(0)}$, and without zero mode $U \in \mathcal{M}_F - \mathcal{M}_F^{(0)}$, because the zero mode contribution does not depend on the distance between plates L.

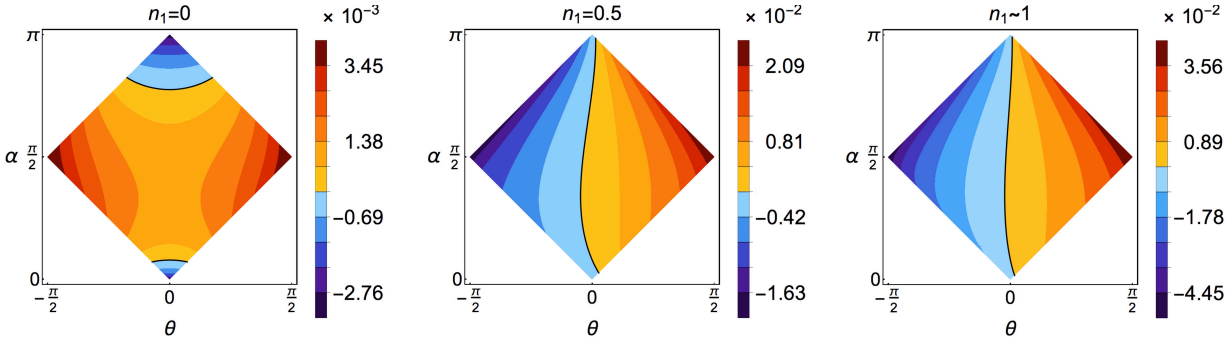

FIGURE 2.7: Pressure in the $\alpha - \theta$ plane for different values of n_1. In these plots, $T = 0.35$ and $L = 1$.

If the temperature is low enough there are attractive, repulsive and null Casimir forces in the system, as happens at zero temperature [34]. Another similarity with the zero temperature case is that the minimum pressure takes place at periodic boundary conditions ($\alpha = -\theta = \pi/2, n_1 = 1$) and the maximum pressure for anti-periodic boundary conditions ($\alpha = \theta = \pi/2, n_1 = 1$). Nonetheless, if the temperature starts to increase, the thermal fluctuations become the dominant contribution to the pressure, giving rise to only repulsive forces in the system (it can be easily seen in Figure 2.8).

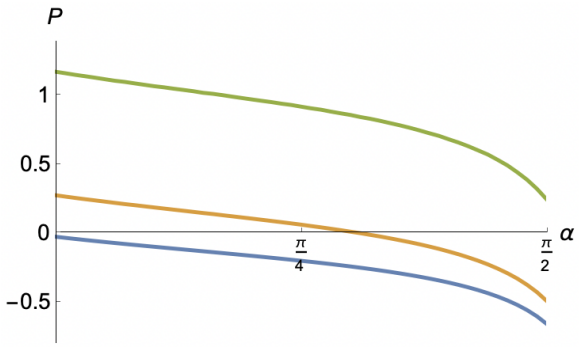

FIGURE 2.8: Pressure in the zero mode line $\{n_1 = 1, \alpha + \theta = 0\}$ for different values of the temperature: $T = 0.75$ (blue), $T = 1.35$ (orange) and $T = 1.85$ (green). In this plot $L = 1$.

This different behaviour of the pressure with respect to the temperature enables to compute a critical temperature that separates both regimes. This critical value occurs when the minimum pressure is equal to zero. It is known that the minimum quantum vacuum pressure at zero temperature happens at periodic boundary conditions[7] $U_p = \sigma_1$ [34]. Hence, since the pressure monotonically increases with the temperature, the equation for the critical temperature T_c^P at a given distance between plates is

$$\Delta_T P(U_p, T_c^P) + P(U_p, T = 0) = \Delta_T P(U_p, T_c^P) - \frac{\pi^2}{15L^4} = 0,$$

and it can be solved numerically to obtain the red curve in Figure 2.9.

[7]The value of the quantum vacuum pressure at $T = 0$ for periodic boundary conditions is $P_0 = -\pi^2/(15L^4)$ [34].

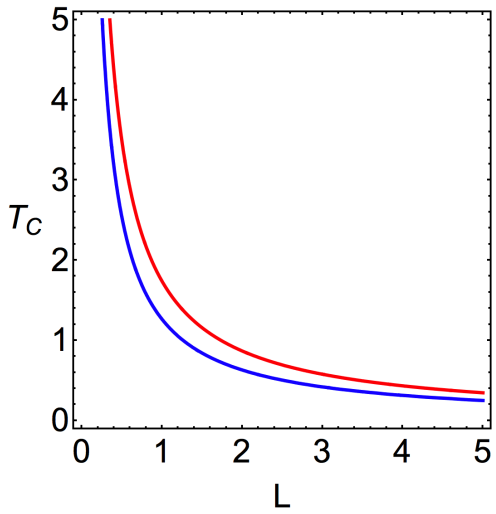

FIGURE 2.9: $T_c^{\mathcal{F}}$ (blue) and T_c^{P} (red) as functions of the distance between plates L.

In the same way and due to the discussion introduced in the previous section, there is a critical temperature such that for temperatures greater than this critical value it is not possible to find boundary conditions giving rise to total positive Helmholtz free energy in the system. On the contrary, for temperatures lower than this critical value $\mathcal{F}$ can be positive, negative or zero. Since the maximum quantum vaccum energy at zero temperature is reached at antiperiodic boundary conditions[8] $U_{ap} = -\sigma_1$ [34] and the free energy monotonically decreases with the temperature, the equation for the critical temperature $T_c^{\mathcal{F}}$ at a given distance between plates is

$$\Delta_T \mathcal{F}(U_{ap}, T_c^{\mathcal{F}}) + E_0(U_{ap}, T = 0) = \Delta_T \mathcal{F}(U_{ap}, T_c^{\mathcal{F}}) + \frac{7\pi^2}{360L^3} = 0.$$

This equation can be solved to obtain the blue curve in Figure 2.9. It is clear from the plot that the temperature T_c^{P}, at which the possibility of having attractive quantum vacuum pressure disappears, is higher than the critical temperature $T_c^{\mathcal{F}}$, at which the total free energy $\mathcal{F}$ becomes definite negative. This is due to the fact that neither the total Helmholtz free energy behaves with the distance between plates like L^{-3} nor the total pressure like L^{-4}. That is to say, both $\mathcal{F}$ and P have different dependence on the variable L, which in turn is also different from the dependence on L of the vacuum energy and pressure at zero temperature.

The existence of this critical temperature is an important conclusion of this analysis. The seminal theorem of *"opposites attract"* by Kenneth and Klich [37] states that the Casimir force induced by quantum vacuum fluctuations between two opposite[9] but not necessarily planar objects separated by a finite distance is always attractive. It is implicit in the assumptions of the theorem that the boundary conditions introduced by the two bodies are each other independent. For the system of a quantum massless scalar field confined between two parallel plates mimicked by the most general type of boundary conditions, the mirror symmetry between independent bodies means that the

[8] The value of the quantum vacuum energy at $T = 0$ for antiperiodic boundary conditions is $E_0 = 7\pi^2/(360L^3)$ [34].

[9] Opposites objects are identical bodies with mirror symmetry with respect to the hyperplane equidistant to the two bodies.

boundary matrix U must be diagonal, i.e. one should only consider the following subset of boundary conditions:

$$\mathcal{M}_F^{ms} = \{U \in \mathcal{M}_F \quad | \quad \theta = 0 \vee n_1 = n_2 = 0\}.$$

In other words, the *"opposites attract"* theorem holds for Robin boundary conditions at $T = 0$ (as stated in [34] and [44]).

At this point it is necessary to distinguish between mirror symmetry and $\mathbb{Z}_2$ symmetry. The physical space of the system of one scalar field confined between several two-dimensional plates is $[0, L] \times \mathbb{R}^2$ (in [44] it is deeply dicussed the general case for any dimension $D-1$ of the plates). The remainder of this paragraph will reproduce the results of [44] related to reflection invariance for completeness. The reflection with respect to a hyperplane placed at $L/2 \times \mathbb{R}^2$ is a unitary bijective application whose action over the fields is given by:

$$\phi^R(z^0, z) = \phi^R(z^0, L - z), \qquad z \in [0, L]. \tag{2.11}$$

It acts over the boundary values of the field through the operator $\hat{O}_{R_b} = \sigma_1$. In order for the self-adjoint extension to the Hamiltonian (1.27) to be $\mathbb{Z}_2$ invariant, the boundary condition must also preserve $\mathbb{Z}_2$ symmetry, i.e.

$$\hat{O}_{R_b}(\varphi - i\partial_n\varphi) = U\hat{O}_{R_b}(\varphi + i\partial_n\varphi).$$

This implies that $[\hat{O}_{R_b}, U] = 0$. Consequently, due to the parametrisation of U given in (1.25), the subset of boundary conditions that preserves $\mathbb{Z}_2$ symmetry is given by:

$$\mathcal{M}_F^{\mathbb{Z}_2} = \{U \in \mathcal{M}_F \quad | \quad n_2 = n_3 = 0\},$$

which is the case of the rhombus in the third column of Figure 2.7 (notice that $n_1^2 + n_2^2 + n_3^2 = 1$). From the definitions of $\mathcal{M}_F^{\mathbb{Z}_2}$ and $\mathcal{M}_F^{ms}$, it is clear that mirror symmetry transformations are included in the $\mathbb{Z}_2$ symmetry ones. In short, one can speak of $\mathbb{Z}_2$ symmetry when there is a symmetry as described in (2.11), whatever the topology of the system, whereas the mirror symmetry is a $\mathbb{Z}_2$ symmetry with a topology necessarily related to two disjoint objects. At $T = 0$ mirror symmetry guarantees attractive forces in the system, whereas $\mathbb{Z}_2$ symmetry does not.

For finite temperatures greater than zero, attractive forces only appear in the regime[10] $T < T_c^P$. Nevertheless, not all the diagonal U matrices yield an attractive force in the system for any non zero temperature. In fact, the subset of Robin boundary conditions which are close to the minimum energy at $\theta = 0$ corresponds to values of pressure not so far from zero at $T = 0$. Consequently, any small thermal perturbation produces a net repulsive force in the system. Hence, at $T \neq 0 \mid T < T_c^P$ neither for mirror nor for $\mathbb{Z}_2$ symmetry is the negative sign of the pressure between plates guaranteed. In the third column of Figure 2.7 it can be seen that not all the boundary conditions which are $\mathbb{Z}_2$ invariant yields attractive forces in the system if $T < T_c^P$. The fact that the Casimir force is not always attractive for any temperature can be easily seen in Figure 2.10, where Neumann boundary conditions have

[10] Notice that for $T > T_c^P$ the thermal fluctuations dominate the behaviour of the pressure, giving rise to only repulsive forces in the system.

been considered as an example of $\mathbb{Z}_2$ invariant boundary condition.

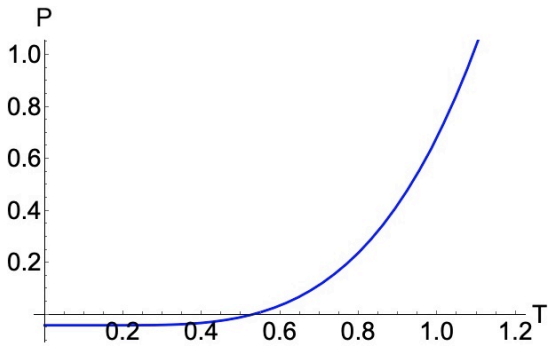

FIGURE 2.10: Quantum vacuum pressure as a function of the temperature for Neumann boundary conditions and $L = 1$.

Furthermore, attractive forces between plates also appear for non diagonal U matrices both at $T = 0$ and $T \neq 0$, as can be seen in [44] and in Figure 2.7, respectively.

2.3. Entropy at finite temperature

Once the total Helmholtz free energy has been studied, it is possible to calculate the one loop quantum correction to the classical entropy per unit area of the plates, as a function of the boundary condition parameters for any non zero temperature (shown in Figure 2.11) by means of $S = -\partial\mathcal{F}/\partial T$.

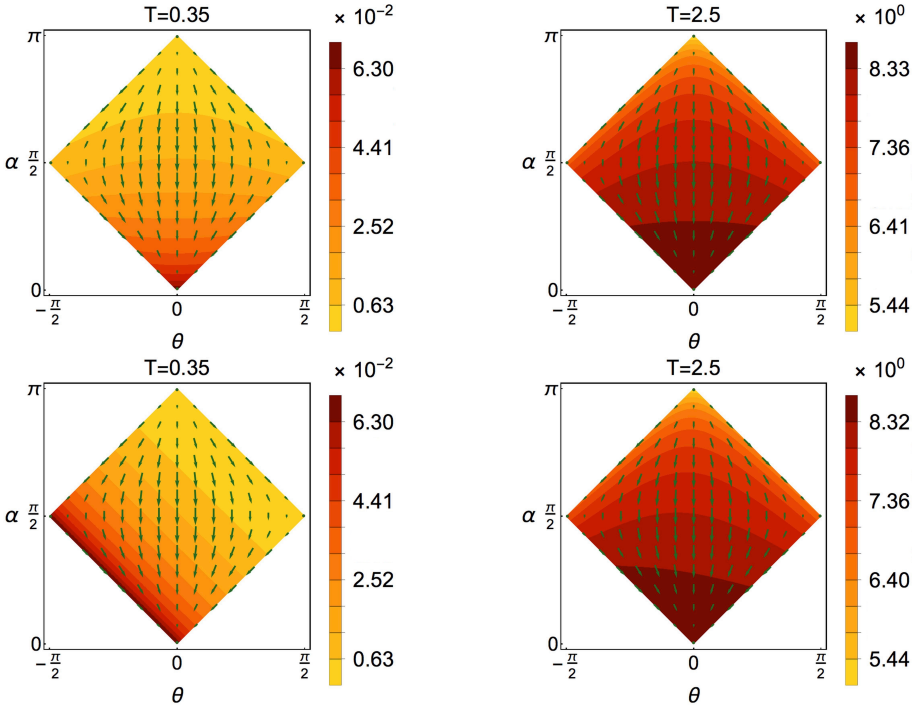

FIGURE 2.11: Entropy per unit area of the plates for low (left) and high (right) temperatures with $n_1 = 0$ (first row) and $n_1 = 0.75$ (second row). In these plots $L = 1$. Green arrows represent the *boundary renormalisation group flow* [44], [135] given in equation (2.12).

From the plots, it is clear that the entropy is positive definite for any boundary condition parameter α, θ, n_1. It shows a monotonically increasing behaviour as the temperature reaches higher values (as can be seen in the different scales in the first and second column of the plots). Moreover, for any $T > 0$ the maximum entropy is reached for Neumann boundary condition ($\alpha = \theta = 0$) and the minimum entropy occurs at Dirichlet boundary condition ($\alpha = \pi$, $\theta = 0$).

The major conclusion is that there is no boundary condition $U \in \mathcal{M}_F$ giving rise to negative one loop quantum corrections to the entropy, unlike the results obtained in some references such as [136]. This negative corrections to the entropy are related to instabilities in the system [137].

Another crucial feature is that the maximum and the minimum of the entropy always occur at Dirichlet and Neumann boundary conditions, which happen to be the most unstable and stable fixed points of the *boundary renormalisation group flow* [138], respectively. The renormalisation of the quantum fields and the typical constants in QFT (such as the couplings or the masses) enables to remove the divergences present in the theories. Since the boundary conditions implement the physical properties of the boundaries, as well as the interaction between them and the quantum fields, they also need to be renormalised. Their renormalisation can be studied while implementing dilation symmetries in the quantum system. The resulting transformations are called transformations of the boundary renormalisation group and they generate a non trivial flux in the boundary condition space, which is the so called *boundary renormalisation group flow*. It can be described by the following equation [139]:

$$\partial_\Lambda U_\Lambda = \frac{1}{2\Lambda} U_\Lambda \left(U_\Lambda^\dagger - U_\Lambda \right), \tag{2.12}$$

being Λ a parameter related to that of the dilatations. 1+1 dimensional massless Quantum Field Theory is conformally invariant but the boundary conditions can break this symmetry. The conformal symmetry is only preserved at the fixed points of the *boundary renormalisation group flow*. At these points (the corners of the rhombus) the boundary conditions are stable under dilatations. Therefore, the implications of the fact that the maximum and the minimum values of the one loop quantum corrections to the entropy in the system occur at some of these fixed points are not yet clear. This work is in progress.

It is worth to point out that part of my results presented in these two sections 2.2 and 2.3 have been summarised and published in the main part of [140].

2.4. High and low temperature expansions

Although the analytic formulae obtained so far are valid for any temperature, more simplified expressions can be reached when considering the limit of low and hight temperatures in the system. These simplifications have been the focus of attention in the last decades, at least for the most commonly used boundary conditions (which are the vertices of the rhombus). Now the aim of this section is to obtain these approximations for most general boundary conditions.

In the system of natural units already chosen, $k_B TL$ is a dimensionless quantity. Hence, it is clear that if $k_B = 1$ then one can define the regimes of low and high temperatures as $TL \ll 1$ and $TL \gg 1$, respectively.

Moreover, notice that the spectral function (1.28), which plays a fundamental role in the computation of the Helmholtz free energy, has terms of different powers of ka and kL. Consequently, h_U depends on both dimensionless quantities in distinct manners. So far, $a = 1$ has been stated just for simplicity. Most of the standard references have only studied this case when proposing approximate formulae for $\Delta_T \mathcal{F}$. Quite the opposite, in this section a is set free to vary because the objective is to study the properties of the thermal correction to the vacuum energy in dependence on the boundary condition parameters and the natural length scales L, a. In fact, it will be proved that a takes on great importance in the limit of low temperatures, so it should not be regarded trivially.

Low temperature expansion: $TL \ll 1$

The dominant contribution of the one loop thermal correction to the quantum vacuum energy if $U \in \mathcal{M}_F^{(0)}$ is the one of the zero mode, namely

$$\frac{\Delta_T^{(0)} \mathcal{F}_{\text{zm}}}{A} = -\frac{\zeta_R(3)}{2\pi} T^3, \quad LT \ll 1.$$

However, for $U \in \mathcal{M}_F - \mathcal{M}_F^{(0)}$ two different scales of energy must be taken into account: the thermal one determined by TL and the intrinsic one characterised by the values of the frequencies of the modes. It is customary [15, 36, 39] to find

$$\frac{\Delta_T \mathcal{F}}{A} \simeq -\frac{k_0}{2\pi} T^2 \exp\left[-\frac{k_0}{T}\right], \quad LT \ll 1,$$

as the dominant contribution to $\Delta_T \mathcal{F}$ in the case of $U \in \mathcal{M}_F - \mathcal{M}_F^{(0)}$, being k_0 the lowest frequency of the field mode. Moreover, this approximation is only valid for $k_0/T > 1$. Despite its widespread use, this standard approximation is only aware of the thermal scale of energy described by the value of TL. In order to cover both scales of energy, one needs to compute an approximate solution of the spectrum of normal modes for boundary conditions in the neighbourhood of $\mathcal{M}_F^{(0)}$, i.e.

$$\{U(\alpha, \theta, \vec{n}) \in \mathcal{M}_F \text{ such that } \alpha + \theta = \epsilon, n_1 = 1\}, \tag{2.13}$$

where $\epsilon > 0$ is a small displacement in the α-θ plane. A perturbative study of the spectrum of the self-adjoint extensions in (2.13) can be performed by substituting $\alpha = -\theta + \epsilon$ and $k_n \sim k_n^{(0)} + \epsilon \delta_n$ in the spectral function f_U given by (1.28) and then expanding it up to first order in ϵ. The frequencies $k_n^{(0)}$ characterise the spectrum of the self-adjoint extensions with zero mode. Solving the resulting spectral equation $f_U = 0$ enables to obtain the lowest transverse mode ($k_0^{(0)} = 0$), indeed

$$k_0 \sim \sqrt{\frac{\epsilon}{aL}}, \qquad k_0 L \ll 1. \tag{2.14}$$

The modes for $n > 1$ can be also computed and they are collected in [140] but they do not contribute in the leading order of $\Delta_T \mathcal{F}$ when $TL \ll 1$. In the neighbourhood of $\mathcal{M}_F^{(0)}$, given by (2.13), the lowest mode k_0 is still the dominant contribution to $\Delta_T \mathcal{F}$. However, two asymptotic behaviours can be distinguished as a function of k_0/T:

- If $k_0/T \ll 1$, the function $I_3(k,T)$ that appears in (2.6) and (2.7) can be expanded up to second order in k_0/T giving rise to a logarithmic correction to the zero mode contribution:

$$\begin{aligned}\frac{\Delta_T \mathcal{F}}{A}\Big|_{\frac{k_0}{T}\ll 1} &= \sum_{k\in Z(f_U)} I_3(k,T)\Big|_{\frac{k_0}{T}\ll 1} \simeq I_3(k_0,T) \simeq -\frac{T^3}{2\pi}\left[\zeta(3) + \frac{1}{4}\frac{k_0^2}{T^2}\left(-1+2\log\frac{k_0}{T}\right) + \mathcal{O}\left(\frac{k_0^3}{T^3}\right)\right] \\ &\simeq \frac{\Delta_T^{(0)}\mathcal{F}_{\rm zm}}{A} - \frac{1}{8\pi}\frac{T\epsilon}{aL}\log\left(\frac{\epsilon}{aLT^2}\right).\end{aligned} \tag{2.15}$$

  Notice that the term $k_0^2/(4T^2)$ into the parenthesis $[\dots]$ in the previous expression is not a dominant term compared to the one proportional to $\log(k_0/T)$, providing k_0/T a small quantity, so it can be ignored.

- If $k_0/T \gtrsim 1$ the Boltzmann factors happens to be exponentially suppressed and the contribution of k_0 is the one given in standard references (c.f. [15]):

$$\frac{\Delta_T \mathcal{F}}{A}\Big|_{\frac{k_0}{T}>1} \simeq I_3(k_0,T)|_{\frac{k_0}{T}>1} \simeq -\frac{T^3}{2\pi}e^{-\frac{k_0}{T}}\left[\frac{k_0}{T}+1\right] \simeq -\frac{T^3}{2\pi}e^{-\frac{k_0}{T}}\frac{k_0}{T} = -\frac{\sqrt{\epsilon}}{2\pi\sqrt{aL}}T^2\exp\left[-\sqrt{\frac{\epsilon}{LaT^2}}\right]. \tag{2.16}$$

  Notice that if $k_0/T \gg 1$, then the term $k_0/T + 1 \simeq k_0/T$. Furthermore, when $x \ll 1$ the function $\mathrm{Li}_s(x)$ with $s = 2,3$ behaves as $x + constant \cdot x^2 + \mathcal{O}(x^3)$.

The ratio $\Delta_T \mathcal{F}/\Delta_T \mathcal{F}_{\rm zm}^{(0)}$ is shown in Figure 2.12, both for the results given by the exact formula (2.8) and their approximations (2.15) and (2.16), for boundary conditions of the form (2.13).

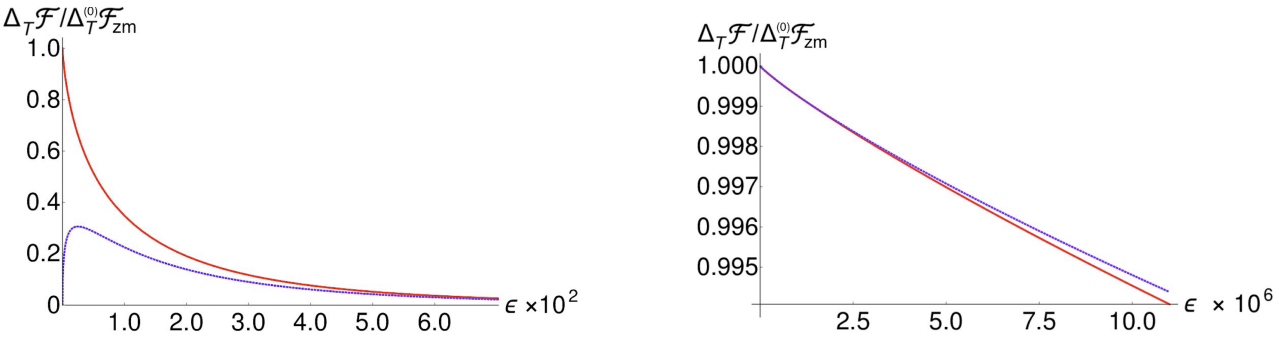

FIGURE 2.12: Graphical representation of $\Delta_T \mathcal{F}/\Delta_T^{(0)}\mathcal{F}_{\rm zm}$ given by (2.8) (solid red line in both graphs) and their asymptotic approximations (2.15) (blue line in the right plot) and (2.16) (blue line in the left plot) as a function of the parameter ϵ for boundary conditions in the subset described by $\{\alpha = -\theta + \epsilon, \theta, n_1 = 1\}$. The numerical values are $T = 1$, $L = 0.1$, and $a = 0.025$.

As can be seen, for fixed values of T and L such that $TL \ll 1$, when ϵ is sufficiently small such that $k_0/T \ll 1$, the logarithm low temperature approximation (2.15) is much better than the standard

one. The standard low temperature approximation given by equation (2.16) is valid only when the boundary conditions are not so close to $\mathcal{M}_F^{(0)}$ for a given temperature, i.e., when $k_0/T > 1$. Therefore, it is clear that the low temperature bibliographic approximation in a neighbourhood of $\mathcal{M}_F^{(0)}$ needs to be refined.

The main conclusion of this analysis is that for a finite non zero low temperature ($TL \ll 1$), a new length scale (k_0/T) appears in the system, and it must be taken into account for establishing which fluctuations constitute a dominant contribution to the expansion of $\mathcal{M}_F$ at low temperatures and which do not. This new scale indicates how close or far the self-adjoint extension is to the zero mode line and whether the temperature can be considered high or low. Consequently, the self-adjoint extension corresponding to the boundary condition matrix U can be considered very close to $\mathcal{M}_F^{(0)}$ when $k_0/T \ll 1$. On the contrary, notice that for $T = 0$ the self-adjoint extension $-\Delta_U$ is very close to $\mathcal{M}_F^{(0)}$ when $\epsilon \to 0$ independently of the value of k_0, since there is no other length scale in the system.

The aforementioned low temperature expansion approximation is the result of a collaboration with J.M. Muñoz-Castañeda, M. Donaire and M. Tello-Fraile and it has been published in the Appendix of [140]. However, although this approximation is a collaborative work with other authors, the discussion has been included here for completeness.

High temperature expansion: $TL >> 1$

The high energy part of the one-particle states spectrum determines the expansion of the Helmholtz free energy in the limit $TL >> 1$ (see [15], [43] and [39]). By using zeta function regularisation[11] and following the method developed by M. Bordag *et al.* in [15], one could write the Helmholtz free energy as

$$\mathcal{F}(s) = A\, q_0 - \frac{1}{2}\frac{\partial}{\partial s}\left[\nu^s \int_0^\infty dt \frac{t^{s-1}}{\Gamma(s)} K_T(t) K_U^{(3)}(t) e^{-tm}\right], \tag{2.17}$$

with

$$K_T(t) = T + 2T\sum_{\ell=1}^{\infty} e^{-t\,\xi_\ell}, \qquad \xi_\ell = 2\pi T\ell. \tag{2.18}$$

Note that, in fact, what is being done above is to write the Matsubara representation using zeta regularisation. The heat trace for the self-adjoint extension $-\Delta_U$ is given by

$$K_U^{(3)}(t) = \sum_{\omega^2 \in \sigma(-\Delta_U)} e^{-t\omega}. \tag{2.19}$$

But since $\omega^2 = \vec{k}_\parallel^2 + k^2$, equation (2.19) factorises as

$$K_U^{(3)}(t) = K_\parallel^{(2)}(t)\; K_U^{(1)}(t), \tag{2.20}$$

[11] Once the whole computation is performed, the physical limit will be obtained by taking $s \to 0$. Notice that ν^s is an arbitrary factor introduced to keep the dimension of the free energy, since ν has dimension of mass. This factor is trivial when $s \to 0$.

being $K^{(2)}_{\|}(t)$ and $K^{(1)}_{U}(t)$ the heat traces for $-\Delta_{\mathbb{R}^2}$ and $-\Delta^{U}_{[0,L]}$, respectively[12]. Replacing (2.18) in (2.17) and performing the derivative of the first term with respect to s yields

$$\begin{aligned}\mathcal{F}(s) &= A\,q_0 - \frac{T}{2}\frac{\partial}{\partial s}\left[\nu^s\left(\zeta_{-\Delta_U}(s) + 2\int_0^\infty dt\frac{t^{s-1}}{\Gamma(s)}\sum_{\ell=1}^{\infty} e^{-t(m+\xi_\ell)}\,K^{(3)}_U(t)\right)\right]\\ &= A\,q_0 - \frac{T}{2}\nu^s\left(\zeta'_{-\Delta_U}(s) + \zeta_{-\Delta_U}(s)\log\nu\right) - T\frac{\partial}{\partial s}\left[\nu^s\int_0^\infty dt\frac{t^{s-1}}{\Gamma(s)}\sum_{\ell=1}^{\infty} e^{-t(m+\xi_\ell)}\,K^{(3)}_U(t)\right].\end{aligned}$$

But in the limit of high temperatures $TL\to\infty$, the last integral above is completely determined by the heat kernel expansion of $K^{(3)}_U(t)$ when $t\to 0$. Following the zeta regularisation method explained in Section 1.3, one could write the heat kernel (2.20) as a series expansion whose coefficients are the heat kernel ones:

$$K^{(3)}_U(t) = \left(\sum_{p=0,1/2,1\ldots}^{\infty} a_p\,t^{p-1}\,\nu^{p-1}\right)\left(\sum_{n=0,1/2,1\ldots}^{\infty} b_n\,t^{n-1/2}\,\nu^{n-1/2}\right).$$

Notice that $a_p\equiv a_p(-\Delta_{\mathbb{R}^2})$ and $b_n\equiv b_n(-\Delta^U_{[0,L]})$. Because the relation

$$\zeta_{\hat{K}}(s) = \frac{\nu^s}{\Gamma(s)}\int_0^\infty dt\; t^{s-1}\sum_{\lambda_n\in\sigma^*(\hat{K}/\nu^2)} e^{-\lambda_n t\nu}$$

holds, the heat kernel coefficients are basically the residues of the zeta function[13].

Consequently, the series expansion of $\mathcal{F}(s)$ at high temperatures can be expressed in terms of the heat kernel coefficients of $-\Delta_U$, i.e. in terms of products of heat kernel coefficients for $-\Delta_{\mathbb{R}^2}$ (collected in [39, 40]) and heat kernel coefficients of $-\Delta^U_{[0,L]}$ (computed in [43]) as

$$\begin{aligned}\mathcal{F}(s) &= A\,q_0 - T\frac{\partial}{\partial s}\left[\nu^s\int_0^\infty dt\frac{t^{s-1}}{\Gamma(s)}\left(\sum_{\ell=1}^{\infty} e^{-t(m+\xi_\ell)}\right)\left(\sum_{p,n=0,\frac{1}{2},1\ldots}^{\infty} a_p\,b_n t^{p+n-3/2}\nu^{p+n-3/2}\right)\right] + (\text{subdom. terms}\propto T)\\ &= A\,q_0 - T\frac{\partial}{\partial s}\left[\nu^s\sum_{\ell,p,n} a_p\,b_n\frac{\Gamma(-3/2+p+n+s)}{\Gamma(s)}(m+\xi_\ell)^{3/2-p-n-s}\nu^{p+n-3/2}\right] + (\text{subdom. terms}\propto T),\end{aligned}$$

as long as $m+\xi_\ell>0$ and $Re(s)>3/2-p-n$. Since the theory is massless, one could consider the limit $m\to 0$ and perform the summation involving the Matsubara frequencies in the parenthesis of the last equality to transform it into

$$-T\frac{\partial}{\partial s}\left[\nu^s\sum_{p,n} a_p\,b_n\frac{\Gamma(-3/2+p+n+s)}{\Gamma(s)}(2\pi T)^{3/2-p-n-s}\,\zeta_R(-3/2+p+n+s)\,\nu^{p+n-3/2}\right], \quad (2.21)$$

[12] The operator $-\Delta^U_{[0,L]}$ is the self-adjoint extension of $-d^2/dz^2$ over the interval $[0,L]$ associated to the boundary condition defined by $U\in\mathcal{M}_F$.

[13] More precisely, the heat kernel coefficients can be computed by means of

$$a_p = \text{Res}\left(\Gamma(s)\zeta_{-\Delta_{\mathbb{R}^2}}(s)\right)\Big|_{s=1-p}, \qquad b_n = \text{Res}\left(\Gamma(s)\zeta_{-\Delta^U_{[0,L]}}(s)\right)\Big|_{s=1/2-n}.$$

where ζ_R is the Riemann zeta function. Finally, one could make the derivative with respect to s and take the physical limit $s \to 0$. However, for doing that one needs to take into account the analytic continuation of $\zeta_R(s)$ and the gamma functions in a neighbourhood of the point $s = 0$.

The derivation of a closed formula for $\mathcal{F}(0)$ is left for further investigation. What does seem clear is that the dominant terms at high temperatures will include only the following heat kernel coefficients[14]: $b_0, b_{1/2}, b_1, a_0, a_1$. Moreover, the physics behind this asymptotic approximation at high temperatures can be discussed at this point. The total Helmholtz free energy at high temperatures can be written as

$$\mathcal{F}(0) = E_0^{ren} + E_0^{div} + \Delta_T\mathcal{F} = E_0^{ren} + E_0^{div} - A\,\frac{\zeta(3)}{2\pi}T^3 + c_{5/2}T^{5/2} + c_2T^2 + (\text{subdominant terms}),$$

where E_0^{ren} is given by (2.2) and E_0^{div} includes the dominant divergence associated to the bulk explained throughout this chapter. Notice that c_i are coefficients which do not depend on the temperature. They have dimensions of L^{i-1}. As previously mentioned, $\Delta_T\mathcal{F}$ is finite and does not include any divergent term. When expanding it in terms of T, the dominant term is cubic in the temperature, which was to be expected given the discussion on pages 39 and 40. The rest of the terms in the expansion will have lower powers of the temperature and will give rise to less and less relevant terms in the present approximation. It is important to highlight that the quartic T-dependent contribution that appears in the analogous expansion in [15] is the Planck's black-body radiation. This term would become a subdominant divergence which must be removed when treating with objects with infinite area, as is the case for the plates considered in this chapter.

[14] On smooth compact Riemannian manifolds of dimension n without boundaries, such as $\mathbb{R}^2$, there exists a heat kernel expansion at $t \to 0$ given by $\mathrm{Tr}_{L^2}(fe^{-tD}) = \sum_{k\gg 0} t^{(k-n)/2}a_k(f, D)$ for any smooth function f and a Laplace-type operator D. The coefficients with odd index vanish and the rest can be computed in terms of geometric invariants. That is the reason that only the coefficient a_0, a_1 is going to be relevant in the approximation at high temperatures. On the other hand, the heat kernel coefficients $b_0, b_{1/2}, b_1$ for $-\Delta^U_{[0,L]}$ only depend on the boundary condition parameters α, θ.

Chapter 3

SCALAR FIELDS IN PERIODIC BACKGROUNDS

In Quantum Field Theory, phonons can be modelled by a quantum scalar field. In this chapter the one-loop quantum corrections to the internal energy of some crystals due to the quantum fluctuations of the phonon field will be studied. The band spectrum will be characterised allowing to compute the total Helmholtz free energy and the entropy at finite non zero temperature by using the techniques developed in Chapter 2.

In particular, two different types of one-dimensional periodic potentials built from the repetition of the same compact supported potential will be addressed. On the one hand, a generalisation of the *Kronig-Penny model* (the compact supported potential will be a combination of Dirac delta potentials and its first derivative) will be analysed. The *Kronig-Penny model* is widely used in Solid State Physics to describe how an electron moves in a rectangular barrier-type lattice [141]. On the other hand, the *Pöschl-Teller comb* (where the potential with compact support is a spatially truncated kink) will be studied. Both cases are examples of systems that can be exactly solved, at least in one dimension. Finally, in Section 3.4 higher dimensional lattices will be handled.

In references [142–144] one could find a problem similar to the one which is going to be addressed in this chapter but for fermions. In these works, the authors studied an electron in a periodic one-dimensional chain of atoms modelled by an infinite periodic potential of Dirac δ with different coefficients inside the unit cell. That model was used by Cerveró *et al.* to study quantum wire band structures and Anderson localisation[1] [145]. The authors proved that the physical properties of the wire depend on the couplings of the different species of δ potentials, their concentration and the presence of short-range correlations in the structure, which affect the transport properties. What is interesting in this example is that although there are signature properties due to the presence of electrons that could not be studied when considering phonons, their treatment for characterising the spectra from a secular function is completely analogous to the one that will be presented here.

[1] When considering the tight binding approximation in a crystal, in which the electrons can hop from atom to atom subject to an external random potential, the system could loose all its conductivity properties for large enough disorder and become an insulator. The electrons thus become trapped due to the external extensive disorder. This effect is called Anderson localisation.

3.1. Analysis of the spectrum

Consider a 1D lattice represented by a periodic potential $U(z)$ built from the repetition of another potential $V(z)$, which stands at the lattice nodes na and vanishes outside small intervals of the form $[na-\epsilon/2, na+\epsilon/2]$ included in the unit cell $[na-a/2, na+a/2]$, i.e.

$$U(z)=\sum_{n\in\mathbb{Z}} V(z-na), \qquad \text{being} \qquad V(z)\begin{cases} \neq 0 & \text{if } |z|\leq \epsilon/2, \\ = 0 & \text{if } |z|>\epsilon/2, \end{cases} \tag{3.1}$$

with[2] $a \geq \epsilon > 0$. The action of a massless scalar field in 1+1 dimensions in such a periodic background is given by

$$S[\phi]=\frac{1}{2}\int dx^{1+1}\left[(\partial\phi)^2-U(z)\phi^2\right].$$

The dimensionless time independent (i.e. after Fourier transform) Schrödinger equation for the one-particle states of the quantum scalar field in the comb is:

$$\left(-\frac{\partial^2}{\partial z^2}+U(z)\right)\phi_\omega(z)=\omega^2\phi_\omega(z),$$

where $\omega = k$ are the frequencies of the quantum field modes $\omega \in \sigma(-\partial_z^2+U(z))$. Given the one particle states Schrödinger operator,

$$\hat{K}=-\frac{d^2}{dz^2}+U(z), \tag{3.2}$$

the band spectrum of the lattice can be written in terms of the transmission amplitude $t(k)$, and the reflection amplitudes[3] $r_L(k)$ and $r_R(k)$ for the scattering problem related to the Schrödinger operator of the compact supported potential from which the comb is built:

$$\hat{H}_V=-\frac{d^2}{dz^2}+V(z). \tag{3.3}$$

From the scattering problem $\hat{H}_V\psi_k(z)=k^2\psi_k(z)$ with $k^2>\mathbb{R}^+$, two independent scattering solutions can be found. For $n=0$ they can be written as:

$$\psi_k^R(z)=\begin{cases} e^{-ikz}r_R(k)+e^{ikz}, & z<-\frac{\epsilon}{2} \\ C_R(k)f_k(z)+D_R(k)f_{-k}(z), & -\frac{\epsilon}{2}<z<\frac{\epsilon}{2} \\ t_R(k)e^{ikz}, & z>\frac{\epsilon}{2} \end{cases} ; \quad \psi_k^L(z)=\begin{cases} t_L(k)e^{-ikz}, & z<-\frac{\epsilon}{2} \\ C_L(k)f_k(z)+D_L(k)f_{-k}(z), & -\frac{\epsilon}{2}<z<\frac{\epsilon}{2} \\ e^{ikz}r_L(k)+e^{-ikz}, & z>\frac{\epsilon}{2} \end{cases}.$$

Notice that $f_{\pm k}(z)$ are eigenfunctions of $-\partial_z^2+V(z)$ for non-constant $V(z)$. Talking about scattering for the potential $U(z)$ is meaningless because these two solutions of scattering ψ_k^R, ψ_k^L can be defined only for potentials with compact support which reduce to zero for asymptotic values of the coordinate, and $U(z)$ is not among them. Nevertheless, this is exactly what happens if one considers only

[2] Here a is the lattice spacing and ϵ represents the compact support of the potential that forms the comb.
[3] The index R refers to incoming particles from the left and L in the opposite direction.

one potential $V(z)$, from which the comb is built, alone in the whole real line. Scattering here does make sense. The scattering solutions for $V(z)$ will then be used to determine the Bloch waves of the whole lattice and to compute the spectrum as a function of the scattering data, in a very convenient way. Moreover, the compact support of $V(z)$ guarantees that all the scattering amplitudes are meromorphic functions over the complex k-plane and that the asymptotic behaviour of the scattering solutions extends to the whole real line except at the interval $[-\epsilon/2, \epsilon/2]$ (see [98]). In the aforementioned interval the solution is the superposition of plane waves with opposite wave vector. Moreover, the time reversal symmetry of the Schrödinger operator ensures that $t_R(k) = t_L(k) = t(k)$.

On any interval of the form $\{z \in [na - a/2, na + a/2] \quad | \quad z \notin [na - \epsilon/2, na + \epsilon/2]\}$ the Bloch waves[4] are linear combinations of the two scattering solutions centred at the lattice node na:

$$\psi_{k,n}(z) = A_n \psi_k^R(z - na) + B_n \psi_k^L(z - na).$$

Imposing the Floquet-Bloch periodicity conditions

$$\psi_q(z + a) = e^{iqa} \psi_q(z), \qquad \partial_y \psi_q(y)|_{y=z+a} = e^{iqa}\, \partial_y \psi_q(y)|_{y=z}, \tag{3.4}$$

for the eigenfunctions of $\hat{K}$ (with any quasi momentum q in the first Brillouin zone[5]) at the boundary point of the primitive cell $z = na - a/2$ yields

$$\begin{pmatrix} \psi_k^R(a/2) - e^{iqa}\psi_k^R(-a/2) & \psi_k^L(a/2) - e^{iqa}\psi_k^L(-a/2) \\ \partial\psi_k^R(a/2) - e^{iqa}\partial\psi_k^R(-a/2) & \partial\psi_k^L(a/2) - e^{iqa}\partial\psi_k^L(-a/2) \end{pmatrix} \begin{pmatrix} A_0 \\ B_0 \end{pmatrix} = 0\,, \tag{3.5}$$

for the cell indexed by $n = 0$.

At this point it is necessary to reinterpret the quantum system of the comb as a one-parameter family of Hamiltonians defined over the finite primitive cell interval, by using general quantum boundary conditions and following the formalism described in [34]. If the origin of the real line is chosen in a way that it is coincident with one of the lattice potential nodes, then it is enough to study the quantum mechanical system characterised by the quantum Hamiltonian $\hat{H}_V$ (3.3) defined over the closed interval $[-a/2, a/2]$, being a the lattice spacing. $\hat{H}_V$ is not essentially self-adjoint when is defined over the square integrable functions over the closed interval $[-a/2, a/2]$, but it admits an infinite set of self-adjoint extensions whose domain is

[4]The Bloch theorem [146] states that the solution of the Schrödinger equation for a periodic potential $V(r)$ is a plane wave modulated by a function $u(r)$ with the same periodicity of the potential, i.e. $\psi(r) = e^{ikr}u(r)$ being r the position and k the wave vector for a constant potential. In Solid State Physics [147] the theorem ensures that knowing the wavefunction in the primitive cell is equivalent to its knowledge in the whole crystal. The wave function only acquires a phase involving the quasi-momentum when passing from one primitive cell to another, i.e. when the translational invariance in the comb is applied.

[5]The first Brillouin zone is the locus of points in the reciprocal lattice that are closer to its origin than they are to another point in the lattice. It is the primitive cell in the reciprocal space and it is uniquely defined.

$$\mathcal{D}_{\hat{H}_V}=\left\{\psi\in L^2\left[-\frac{a}{2}',\frac{a}{2}\right] \;\middle|\; \begin{pmatrix}\psi(-a/2)+i\psi'(-a/2)\\ \psi(a/2)-i\psi'(a/2)\end{pmatrix}=U\begin{pmatrix}\psi(-a/2)-i\psi'(-a/2)\\ \psi(a/2)+i\psi'(a/2)\end{pmatrix}\right\}, \tag{3.6}$$

where $U\in SU(2)$. If in addition such boundary conditions at the extremal points of the unit cell ensures that the domain of the corresponding self-adjoint extension is a set of wave functions that satisfy Bloch's semi-periodicity condition, then the comb can be interpreted as a one-parameter family of self-adjoint extensions where the parameter is the quasi-momentum. In other words, when using the unitary matrix

$$U_B=\begin{pmatrix}0 & e^{i\theta}\\ e^{-i\theta} & 0\end{pmatrix} \tag{3.7}$$

to define the self-adjoint extensions of $\hat{H}_V$, one could recover the Bloch semi-periodicity condition (3.4) from the boundary conditions in (3.6). This approach enables to interpret the comb as a one-parameter family of quantum pistons [148–150] where

1. The middle piston membrane is represented by the individual potential $V(z)$ given in (3.1) placed at the middle point of the primitive cell.

2. The extremal points of the primitive cell correspond to the external walls of the piston placed at $z=na\pm a/2$. The quantum field satisfies the one-parameter family of quantum boundary conditions depending on the parameter $\theta=-qa$ given by the unitary matrix U_B in (3.7). θ is thus related to the quasi-momentum of the Bloch wave.

The existence of non trivial solutions for the coefficients A_0, B_0 in (3.5) requires that the determinant of the matrix vanishes. The real solutions of the resulting spectral equation

$$\begin{aligned} &f_\theta(k)\equiv\cos(\theta)-h_V(k)=0, \qquad \text{with} \qquad \theta\in[-\pi/\pi],\\ &\text{and} \qquad h_V(k)=\frac{1}{2t(k)}\left[e^{-ika}+e^{ika}(t^2(k)-r_R(k)r_L(k))\right], \end{aligned} \tag{3.8}$$

determine the energy levels of the crystal. Hence, the band spectrum arises as the different branches $E(q)$ of the equation $f_{-qa}(k=\sqrt{E})=0$ for $q\in[-\pi/a,\pi/a]$. Since $\cos(\theta)$ in (3.8) is a bounded function and consequently

$$|h_V(k)|\leq 1,$$

the energy spectrum of the system is organised into allowed and forbidden energy bands and gaps. Additionally, the discrete set of wave vectors satisfying $\{k_i\in\mathbb{R}\,/\,|h_V(k_i)|=1\}$ determines the lower and higher values of k for each allowed band. The band spectrum disappears in two special cases:

1. If the compact potential $V(z)$ in (3.1) is opaque (i.e. $t(k)=0$), the band spectrum becomes the discrete energy spectrum of a square well with opaque edges.

2. If $V(z)$ in (3.1) is transparent (i.e. $|t(k)| = 1$), the spectrum coincides with the gapless free particle spectrum. Actually, the spectrum of the free particle constitutes only one band of infinite width.

So far the attention has been focused on the positive energy band spectrum. This spectrum of positive energy bands contains an infinite number of allowed bands, since an effective model of an infinite linear chain is considered. However, it is worth stressing that the possible solutions of (3.8) for imaginary momenta ($k = i\kappa$, with $\kappa > 0$) so that the energy is negative ($E = -\kappa^2$) form negative energy bands. Again, the allowed energies for these bands satisfy $|h_V(k = i\kappa)| \leq 1$.

All the characterisation of the spectrum described in this section applies for any comb built as a repetition of a potential with compact support smaller than the lattice spacing sitting at the lattice nodes. Hereafter, two different types of such a potential will be considered: one contact potential (the *generalised Dirac comb*) and another one with extended compact support (the *Pöschl-Teller comb*).

3.1.1. Generalised Dirac comb

The so called *Dirac comb* is a variation of the *Kronig-Penney model* in which the rectangular barriers (or wells) transform into Dirac delta potentials with positive (or negative) coefficients. Dirac delta potentials are widely used as toy models for realistic materials like quantum wires [142], and to analyse physical phenomena such as Bose-Einstein condensation in periodic backgrounds [151] or light propagation in 1D relativistic dielectric superlattices [152]. Despite being a rather simple idealisation of the real system, the δ function has been proved to correctly represent surface interactions in many models related to the Casimir effect. For instance, Dirac δ functions have been set on the plates as models of the electrostatic potential [153], to represent two finite-width mirrors [154], or to describe the permittivity and magnetic permeability in an electromagnetic context, by associating them to the plasma frequency in Barton's model on spherical shells [155, 156]. On the other hand, the first derivative of the delta potential has been used by M. Bordag in the study of monoatomically thin polarisable plates formed by lattices of dipoles. In fact, the δ' potentials appear in the interaction between the orthogonal polarisability of the monoatomically thin plate and the electromagnetic field [157]. The δ' potential has also been used to study resonances in 1D oscillators [158], to mention just a few of applications.

The *generalised Dirac comb* is built as a repetition of the following potential with compact support smaller than the lattice spacing:

$$V_{\delta\delta'}(z) = w_0\delta(z) + 2w_1\delta'(z), \qquad w_0, w_1 \in \mathbb{R}. \tag{3.9}$$

The non relativistic Schrödinger operator for the above δ-δ' point interaction potential is given by $\hat{K}_{\delta\delta'} = -\partial_z^2 + w_0\delta(z) + 2w_1\delta'(z)$ and it acts on the Sobolev space of second class [159]. The definition of the first derivative of the Dirac delta here must be understood in the following sense: the operator $\hat{K} = -\partial_z^2$ acting on functions $\phi \in W_2^2$ in the finite interval $I_n = [na - a/2, na + a/2]$ defined by the unit cell is not essentially self-adjoint. However, it admits an infinite set of self-adjoint extensions

$\hat{K}_{\delta\delta'}$, whose domain is given by the set of functions satisfying the following matching conditions related to the couplings of the δ-δ' potential

$$\mathcal{D}_{\delta\delta'} = \left\{ \phi \in W_2^2(I_n, \mathbb{C}) \quad \middle| \quad \begin{pmatrix} \phi(na)^+ \\ \phi'(na)^+ \end{pmatrix} = \begin{pmatrix} \frac{1+w_1}{1-w_1} & 0 \\ \frac{w_0}{1-w_1^2} & \frac{1-w_1}{1+w_1} \end{pmatrix} \begin{pmatrix} \phi(na)^- \\ \phi'(na)^- \end{pmatrix} \right\}, \tag{3.10}$$

being $\phi(na)^{\pm} = \lim_{z \to (na)^{\pm}} \phi(z)$.

As previously mentioned, the band spectrum can be analysed by means of the scattering data of the potential $V(z)$ and the spectral equation (3.8). The scattering data for $V_{\delta\delta'}$ (3.9) was previously studied in [159]:

$$t(k) = \frac{2(1-w_1^2)k}{2(1+w_1^2)k + iw_0}, \qquad r_R(k) = -\frac{4kw_1 + iw_0}{2(1+w_1^2)k + iw_0}, \qquad r_L(k) = \frac{4kw_1 - iw_0}{2(1+w_1^2)k + iw_0}.$$

Plugging these coefficients into equation (3.8) yields the secular equation:

$$f_q^{Dc}(\Omega, \gamma, k, a) \equiv \Omega \cos(qa) + \cos(ka) + \frac{\gamma}{2}\frac{\sin(ka)}{k} = 0, \qquad \text{with} \quad \gamma = \frac{w_0}{1+w_1^2}, \ \Omega = \frac{w_1^2 - 1}{w_1^2 + 1}. \tag{3.11}$$

Once the spectral equation is solved numerically with *Mathematica*, one can evaluate the energy of the allowed bands by means of $E = k^2$. Two different cases arise depending on the values of the couplings w_0, w_1: situations in which there is a negative energy band[6] of localised states (because if $w_0 < 0$ the δ-δ' potential admits one bound state) and occasions in which the lowest energy band is positive and the phonons propagate freely along the crystal as plane waves. Figure 3.1 allows the comparison between the first two allowed energy bands for the pure Dirac comb ($w_1 = 0$) and for the generalised Dirac comb.

It is well-known that for spin 1/2 fermionic carriers in crystals, depending on the existence or not of a gap between the negative energy band and the first positive one, the charge carriers could spontaneously go or not from localised states of negative energy to propagating states of positive energy. The first situation corresponds to a conductor behaviour if the lowest energy band is not completely filled. The second case above described represents a semiconductor or insulator behaviour (depending on the size of the gap) whenever the valence band is completely filled. Notice that when there are many charge carriers, the Dirac-Fermi statistics must be introduced in the analysis. However, in the problem present in this chapter, only scalar fields are involved. Since their vibrational spectrum has been studied, and due to the Bose-Einstein statistic, all the modes of the spectrum are available to be occupied by bosons without any restriction as to their number. One cannot talk about valence and conducting bands separated by a gap of prohibited energy because the way in which modes are occupied is completely different from the fermionic case. What really happens in the bosonic case is that certain frequencies are forbidden for phonon propagation. This is how these band spectra are to

[6] Whenever there is a negative energy band, the QFT ceases to be unitary and absorption phenomena in quantum wires can be studied at zero and non zero temperature.

be interpreted in this chapter.

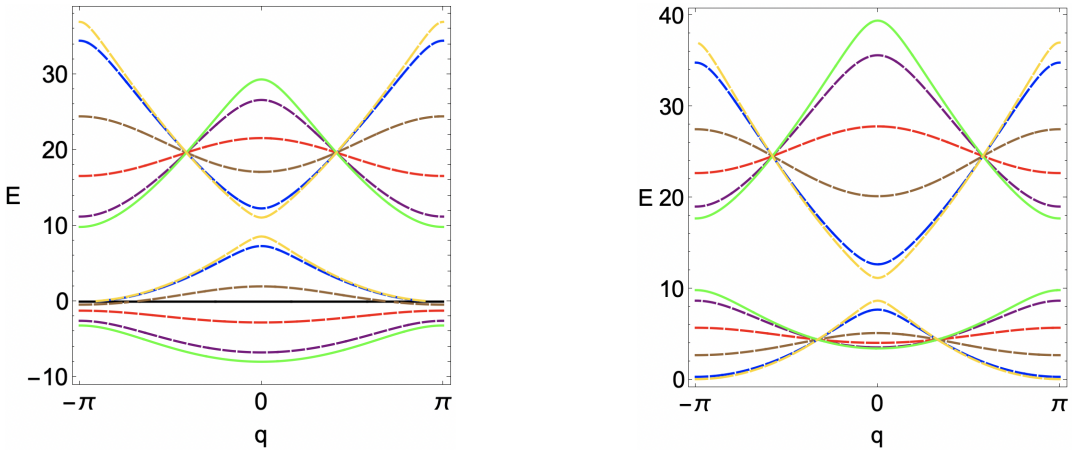

FIGURE 3.1: First two allowed energy bands for the pure Dirac comb (solid green curve) and the generalised Dirac comb (dashed lines). On the left $w_0 = -5$ for all the cases and on the right $w_0 = 5$. In both plots $w_1 = 0.3$ (purple), $w_1 = 0.75$ (red), $w_1 = 1.5$ (brown), $w_1 = 5$ (blue) and $w_1 = -10$ (yellow). The black line in the left plot represents the zero energy level. In these plots $a = 1$ and $E = k^2$.

Concerning the two graphs of Figure 3.1 and the spectrum of the comb, there are some caveats that are worth highlighting:

- If $w_1 = \pm 1$, the width of the allowed energy bands are zero and a discrete spectrum is recovered. This discrete spectrum coincides with the fixed points of the n-th allowed energy band for other values of w_0, w_1. The fixed points are given by $f_q^{Dc}(\Omega = 0, \gamma = w_0/2, k, a) = 0$, i.e. by

$$\frac{\tan\left(a\sqrt{E}\right)}{\sqrt{E}} = -\frac{4}{w_0}.$$

- For a fixed value of w_0, if $|w_1| \to \infty$ the forbidden energy bands disappear and the system behaves as a free particle on the real line. In this limit, the scattering potential due to the δ-δ' potential becomes almost transparent.

- When $w_0 > 0$, the appearance of a δ' term shifts the maximum and minimum energy of each band. If $w_0 > 0$, there are no negative energy bands even if one takes $w_1 \ll 0$.

- In all cases, the introduction of the δ' term changes the absolute value of the curvature of the allowed energy bands. Whenever $|w_1| < 1$, the sign of the curvature of the allowed energy bands is the same as in the Dirac δ comb case whereas when $|w_1| > 1$, it changes with respect to the Dirac δ comb case.

A rather comprehensive analysis of the density of states and the spectrum of some generalised Dirac combs has been published in [160] but it goes beyond the scope of this chapter. In fact, I have published part of the results collected in Section 3.1 so far in [160–162]. However, the band spectra for the Pöschl-Teller comb which is going to appear in the following subsection is original work, not

yet published.

3.1.2. Pöschl-Teller comb

The Pöschl-Teller potential [163] is known to have application in a variety of areas in physics such as astrophysics, quantum many-body systems or supersymmetric quantum mechanics but also in condensed matter. For instance, it has been employed in [164] to numerically represent potential barriers in bilayer graphene. In [165] the relativistic one-dimensional Pöschl-Teller potential problem has been studied to describe graphene waveguides. Another promising example is given in [166] where quantum wells[7] mimicked by Pöschl-Teller confining potentials are considered to calculate intersubband absorption and other nonlinear optical properties. It seems to be possible to create this type of quantum wells with the recent nanotechnology progress. The spectra of bound, antibound or resonance states of different types of Pöschl-Teller potentials (potential wells, low and high barriers) have been studied in [169], allowing the authors to also build supersymmetric partners. It is worth mentioning that only the Pöschl-Teller well is the focus of this section.

The *Pöschl-Teller comb* is built as a repetition of the following potential with compact support ϵ smaller than the lattice spacing a:

$$V_{PT}(z) = -\frac{2\Theta(-z+\epsilon/2)\Theta(z+\epsilon/2)}{\cosh^2(z)}, \tag{3.12}$$

being $\Theta(z)$ the Heaviside function. Following [170], the scattering coefficients for $V_{PT}(z)$ are

$$\begin{aligned} r(k) &= \frac{e^{i\epsilon k}\Lambda(\Lambda+2k(k+i\tanh(\epsilon/2)))}{\Delta(k)} - \frac{e^{-i\epsilon k}\Lambda(\Lambda+2k(k-i\tanh(\epsilon/2)))}{\Delta(k)}, \\ t(k) &= \frac{4k^2(k^2+1)}{\Delta(k)}, \qquad \Delta(k) = -e^{2i\epsilon k}\Lambda^2 + [\Lambda+2k(k-i\tanh(\epsilon/2))]^2, \end{aligned} \tag{3.13}$$

with $\Lambda = 1-\tanh^2(\epsilon/2)$. Notice that $r_R(k) = r_L(k) = r(k)$ due to the parity symmetry of the potential. The poles $k = i\kappa$ with $\kappa > 0$ of the determinant of the scattering matrix ($\det S = t^2 - r_R r_L$) are the bound states of the kink-comb spectrum. In this comb, the well known state of the kink potential with $k = i$ is not a bound state.

Once more, the allowed bands are determined by the real solutions of the spectral equation (obtained by replacing (3.13) into (3.8)), which takes the form

$$\begin{aligned} & f_q^{PTc}(a,k,\epsilon) \equiv \cos(qa) - \frac{\Sigma\cos(ka) - \Upsilon\sin(ka)}{k^2(k^2+1)(1+\cosh\epsilon)} = 0, \qquad \text{with} \\ & \Upsilon = 2k\tanh\left(\frac{\epsilon}{2}\right)(1+k^2+k^2\cosh(\epsilon)) + \Lambda\cos(k\epsilon)\sin(k\epsilon), \qquad \text{and} \\ & \Sigma = k^2(3+k^2) + k^2(-1+k^2)\cosh(\epsilon) + \Lambda\sin^2(k\epsilon). \end{aligned} \tag{3.14}$$

[7] Quantum wells are structures consisting of alternating thin layers of semiconductors with different band-gaps. They can confine particles in the dimension perpendicular to the layer surface, whereas the movement in the other dimensions is not restricted. The concept was proposed by H. Kroemer [167] and by Z. Alferov and R.F. Kazarinov [168] in the mid-1960s.

In Figure 3.2 the two lowest energy bands of the Pöschl-Teller comb are shown for different values of the unit cell size.

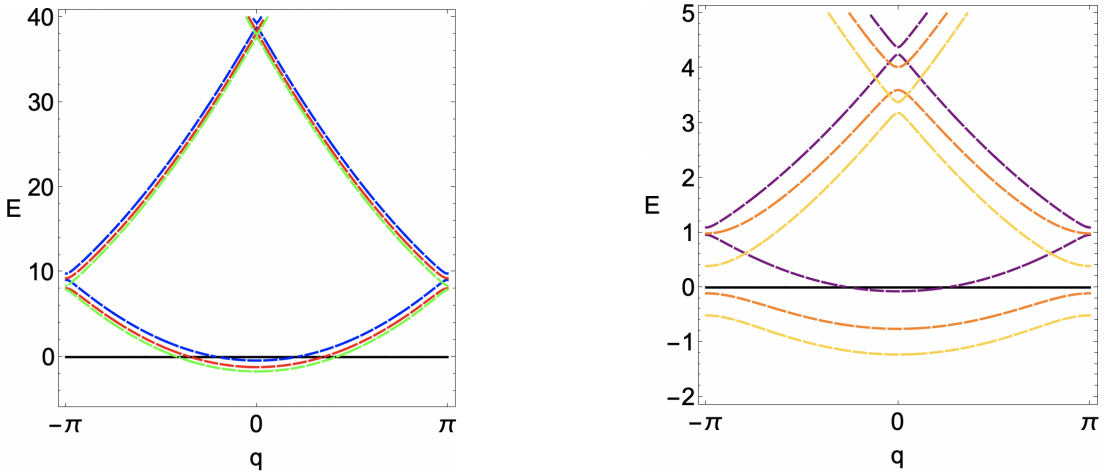

FIGURE 3.2: Left: First two allowed energy bands for the Pöschl-Teller comb for $a = 1$ and different values of the compact support $\epsilon = 0.2$ (blue), $\epsilon = 0.6$ (red) and $\epsilon = 0.9$ (green). Right: First two allowed bands for $a = 3$ as a function of the compact support $\epsilon = 0.1$ (purple), $\epsilon = 1$ (orange) and $\epsilon = 2.5$ (yellow). In these plots $E = k^2$.

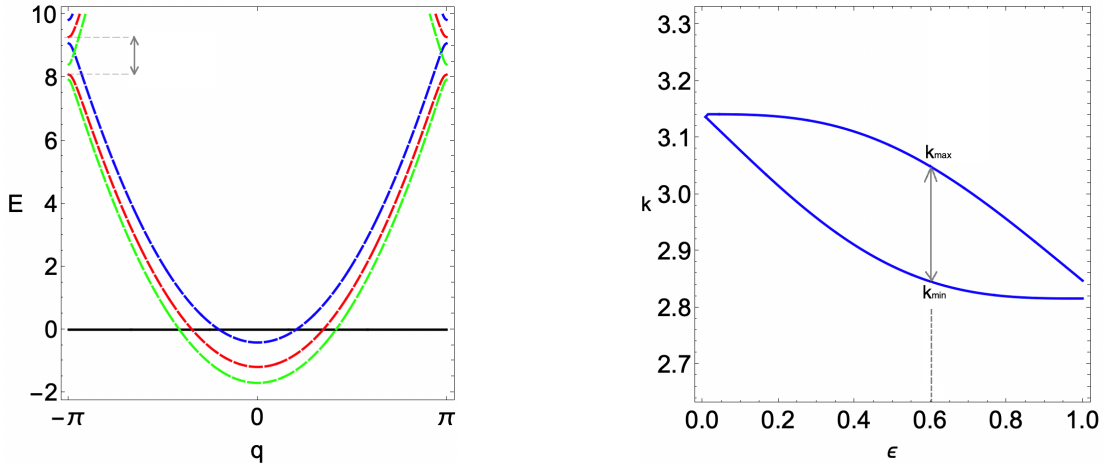

FIGURE 3.3: Left: Zoom of the first band for $a = 1$. Right: Gap size at $q = \pm\pi$ between the first two allowed bands for $a = 1$ as a function of the compact support. The gray arrow denotes the length of the gap between allowed bands. k_{min} and k_{max} are the solutions of equation (3.15).

As there can be seen in Figure 3.3, whenever $a > \epsilon > 0$, there is gap between the maximum value of the energy in the first band and the minimum of the second band for $a = 1$. Both values of the energy can be obtained by solving the equation $\cos(qa) - h_V(k, a, \epsilon) = 0$ for $q = -\pi$, $a = 1$ and $\sqrt{7} < k < \sqrt{14}$, that is:

$$h_V(k, 1, \epsilon) = -1, \qquad \text{for} \qquad \sqrt{7} < k < \sqrt{14}. \tag{3.15}$$

The length of this gap (indicated by the gray arrows in Figure 3.3) varies with the value of the compact support ϵ in a non monotonically way. Firstly, the length increases while ϵ does just until a critical value $\epsilon_{cr} = 0.5105$, from which the length of the gap decreases again, as is shown in Figure 3.3. Only for $\epsilon = 0$ one recovers a comb in the plain real line, without any potential in the middle of the piston.

Consequently, the band spectrum no longer appears. Moreover, from the left graph in Figure 3.2 it is clear that the kink comb has a band with negative energy. This comes from the fact that the potential (3.12) has always one bound state with momentum $k = i\kappa$, being $0 < \kappa < 1$ for $a = 1$. If a increases, there is still a negative energy band for any value of the compact support ϵ, as shown in Figure 3.2 right. It will be crucial to take this fact into account when calculating the vacuum energy of this system in the corresponding QFT.

3.2. Vacuum energy at zero temperature

Once the non relativistic quantum mechanical problem has been solved, one could perform the second quantisation of the fields to focus on computing some relevant magnitudes of the associated QFT. In the periodic structure (3.1), E_0 physically gives the phonon contribution to the internal pressure of the chain if one interprets the quantum scalar field as phonons in the crystal. Hence, E_0 enables to study the dilatation or reduction of the primitive cells in the lattice due to the fluctuations of the phonons.

The quantum vacuum energy per unit cell of the comb E_0 will be computed by using the spectral zeta function, instead of calculating the Green's function of the quantum field on the crystal and the energy density $\langle 0| T_{00} |0\rangle$ per unit length within a unit cell. The zeta function method, explained in detail in Chapter 1, allows to subtract the infinite self-energy of the individual potential that makes up the comb and the fluctuations of the field in the background. In order to perform the summation over the spectrum of the comb:

$$E_0^{comb} = \frac{1}{2} \sum_{\omega^2 \in \sigma(\hat{K}_{comb})} \omega = \frac{1}{2\nu} \sum_{bands} \int_{\sqrt{\epsilon_{min}^{(n)}}}^{\sqrt{\epsilon_{max}^{(n)}}} dkk = \frac{1}{2} \lim_{s \to 0} \nu \, \zeta_{\hat{K}}^{comb} \left(s - \frac{1}{2} \right), \tag{3.16}$$

equation (1.21) can be applied but replacing the phase shift by the spectral function $f_\theta(k)$ defined in (3.8). Note that the $1/2$ factor in the equation above appears because a real scalar field is being considered. Furthermore, performing the summation over eigenvalues by using the residue theorem is useful because in general the secular equation cannot be solved.

In the reinterpretation of the comb as a one parameter family of self-adjoint extensions, for a fixed value of the parameter $q \in [-\pi/a, \pi/a]$, the spectral equation $f_q(k) = 0$ gives a discrete set of values of k in one-to-one correspondence with $\mathbb{N}$. Then, when q takes values from $-\pi/a$ to π/a, the allowed energy bands arise when putting together all the discrete spectra obtained by $f_q(k) = 0$. Consequently, and due to the definition of the spectral function in (3.8), it is clear that the scattering amplitudes for a single potential of compact support over the real line is all that is needed to carry on the computation of the quantum vacuum energy of the comb.

The spectral zeta function corresponding to the Schrödinger Hamiltonian of the comb (3.2) is

$$\zeta^{comb}(s) = \frac{a}{2\pi} \int_{-\pi/a}^{\pi/a} dq \, \zeta_q(s), \tag{3.17}$$

or which is the same,

$$\zeta^{comb}(s) = \frac{a}{2\pi}\int_{-\pi/a}^{\pi/a} dq \frac{\sin(\pi s)}{\pi}\int_0^\infty dk k^{-2s}\nu^{2s}\partial_k \log f_q(ik). \tag{3.18}$$

From this equation, some conclusions can be drawn. Firstly, equation (3.18) implies that the zeta function of a comb is the continuous sum of zeta functions over the dual primitive cell of Bloch quasi-momenta. Secondly, the finite Casimir energy per unit cell of the comb,

$$E_0^{comb} = -\frac{1}{2}\lim_{s\to 0}\nu^{2s}\frac{a}{2\pi}\int_{-\pi/a}^{\pi/a} dq \frac{\cos(\pi s)}{\pi}\int_0^\infty dk k^{1-2s}\partial_k \log f_q(ik) = \frac{a}{2\pi}\int_{-\pi/a}^{\pi/a} dq\, E_0^V(q), \tag{3.19}$$

is the summation over the quasi momentum of all the discrete spectra characterised by $f_\theta(k) = 0$ that arises for each value of the parameter θ. That is, the finite quantum vacuum energy of the comb E_0^{comb} can be obtained from the finite quantum vacuum energy $E_0^V(q)$ of the quantum scalar field confined between two plates placed at $z = \pm a/2$ represented by the boundary condition associated to (3.7), and under the influence of the individual potential that forms the comb $V(z)$(3.1) placed at $z = 0$.

Whenever there are no states with negative energy in the spectrum of the comb, $E_0^V(q)$ can be computed by means of (1.29), replacing the distance between plates by the lattice spacing. Furthermore, from (2.2) it is clear that $h_U^\infty(ik) = \lim_{L_0\to\infty} h_u(ik, L_0)/e^{kL_0}$. Evaluating this limit in an analogous way for the secular function of the comb (3.8) yields:

$$\lim_{a_0\to\infty}\frac{f_\theta(ik)}{e^{ka_0}} = \lim_{a_0\to\infty} e^{-ka_0}\cos\theta - \frac{1}{2t(ik)}\left(1 + e^{-2ka_0}(t^2(ik) - r_R(ik)r_L(ik)\right) = -\frac{1}{2t(ik)}.$$

In this way, one can rewrite $E_0^V(\theta)$ from formula (2.2) as

$$E_0^V(\theta) = -\frac{1}{2\pi}\int_0^\infty dk\, k\left[-L + \frac{d}{dk}\log(f_\theta(ik)) + \frac{d}{dk}\log(t(ik))\right]. \tag{3.20}$$

It is important to mention that the zero point energy has been assumed to be the one of a free quantum scalar field over the real line when the potentials of compact support of the primitive cells are identically zero, i.e. when $\{t(k) = 1, r_R(k) = 0, r_L(k) = 0\}$. In this case, the scalar quantum vacuum interaction energy between two plates mimicked by quasiperiodic boundary conditions is neither zero not infinite (see [34] and [171]) but

$$E_0(\theta) = \frac{1}{2a}\left(|\theta| - \frac{\theta^2}{2\pi} - \frac{\pi}{3}\right), \tag{3.21}$$

and consequently:

$$E_0^{comb}(t = 1, r_R = 0, r_L = 0) = \int_{-\pi}^{\pi}\frac{d\theta}{2\pi}E_0(\theta) = 0, \tag{3.22}$$

as it should be. This is because when the compact support potential $V(z)$ is zero, a quantum scalar field in the real line with Bloch periodicity conditions remains. But its energy is the same as the energy of the free scalar field on the real line (i.e. zero), since any plane wave on the real line satisfies

Bloch periodicity.

Part of the discussion I make in this section, as well as the example of Subsection 3.2.1, have been included in [133, 172]. On the contrary, the results that will be shown in 3.2.2 are original work, not yet published.

3.2.1. Generalised Dirac comb

The quantum vacuum energy of the *generalised Dirac comb* is obtained from equation (1.29) by using the spectral function (3.11) and after taking the limit $a_0 \to \infty$. The resulting expression is

$$E_0^{\delta\delta' \text{comb}} = \int_{-\pi}^{\pi} \frac{d\theta}{4\pi^2} \int_0^{\infty} dk \left(\frac{A(k)}{B(k) + C(k)\cos\theta} + ak - \frac{\gamma}{\gamma + 2k} \right), \tag{3.23}$$

being $A(k)$, $B(k)$ and $C(k)$ defined as

$$\begin{aligned} A(k) &= -ak\gamma\cosh(ka) + (-2ak^2 + \gamma)\sinh(ka), \\ B(k) &= 2k\cosh(ka) + \gamma\sinh(ka), \quad C(k) = 2k\Omega. \end{aligned}$$

One can exchange the order of integration in (3.23) to do the integration in θ first. Hence,

$$I_{\delta\delta'}(k) = \int_{-\pi}^{\pi} \frac{d\theta}{4\pi^2} \left(\frac{A(k)}{B(k) + C(k)\cos\theta} + ak - \frac{\gamma}{\gamma + 2k} \right) \tag{3.24}$$

can be computed from [173] by making use of

$$\int_0^{\pi} \frac{\cos^n(y)dy}{(b + a\cos y)^{n+1}} = \frac{\pi}{2^n(b+a)^n\sqrt{b^2 - a^2}} \sum_{k=0}^{n} (-1)^k \frac{(2n-2k-1)!!(2k-1)!!}{(n-k)!k!} \left(\frac{a+b}{b-a} \right)^k,$$

for $b^2 > a^2$. Taking into account the definition of $B(k)$ and $C(k)$, the condition $B^2(k,a) > C^2(k,a)$ is always fulfilled because $-1 < \Omega < 1$ and

$$\cosh(ka) + \frac{\gamma}{2k}\sinh(ka) > 1, \quad \forall k, a, \gamma > 0. \tag{3.25}$$

Consequently, the result of the integration in θ is given by

$$I_{\delta\delta'}(k) = \frac{1}{2\pi} \left[\frac{A(k)}{\sqrt{B^2(k) - C^2(k)}} + ak - \frac{\gamma}{\gamma + 2k} \right]. \tag{3.26}$$

With this result, the quantum vacuum energy for the comb is finally reduced to a single integration in k:

$$E_0^{\delta\delta' \text{comb}} = \int_0^{\infty} dk I_{\delta\delta'}(k), \tag{3.27}$$

that can be computed numerically. The results for $a = 0.5$ are plotted in Figure 3.4.

The δ-δ' potentials placed at each lattice node mimic atoms that have lost their most external

electron. The classical force between them is repulsive (all the atoms have positive charge). However, as can be seen in Figure 3.4, the quantum vacuum energy produced by the phonon field can be positive, negative or zero. Similarly, the quantum vacuum force in the system can be repulsive, attractive or zero, because it is obtained from $-\partial E_0/\partial a$. The negative values of the quantum vacuum force implies the reduction of the repulsive classical one, giving rise to a smaller lattice spacing. On the opposite, the positive values means that the classical repulsion is enhanced and the lattice spacing in the crystal becomes bigger.

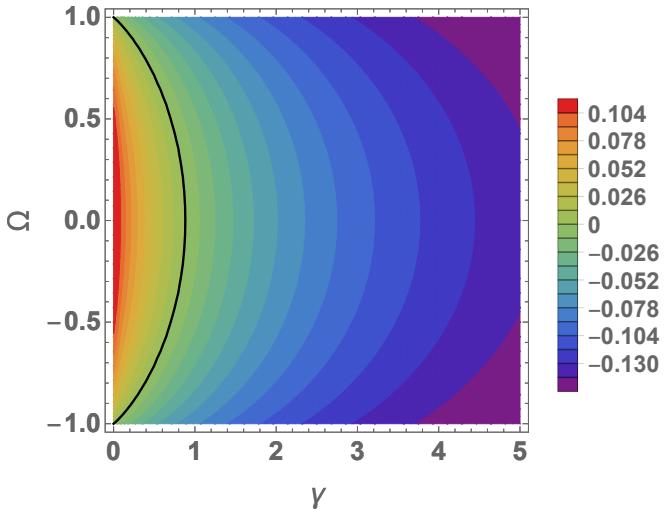

FIGURE 3.4: Quantum vacuum energy $E_0^{\delta\delta' comb}$ (3.27) for $a = 0.5$ in the coupling space γ-Ω.

Figure 3.5 shows the behaviour of the quantum vacuum energy (3.27) as a function of the lattice spacing a.

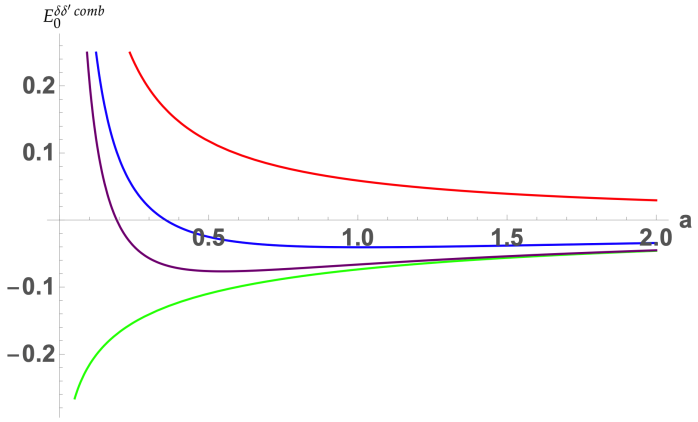

FIGURE 3.5: Quantum vacuum energy $E_0^{\delta\delta' comb}$ (3.27) as a function of the distance between nodes a, for different values of the $\delta\delta'$ couplings: $\gamma = 1.2, \Omega = -0.2$ (blue), $\gamma = 0, \Omega = 0.4$ (red),$\gamma = 2, \Omega = -1$ (green) and $\gamma = 2.3, \Omega = 0$ (purple).

In all the cases shown the quantum vacuum energy becomes zero as $a \to \infty$ because when lattice centres are moved away from each other, they stop interacting. At zero temperature and with lattice centres far away from each other, the energy contributed by the phonons is zero. On the opposite

situation, if $a \to 0$ the energy goes to $\pm\infty$. The reason is that for all the cases considered, the quantum vacuum energy behaves as the inverse of the distance between plates to the power of a positive number. Hence, if the distance between plates goes to zero, E_0 will diverge.

The limit $w_0 \to \infty$ gives the minimum quantum vacuum energy that the δ-δ' can have: the quantum vacuum energy between two Dirichlet plates $E_0^{Dbc} = -\pi/(24a)$. On the other hand, the limit $w_1 = \pm 1$ and $w_0 = 0$ allows to recover the maximum possible value of positive energy $E_0^{mbc} = \pi/(48a)$, corresponding to mixed boundary conditions [174] (i.e. Dirichlet boundary conditions on one side of the plates and Neumann ones on the other). It is easy to check that the integral (3.27) can be computed analytically for these two particular cases, giving rise to the aforementioned values of the energy. Moreover, $\lim_{w_0 \to 0} E_0^{\delta\delta' \, comb}(w_1 = 0, w_0)$ behaves proportional to $w_0 \cdot \log w_0$, implying that $E_0^{\delta\delta'}$ is not analytic in w_0 due to the quadratic infrared divergence[8] that appears in the Feyman diagram of Figure 3.6 because of the masslessness of the phonon field.

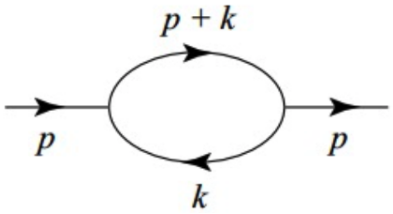

$$I = \int \mathrm{d}^D k \, \frac{1}{k^2 + m^2} \frac{1}{(p+k)^2 + m^2}.$$

FIGURE 3.6: One-loop Feynman diagram and amplitude corresponding to the process $\phi \to \phi$ for an incoming scalar particle of momentum p. Notice that in this massless scalar QFT, one has to consider $m \to 0$ in the Feynman amplitude I. As the propagator is defined in terms of a two point correlation function, this process can be interpreted as the one loop quantum correction to the propagator.

In conclusion, $E_0^{\delta\delta' \, \mathrm{comb}}$ does not admit a perturbative expansion in w_0 around $w_0 = 0$ when $w_1 = 0$. This is in agreement with [175] (and references [17]-[20] of the MIT group research therein).

3.2.2. Pöschl-Teller comb

This second example of crystal is appealing because there is always a band of negative energies regardless of the value of a and ϵ, as shown in Figure 3.2. There is always a bound state in the spectra of $V(z)$ (3.12) fulfilling the condition $k = i\kappa$, $0 < \kappa < 1$. In the previous example of the *Dirac comb*, only the cases where there was no negative energy band (i.e. with $w_0 > 0$) were considered when calculating the vacuum energy, so now the computation has to be changed a bit.

It has already been explained that the vacuum energy is computed as the summation of k over the quantum field modes that form the comb spectrum. But in the case of combs, since the spectrum is $\sigma(\hat{K}) = \{\omega / f_\theta(\omega) = 0\}_{\theta \in [-\pi, \pi]}$, it is necessary to sum up the energies of each band for all the bands that form the spectrum. When bound states exist, a mass term should be introduced in order for the QFT to be well defined and for the Hamiltonian to be a non-negative self-adjoint operator. The action

[8] The infrared divergences occur for theories with massless particles or fields in the limit of very low frequencies or energies. They cannot be renormalised. For instance, in QED there are infrared divergences due to the masslessness of the photon in graphs in which both ends of a photon propagator are attached to an external charged line.

of a scalar massive field $\phi(x)$ in (1+1)-dimensions is

$$S[\phi] = \frac{1}{2}\int d^2x \left[\partial_\mu\phi(x)\partial^\mu\phi(x) - (m^2 + U(z))\phi^2(x)\right], \tag{3.28}$$

where $U(z)$ is the general periodic potential considered in (3.1) and $x = (t, z)$. The modes of this scalar field obey the Schrödinger equation, after Fourier transform,

$$\left(-\frac{\partial^2}{\partial z^2} + V(z)\right)\phi_\omega(z) = (\omega^2 - m^2)\phi_\omega(z) = k^2\phi_\omega(z), \tag{3.29}$$

being $\omega = \sqrt{k^2 + m^2}$ the frequencies of the quantum field modes. The sum over the band spectrum is to be carried out following these steps (see Figure 3.7): firstly a value of the quasi-momentum in the first Brillouin zone is fixed, secondly all the discrete set of zeroes of the spectral function corresponding to those k that make up the spectrum for that value of θ are summed, and finally the process is repeated for all the values of the quasi-momentum $q \in [-\pi/a, \pi/a]$, i.e.:

$$E_0^{PT\,comb} = \frac{1}{2}\sum_{w^2\in\sigma(\hat{K}_{comb})}\omega = \frac{1}{2}\int_0^\pi \frac{d\theta}{\pi}\sum_{w^2\in\sigma(\hat{K}_\theta)}\omega$$

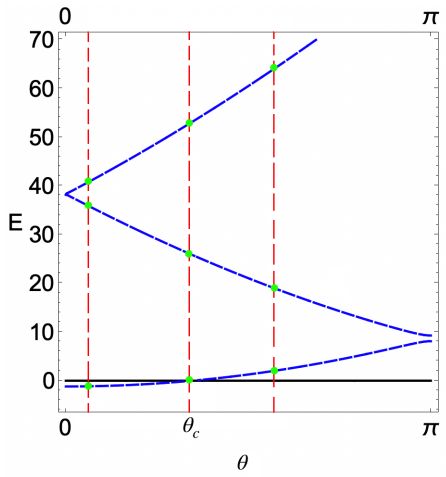

FIGURE 3.7: First three bands of the spectrum for the PT comb characterised by $a = 1, \epsilon = 0.6$. For each fixed value of $\theta \in [0, \pi]$, one has to sum over the wave vector k or κ associated to the states highlighted by green dots. Notice that $E = k^2$ when $E > 0$ and $E = (i\kappa)^2$ when $E < 0$.

But now, the last sum in the equation above must be splitted into two terms: the one corresponding to the part of the first band which corresponds to states with negative energy, and the other related to all the positive energy bands, either the rest of the first band and all the upper bands, as the latter only contain positive energy states.

Regarding the part of the first band with negative energy, one has to sum up the momentum of the bound state $k = i\kappa$, $\kappa > 0$ and then integrate over the quasi-momentum. But instead of considering the whole Brillouin zone, one has to integrate only over the interval $[-\theta_c, \theta_c]$. θ_c is related to the value of the quasi-momentum in the first Brillouin zone beyond which there are no negative energies in the

first band of the comb spectrum. It could be obtained from the secular equation as:

$$\cos\theta_c - h_V(k=0) = 0. \tag{3.30}$$

Furthermore, the mass which should be introduced in the theory must satisfy the condition $m \geq \kappa$ being κ the wave vector of the unique negative energy bound state of the spectrum for a given $\theta < \theta_c$. In this case, κ could be obtained from the spectral equation

$$\cos\theta - h_V(i\kappa) = 0, \qquad \text{for} \qquad \theta < \theta_c. \tag{3.31}$$

Nevertheless, instead of considering one value of the mass for each fixed value of the quasi-momentum, it is possible to define $m = \kappa_{min}$ being $i\kappa_{min}$ the wave vector associated to the bound state with minimum energy for the comb, which happens at $\theta = 0$. This value of the wave vector can be computed from

$$\cos 0 - h_V(i\kappa_{min}) = 0, \qquad \text{i.e.} \qquad h_V(i\kappa_{min}) = 1. \tag{3.32}$$

Notice that $k = 0$ for $\theta = \theta_c$. If all the first band is a negative energy band, then $\theta_c = \pi$. On the other hand, if $\theta_c < \pi$, from $\theta \in (\theta_c, \pi]$ the first band only includes states with positive energy.

Now that all the negative energy states of the spectrum have been taken into account, the positive energy states must be added. Their wave vectors $k \in \mathbb{R}^+$ can be calculated from

$$\cos\theta - h_V(k) = 0.$$

One could proceed in the same way as in the Dirac comb case and perform the summation by using Cauchy's residue theorem for a complex integral over a contour which enclose all the real positive zeroes of the spectral function. These zeroes characterise both to the states related to the upper bands and to the fragment of the first band in which $E > 0$. To sum up, the quantum vacuum energy for the PT comb (and for any other comb with bound states in its spectrum[9]) is given by

$$\begin{aligned} E_0^{PT\,comb} &= \frac{1}{2}\int_0^{\theta_c}\frac{d\theta}{\pi}\sqrt{m^2-\kappa_\theta^2} + \frac{1}{2}\int_0^{\pi}\frac{d\theta}{\pi}\sum_{w^2>0\,|\,w^2\in\sigma(\hat{K}_\theta)}\omega \\ &= \frac{1}{2}\int_0^{\theta_c}\frac{d\theta}{\pi}\sqrt{m^2-\kappa_\theta^2} + \frac{1}{2}\int_0^{\pi}\frac{d\theta}{\pi}\oint_\Gamma\frac{dk}{2\pi i}\,\sqrt{k^2+m^2}\,\partial_k\log f_\theta(k), \end{aligned} \tag{3.33}$$

where Γ is the contour represented in Figure 2.1 but displaced a positive distance m on the real axis, as shown in Figure 3.8. The choice of this contour guarantees that only the real zeros of the spectral function are summed over when performing the integral in k of the above expression and that the bound states in the positive imaginary axis are disregarded. Take into account that the bound states have already been considered in the first summand of (3.33).

[9] For another potential $V(z)$ that had more than one bound state in the spectrum, $m \geq \kappa_{min}$ where κ_{min} will correspond to the lowest energy state among all the bound states of the spectrum. Moreover, the first summand of (3.33) would contain as many terms as bound states in the spectrum, i.e. $\frac{1}{2}\int_0^{\theta_c}\frac{d\theta}{\pi}\sum_n\sqrt{m^2-\kappa_{\theta,n}^2}$. This reasoning would also be applied to all other results presented in the following sections.

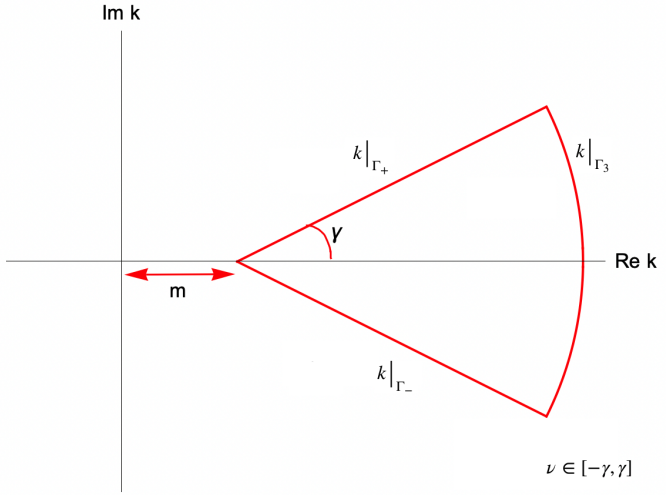

FIGURE 3.8: Complex contour Γ that encloses all the zeroes of $f_\theta(k)$ as $R \to \infty$ when there are bound states in the spectrum. Notice that $R > 0$ and $0 < \gamma < \pi/2$ are constants. In the contour, $k|_{\Gamma_3} = \{(m + R\cos\nu) + iR\sin\nu, \nu \in [-\gamma, \gamma]\}$ and $k|_{\Gamma_\pm} = \{m + \xi e^{\pm i\gamma}, \xi \in [0, R]\}$.

The secular function $f_\theta(k)$ is a holomorphic function on k and the logarithmic derivative of the secular equation has poles at the zeroes of $f_\theta(k)$, which are the bands in the real axis when summing over the quasi-momentum. Furthermore, in the limit $R \to \infty$, the integral over the circumference arc of the contour Γ goes to zero since following [98] the asymptotic behaviour of the scattering amplitudes is

$$t(|k| \to \infty) \to 1, \quad r_{R,L}(|k| \to \infty) \to 0.$$

Therefore

$$\lim_{R\to\infty} \left| \int_{\Gamma_3} \frac{dk}{2\pi i} \sqrt{k^2 + m^2}\, \partial_k \log f_\theta(k) \right| \leq \lim_{R\to\infty} \int_{-\gamma}^{\gamma} \frac{R d\nu}{2\pi} \left| \sqrt{\left(\frac{m}{R}\right)^2 + \left(\frac{m}{R} + e^{i\nu}\right)^2} \right| |\partial_\nu \log f_\theta(k|_{\Gamma_3})|.$$

It can be checked numerically that the contribution of this integral becomes negliglible when R takes large values. However, it can also be seen that $\int_{\Gamma_3} \to 0$ if $R \to \infty$ when considering a regularisation procedure by means of the heat trace, which is the Mellin transform of the zeta function. In this way, explained in [44], one considers

$$\lim_{R\to\infty} \oint_\Gamma \frac{dk}{2\pi i}\, e^{-y(k^2+m^2)} \sqrt{k^2 + m^2}\, \partial_k \log f_\theta(k), \tag{3.34}$$

where it is easy to show that the integral over the arc of the contour cancels out thanks to the decaying exponential function. Note that y is an ultraviolet regulator parameter such that the theory is finally recovered by taking the limit $y \to 0$. In conclusion, irrespective of the method followed, integrating over the whole contour is equivalent to integrating over the straight lines $k|_{\Gamma_\pm} \equiv \xi_\pm = m + \xi e^{\pm i\gamma}$ with $\xi \in [0, R]$. Thus,

$$\begin{aligned} E_0^{PT\,comb} &= \frac{1}{2}\int_0^{\theta_c} \frac{d\theta}{\pi} \sqrt{m^2 - \kappa_\theta^2} + \lim_{R\to\infty} \frac{1}{2}\int_0^{\pi} \frac{d\theta}{\pi} \int_0^R \frac{d\xi}{2\pi i} \left[-\sqrt{m^2 + \xi_+^2}\, \partial_\xi \log f_\theta(\xi_+) + \sqrt{m^2 + \xi_-^2}\, \partial_\xi \log f_\theta(\xi_-) \right] \\ &= \frac{1}{2}\int_0^{\theta_c} \frac{d\theta}{\pi} \sqrt{m^2 - \kappa_\theta^2} + \frac{1}{2}\int_0^{\pi} \frac{d\theta}{\pi} \int_0^{\infty} \frac{d\xi}{\pi} \mathrm{Re}\left[i\sqrt{m^2 + \xi_+^2}\, \partial_\xi \log f_\theta(\xi_+) \right] \end{aligned}$$

At this point the integral remains divergent and one has to subtract de contribution to the energy density of the theory in the bulk and the term related to the subdominant divergence. Notice that if $m \to 0$ and $\gamma = \pi/2$ the above expression becomes (2.1) and hence, the same reasoning given both in that section and in the derivation of formula (3.20) can be followed to calculate the finite contribution of this integral here. That is, computing

$$\lim_{a_0\to\infty} \frac{1}{2}\int_0^{\pi}\frac{d\theta}{\pi}\int_0^{\infty}\frac{d\xi}{2\pi i}\ \Big[\sqrt{m^2+\xi_+^2}\ \left(a-\partial_\xi \log f_\theta(\xi_+,a)-a_0+\partial_\xi \log f_\theta(\xi_+,a_0)\right) \\ -\sqrt{m^2+\xi_-^2}\ \left(a-\partial_\xi \log f_\theta(\xi_-,a)-a_0+\partial_\xi \log f_\theta(\xi_-,a_0)\right)\Big]$$

yields the quantum vacuum energy for the Pöschl-Teller comb:

$$E_0^{PT\,comb} \;=\; \frac{1}{2}\int_0^{\theta_c}\frac{d\theta}{\pi}\sqrt{m^2-\kappa_\theta^2}+\frac{1}{2}\int_0^{\pi}\frac{d\theta}{\pi}\int_0^{\infty}\frac{d\xi}{2\pi i}\left[\Omega(\xi_+)-\Omega(\xi_-)+\,i\,2\,\partial_\xi\delta(\xi_-)\right] \tag{3.35}$$

being $\Omega(\xi_\pm)=\sqrt{m^2+\xi_\pm^2}\ \left(a-\partial_\xi \log f_\theta(\xi_\pm,a)-\partial_\xi \log t(\xi_\pm)\right)$ and $\delta(\xi)$ the phase shift obtained from the scattering data.

There is another interesting caveat which becomes apparent when one subtracts either the dominant and subdominant divergences directly in the integrand of the closed complex integral given in equation (3.33). This detail can be also seen from the analogous integrals which appear for combs without bound states in the spectrum. When considering this last case, only for simplicity, one has to study

$$\oint_\Gamma \frac{dk}{2\pi i}\ k\ \left(a-\partial_k \log f_\theta(k)-\partial_k \log t(k)\right),$$

with Γ the complex contour given in Figure 2.1, taking for instance $\gamma = \pi/2$ as done in [34]. Scattering theory states that the trasmission coefficient can be written in terms of the phase shift as $t(k) = |t(k)|e^{i\delta(k)}$. And the logarithmic integral of $t(k)$ along the complex contour Γ is the increase on the argument of $t(k)$ (i.e. the phase shift), by the Argument Principle[10] [176]. Consequently, subtracting the subdominant divergence implies the emergence of the phase shift derivative. This would be relevant for obtaining the Dashen-Hasslacher-Neveu formula in subsequent sections and chapters.

Figure 3.9 shows $E_0^{PT\,comb}$ for different values of the lattice spacing a and the compact support ϵ of the Pöschl-Teller potential which composes the lattice.

Either for the Dirac comb and the Pöschl-Teller one, the classical force between the lattice nodes is repulsive. However, it has been found that at zero temperature, the vacuum quantum energy produced by the phonon field takes positive, negative or zero values in the Dirac lattice. This means that the lattice spacing can increase, remain unchanged or decrease with respect to its classical analogue as a consequence of this quantum interaction. In contrast, in the PT comb, the quantum vacuum interaction energy always takes positive values (as can be seen in Figure 3.9), which enhances the

[10] It is possible to rewrite the logarithmic integral of t as $\oint d\log t = \oint d\log|t(k)| + i\oint d\delta(k)$. The differential $d\log|t(k)|$ is exact so its integral over a closed contour is zero. But the differential $d\delta(k)$ is closed but not exact. Its integral is the increase of the phase shift along the contour.

repulsive classical force between lattice nodes.

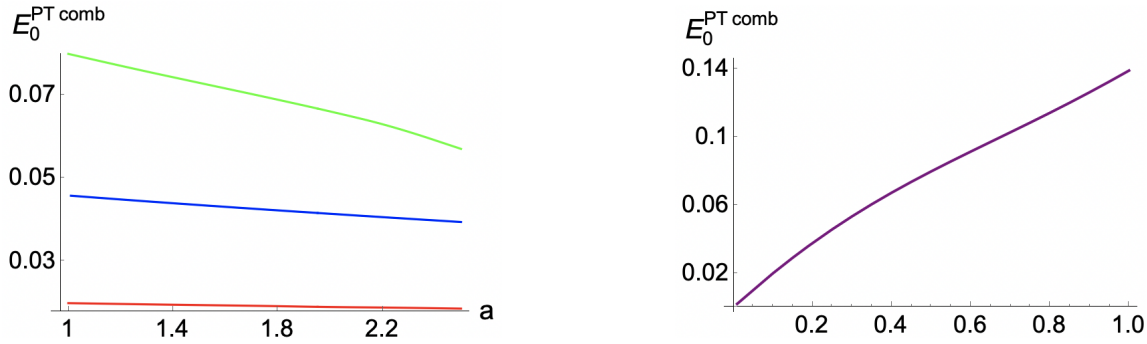

FIGURE 3.9: Left: Quantum vacuum energy $E_0^{PT\,comb}$ (3.35) for $\epsilon = 0.1$ (red) and $\epsilon = 0.25$ (blue) and $\epsilon = 0.5$ (green) as a function of the lattice spacing a. Right: Quantum vacuum energy $E_0^{PT\,comb}$ (3.35) for $a = 1$ (purple) as a function of the compact support ϵ.

Notice that when the lattice spacing increases, the quantum vacuum energy between nodes decreases to zero (see the left plot in Figure 3.9), as expected. In the limit case where the lattice nodes are far apart, the phonons propagation initiated at one node ends before reaching the following one and there is no interaction between nodes.

3.3. Free energy and entropy at finite temperature

The temperature dependent part of the total Helmholtz free energy[11] is computed as the summation of the Boltzmann factors over the quantum field modes that form the comb spectrum:

$$\triangle_T \mathcal{F} = \sum_{\omega \in \text{spec}(\hat{K})} B(\omega, T) = \int_{-\pi}^{\pi} \frac{d\theta}{2\pi} \sum_{\omega \in \text{spec}(\hat{K})_\theta} B(\omega, T) = \int_{-\pi}^{\pi} \frac{d\theta}{2\pi} \oint_\Gamma \frac{dk}{2\pi i} B(k, T) \partial_k \log f_\theta(k), \tag{3.36}$$

being $\omega = k$ the energy of the one-particle states of the Quantum Field Theory and Γ the contour given in Figure 2.1. The Boltzmann factor has a discrete set of branch points on the imaginary axis[12]. As stated in the previous section, the logarithmic derivative of the secular function has poles at the zeroes of $f_\theta(k)$, which are the bands in the real axis when summing over the quasi-momentum. Furthermore, in the limit $R \to \infty$, the integral over the circumference arc of the contour Γ goes to zero following the reasoning given in the previous section and taking into account that

$$\lim_{R\to\infty} |B(k,T)| = \lim_{R\to\infty} \left| T \log\left(1 - e^{-(R\cos\nu + iR\sin\nu)/T}\right)\right| = \lim_{R\to\infty} T \left| \arctan\left[\frac{e^{-R\cos(\nu)/T}\sin(R\sin(\nu)/T)}{1 - e^{-R\cos(\nu)/T}\cos(R\sin(\nu)/T)}\right]\right|$$
$$+ \lim_{R\to\infty} T \left| \ln\sqrt{1 + e^{-2R\cos(\nu)/T} - 2e^{-R\cos(\nu)/T}\cos(R\sin(\nu)/T)}\right| = 0.$$

[11] A summary of this entire section has been published in [161], with the exception of subsection 3.3.2 which I have corrected and included in this thesis.

[12] $B(\omega, T) = \log_\pi(1 - e^{-\omega/T})$ is not an analytic function if $w = 0$ and whenever $\omega = |\omega| e^{i \arcsin(2\pi pT/R)}$ being $p \in \mathbb{Z}$ and the argument is in $[\pi/2, \pi] \cup (-\pi, -\pi/2]$. Nevertheless if one chooses $R = \pi pT$ then, the non-analytic points of the Boltzmann factor reduce to $\omega = i\pi pT, \forall p \in \mathbb{Z}$, i.e. a discrete set of purely imaginary points.

In conclusion, integrating over the whole contour is again equivalent to integrating over the two straight lines $k = \xi e^{i\gamma}$ and $k = \xi e^{-i\gamma}$ being γ a constant angle. In such a way $\triangle_T\mathcal{F}$ reads as

$$\begin{aligned}\triangle_T\mathcal{F} &= \int_0^{\pi}\frac{d\theta}{\pi}\int_0^{\infty}\frac{d\xi}{2\pi i}\left[-B(\xi e^{i\gamma},T)\partial_{\xi}\log f_\theta(\xi e^{i\gamma})+B(\xi e^{-i\gamma},T)\partial_{\xi}\log f_\theta(\xi e^{-i\gamma})\right]\\ &= \int_0^{\pi}\frac{d\theta}{\pi}\int_0^{\infty}\frac{d\xi}{\pi}\mathrm{Re}\left[iB(\xi e^{i\gamma},T)\partial_{\xi}\log f_\theta(\xi e^{i\gamma})\right]\end{aligned} \tag{3.37}$$

If there is a negative energy band in the spectrum, it is necessary to perform a summation over bound states ($k = i\kappa$ with $\kappa > 0$) of the Boltzmann factor and a Cauchy integral over the positive energy states of the spectrum (notice that the secular function f_θ is holomorphic in k, not in ω). Consequently:

$$\triangle_T\mathcal{F} = \int_0^{\theta_c}\frac{d\theta}{\pi}T\log\left(1-e^{\frac{\sqrt{m^2-\kappa_\theta^2}}{T}}\right)+\int_0^{\pi}\frac{d\theta}{\pi}\oint_\Gamma\frac{dk}{2\pi i}B\left(\sqrt{k^2+m^2},T\right)\partial_k\log f_\theta(k), \tag{3.38}$$

where Γ is the contour represented in Figure 3.8. Again, the whole contour integral is reduced to the integral on the two half lines $\xi_\pm \equiv \{k = \xi e^{\pm i\gamma}+m,\ |\ \xi\in[0,\infty),\ 0<\gamma<\pi/2,\ m>0\}$ giving rise to:

$$\triangle_T\mathcal{F} = \int_0^{\theta_c}\frac{d\theta}{\pi}T\log\left(1-e^{\frac{\sqrt{m^2-\kappa_\theta^2}}{T}}\right)+\int_0^{\pi}\frac{d\theta}{\pi}\int_0^{\infty}\frac{d\xi}{\pi}\mathrm{Re}\left[iB\left(\sqrt{\xi_+^2+m^2},T\right)\partial_\xi\log f_\theta(\xi_+)\right]. \tag{3.39}$$

The result of the integration in (3.36) and (3.38) does not depend on the angle γ taken in the contour, according to the residue theorem. The major advantage of choosing the angle of the contour such that $0<\gamma<\pi/2$, is that it avoids either the oscillations of the integrand caused by the zeroes of the secular function on the real axis and the branch points of the Boltzmann factors on the imaginary axis. Moreover, the integrand has an exponential decrease which makes numerical evaluation easier. Nonetheless, it is possible to choose either $\gamma = 0$ recovering the well-known real frequencies approach, or $\gamma = \pi/2$ to work on the Matsubara representation. Just some further words about these two widely used approaches will be added below.

Real frequencies representation

As stated before, $\triangle_T\mathcal{F}$ is given by the summation of the Boltzmann factors over the zeroes of the secular equation (3.8), which can be rewritten as $\theta(\omega) = \arccos h_V(\omega)$. The allowed modes of the quantum scalar field are given by $|h_V(\omega)|\leq 1$. Consequently, the allowed ω in the spectrum are such that[13] $\theta(\omega) = \arccos h_V(\omega)\in\mathbb{R}$, and the forbidden ones by $\theta(\omega) = \arccos h_V(\omega)\in i\mathbb{R}$. It should be clear that the allowed energy bands of the spectrum are given by real frequencies ω.

[13]Notice that $\theta(\omega) = \arccos h_V(\omega) = -i\log_{-\pi}\left(h_V(\omega)+\sqrt{h_V^2(\omega)-1}\right)$. Moreover $h_V(\omega)\in\mathbb{R}$ whenever $\omega\in\mathbb{R}$. Hence, if $h_V(\omega)\geq 1$, then $\theta(\omega) = -i\ln\left|h_V(\omega)+\sqrt{h_V^2(\omega)-1}\right|$. And on the contrary, whenever $h_V(\omega)\leq 1$ then $\theta(\omega) = \arctan\left(\frac{\sqrt{-h_V^2(\omega)+1}}{h_V(\omega)}\right)$.

In order to compute the free energy, ω should be integrated from the minimum energy to the maximum energy of each band by means of

$$\triangle_T \mathcal{F} = \int_0^{\pi} \frac{d\theta}{\pi} \sum_{\omega \in \sigma(\hat{K}_\theta)} B(\omega, T) \qquad \longrightarrow \qquad \triangle_T \mathcal{F} = \sum_n \int_{\omega_n(0)}^{\omega_n(\pi)} \frac{d\omega}{\pi} \frac{d\theta}{d\omega} B(\omega, T), \tag{3.40}$$

where $n \in \mathbb{N}$ indexes the bands. In the previous expression a change of variable $\theta \to \omega$ has been performed. The Jacobian of the transformation is well defined because in the expression

$$\frac{\partial \omega}{\partial \theta} = \frac{-\sin\theta}{\partial_\omega h_V(\omega)} \qquad \longrightarrow \qquad -\sin\theta = \partial_\omega h_V(\omega) \frac{\partial \omega}{\partial \theta}, \tag{3.41}$$

the sine function only has zeroes at $\theta = 0, \pm\pi$ and not at any other intermediate point of the first Brillouin zone. Consequently, $\omega_n(\theta)$ is a monotone function between $\theta = 0$ and $\theta = \pi$ for all the bands. Furthermore, for the extremal integration points $\theta = 0, \pi$ there is always a maximum or a minimum of the band. Two scenarios can be distinguished:

- If $\omega_n(0) = \omega_{min}$ and $\omega_n(\pi) = \omega_{max}$ of the band, then

$$\frac{\partial \theta}{\partial \omega} = \left| \frac{\partial \theta}{\partial \omega} \right| > 0, \qquad \forall \omega \in [\omega_n(0), \omega_n(\pi)]. \tag{3.42}$$

- If $\omega_n(0) = \omega_{max}$ and $\omega_n(\pi) = \omega_{min}$ of the band, then

$$\frac{\partial \theta}{\partial \omega} = -\left| \frac{\partial \theta}{\partial \omega} \right| < 0, \qquad \forall \omega \in [\omega_n(0), \omega_n(\pi)]. \tag{3.43}$$

Hence, in order for both cases to be taken into account an absolute value of the Jacobian must be added:

$$\triangle_T \mathcal{F} = \sum_n \int_{\omega_n^{min}}^{\omega_n^{max}} \frac{d\omega}{\pi} \left| \frac{\partial \theta}{\partial \omega} \right| B(\omega, T). \tag{3.44}$$

Due to the fact that whenever $\mathrm{Re}\,[\theta(\omega)] \neq 0$ there is an energy in the allowed band and $\mathrm{Re}[\theta(\omega)] = 0$ represents forbidden bands, summing over the allowed bands is the same as integrating ω from 0 to ∞. In this way, the temperature dependent part of the free energy takes the form

$$\triangle_T \mathcal{F} \;\; = \;\; \int_0^{\infty} \frac{d\omega}{\pi} \left| \mathrm{Re} \left(\frac{\partial \theta}{\partial \omega} \right) \right| B(\omega, T), \tag{3.45}$$

with

$$g(\omega) = \frac{a}{\pi} \left| \mathrm{Re} \left(\frac{\partial q}{\partial \omega} \right) \right|$$

the general expression for the **density of states of the comb**[14] as a function of ω. It can be given the

[14] In Solid State physics the density of states is defined as the number of energy states between E and $E + dE$ per unit volume of the first Brillouin zone to be occupied by the charge carriers. Its product by the probability distribution function (following the Fermi-Dirac statistics for fermions and the Bose-Einstein one for bosons) is the number of occupied states per unit volume at a given energy for a system in thermal equilibrium. This product allows to compute thermodynamic properties involving averages over occupied levels such as the specific heat capacity, the thermal conductivity or the internal energy [147].

physical meaning of the derivative of the *phase shift*[15] for the particles propagating along the comb, if one follows the representation through self-adjoint extensions given in section 3.2. To see this, notice that when the lattice spacing increases, in particular when taking the limit $a \to \infty$, the operator $\hat{H}_V$ becomes self-adjoint just as $\hat{H}^{(0)}$. In this limit one recovers the quantum mechanical problem of the single potential $V(z)$ (defined in (3.1)) in the real line yielding the well-known result [177]

$$\triangle_T \mathcal{F} \;=\; \int_0^\infty \frac{d\omega}{\pi} \frac{d\delta(\omega)}{d\omega} B(\omega, T), \tag{3.47}$$

with $\delta(\omega)$ the phase shift associated to the scattering problem. In fact, if in the limit $a \to \infty$ one considers the contribution of the continuum states of the spectra to the zero point energy, and replaces the density of states of the comb by the derivative of the phase shift related to the individual potential from which the comb is made up, one recovers the Dashen-Hasslacher-Neveu formula [82, 123]:

$$E_0 = \frac{1}{2} \int \frac{d\omega}{2\pi} \omega \frac{d\delta(\omega)}{d\omega}.$$

Matsubara representation

The Matsubara formalism [15] is another alternative to the previous ones. It works with imaginary discrete frequencies $\omega = i\xi_\ell = i2\pi\ell T$, being $\ell \in \mathbb{Z}$ for bosons and $\ell \in \mathbb{Z} + 1/2$ for fermions. The Matsubara approach emerges either when taking a Wick rotation of the real frequencies one and by taking $\gamma = \pi/2$ both in the contour Γ (Figure 2.1) and in the equation (3.37). In the second case, a small displacement $\varepsilon > 0$ on the resulting vertical line must be introduced to avoid the branch points of $B(k, T)$ on the imaginary axis (see Figure 3.10).

Before taking the limit $\varepsilon \to 0$ the singular terms of the quantum vacuum energy cancel[16], as explained in [39, 178, 179]. For the thermal correction, one reaches the expression

$$\triangle_T \mathcal{F} = \lim_{\varepsilon \to 0} \int_0^\pi \frac{d\theta}{\pi} \int_0^\infty \frac{d\xi}{2\pi i} \left[-B(i\xi + \varepsilon, T) \partial_\xi \log f_\theta(i\xi + \varepsilon) + B(-i\xi + \varepsilon, T) \partial_\xi \log f_\theta(-i\xi + \varepsilon) \right]. \tag{3.48}$$

[15] In scattering theory, the phase shift gives information regarding how far the asymptotic solution of the scattering problem is displaced at the origin from the asymptotic free solution. The spectral equation (3.8) can be written in terms of the phase shift and the transmission coefficient as

$$\cos\theta = \frac{e^{i\delta(\omega)}}{t(\omega)} \cos[\omega a + \delta(\omega)] = \frac{1}{|t(\omega)|} \cos[\omega a + \delta(\omega)], \tag{3.46}$$

where the relations $e^{i2\delta(\omega)} = t^2(\omega) - r_R(\omega) r_L(\omega)$ and $\delta(\omega) = \log[t(\omega)/t^*(\omega)]/(2i)$ have been used. Furthermore, computing the density of states of the comb given by $g(\omega)$ in (3.45) from (3.46), allows to recover the derivative of the phase shift for $V(z)$.

[16] The representation of the zeta function for a second order elliptic operator in a one dimensional manifold, in the form of a contour integral in the complex plane (3.18), is valid for $Re(s) > 1/2$ only. So to evaluate the Casimir energy, one needs to perform the analytic continuation to the left of this converegence strip. In [178], firstly the system is putting within a large box of length L so that the spectrum is discrete. Secondly, the asymptotic behaviour of the integrand at $L \to \infty$ is studied to eliminate the divergent terms proportional to L and those independent of the potential, and finally the integration contour is shifted to the imaginary axis. The integral is finite at $s = 0$.

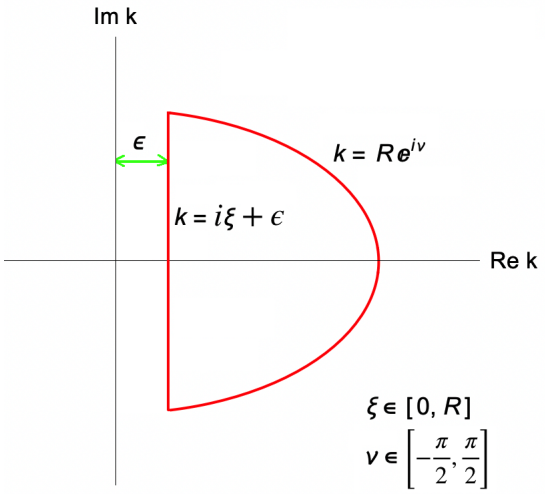

FIGURE 3.10: Complex contour that should be used to recover the Matsubara approach from equation (3.37) in the particular case $\gamma = \pi/2$, after taking the limit $\varepsilon \to 0$. Notice that $R > 0$.

Notice that

$$\begin{aligned} B(\pm i\xi + \varepsilon, T) &= T \log\left(1 - e^{\mp i\xi/T} e^{\varepsilon/T}\right) = T \ln \sqrt{(1 - e^{-\varepsilon/T}\cos(\xi/T))^2 + \sin^2(\xi/T) e^{-2\varepsilon/T}} \\ &\mp \frac{i\xi e^{-\varepsilon/T}}{2} \pm \frac{i\pi T}{2} \pm i\pi T \sum_{\ell=1} \Theta(\xi - \xi_\ell) \end{aligned}$$

with $\xi_\ell = 2\pi T\ell, \ell \in \mathbb{Z}$ the Matsubara frequencies for bosons (for fermions one can follow a similar procedure). This specific value for the frequencies in the last term of the previous equation comes from the fact that the argument of $1 - e^{\mp i\xi/T} e^{\varepsilon/T}$ is 2π periodic in ξ/T. It is necessary to add the summation over the Heaviside functions to work with the principal branch of the logarithm. Since for the potentials studied the property $f_\theta(i\xi) = f_\theta(-i\xi)$ is fulfilled, hence

$$\begin{aligned} \triangle_T \mathcal{F} &= \lim_{\varepsilon \to 0} \int_0^\pi \frac{d\theta}{\pi} \int_0^\infty \frac{d\xi}{2\pi i} \left[-B(i\xi + \varepsilon, T) + B(-i\xi + \varepsilon, T)\right] \partial_\xi \log f_\theta(i\xi), \\ \triangle_T \mathcal{F} &= \lim_{\varepsilon \to 0} \int_0^\pi \frac{d\theta}{\pi} \int_0^\infty \frac{d\xi}{2\pi} \xi\, e^{-\varepsilon/T} \partial_\xi \log f_\theta(i\xi) - \int_0^\pi \frac{d\theta}{\pi} \int_0^\infty d\xi\, T\, \partial_\xi \log f_\theta(i\xi) \left[\frac{1}{2} + \sum_{\ell=1} \Theta(\xi - \xi_\ell)\right] \end{aligned} \tag{3.49}$$

Finally, applying $\triangle_T \mathcal{F} = -E_0 + \mathcal{F}$ and integrating by parts taking into account that the boundary terms give divergences because E_0 and $\mathcal{F}$ also present them, the second term in (3.49) yields the result

$$\mathcal{F} = T \sum_{\ell=1}^{\infty} \int_0^\pi \frac{d\theta}{\pi} \log f_\theta(i\xi_\ell)\theta(\xi_\ell) = T \sum_{\ell=1}^{\infty} \int_0^\pi \frac{d\theta}{\pi} \log f_\theta(i\xi_\ell) \tag{3.50}$$

for the total Helmholtz free energy per unit cell at $T \neq 0$ in the Matsubara representation. The analogue of the last formula for $\mathcal{F}$ can be easily found in the literature (for instance in Chapter 5 of [15]), for simpler cases where the system consists of a solely potential $V(z)$ instead of a comb built from its periodic repetition.

Although the Matsubara representation can be recovered from the novel representation with complex frequencies obtained in this chapter, it is not going to be used for obtaining the graphical results for the remainder of this chapter because it converges more slowly.

3.3.1. Generalised Dirac comb

Replacing the spectral equation f_θ^{Dc} (3.11) in (3.37) and evaluating the resulting formula numerically with *Mathematica*, one obtains the thermal correction to the vacuum energy of the *generalised Dirac comb* at any temperature for different configurations of couplings (left graph in Figure 3.11 and both in Figure 3.12).

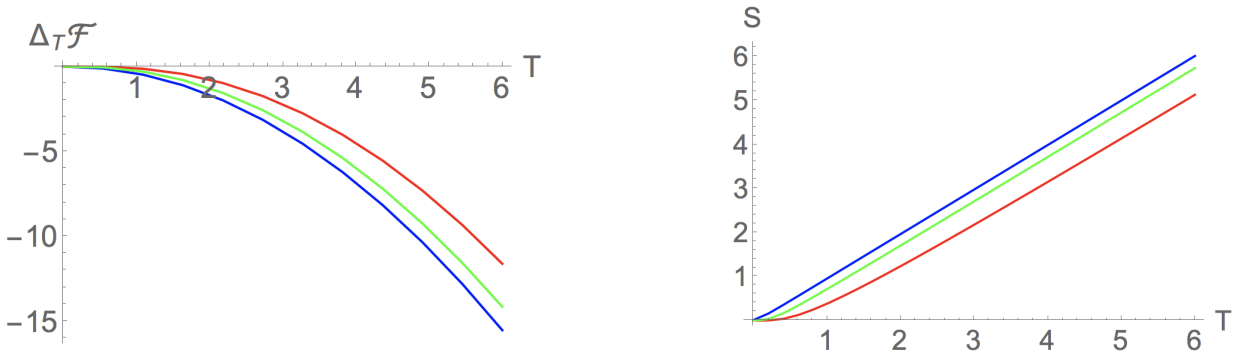

FIGURE 3.11: Free energy (left) $\triangle_T\mathcal{F}$ (3.37) and entropy (right), as a function of T for the comb with individual potential (3.9) for $w_0 = 0.1, w_1 = 5$ (blue), $w_0 = 8, w_1 = 0$ (red), $w_0 = 3, w_1 = 2$ (green). In this plot the lattice spacing is $a = 1$.

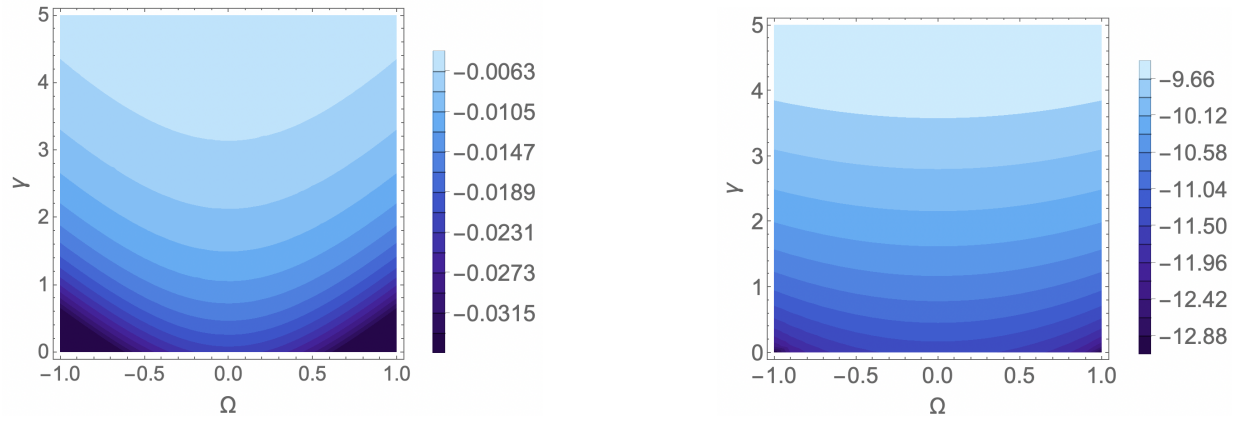

FIGURE 3.12: Free energy $\triangle_T\mathcal{F}$, (3.37) for $T = 0.5$ (left) and $T = 5$ (right) for the comb built from the potential (3.9) in the parameter space $\Omega - \gamma$. In this plot the lattice spacing is $a = 1$.

Either in the regime of low temperatures as well as at high temperatures, $\Delta_T\mathcal{F}$ is definite negative and rapidly decreasing with the temperature. However, in the limit of low temperature the vacuum energy at zero temperature provides the leading contribution whereas the thermal correction is a small deviation. At high temperatures the opposite situations happens due to the thermalisation, as it should be.

By computing $-\partial_T \Delta_T \mathcal{F}$, the entropy can be evaluated in the coupling space for any finite non zero temperature (see right plot in Figure 3.11 and both in Figure 3.13). The quantum system is thermodynamically stable because the one loop quantum corrections for the entropy always take positive values.

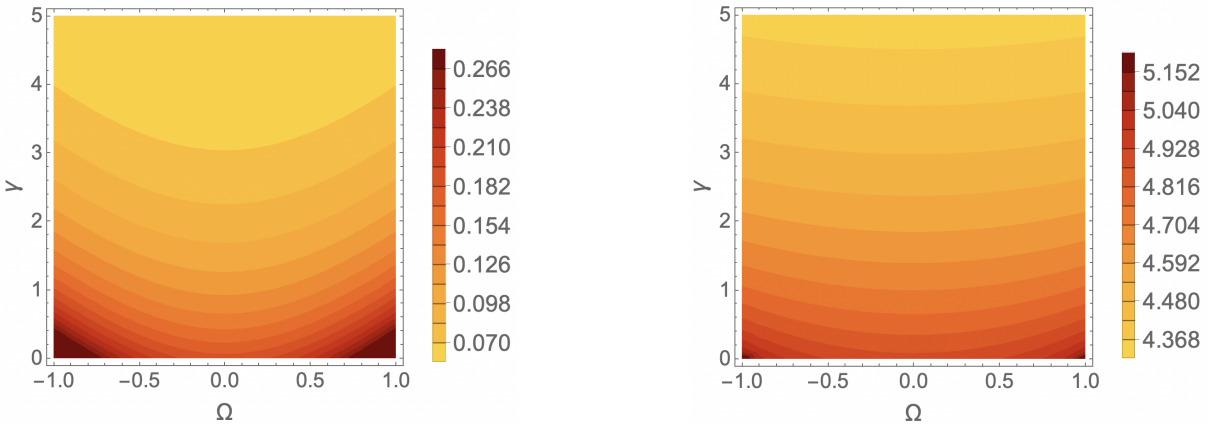

FIGURE 3.13: The entropy S for $T = 0.5$ (left) and $T = 5$ (right) for the Dirac comb built from the δ-δ' potential (3.9), in the parameter space $\Omega - \gamma$. In this plot the lattice spacing is $a = 1$.

3.3.2. Pöschl-Teller comb

Plugging the spectral function (3.14) into (3.39), the thermal correction to the vacuum energy in the Pöschl-Teller comb is obtained. It can be evaluated numerically with *Mathematica*. The results are shown in the left graph of Figure 3.14 as a function of the temperature for different values of the compact support ϵ of the Pöschl-Teller potential (3.12).

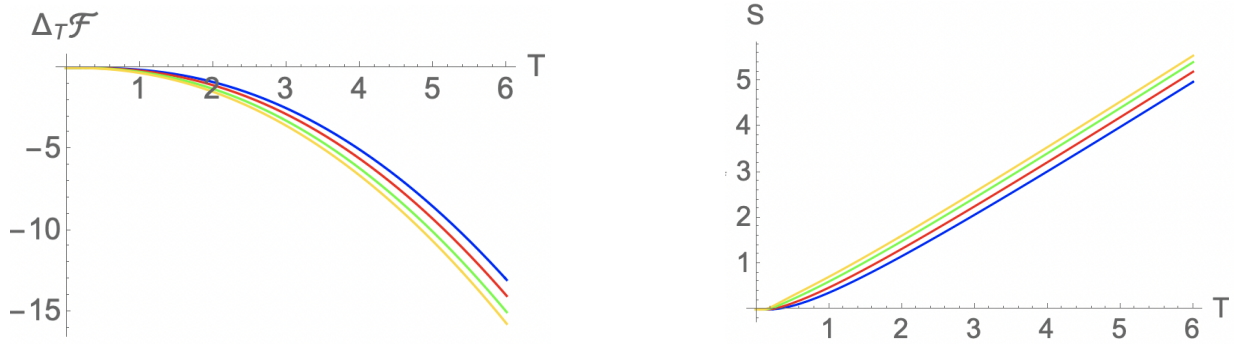

FIGURE 3.14: Free energy (left) $\triangle_T \mathcal{F}$ (3.39) and entropy (right), for the Pöschl-Teller comb (3.12) as a function of T for: $\epsilon = 0.25$ (blue line), $\epsilon = 0.5$ (red line), $\epsilon = 0.75$ (green line), $\epsilon = 0.9$ (yellow line). In this plot the lattice spacing is $a = 1$ and $m = 1.5$.

The one loop quantum corrections to the classical entropy can be obtained by performing the derivative of $\Delta_T \mathcal{F}$ with respect to the temperature and changing the global sign of the resulting value. The results are shown in the right graph of Figure 3.14. It is clear that qualitatively the same results are obtained for the thermal correction to the vacuum energy and the entropy as in the case of the Dirac comb, so the conclusions given in the previous section are also valid here.

3.4. Generalisation to combs in higher dimensions

The study of one dimensional chains naturally brings forward the question of combs in theories with $D+1$ dimensions. The aim of this section will be the computation of the quantum vacuum interaction energy of a stack of parallel plates constructed by positioning $\delta\delta'$-function plates or $D-1$ Pöschl-Teller dimensional wells at the lattice nodes, as represented in Figure 3.15.

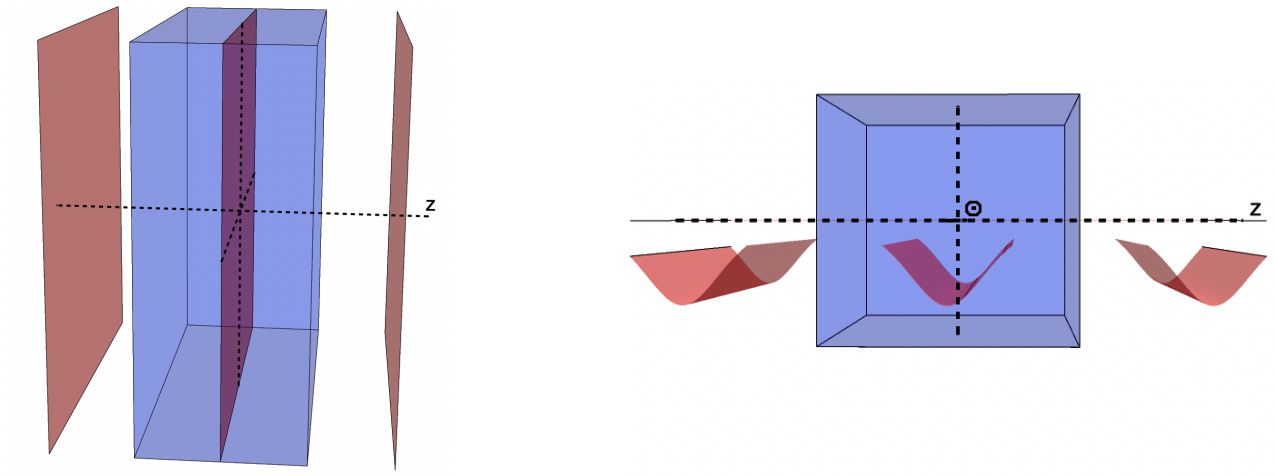

FIGURE 3.15: Left: Lattice of parallel Dirac delta plates (red) in three spatial dimensions and primitive cell (blue). Right: Lattice of PT potentials (red) in three spatial dimensions and primitive cell (blue).

The potential representing the three dimensional comb is:

$$U(\vec{x}) = \sum_{n\in\mathbb{Z}} V(z-na), \qquad \text{being} \qquad V(z)\begin{cases} \neq 0 & \text{if } |z| \leq \epsilon/2, \\ = 0 & \text{if } |z| > \epsilon/2, \end{cases} \tag{3.51}$$

being $\vec{x} = (\vec{x_\parallel}, z)$, with $\vec{x_\parallel} \in \mathbb{R}^2$. Again, z is the spatial coordinate corresponding to the direction orthogonal to the surface of the bodies (the plates or the wells). Likewise, the wave vector in this section will be denoted by $\vec{k} = (\vec{k_\parallel}, k)$.

In [180] the Casimir energy of a stack of parallel plates mimicked by δ plates at the points constituting a Cantor set has been studied by means of the Green's function formalism. The resulting Casimir energy turns out to be positive, involving a separation between the plates and a widening of the whole self-similar configuration. Now the objective is quite similar, namely using the technique developed in section 2.2.1 to study the thermal correction to the energy between the plates sitting at the lattice nodes, in order to determine how the lattice spacing is affected. The results presented in this section are original work, not yet published.

Consider a comb built from the repetition of infinite two dimensional Dirac plates sitting at the lattice nodes. In the direction orthogonal to the plates, i.e. (0,0,1), the same problem as the one presented in previous sections appears. However, in the two directions parallel to the plate, (1,0,0)

and (0,1,0), the scalar field moves freely without boundaries[17] and consequently, one recovers the spectrum of a free particle in these two directions. The frequency of the field modes in the system would be $\omega = \sqrt{\vec{k}_{\parallel}^{\,2} + k^2}$. And summing over the frequencies translates into integrating over the continuous parallel momenta and summing over the discrete transverse momenta. For combs whose spectrum do not present negative energy bands, the temperature dependent part of the Helmholtz free energy can be computed as

$$\begin{aligned}\frac{\triangle_T \mathcal{F}}{A} &= \sum_{\omega^2\in\sigma(\hat{K}_{comb})} B(\omega,T) = \int_{-\pi}^{\pi}\frac{d\theta}{2\pi}\sum_{\omega^2\in\sigma(\hat{K}_\theta)} B(\omega,T) = \int_{-\pi}^{\pi}\frac{d\theta}{2\pi}\int_{\mathbb{R}^2}\frac{d^2\vec{k}_{\parallel}}{(2\pi)^2}\sum_{k\in Z(f_\theta)} B\left(\sqrt{k^2+\vec{k}_{\parallel}^{\,2}},T\right)\\ &= \int_{-\pi}^{\pi}\frac{d\theta}{2\pi}\sum_{k\in Z(f_\theta)} I_3(k,T) = \lim_{R\to\infty}\int_0^{\pi}\frac{d\theta}{\pi}\oint_\Gamma \frac{dk}{2\pi i}\, I_3(k,T)\,\partial_k \log f_\theta(k)\end{aligned} \tag{3.52}$$

where Γ is the contour represented in Figure 2.1 and $I_3(k,T)$ is given by (2.6). The reason stated in section 2.2.1 as to why the integral over the circumference arc Γ_3 is zero is applicable here as well. Consequently, the integration over the whole contour Γ reduces to the integration over the two straight lines $z = \xi e^{\pm i\gamma}$ with being γ a constant angle and $\xi \in [0,\infty)$. It yields

$$\begin{aligned}\frac{\triangle_T \mathcal{F}}{A} &= \int_0^{\pi}\frac{d\theta}{\pi}\int_0^{\infty}\frac{d\xi}{2\pi i}\left[-I_3(\xi e^{i\gamma},T)\partial_\xi \log f_\theta(\xi e^{i\gamma}) + I_3(\xi e^{-i\gamma},T)\partial_\xi \log f_\theta(\xi e^{-i\gamma})\right]\\ &= \int_0^{\pi}\frac{d\theta}{\pi}\int_0^{\infty}\frac{d\xi}{\pi}\mathrm{Re}\left[iI_3(\xi e^{i\gamma},T)\partial_\xi \log f_\theta(\xi e^{i\gamma})\right]\end{aligned} \tag{3.53}$$

This integral can be computed numerically by using *Mathematica* for any finite temperature T. From this expression one could obtain the entropy and the Casimir pressure by means of

$$\frac{S}{A} = \frac{d}{dT}\triangle_T \mathcal{F}, \qquad P = -\frac{d}{d\,a}\triangle_T \mathcal{F}. \tag{3.54}$$

For combs whose spectrum do present negative energy bands, and consequently with dispersion relation $\omega^2 = m^2 + k^2 + \vec{k}_{\parallel}^2$, the temperature dependent part of the Helmholtz free energy can be computed as

$$\begin{aligned}\frac{\triangle_T \mathcal{F}}{A} &= \sum_{\omega^2\in\sigma(\hat{K}_{comb})} B(\omega,T) = \int_0^{\theta_c}\frac{d\theta}{\pi}\int_{\mathbb{R}^2}\frac{d\vec{k}_{\parallel}^2}{(2\pi)^2}\left[B\left(\sqrt{m^2-\kappa^2+\vec{k}_{\parallel}^2},T\right) + \sum_{k\in Z(f_\theta)} B\left(\sqrt{m^2+k^2+\vec{k}_{\parallel}^2},T\right)\right]\\ &+ \int_{\theta_c}^{\pi}\frac{d\theta}{\pi}\int_{\mathbb{R}^2}\frac{d\vec{k}_{\parallel}^2}{(2\pi)^2}\sum_{k\in Z(f_\theta)} B\left(\sqrt{m^2+k^2+\vec{k}_{\parallel}^2},T\right)\end{aligned}$$

[17] If the plates had a finite area and some boundary conditions for the wave function of the scalar field were imposed representing a more realistic material, the frequencies on the parallel dimensions would be quantised. Thus, instead of performing an integration over the whole $\mathbb{R}^2$, one would make a summation over a discrete set of parallel momenta. For instance, if Dirichlet boundary conditions were imposed over the edges of a squared plate of length b, then the field must fulfil the relations $\phi(x=b) = \phi(x=-b) = \phi(y=b) = \phi(y=-b) = 0$ and

$$\sum_{\omega^2\in\sigma(\hat{K}_{comb})} B(\omega,T) = \int_0^{\pi}\frac{d\theta}{\pi}\sum_{n_x=1}^{\infty}\sum_{n_y=1}^{\infty}\sum_{k\in Z(f_\theta)} B\left(\sqrt{k^2+\frac{n_x^2\pi^2}{b^2}+\frac{n_y^2\pi^2}{b^2}},T\right).$$

This type of cases are left for future further investigation.

Following the same steps that were used to derive the equation (2.6) but for $\omega = \sqrt{m^2 + k^2 + \vec{k}_{\parallel}^2}$ one arrives at

$$\begin{aligned}\frac{\triangle_T \mathcal{F}}{A} &= \int_0^{\theta_c} \frac{d\theta}{\pi} I_3\left(\sqrt{m^2 - \kappa_\theta^2}\,, T\right) + \int_0^{\pi} \frac{d\theta}{\pi} \sum_{k \in Z(f_\theta)} I_3\left(\sqrt{m^2 + k^2}, T\right) \\ &= \int_0^{\theta_c} \frac{d\theta}{\pi} I_3\left(\sqrt{m^2 - \kappa_\theta^2}\,, T\right) + \int_0^{\pi} \frac{d\theta}{\pi} \oint_\Gamma \frac{dk}{2\pi i} I_3\left(\sqrt{m^2 + k^2}, T\right) \partial_k \log f_\theta(k)\end{aligned}$$

where Γ is the contour of Figure 3.8 and $I_3(k, T)$ is given by (2.6). Again, the integral over the circumference arc Γ_3 vanishes and one only has to integrate over the two straight lines $\xi_\pm = \xi e^{\pm i\gamma} + m$ with $\xi \in [0, \infty]$, $m > 0$ and $\gamma \in [0, \pi/2]$. So finally

$$\frac{\triangle_T \mathcal{F}}{A} = \int_0^{\theta_c} \frac{d\theta}{\pi} I_3\left(\sqrt{m^2 - \kappa_\theta^2}\,, T\right) + \int_0^{\pi} \frac{d\theta}{\pi} \int_0^{\infty} \frac{d\xi}{\pi} \mathrm{Re}\left[i I_3\left(\sqrt{m^2 + \xi_+^2}, T\right) \partial_\xi \log f_\theta(\xi_+)\right]$$

This integral can be computed numerically by using *Mathematica* for any finite temperature T. The numerical results for both the Dirac and Pöschl-Teller comb in three dimensions are qualitatively analogous to those obtained for one dimension and are therefore not included here to avoid being repetitive. It can be easily checked that $\triangle_T \mathcal{F}$ takes always negative values which decrease rapidly with increasing temperature. On the contrary, the entropy is a monotonically increasing function of the temperature, meaning that the systems are thermodynamically stable. Finally, the Casimir force takes positive values too, which can be interpreted as the lattice spacing increases and the unit cell blows up as a consequence of the quantum interaction.

Chapter 4

SCALAR FIELDS IN KINK BACKGROUNDS

The main objective of this chapter is to study the quantum vacuum interaction energy between a pair of two-dimensional homogeneous plates placed[1] at $z = a, b$, mimicked by the punctual potential

$$V_{2\delta}(z) = v_0\delta(z-a) + v_1\delta(z-b), \qquad \text{being} \quad v_0, v_1, a, b \in \mathbb{R}, \qquad \text{and} \quad a < b,$$

embedded in a Pöschl-Teller (PT) classical background potential centred at the origin of the direction orthogonal to the plates, i.e.

$$V_{PT}(z) = -\frac{2}{\cosh^2 z}.$$

The PT potential models the propagation of mesons moving in a sine-Gordon kink background [111, 112, 170]. This is another example of QFT in which the ultraviolet divergences present in the vacuum energy are not eliminated just by taking the normal ordering of the operators. In fact, corrections of order $\hbar$ to the mass will appear.

In the first part of the chapter, a brief introduction regarding relevant concepts of QFT in curved spaces is presented. Then, the spectrum of scattering and bound states as well as the Green's functions will be computed. Finally, the *TGTG* formalism is the approach which will be used to calculate the quantum vacuum interaction energy and to study the Casimir pressure between plates. All this chapter is original work not yet published.

4.1. QFT in curved spaces

The Klein-Gordon action of a scalar quantum field ϕ in a curved background [181–183] with boundaries is given by the first integral of (1.11). In fact, the total action has a term concerning

[1]The position four-vector is expressed along the chapter as $x^\mu = (t, \vec{x}_\parallel, z) \in \mathbb{R}^{1,3}$. Notice that $\vec{x}_\parallel \in \mathbb{R}^2$. Likewise, the four-momentum will be $K^\mu = (E, \vec{k}_\parallel, k)$. Note that z and k are the position and the momentum coordinates in the direction orthogonal to the surfaces of the plates.

matter (1.11) and another one related to gravitation:

$$S = S_g + S_m = \int d^{D+1}x \sqrt{-g}\, \frac{R - 2\Lambda}{16\pi \mathtt{G}} + \frac{1}{2}\int d^{D+1}x \sqrt{-g}\, \left[g_{\mu\nu} D_\mu \phi D_\nu \phi - m^2 |\phi|^2 - \xi R |\phi|^2 \right]. \quad (4.1)$$

$\mathtt{G}$ is the universal gravitational constant and Λ the cosmological constant. Remember that, as mentioned in Chapter 1, g is the determinant of the metric tensor, D_μ the covariant derivative obtained from the connection, R the Ricci scalar curvature and ξ the coupling to the gravitational field. Notice that for scalar fields D_μ reduces to ∂_μ.

On the one hand, varying the action with respect to ϕ yields the field equations:

$$g^{\mu\nu} D_\mu D_\nu \phi + (m^2 + \xi R)\phi = 0. \quad (4.2)$$

When considering four-dimensional spacetimes, if $m = 0$ and $\xi = 1/6$, the action and the field equations are invariant under conformal transformations of the metric, namely $g'_{\mu\nu} = \Omega g^{\mu\nu}$ being Ω a real continuous positive definite function. The light cone structure remains invariant under this type of transformations. When using the Minkowski metric in (4.2), one recovers the Klein-Gordon equations. The main differences of the field equations in a generic curved spacetime with respect to those present in the flat Minkowski one, are the terms proportional to the scalar curvature R and the ones which couple the metric with the scalar field by means of the covariant derivatives in the first term of (4.2). Both terms are indispensable when renormalising the theory with counter terms.

On the other hand, varying the action with respect to $g_{\mu\nu}$ yields the Einstein equations:

$$\mathcal{G}_{\mu\nu} = R_{\mu\nu} - \frac{1}{2} R g_{\mu\nu} + \Lambda g_{\mu\nu} = 8\pi \mathtt{G} T_{\mu\nu}, \qquad \text{with} \qquad T_{\mu\nu} = \frac{2}{\sqrt{g}} \frac{\delta}{\delta g^{\mu\nu}} S_m, \quad (4.3)$$

being $T_{\mu\nu}$ the energy-momentum tensor and $R_{\mu\nu}$ the Ricci curvature tensor.

There are relevant differences between working with static flat metrics and curved ones. Those most relevant to the forthcoming discussion are summarised in Table 4.1.

FLAT SPACETIME	**CURVED SPACETIME**
Global time-like Killing vector ∂_t ensuring global conservation laws in special relativity	No global time-like Killing vector
Global space-like hypersurfaces parametrised by the temporal coordinate	Local space-like hypersurfaces parametrised by the temporal coordinate. Only global hyperbolic spacetimes admit a foliation by Cauchy hypersurfaces
Vacuum state invariant under Poincaré group	No preferred coordinates to choose an invariant vacuum state

FLAT SPACETIME	CURVED SPACETIME
Poincaré symmetry group and particles as irreducible representations of this group	No global Poincaré symmetry. The curvature of the spacetime could create particles. The concept of particle makes sense only if its wavelength is much smaller than the curvature scale. Otherwise, it is mean values of the fields that describe the states
Global field decomposition in modes whose coefficients are related to creation and annihilation of particles operators. Field modes are eigenvectors orthogonal to the Killing vector with eigenvalue $-i\omega$ being $\omega > 0$. The modes are plane waves in Minkowski spacetime	Local field modes divided into terms of positive and negative frequencies, which depend on the point in space the observer is sitting at
Global canonical quantisation procedure	Local canonical quantisation procedure

TABLE 4.1: Quantum Field Theory in flat versus curved spacetime.

To sum up, only for Cauchy surfaces in globally hyperbolic [184, 185] curved spacetimes endowed with a complete lightlike Killing vector field, the solutions of the field equations and the temporal coordinate are globally defined and one could perform the usual canonical quantisation. Notice that only in this case, there is a goblal Killing vector and one can express the spacetime as a set of spatial slices which evolve in time. This means that the curved spacetime is a fiber bundle where the temporal one-dimensional manifold is the fiber over each point of the “spatial" manifold. For each fixed value of the temporal coordinate, one could solve the spectra of the Laplacian-Beltrami operator in the spatial slice as done in previous chapters for the Minkowski metric. However, in another more general case, if the curved spacetime is such that the fiber bundle do not allow an interpretation in terms of particle spectra independent of the observer, scattering does not make sense. Consequently, the T_{00} and the transfer operator T defined in Chapter 1 in terms of the scattering data, will not be a universal result independent of the observer. In fact, there are not many results about the *TGTG*-formula in curved backgrounds and sometimes it does not even exist [186]. In these cases, the correct way to compute the Casimir energy is considering the wave function of the fundamental state of the field configuration. Spectral functions associated to the Laplacian operator could be used. Hence, the trace of the determinant of the Laplacian operator would be interpreted as the energy and by using zeta regularisation, it is possible to find a universal result.

The principal problems mentioned above regarding the abscence of the concept of particle, the abscence of a reference vacuum state and the unitarily inequivalent representations of the algebra of the observables in curved spacetime are arisen for instance in [187, 188]. There is a special case to be

taken into account. When the frequencies of the particles created by the gravitational background are much smaller than the Planck frequency, one could use the perturbation theory for this curved spacetime as a semi-classical approach to quantum gravity [189, 190]. In doing so, this weak gravitational backgrounds are treated classically and the matter fields are the ones which will be quantised. In this chapter, an example of weak gravitational field is going to be studied: a 3+1 dimensional spacetime with a Pöschl-Teller kink in one of the spatial dimensions. This gravity would be strong enough to produce some effects to the quantum matter but not so strong as to require an own quantisation. Furthermore, the PT potential is transparent in the sense that the fields could be asymptotically interpreted as particles. Thus it is possible to define incoming and outgoing waves and to derive a S-matrix in a similar way to the usual for flat spacetimes.

The next question that arises is whether it is possible to determine a metric for a curved spacetime, in such a way that the equation describing the dynamics of the quantum vacuum fluctuations around a kink solution in a flat spacetime, i.e.

$$\partial_t^2\phi - \partial_z^2\phi - \left(m^2 + \frac{2}{\cosh^2 z}\right)\phi = 0,$$

be the equation of motion for a scalar field coupled to the gravitational background of a domain wall[2]. It is possible to find a solution for this problem from (4.2) or (4.3), but it is undoubtedly complicated. One of the several difficulties is that very little is known about the distribution of momentum and energy in such a curved spacetime. Is it sufficient for the domain wall to be the only gravitational source of mass? If yes, and considering z as the spatial coordinate in which the one-dimensional domain wall extends along, can $T_{\mu\nu}$ be written as

$$T_{\mu\nu} = \begin{pmatrix} \rho(z) & 0 \\ 0 & f_\Pi \end{pmatrix},$$

with $\rho(z)$ the energy density? If so, what is the flux of momentum f_Π? As can be seen, being able to derive the components of the metric from the Einstein's equations without knowing in advance the exact form of the $T_{\mu\nu}$ tensor may not be guaranteed. However, taking into account the symmetry of the system, perhaps it might be possible to apply the same reasoning given in [192]. In this work, the authors derive the metric components just by solving two differential equations that arise when imposing the spherical symmetry over the Einstein's equations, written in terms of the sectional curvatures[3] [193, 194], and the Bianchi's identities. Due to the spherical symmetry, all sectional curvatures as well as the proper energy density and the proper pressures across the transversal spatial two planes, depend only on the radial coordinate. The rest of the components of $T_{\mu\nu}$ are zero. All this significantly reduces the problem of finding the sectional curvatures and then the metric components.

[2]Domain walls can be thought as membrane-like two dimensional structures embedded in three dimensional spaces. In the early stages of the Universe, the spontaneous breaking of discrete symmetries produced this kind of topological defects [191].

[3]Sectional curvatures allows to compute the second derivative of the separation between any to nearby geodesic curves, with tangent vectors at a given point contained in the corresponding two-plane indicated by the subindeces. They are geometrical quantities independent of the coordinate system.

Back to the case of the metric for the domain wall, there is also a certain degree of symmetry in the configuration of the system. Notice that the domain wall extends along a spatial coordinate but the other two are totally symmetric. Consequently, the sectional curvatures $(K_{tx}, K_{ty}, K_{tz}, K_{yz}, K_{zx}, K_{xy})$ to be found only depend on the spatial coordinate z. Moreover, they fulfil the properties $K_{tx}(z) = K_{ty}(z)$ and $K_{yz}(z) = K_{zx}(z)$. The Einstein's equations

$$\begin{aligned} 2K_{tx}(z) + K_{tz}(z) &= \frac{4\pi \mathtt{G}}{c^2}(\rho(z) + \operatorname{tr} f_{\Pi}), \\ K_{xy}(z) + 2K_{yz}(z) &= \frac{8\pi \mathtt{G}}{c^4}\rho(z), \\ K_{xy}(z) + \frac{1}{c^2}K_{tz}(z) &= \frac{4\pi \mathtt{G}}{c^2}(\rho(z) + \operatorname{tr} f_{\Pi} - 2\sigma^{zz}), \end{aligned}$$

should be solved together with the Bianchi's identities but due to the symmetry, the problem can be tackled. In the equations above, σ^{zz} is the flux of the z component of the momentum transferred per unit time across the unit area along the xy parallel two-plane. This discussion could be a beautiful problem to solve in the future, but it is not necessary to do it right now in order to understand what will appear in the rest of chapter. I would like to remark again that this is due to the fact that the case presented in this chapter is a weak gravitational field which is going to be treated classically, without an own quantisation. And furthermore, the PT potential is transparent so that the notion of incoming and outgoing particle applies here. Hence, for the purposes of this chapter, a quantum scalar field in the presence of an external classical background potential will be considered, in a similar way to what has been done in previous chapters for flat spacetimes.

The aim of the rest of the chapter is to compute the Casimir energy for the quantum vacuum fluctuations of a scalar field interacting with semitransparent plates rather than impenetrable ones (which would be the case when using Dirichlet boundary conditions to mimic the plates, instead of the matching conditions for the double delta potential). In this picture, the delta couplings v_0, v_1 represent the plasma frequencies mimicking the plates in [156]. Previous work concerning the 00 component of $T_{\mu\nu}$ in a system with a kink in the real line, and the scattering problem of two delta potentials symmetrically placed around a kink, can be found in [170, 195]. This chapter tackles a more general situation. The starting point would be the Lagrangian density

$$\mathcal{L} = \frac{1}{2}\left(\partial_\mu \phi \partial^\mu \phi + \frac{2}{\cosh^2 z}\phi^2 - v_0\delta(z-a)\phi^2 - v_1\delta(z-b)\phi^2\right), \qquad v_0, v_1, a < b \in \mathbb{R}.$$

It is important to note that the thermodynamics at non zero temperature are not going to be considered. This is due to the fact that the Pöschl-Teller potential is an example of weak gravitational background so once the thermal fluctuations be the dominant ones, the effects of the curved background will not be noticeable. One will find the same results as in a flat background and more specifically, the results presented in Chapter 2.

4.2. Scattering data and spectrum

A detailed description of the spectrum of the non relativistic Schrödinger operator in the dimension orthogonal to the plates,

$$\hat{K} = -\nabla_\perp + V_{PT}(z) + V_{2\delta}(z), \tag{4.4}$$

is needed to identify the eigenmodes of the scalar field fluctuations. The plates divide the real line into three different zones. The system has an open geometry so the positive energy spectrum would be continuous. Scattering states correspond to solutions of the Schrödinger equation $\hat{K}\psi = k^2\psi$ with $k \in \mathbb{R}$ (such that $k^2 > 0$). Given a linear momentum k there are two independent scattering solutions. Away from the singular points, the "*diestro*" scattering solutions (incoming particles from the left) are of the form:

$$\psi^R(k,z) = \begin{cases} f_k(z) + r_R(k)\, f_{-k}(z), & \text{if} \quad z < a, \\ A_R(k)\, f_k(z) + B_R(k)\, f_{-k}(z), & \text{if} \quad a < z < b, \\ t_R(k)\, f_k(z), & \text{if} \quad z > b, \end{cases} \tag{4.5}$$

being $f_k(z) = e^{ikz}(\tanh(z) - ik)$ the free waves of the Pöschl-Teller potential (i.e., plane waves times first order Jacobi polynomials). Hence, the scattering problem will be solved analogously to a flat background case, but replacing the free waves $e^{\pm ikz}$ by $f_{\pm k}(z)$. Likewise, for "*zurdo*" scattering (incoming particles from the right) one gets:

$$\psi^L(k,z) = \begin{cases} t_L(k)\, f_{-k}(z), & \text{if} \quad z < a, \\ A_L(k)\, f_{-k}(z) + B_L(k)\, f_k(z), & \text{if} \quad a < z < b, \\ r_L(k)\, f_k(z) + f_{-k}(z), & \text{if} \quad z > b. \end{cases} \tag{4.6}$$

The transmission amplitudes $t_R(k) = t_L(k) = t(k)$ are identical to each other due to the time-reversal invariance of the Schrödinger operator (4.4).

Notice that $-\nabla^2 + V_{PT}(z)$ is not essentially self-adjoint in the whole real line excluding the points at which the delta potentials are centred, i.e. when its domain is the Sobolev space of functions $W_2^2(\mathbb{R} - \{a,b\}, \mathbb{C})$. It is necessary to add some matching conditions concerning the continuity of the wave function and the discontinuity of its derivative at the boundary points $\{a,b\}$ in order to define the self-adjoint extensions of $-\nabla^2 + V_{PT}(z)$ in the aforementioned domain. These boundary conditions are given by:

$$\begin{pmatrix} \psi(a^+) \\ \psi'(a^+) \end{pmatrix} = \begin{pmatrix} 1 & 0 \\ v_0 & 1 \end{pmatrix} \begin{pmatrix} \psi(a^-) \\ \psi'(a^-) \end{pmatrix}, \qquad \begin{pmatrix} \psi(b^+) \\ \psi'(b^+) \end{pmatrix} = \begin{pmatrix} 1 & 0 \\ v_1 & 1 \end{pmatrix} \begin{pmatrix} \psi(b^-) \\ \psi'(b^-) \end{pmatrix}. \tag{4.7}$$

Replacing (4.5) and (4.6) in (4.7) and solving the resulting two systems of equations with unknowns $\{r_R, r_L, t_R = t_L, A_R, B_r, A_L, B_L\}$, one obtains the following scattering data:

$$\begin{aligned}
t &= \frac{W^2}{\Upsilon(k)},\\
r_R &= \frac{-v_0 W f_k^2(a) - v_1 W f_k^2(b) + v_0 v_1 f_k(a) f_k(b)[f_{-k}(a) f_k(b) - f_k(a) f_{-k}(b)]}{\Upsilon(k)},\\
r_L &= \frac{-v_0 W f_{-k}^2(a) - v_1 W f_{-k}^2(b) - v_0 v_1 f_{-k}(a) f_{-k}(b)[f_k(a) f_{-k}(b) - f_{-k}(a) f_k(b)]}{\Upsilon(k)},\\
A_R &= \frac{W^2 + v_1 W f_k(b) f_{-k}(b)}{\Upsilon(k)},\\
A_L &= \frac{W^2 + v_0 W f_k(a) f_{-k}(a)}{\Upsilon(k)},\\
B_R &= -\frac{v_1 W f_k^2(b)}{\Upsilon(k)},\\
B_L &= -\frac{v_0 W f_{-k}^2(a)}{\Upsilon(k)},\\
\Upsilon(k) &= W^2 + v_0 W f_k(a) f_{-k}(a) + v_1 W f_k(b) f_{-k}(b) + v_0 v_1 f_{-k}(a) f_k(b)[f_k(a) f_{-k}(b) - f_{-k}(a) f_k(b)],
\end{aligned} \tag{4.8}$$

where W is the following Wronskian

$$W \equiv W[f_k(a), f_{-k}(a)] = f_k(a) f'_{-k}(a) - f_{-k}(a) f'_k(a) = -2ik(k^2+1).$$

A rather important fact is that due to the Pöschl-Teller background potential, the translational invariance of the system is broken. $V_{PT}(z)$ breaks the isotropy of the space and consequently if $f_k(z)$ is an eigenfunction of the non-relativistic Schrödinger operator $\hat{K} = -\partial_z^2 + V_{PT}(z)$, then $f_k(z+a)$ with $a \in \mathbb{R} - \{0\}$ will no longer be another. This means that the scattering data explicitly depend on the position of the plates in a non-trivial way. In contrast, a free flat spacetime with Schrödinger operator $\hat{K}_0 = -\partial_z^2$ is isotropic.

The denominator of all the scattering parameters, $\Upsilon(k)$, is the spectral function. The set of zeroes of $\Upsilon(k)$ gives the poles of the scattering matrix $S(k)$. Notice that the $S(k)$-matrix admits an analytical continuation to the entire complex momentum plane. Studying the solutions of $\Upsilon(k) = 0$ with $k \in \mathbb{R}$ allows to know the region in the coupling parameter space (v_0, v_1) where there are no bound states. The zeroes on the positive imaginary axis in the complex momentum k-plane gives the bound states of the spectrum of the Hamiltonian. Making $k \to i\xi$ in $\Upsilon(k) = 0$, one can study the bound states as the intersections between an exponential and a rational function via the following transcendent equation:

$$\frac{\Upsilon_1}{\Upsilon_2} = e^{-2\xi(b-a)},$$

where

$$\begin{aligned} Y_1 &= [v_0(\xi^2 - \tanh^2 a) + 2\xi(\xi^2 - 1)][v_1(\xi^2 - \tanh^2 b) + 2\xi(\xi^2 - 1)], \\ Y_2 &= v_0 v_1 (\xi - \tanh a)^2 (\xi + \tanh b)^2. \end{aligned}$$

It can be checked numerically that there are no bound states with energy below a certain quantity E_{min}, which takes the value:

$$E_{min} = -\frac{\left[(|v_1| + |v_0|) + \sqrt{(|v_1| + |v_0|)^2 + 16}\right]^2}{16}, \qquad \forall v_0, v_1 \in \mathbb{R}, \tag{4.9}$$

for all $a, b \neq 0$. If $a = b = 0$ then the minimum energy of the bound state of the system is given by:

$$E_{min} = -\frac{\left[-(v_1 + v_0) + \sqrt{(v_1 + v_0)^2 + 16}\right]^2}{16}, \qquad \forall v_0, v_1 \in \mathbb{R}.$$

If one of the delta potentials is switched off (for example, $v_0 = 0$), the scattering data of the reduced system is given by (4.8) with $v_0 = 0$ and the spectral function is:

$$2\xi^3 + v\xi^2 - 2\xi - v\tanh^2(b) = 0. \tag{4.10}$$

The polynomial (4.10) has three real roots. By studying the asymptotic behaviour of the spectral function as well as its maxima and minima for different values of the parameters, it can be seen that there may be several cases: only one bound state or two bound states, as one can see in Figure 4.1.

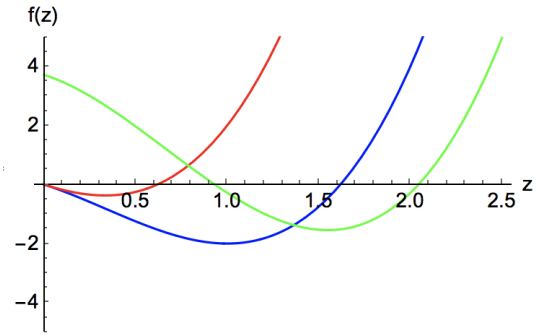

FIGURE 4.1: Zeroes of the spectral function $f(\xi)$ for a single delta potential in the PT background. Green line: $(b = 2, v_1 = -4)$; red line: $(b = 0, v_1 = 2)$; blue line: $(b = 0, v_1 = -2)$.

There is no zero mode because the state with wave vector $k = 0$ does not constitute a pole of the S-matrix. If $b = 0$ there is always a bound state with energy:

$$E = -\frac{\left(-v_1 + \sqrt{v_1^2 + 16}\right)^2}{16}.$$

The minimum energy related to the bound state that appears in the system for all $b \neq 0$ is

$$E_{min} = \begin{cases} -\frac{\left(-v_1+\sqrt{v_1^2+16}\right)^2}{16}, & \text{if} \quad v_1 < 0, \\ -1 & \text{if} \quad v_1 \geq 0. \end{cases} \tag{4.11}$$

Either for the general case $v_0, v_1 \in \mathbb{R} - \{0\}$ and for the simpler case mentioned above in which one of the potentials is "turned off" ($v_0 = 0, v_1 \neq 0$ or $v_1 = 0, v_0 \neq 0$), the value of E_{min} is essential for the computation of the quantum vacuum interaction energy in the corresponding QFT. Since the bound state with the lowest energy is characterised by E_{min}, the mass of the fluctuations in the theory will be balanced with this value E_{min} for making fluctuation absorption impossible. The unitarity of the QFT sets this lower bound for the mass of the quantum vacuum fluctuations, so that the total energy of the lowest energy state of the spectrum will be zero.

4.3. Green's function

To compute the Casimir energy induced by the quantum vacuum fluctuations of a real massive scalar field in the system, it is necessary to know the Green's function. One could obtain it by solving the differential equation

$$\left(\partial_\mu \partial^\mu - \frac{2}{\cosh^2 z} + V_{2\delta}(z) + m^2\right) G(x^\mu, y^\mu) = \delta(x^\mu - y^\mu),$$

for the complete Green's function given in (1.12) or, equivalently, by solving

$$\begin{aligned} \left(-\partial_{z_1}^2 - \omega^2 + \vec{k}_\parallel^2 - \frac{2}{\cosh^2 z_1} + m^2 + V_{2\delta}(z_1)\right) G_k(z_1, z_2) &= \delta(z_1 - z_2), \\ \left(-\partial_{z_1}^2 - k^2 - \frac{2}{\cosh^2 z_1} + V_{2\delta}(z_1)\right) G_k(z_1, z_2) &= \delta(z_1 - z_2), \end{aligned}$$

for the reduced one. For solving it, it is also necessary to assume continuity of $G_k(z_1, z_2)$ and discontinuity of its derivative at the points a, b and to impose an exponentially decaying behaviour of the solutions at infinity. Another way to compute the reduced Green's function in the spatial dimension orthogonal to the surfaces of the plates, is by using (1.13) and the two linear independent scattering solutions given in (4.5), (4.6), being

$$W[\psi_k^R(a), \psi_k^L(a)] = \psi_k^R(a)\psi_k^L(a)' - \psi_k^L(a)\psi_k^R(a)' = t\, W = t[-2ik(k^2+1)].$$

The Wronskian has to be the same for the three zones in which the two delta plates divide the space. This imposes the following relation between the scattering coefficients: $t = A_R A_L - B_R B_L$. This relation would be useful to simplify the solutions of the Green's function in the different zones which the plates divide the space into, and to rewrite them as $G_k(z_1, z_2) = G_k^{PT} + \Delta G_k(z_1, z_2)$. Both aforementioned methods yield the same following solutions for the correlator when the two points are in

the same region of the space:

$$\Delta G_k(z_1,z_2)=\begin{cases}\frac{r_L}{W}f_k(z_1)f_k(z_2), & \text{if } z_1,z_2>b,\\ \frac{r_R}{W}f_{-k}(z_1)f_{-k}(z_2), & \text{if } z_1,z_2<a,\\ \frac{A_RB_L}{tW}f_k(z_1)f_k(z_2)+\frac{B_RA_L}{tW}f_{-k}(z_1)f_{-k}(z_2) & \text{if } a<z_1,z_2<b,\\ +\frac{B_RB_L}{tW}(f_{-k}(z_>)f_k(z_<)+f_k(z_>)f_{-k}(z_<)), & \end{cases} \tag{4.12}$$

where $z_<$ and $z_>$ are the lesser or the greater of z_1 and z_2.

When z_1, z_2 are in different regions of the space, the reduced Green's function can be written as:

$$\Delta G_k(z_1,z_2)=\begin{cases}(t-1)\,G_k^{PT}(z_1,z_2), & \text{if } z_2>b,\ z_1<a\,(\text{or } z_1\leftrightarrow z_2),\\ (A_L-1)\,G_k^{PT}(z_1,z_2)+\frac{B_L}{W}f_k(z_1)f_k(z_2), & \text{if } z_2>b,\ a<z_1<b\,(\text{or } z_1\leftrightarrow z_2),\\ (A_R-1)\,G_k^{PT}(z_1,z_2)+\frac{B_R}{W}f_{-k}(z_1)f_{-k}(z_2), & \text{if } z_2<a\ a<z_1<b,(\text{or } z_1\leftrightarrow z_2),\end{cases} \tag{4.13}$$

In both (4.12) and (4.13) the scattering data is given by (4.8). Notice that the Green's function for the kink potential centred at the origin without any delta interactions ($v_0, v_1 = 0$),

$$G_k^{PT}(z_<,z_>)=\frac{1}{W}f_{-k}(z_<)f_k(z_>)=\frac{e^{ik|z_1-z_2|}}{W}\left(k^2-ik|\tanh z_1-\tanh z_2|+\tanh z_1\tanh z_2\right),$$

plays the same role as $G_k^0(z_1,z_2)=e^{ik|z_1-z_2|}/(-2ik)$ in plain backgrounds. This is due to the fact that the Pöschl-Teller potential is transparent (there is not additional reflection with respect to the free case). Furthermore, since the Pöschl-Teller potential breaks the isotropy of the space, the Green's function is such that $G_k^{PT}(z_1,z_2)\neq G(z_1-z_2)$. In fact, $G^{PT}(z,z)$ is not a constant as happens in the free flat case, but depends on the spatial coordinate in a non trivial way and thus, spatial translations are no longer symmetries of the system.

4.4. *TGTG* formula

The energy induced by the quantum vacuum fluctuations around the plates is given by

$$E_0=\frac{1}{2}\sum_{\omega^2\in\sigma(\hat{K})}\omega=\frac{A}{2}\int_{\mathbb{R}^2}\frac{d\vec{k}_\parallel}{(2\pi)^2}\left(\sum_{j=1}^{N}\sqrt{\vec{k}_\parallel^2+(i\kappa_j)^2+m^2}+2\int_m^\infty\frac{dk}{2\pi}\sqrt{\vec{k}_\parallel^2+k^2+m^2}\,\frac{d\delta(k)}{dk}\right), \tag{4.14}$$

being A the area of the plates and $\delta(k)$ the phase shift related to the scattering problem in the direction orthogonal to the plate:

$$\delta(k)=\frac{1}{2i}\log_{-\pi}\left[t^2(k)-r_R(k)r_L(k)\right]. \tag{4.15}$$

The summation over ω^2 in (4.14) is performed over $\omega^2 \in \sigma(-\nabla + V_{PT})$. The sum over modes of the spectrum in the orthogonal direction splits into the summation over a finite number of bound states with positive energy in the gap[4] and the integral over the continuous states. Since the integral over $\mathbb{R}^2$ is divergent, it is necessary to add a regulator such that:

$$\lim_{\epsilon\to 0}\int_{\mathbb{R}^2}\frac{d\vec{k}_\parallel}{(2\pi)^2}\sqrt{\vec{k}_\parallel^2+k^2+m^2}\,e^{-\epsilon(\vec{k}_\parallel^2+k^2+m^2)} = \lim_{\epsilon\to 0}\frac{1}{2\pi}\chi(k,\epsilon),$$
$$\chi(k,\epsilon) = \frac{\sqrt{\pi}}{4\,\epsilon^{3/2}} - \frac{1}{3}\left(k^2+m^2\right)^{3/2} + o(\epsilon).$$

The result is still divergent making it necessary to remove the first term in the Laurent series of $\chi(\epsilon,k)$ and $\chi(\epsilon,i\kappa)$ to then perform the limit $\epsilon\to 0$ and obtain

$$E_0 = -\frac{A}{2}\sum_{j=1}^{N}\frac{\left(\sqrt{-(\kappa_j)^2+m^2}\right)^3}{6\pi} - \frac{A}{12\pi^2}\int_m^\infty dk\,\left(\sqrt{k^2+m^2}\right)^3\frac{d\delta(k)}{dk}, \tag{4.16}$$

with $m^2 = |E_{min}|$ as appears in (4.9).

Notice that removing the pole in the series expansion of $\chi(\epsilon,k)$ implies subtracting the divergence associated to the bulk. However, the subdominant divergences associated to the plates are still present and a renormalisation mode-by-mode is necessary. This step is achieved by subtracting from the phase shift of the whole system with two plates, the corresponding phase shifts associated to a reduced problem with only one delta plate:

$$\tilde{\delta}(k) = \delta_{v_0,v_1}(k) - \delta_{v_0}(k) - \delta_{v_1}(k). \tag{4.17}$$

It is worth highlighting that this last equation constitutes a subtraction mode by mode of the spectrum to complete the renormalisation. This method is different from setting a cutoff in the integral over modes to remove the high energetic spectrum that does not feel the background. The DHN formula [123] arises from (4.16) when using the phase shift (4.17). It is also possible to integrate it by parts to derive a simplified expression:

$$E_0 = -\frac{A}{2}\sum_{j=1}^{N}\frac{\left(\sqrt{-(\kappa_j)^2+m^2}\right)^3}{6\pi} - \frac{A}{12\pi^2}\left(\sqrt{k^2+m^2}\right)^3\tilde{\delta}(k)\Big|_m^\infty + \frac{A}{4\pi^2}\int_m^\infty dk\,k\sqrt{k^2+m^2}\,\tilde{\delta}(k). \tag{4.18}$$

The frequencies of the bound states for each configuration (v_0,v_1,a,b) would be determined numerically through $\Upsilon(i\kappa) = 0$ from (4.8). The second term of (4.18) would be zero due to the Levinson theorem[5] [98, 196], so finally

[4] When introducing a mass in the theory and the lowest energy of the eigenstates of $\hat{K}$ becomes zero, the threshold of the continuous spectrum is also displaced. Hence, the discrete part of the spectrum related to bound states moves to the gap $[0,m]$, and the continuous spectrum of eigenstates starts at the upper threshold of this interval, i.e. $E = m^2$.

[5] The Levinson's theorem states that there is a relation between the number of bound states with energy smaller or equal to zero, and the variation in the phase shift as the moment changes. In this case, since in the interval $[m,\infty]$ there are no bound states, the variation $\delta(\infty) - \delta(m)$ must be zero. Furthermore, if one chooses the branch of the logarithm in the definition of the phase shift in such a way that $\delta(\infty) = 0$ then $\delta(m) = 0$ too and the second term in (4.18) vanishes. The condition $\delta(\infty) = 0$ is what makes physical sense, since the high energetic modes are not scattered when passing through the system.

$$E_0 = -\frac{A}{2}\sum_{j=1}^{N}\frac{\left(\sqrt{-(\kappa_j)^2+m^2}\right)^3}{6\pi} + \frac{A}{4\pi^2}\int_m^\infty dk\, k\,\sqrt{k^2+m^2}\,\tilde{\delta}(k). \tag{4.19}$$

If there were half bound states in the spectrum (i.e. states with energies that lie in the threshold of the continuum spectrum), they would have to be accounted for in the first term of the equation above with a weight of $1/2$. But this is not the case covered by this chapter. Appendix B contains a derivation of the DHN formula from basic principles.

Nevertheless, instead of using the aforementioned approach with the derivative of the phase shifts acting as the density of states, the *TGTG* formula will be used. The result will be the same using either of these two procedures. The major advantage of using the *TGTG* formalism explained in Section 1.3 is that only the scattering problem for the Pösch-Teller potential with one delta plate is necessary to compute the vacuum interaction energy between plates. This could be a crucial factor whenever the scattering problem for the complete potential with two plates in a classical background is hard to be solved. Furthermore, using the *TGTG* formula significantly reduces the complexity of the analytical computation.

From the Lippmann-Schwinger equation (1.15) and $\hat{K}_{z_1} G_k^{PT}(z_1 - z_2) = \delta(z_1 - z_2)$, it is easy to see that

$$-\hat{K}_{z_2}\,\hat{K}_{z_1}\,\Delta G_k(z_1,z_2) = \int dz_3\, dz_4\, \delta(z_1-z_3) T_k(z_3,z_4)\delta(z_4-z_2) = T_k(z_1,z_2),$$

being $\hat{K}_z = -\partial_z^2 - k^2 + V_{PT}(z)$ the free Schrödinger operator for the one-particle states. Notice that in the above formula, $\Delta G_k(z_1,z_2)$ corresponds to the Green's function of only one plate in the Pösch-Teller potential. For obtaining the transfer matrix $T_k(z_1,z_2)$ corresponding to one plate from (4.12) and (4.13) with one of the deltas switched off, the only non trivial contribution comes from the case in which one point is on the left and the other one on the right of the plate, due to the absolute values contained in G_k^{PT}. Hence, since in this case $\Delta G_k(z_1,z_2) = (t-1)G_k^{PT}(z_1,z_2)$, it is necessary to compute:

$$T_k(z_1,z_2) = -(t-1)\hat{K}_{z_2}\,\hat{K}_{z_1}\,G_k^{PT}(z_1,z_2). \tag{4.20}$$

Now the objective is to compute the transfer matrix associated to the plate on the right[6]. Again, for simplicity, one assumes the plate sitting at the origin ($b = 0$) and hence, one of the coordinates z_1, z_2 will be greater than zero and the other less than zero. Taking into account that in such a case

$$e^{ik|z_1-z_2|} = e^{ik(|z_1|+|z_2|)}, \qquad \text{both in the cases } z_1<0, z_2>0 \text{ and } z_1>0, z_2<0,$$

$$|\tanh z_1 - \tanh z_2| = \tanh|z_1| + \tanh|z_2|, \qquad \text{both in the cases } z_1<0, z_2>0 \text{ and } z_1>0, z_2<0,$$

$$\tanh z_1 \tanh z_2 = -\tanh|z_1|\tanh|z_2|, \qquad \text{both in the cases } z_1<0, z_2>0 \text{ and } z_1>0, z_2<0,$$

[6]For computing the transfer matrix of the left hand sided plate one sets $v_1 = 0$ in the transmission coefficient (4.8) involved in the Green's function and considers the case in which the left plate is centred at $a = 0$. Similarly, one should take $v_0 = 0$ in the general scattering data (4.8) for calculating the T matrix of the right hand side plate.

it is possible to rewrite the free Green's function in the background of the kink as

$$G_k^{PT}(z_1,z_2) = -\frac{1}{W}e^{ik|z_1|}(\tanh|z_1| - ik)e^{ik|z_2|}(\tanh|z_2| - ik) = -\frac{1}{W}f_k(|z_1|)f_k(|z_2|). \tag{4.21}$$

Because of the Green's differential equation

$$\left(-\partial_z^2 - k^2 - \frac{2}{\cosh^2 z}\right) f_{\pm k}(|z|) = 0,$$

and using the formulas for the derivatives of functions depending on absolute values

$$\frac{df_k(|z|)}{dz} = f_k(|z|)'\operatorname{sign} z, \qquad \frac{d^2 f_k(|z|)}{dz^2} = f_k(|z|)'' + f_k(|z|)'2\delta(z),$$

the transfer matrix for the right plate can be written as

$$\begin{aligned} T_k(z_1,z_2) &= \frac{t-1}{W}4\delta(z_1)\delta(z_2)e^{ik|z_1|}(ik\tanh|z_1| + k^2 + \operatorname{sech}^2|z_1|)e^{ik|z_2|}(ik\tanh|z_2| + k^2 + \operatorname{sech}^2|z_2|) \\ &= \frac{t-1}{W}4\delta(z_1)\delta(z_2)(k^2+1)^2 = \frac{|W|^2}{k^4}\delta(z_1)\delta(z_2)\Delta G_k(z_1,z_2). \end{aligned}$$

When the delta potential which mimics the plate is evaluated at another point different from the origin, the just-computed result for $T_k(z_1,z_2)$ is valid once after performing the following translations: $z_1 \mapsto z_1 - b$ and $z_2 \mapsto z_2 - b$. Consequently,

$$T_k(z_1,z_2) = \frac{|W|^2}{k^4}\delta(z_1-b)\delta(z_2-b)\Delta G_k(b,b). \tag{4.22}$$

The only difference is that now $\Delta G_k(b,b)$ is not a continuous function as it is the case for $\Delta G_k(0,0)$ and it should be defined as the following piecewise function:

$$\Delta G_k(b,b) = \begin{cases} \frac{r_R}{W}f_{-k}^2(b), & \text{if } z_1, z_2 \to b^-, \\ \frac{r_L}{W}f_k^2(b), & \text{if } z_1, z_2 \to b^+, \\ \frac{t-1}{W}f_k(b)f_{-k}(b), & \text{if } z_1 \to b^-, z_2 \to b^+ (\text{or } z_1 \leftrightarrow z_2), \end{cases} \tag{4.23}$$

being the scattering data given in (4.8) but for $v_0 = 0$. Notice that in the definition of T at a point different to $z = 0$, translation must be understood as replacing $\delta G_k(0,0)$ and the scattering coefficients at $z = 0$ contained in its definition, by $\delta G_k(b,b)$ and the scattering data at $z = b$. Notice that due to the PT potential the isotropy of the spacetime is broken and $r_{R,L}(b) \neq r_{R,L}(0)e^{ikb}$, so the translation $z_1 \mapsto z_1 - b$ and $z_2 \mapsto z_2 - b$ aforementioned must not be interpreted in this usual sense. The T matrix for the left-hand side plate is

$$T_k(z_1,z_2) = \frac{|W|^2}{k^4}\delta(z_1-a)\delta(z_2-a)\Delta G_k(a,a). \tag{4.24}$$

Again, for computing $\Delta G_k(a,a)$ the coefficient v_1 must be taken equal to zero in (4.8) and (4.12).

The Green's function or correlator $G(z_1, z_2) = G^{PT}(z_1, z_2) + \Delta G(z_1, z_2)$ represents the probability transition amplitude for a particle to propagate from one point to another while moving freely in the background spacetime ($G^{PT}(z_1, z_2)$ term), or while interacting with different potentials ($\Delta G(z_1, z_2)$ contribution). Besides that, the T matrix is the probability amplitude for a particle to interact with the potential but without propagation. Hence, in the system of two plates mimicked by punctual delta potentials in the background of a kink, the definition of the T operator must depend on ΔG evaluated at the point at which the delta potential is centred, as it is the case in (4.24). It could not depend on an arbitrary point of the spacetime for the causality not to be violated. Notice that when the potential is not supported at a point but a compact interval, then T is local. Although in this case T would depend on the points that constitute the support of the potential, it does not violate causality because it does not depend on arbitrary points. When the particle interacts with a potential of compact support, $\Delta G(z_1, z_2)$ includes the probability of interaction with the potential (T contribution) as well as the propagation of the particle within the support of the potential.

Notice that $G^{PT}(z_1, z_2) = \langle \mathcal{T}\phi(z_1)\phi(z_2)\rangle$, expression in which the time-ordering operator product has been considered. All eigenstates of $\hat{K} = -\partial_z^2 + V_{PT}(z)$ with fixed energy k^2 can be described in terms of the orthonormal basis of left and right Pöschl-Teller free waves. By labelling $R = f_k(z)$ and $L = f_{-k}(z)$, the Green's function or propagator can be written in this basis as

$$G^{PT}(a,b) = \frac{1}{W} |L(a)\rangle \langle L(b)|, \qquad G^{PT}(b,a) = \frac{1}{W} |R(b)\rangle \langle R(a)|, \qquad \text{being} \quad a < b, \tag{4.25}$$

and the *TGTG* operator has the following behaviour:

$$\operatorname{tr} T^\ell G^{PT} T^r G^{PT} = \frac{1}{W^2} \langle R(a)| T^\ell |L(a)\rangle \langle L(b)| T^r |R(b)\rangle \langle R(a)|R(a)\rangle .$$

The superscript ℓ, r indicates which plate is being considered: ℓ for the plate placed on the left of the system and r on the right. It has been taken into account that $T|R\rangle = |L\rangle$ and vice versa. So by (4.23) and (4.24), the *TGTG* formula will be calculated using the reflection coefficients, which depend explicitly on the position of each plate. As a consequence of this reasoning, the only combinations of the T operator components that allow coincidences of the z_1, z_2 points in $[a, b]$ and contribute to the quantum vacuum interaction energy between plates are:

$$\begin{aligned} \operatorname{Tr} \mathbf{TGTG}_k &= \int dz_1\, dz_2\, dz_3\, dz_4\, T^\ell(z_1, z_2) G^{PT}(z_2, z_3) T^r(z_3, z_4) G^{PT}(z_4, z_1) = \left[G^{PT}(a,b)\right]^2 T_2^\ell(a,a)\, T_1^r(b,b) \\ &= \left[G^{PT}(a,b)\right]^2 \frac{(W^*)^2}{k^8}\, r_L^\ell(v_0, a, k)\, r_R^r(v_1, b, k) f_k^2(a) f_{-k}^2(b), \end{aligned} \tag{4.26}$$

where the asterisk means complex conjugate. The subindex of T refers to the different zones in which the plates divides the real line: 1 is for the zone to the left of the plate and 2 to the right. On the other hand, the subscript in the reflection coefficients denotes whether one is working with the "*zurdo*" (L) or "*diestro*" (R) scattering solution. Taking into account the scattering reflection coefficients given in (4.8) and the Green's function for the PT background (4.25), the trace mentioned above could be written more specifically as

$$\mathrm{Tr}\,\mathbf{TGTG}_k = \frac{v_0 v_1}{k^8}\frac{f^4_{-k}(a)f^4_k(b)f^2_{-k}(b)f^2_k(a)}{(W+v_1 f_k(b)f_{-k}(b))\,(W+v_0 f_k(a)f_{-k}(a))}. \tag{4.27}$$

In the seminal paper [38], Kenneth and Klich give the following formula for the quantum vacuum interaction energy between compact bodies in one dimensional flat spacetime:

$$E_0 = -i\int_0^\infty \frac{d\omega}{2\pi}\,\mathrm{tr}\log\left(1-\mathbf{TGTG}_\omega\right). \tag{4.28}$$

Notice that the case the authors consider does not present bound states with negative energy in the spectrum. Furthermore, in Appendix B and C of [38] the authors prove that for any pair of disjoint finite bodies separated by a finite distance and any Green's function that is finite away from the diagonal, the operator $TGTG$ is trace class. The modulus of its eigenvalues is less than one (Theorem B.6 in [38]) and $\log(1-\boldsymbol{TGTG})$ is well defined. A similar reasoning can be followed here for the system of two dimensional plates, that are assumed not to touch, in the curved background of a kink. Since the modulus of the eigenvalues of the $TGTG$ operator is less than one, it is possible to use

$$\mathrm{Tr}\log(1-\mathbf{TGTG}_k) = \log\det(1-\mathbf{TGTG}_k) \approx \log(1-\mathrm{Tr}\,\mathbf{TGTG}_k) \tag{4.29}$$

as a good approximation up to first order to simplify (4.28). The above first equality can be proven by taking into account that any Hermitian matrix A representing an Hermitian operator can be transformed into a diagonal matrix, so that $A_D = BAB^{-1}$. In this way:

$$\begin{aligned} e^{\mathrm{Tr}\log A} &= e^{\mathrm{Tr}\log\left(B^{-1}A_D B\right)} = e^{\mathrm{Tr}\left[B^{-1}(\log A_D)B\right]} = e^{\mathrm{Tr}\log A_D} = e^{\sum_i \log\lambda_i} = \prod_i \lambda_i \\ &= \det A_D = \det\left(BAB^{-1}\right) = \det A. \end{aligned}$$

In this demonstration the cyclic property of the trace has been used, and the eigenvalues of the diagonal matrix A_D have been denoted by λ_i. On the other hand, denoting by α_i the eigenvalues of $M = TGTG$, it is easy to prove the second claim in (4.29) because

$$\begin{aligned} \log\det(1-M) &= \log\det\left[B_1^{-1}(1-M_D)B_1\right] = \log\prod_i(1-\alpha_i) = \log[1-(\sum_i \alpha_i)+o(\alpha_i\alpha_j)] \\ &\approx \log[1-\mathrm{Tr}\,M_D] = \log[1-\mathrm{Tr}(B_1 M B_1^{-1})] = \log[1-\mathrm{Tr}\,M], \end{aligned}$$

because the norm of M is less than one.

In summary, replacing (4.27) and (4.29) in (4.28) and generalising it to three dimensions leads the final expression:

$$\frac{E_0}{A} = -\frac{1}{2}\sum_{j=1}^{N}\frac{\left(\sqrt{-\kappa_j^2+m^2}\right)^3}{6\pi} + \frac{1}{8\pi^2}\int_m^\infty d\xi\,\xi\sqrt{\xi^2-m^2}\log(1-\mathrm{Tr}\,\mathbf{GTGT}_\xi),$$

$$\frac{E_0}{A} = \frac{1}{8\pi^2}\int_m^\infty d\xi\,\xi\,\sqrt{\xi^2-m^2}\log\left[1-\frac{v_0v_1}{\xi^8}\frac{f^4_{-i\xi}(a)f^4_{i\xi}(b)f^2_{-i\xi}(b)f^2_{i\xi}(a)}{\left[W(i\xi)+v_1f_{i\xi}(b)f_{-i\xi}(b)\right]\left[W(i\xi)+v_0f_{i\xi}(a)f_{-i\xi}(a)\right]}\right] - \frac{1}{2}\sum_{j=1}^{N}\frac{\left(\sqrt{-\kappa_j^2+m^2}\right)^3}{6\pi}, \tag{4.30}$$

with $m^2 = |E_{min}|$ given by (4.9). When defining $V_i(z) = v_i\,\delta(z-z_i)$ (with $i = 0, 1$ and $z_0 = a, z_1 = b$) for describing each of the the two plates, it is clear that $\hat{K}_i = -\partial_z^2 + V_i(z)$ are defined over a Hilbert space that, in general, is not isomorphic to $\hat{K} = -\partial_z^2 + V_{PT}(z)$. Hence, G^{PT} and $T^{r,\ell}$ do not act in the same spaces and $G^{PT}T^\ell G^{PT}T^r$ is ill defined. To avoid this problem, a Wick rotation of the momentum k must be performed in order for all the operators to act in the same Hilbert space. The integral (4.30) is thus convergent and can be evaluated numerically with *Mathematica*. In the next section, the results of the Casimir pressure for some examples of configurations of the plates in the background potential are going to be discussed, as a way to close this chapter.

4.5. Casimir pressure

Once the quantum vacuum interaction energy is determined, one can study the Casimir force between plates as

$$F = -\frac{\partial E_0}{\partial d}.$$

being d the distance between plates. Nevertheless, the translational invariance is broken due to the PT background, which means that the scattering data for the plates explicitly depend on the position in a non-trivial way. Hence, when computing the Casimir force, a non-trivial contribution coming from the derivatives of the scattering amplitudes of one of the plates with respect to the position will appear. There is an ambiguity yet not clarified in this calculation. One can either introduce the dependence on the distance between plates in three different ways:

1. Putting the left plate at $z_1 = a$ and the right one at $z_2 = a + d$. In this case, only the right plate scattering data will depend on the distance, and only the derivative of $r_R^r(v_1, a+d, k)$ with respect to the position will appear.

2. Considering the right plate placed at $z_2 = b$ and the left plate at $z_1 = b - d$. Analogously to the previous case, only the left plate scattering data will depend on d and the derivative of $r_L^\ell(v_0, b-d, k)$ with respect to the position is the only possible contribution.

3. When one of the plates is to the left of the origin and the other one to the right, one could describe the location of the plates as the left one being at $z_1 = -d + b$ and the other one at $z_2 = d - a$. This case is different because the derivatives of the reflection coefficients of both plates $r_R^r(v_1, d-a, k)$ and $r_L^\ell(v_0, -d+b, k)$ will be taken into account.

It is work in progress to check that these three situations give rise to the same force. However, it is

obvious that if the Casimir energy between plates has a change in the sign for some values of the parameters $\{v_0, v_1, a, b\}$, the Casimir force will present it too. Consequently, studying numerical results for the quantum vacuum interaction energy is enough to discuss whether this important property is fulfilled, which is one of the main points of interest of the work.

Figure 4.2 shows the quantum vacuum interaction energy for different configurations of the system of two plates in the PT background. As can be seen, the energy is always negative, independently of the value of the coefficients of the delta potentials and its location in relation to the kink centre. This implies that the Casimir force between plates will always be attractive in this system. Furthermore, when the Pöschl-Teller well is not confined at all between the plates and they are far from the kink centre, the system of two δ-plates in flat spacetime is recovered. This is the reason that the numerical representation for this situation, which has already been studied in the literature, is not included here. However, it is available in [54].

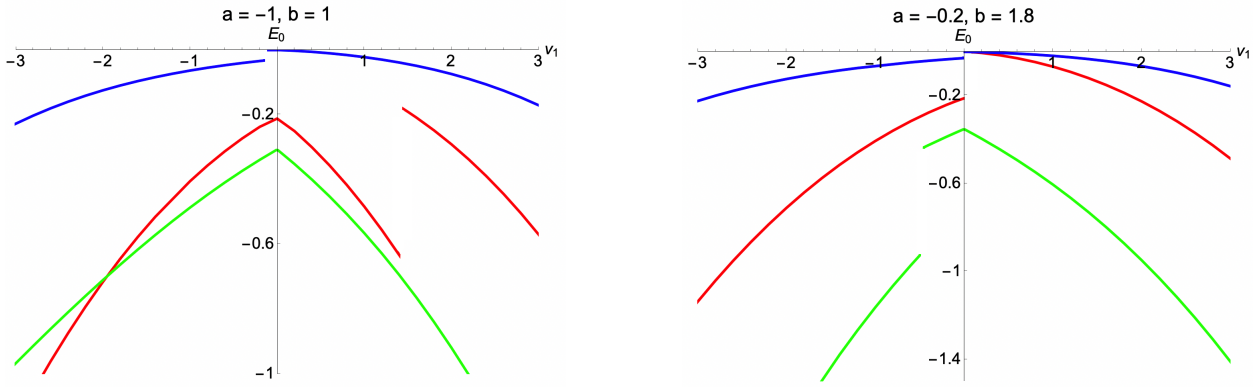

FIGURE 4.2: Casimir energy between plates for $a = -b = -1$ (first column) and in the case $a = -0.2, b = 1.8$ (second column). In both cases, the plates are mimicked by delta potentials with coefficients v_0, v_1. In these plots $v_0 = -3$ (red), $v_0 = 0.1$ (blue) and $v_0 = 4$ (green).

A relevant characteristic of the spectra can be observed in the plots of Figure 4.2. The sudden jump discontinuities present in these plots are related to the loss of one bound state with very low $k = i\kappa$ (nearly zero) in the spectrum of the system. At this point it is necessary to realise that the whole system of the two deltas together with the PT potential acts as a well with a fixed depth and width. Consequently, at the configuration in the space of parameters at which the jump appears, the resulting well is not deep enough to hold more bound states with large negative energy. This loss of a bound state translates into a jump in the energy.

In general terms, it can be seen that the larger the magnitude of the delta coefficients, the larger the one of the quantum vacuum interaction energy. However, due to the changes of the spectrum of bound states as a function of v_0, v_1 and the relative position between the plates and the kink, there is a peculiar fact shown in the figures above. When the plates are not symmetrically placed with respect to the kink centre, the force between plates is greater if $v_0 \gg 0$ and $v_1 < 0$ (green line of the right graph of Figure 4.2) than if both coefficients are negative (red line in the same graph), which is exactly the opposite to what happens in the symmetric case.

Finally, is worth pointing that even in the case where one of the delta coefficients is zero (and as a

consequence, there is only one plate in the system), the other plate feels the interaction because there is still a non zero quantum vacuum interaction energy in the system. This can be checked by looking at the non zero values of the energy appearing in the vertical axis (at which $v_1 = 0$ and there is no right plate in the system) in both graphs of Figure 4.2.

As said before, the system described so far is characterised by only attractive forces between plates. Nevertheless, the virtue of the method presented in this chapter for obtaining a *TGTG* formula valid in curved spacetimes, which has not been studied until now, is that it can be easily generalised to other type of configurations, either for another background and for other potentials that could properly mimic the plates. For instance, when considering two plates represented by the potential

$$V_{\delta\delta'}(z) = C_1\,\delta(z-a) + C_2\,\delta'(z-a) + C_3\,\delta(z-b) + C_4\,\delta'(z-b)$$

in the background of the Pösch-Teller kink, the only change that needs to be made is to modify the reflection coefficients in

$$\mathrm{Tr}\,\mathbf{TGTG}_k = \Big[G^{PT}(a,b)\Big]^2\; T_2^{\ell}\,T_1^{r} = \Big[G^{PT}(a,b)\Big]^2\;\frac{(W^*)^2}{k^8}\;r_L^{\ell}(v_0,a,k)\;r_R^{r}(v_1,b,k) f_k^2(a) f_{-k}^2(b).$$

I am currently working on this issue and there are indications that the introduction of the first derivative of the delta potential[7] causes the sign of the force to change in different areas of the space parameter, given by $\{C_1, C_2, C_3, C_4\}$. This behaviour has also been observed for the vacuum interaction energy of a scalar field and two concentric spheres defined by such a singular $\delta\delta'$ potential on their surfaces [100]. The generalisation of the work collected in this chapter to $\delta\delta'$ potentials, still incomplete to be introduced in this thesis, will be submitted for publication in the near future.

[7] In [197] Fulling relates the problem of Robin boundary conditions on an interval (fundamental for the mathematical modelling of superconducting quantum interferences devices or SQUIDs), with a quantum graph vertex with a Dirac δ-function as well as matching conditions for some kind of δ' potentials. In order to define the δ' potential, one could regularise it by including a δ interaction at the same point following [159].

Chapter 5

FERMI FIELDS BETWEEN PLATES

So far, only scalar field theory has been discussed. However, the self-adjoint extensions formalism explained in previous chapters can be generalised to fermionic fields. The great interest that has arisen around 2D materials such as graphene has certainly stimulated again the interest in the Dirac equation with singular potentials, as the Kronig Penny or de Dirac-δ chain one [198, 199]. On the other hand, this formalism can be also applied to study topological insulators[1] and edge states [203].

The goal of this chapter is to study the bound states and the scattering wave functions of the quantum mechanical one dimensional system of a Dirac fermionic field propagating in the real line under the influence of the static potential

$$V(z) = (q_1 \mathbb{1} + \lambda_1 \beta)\, \delta(z+a) + (q_2 \mathbb{1} + \lambda_2 \beta)\, \delta(z-a), \qquad \beta = \gamma^0 \qquad q_1, q_2, \lambda_1, \lambda_2 \in \mathbb{R}, \tag{5.1}$$

where γ^0 is one of the gamma matrices of the corresponding Clifford algebra. Firstly, a review of fundamental concepts of relativistic quantum mechanics will be given and the notation of the chapter will be established. Then, the spectra of bound and scattering states for either a single electric delta potential (obtained from (5.1) by taking $\lambda_1 = \lambda_2 = q_2 = a = 0$) and a single massive delta potential (arisen when choosing $\lambda_2 = q_1 = q_2 = a = 0$ in (5.1)) is computed. Hereafter, the spectrum of bound and scattering states for either a double electric delta potential (derived from (5.1) in the case $\lambda_1 = \lambda_2 = 0$) and a double massive delta potential (obtained from (5.1) by taking $q_1 = q_2 = 0$) is collected. Finally, the second quantisation is performed in order to promote the relativistic quantum mechanical theory presented so far to a relativistic QFT. The transformations of the potential under the symmetries $\mathcal{C}, \mathcal{P}, \mathcal{T}$ are studied. To conclude this chapter, the calculation of the quantum vacuum interaction energy for fermions confined between plates mimicked by unitary boundary conditions is briefly introduced. Notice that the eigenwave functions of the Dirac operator studied in the first part of the chapter, provide the one particle states of the associated 1+1 dimensional QFT. Moreover and similarly to the bosonic case, the perturbative analysis of the relativistic quantum mechanical problem gives information concerning the tree diagrams of the associated QFT, as explained in [204].

[1] A topological insulator is a material which behaves as a insulator in its interior but can feature a flow of Dirac electrons on its surface. These edge states are protected by time-reversal symmetry [200, 201]. Here protected state must be understood as one which is robust or topologically stable against perturbations. The $\mathbb{Z}_2$ topological invariant associated to these materials is analogous to the Chern number in the quantum Hall effect [202].

5.1. Relativistic quantum mechanics

Consider the Minkowski space $\mathbb{R}^{1,1}$ with a hyperbolic Lorentzian metric totally characterised by $g_{\mu\nu} = \text{diag}\{1, -1\}$. The one dimensional Lagrangian for a free massive fermionic Dirac field $\Psi(t, z)$ propagating in this spacetime is given by

$$\mathcal{L} = \Psi^\dagger(t,z)\gamma^0(i\gamma^\mu\partial_\mu - m)\Psi(t,z), \qquad \mu = 0, 1.$$

There are two basic elements in the above Lagrangian:

1. The gamma matrices $\{\gamma^\mu\}$, which are the minimal representation[2] of the Clifford algebra of $\mathbb{R}^{1,1}$:

$$\{\gamma^\mu, \gamma^\nu\} \equiv \gamma^\mu\gamma^\nu + \gamma^\nu\gamma^\mu = 2g^{\mu\nu}, \qquad (\gamma^\mu)^\dagger = \gamma^0\gamma^\mu\gamma^0 \quad \Rightarrow \quad \gamma^0\gamma^0 = \mathbb{1} = -\gamma^1\gamma^1,$$
$$\gamma^2 \equiv \gamma^0\gamma^1 = -\gamma^1\gamma^0, \qquad \{\gamma^2, \gamma^\mu\} = 0, \quad (\gamma^2)^2 = \mathbb{1},$$

   with γ^2 the 1+1 dimensional analogue of the element of $\text{Cl}_{1,3}(\mathbb{R})$ defined as $\gamma^5 = \mathbb{1}\gamma^0\gamma^1\gamma^2\gamma^3$.

2. $\Psi(t, z)$ are spinors, i.e. quanta emerging from spinor fields. Spinors are usually represented by column vectors of two components taking values in $\mathbb{C}$:

$$\Psi(t,z) = \begin{pmatrix} \psi_1(t,z) \\ \psi_2(t,z) \end{pmatrix} \quad ; \qquad \psi_i(t,z) : \mathbb{R}^{1,1} \to \mathbb{C}, \quad i = 1, 2.$$

   In the natural system of units $\hbar = c = 1$, the dimension of the Dirac field is: $[\Psi] = L^{-1/2}$.

   Notice that in 1+1 dimensional spacetimes there are no rotations and consequently, spin is meaningless from this point of view. Nevertheless, spinors can be defined in one spatial dimension as the elements of the fundamental representation of the spin group [205, 206]. The elements of the group are such that

$$S \in Spin(1, 1, \mathbb{R}) \qquad \to \qquad S = e^{\frac{i}{2}\kappa_{\mu\nu}\sigma^{\mu\nu}}, \qquad \sigma^{\mu\nu} = \frac{i}{4}[\gamma^\mu, \gamma^\nu].$$

   $Spin(1, 1; \mathbb{R})$ can be defined as the double cover of the special orthogonal group $SO(1, 1; \mathbb{R})$, that describes the boost transformations along the real line. Here $\kappa_{01} = -\kappa_{10} \in \mathbb{R}$ will be the parameter of the Lorentz boost in the spatial dimension of the spacetime:

$$\cosh\kappa_{01} = \frac{1}{\sqrt{1-v^2}}, \qquad \sinh\kappa_{01} = \frac{v}{\sqrt{1-v^2}}.$$

   The Lie algebra of $Spin(n, \mathbb{R})$ is a subgroup of the invertible elements of the aforementioned Clifford algebra $\text{Cl}_{1,1}(\mathbb{R})$. Spinor fields are hence maps from $\mathbb{R}^{1,1}$ to the fundamental representation of the spin group.

[2] $\{\gamma^\mu\}$ are going to be represented by two-by-two matrices. γ^0, γ^2 would be Hermitian and γ^1 anti-Hermitian.

It is interesting to highlight that from a geometrical point of view, the spinor group is the structure group of a spinor bundle. In references [206, 207] it is explained that given an oriented general differentiable n-dimensional manifold $\mathcal{M}$, the tangent bundle has the connected component to the identity of $GL(1,n-1,\mathbb{R})$ as structure group. If $GL(1,n-1,\mathbb{R})$ can be lifted to the universal covering $\widetilde{GL}(1,n-1,\mathbb{R})$, then $\mathcal{M}$ is a spin manifold. The problem is that there could be finite representations of $\widetilde{GL}(1,n-1,\mathbb{R})$ which do not come from the connected component to the identity of $GL(1,n-1,\mathbb{R})$. Nevertheless, one could avoid the problem by fixing a Lorentzian metric on the manifold and consequently, passing from $GL(1,n-1,\mathbb{R})$ to $SO(1,n-1,\mathbb{R})$. In this case, it is sometimes possible to define a spin structure [208] when lifting the structure group $SO(1,n-1,\mathbb{R})$ to its universal covering $Spin(1,n-1,\mathbb{R})$. Hence, in this context one could see a spinor in a Lorentz manifold as a section of the spin bundle in which a spin representation has been associated to every point of $\mathcal{M}$. $Spin(1,n-1,\mathbb{R})$ is a $\mathbb{Z}_2$ group extension of the corresponding pseudo-orthogonal group so that the short sequence

$$\mathbb{Z}_2 \quad \hookrightarrow \quad Spin(1,n-1) \quad \rightarrow \quad SO(1,n-1)$$

is exact and therefore $Spin(n)/\mathbb{Z}_2 \cong SO(n)$. Although interesting, these concepts go beyond the scope of this work and there will be no further emphasis on this issue.

The Hamiltonian form of the Dirac equation

$$(i\gamma^\mu\partial_\mu - m\,)\Psi(x) = 0, \qquad \rightarrow \qquad i\partial_t\Psi(t,z) = \boldsymbol{H}_D^{(0)}\Psi(t,z), \qquad \boldsymbol{H}_D^{(0)} = [-i\alpha\partial_z + \beta m]. \tag{5.2}$$

governs the dynamics of a free fermionic particle of mass m moving on a line. Analogously, the dynamics of the the fermionic anti-particle are described by minus the conjugate Dirac Hamiltonian

$$(i\gamma^\mu\partial_\mu + m\,)\Phi(x) = 0, \qquad \rightarrow \qquad i\partial_t\Phi(t,z) = \overline{\boldsymbol{H}}_D^{(0)}\Phi(t,z), \qquad \overline{\boldsymbol{H}}_D^{(0)} = [-i\alpha\partial_z - \beta m]. \tag{5.3}$$

The Dirac matrices and the gamma ones are going to be chosen as

$$\beta = \gamma^0 = \sigma_3, \qquad \alpha = \gamma^0\gamma^1 = \gamma^2 = \sigma_1, \qquad \gamma^1 = i\sigma_2, \tag{5.4}$$

where σ_1, σ_2, σ_3 are the 2×2 Pauli matrices:

$$\sigma_1 = \begin{pmatrix} 0 & 1 \\ 1 & 0 \end{pmatrix}, \quad \sigma_2 = \begin{pmatrix} 0 & -i \\ i & 0 \end{pmatrix}, \quad \sigma_3 = \begin{pmatrix} 1 & 0 \\ 0 & -1 \end{pmatrix}.$$

When considering the normal modes expansion of the fermionic fields by means of the time-energy Fourier transform

$$\Psi(t,z) = \int d\omega\, e^{-i\omega t}\,\Psi_\omega(z), \qquad \Phi(t,z) = \int d\omega\, e^{-i\omega t}\,\Phi_\omega(z),$$

one could transform the matricial PDE Dirac equations (5.2), (5.3) into the ODE eigenvalue systems for electrons and for positrons

$$[-i\sigma_1\partial_z + \sigma_3 m]\Psi_\omega(z) = \omega\Psi_\omega(z), \qquad [-i\sigma_1\partial_z - \sigma_3 m]\Phi_\omega(z) = \omega\Phi_\omega(z).$$

Performing the position-momentum Fourier transform

$$\Psi_\omega(z) = \int dk\, u(k)e^{ikz}, \qquad \Phi_\omega(z) = \int dk\, v(k)e^{ikz},$$

one obtains the algebraic homogeneous systems

$$[\sigma_1 k + \sigma_3 m - \omega\,\mathbb{1}]u(k) = 0, \qquad \text{with} \qquad u(k) = \begin{pmatrix} A(k) \\ B(k) \end{pmatrix} \quad \text{for electrons,} \tag{5.5}$$

$$[\sigma_1 k - \sigma_3 m - \omega\,\mathbb{1}]v(k) = 0, \qquad \text{with} \qquad v(k) = \begin{pmatrix} C(k) \\ D(k) \end{pmatrix} \quad \text{for positrons.} \tag{5.6}$$

Notice that the specific behaviour of $u(k), v(k)$ depends on the choice of $\{\gamma^\mu\}$. Non trivial solutions of this system arise when the determinant of the matrices $[\sigma_1 k \pm \sigma_3 m - \omega\,\mathbb{1}]$ is zero. The spectral equation thus satisfies $\omega^2 = m^2 + k^2$. There are two possible eigenvalues $\omega_\pm = \pm\sqrt{k^2+m^2}$, but following the Dirac sea and the electron/hole prescription[3], only the positive energy eigenspinors have a physical meaning. Hence, the eigenspinors of moving fermions are classified in two classes in terms of plane waves:

1. Positive energy ω_+ electron spinor plane waves moving along the real axis with momentum $k \in \mathbb{R}$. The solution of (5.5) is $B(k) = A(k)k/(\omega_+ + m)$. Hence

$$u_+(k) = \begin{pmatrix} 1 \\ \frac{k}{\omega_+ + m} \end{pmatrix}. \tag{5.7}$$

2. Positive energy ω_+ positron spinor plane waves moving along the real axis with momentum $k \in \mathbb{R}$. The solution of (5.6) is $C(k) = D(k)k/(m + \omega_+)$. Hence

$$v_+(k) = \gamma^2 u_+^*(k) = \begin{pmatrix} \frac{k}{\omega_+ + m} \\ 1 \end{pmatrix}. \tag{5.8}$$

[3]The infinite Dirac sea proposed by P. Dirac [209] is a theoretical vacuum with only particles with negative energy. The positron was thought as a hole or absence of a particle in the Dirac sea until its discovery as real particle by Carl Anderson [210]. Note that due to the exclusion principle imposed by the Fermi statistics, all the negative energy states of this vacuum are filled.

The basis of states to be used to generate the bound and scattering spinors of the quantum problem are included in Table 5.1.

MOVEMENT	**ELECTRONS WITH ENERGY** $\omega_+ > 0$	**POSITRONS WITH ENERGY** $\omega_+ > 0$
From left to right with momentum $k \in \mathbb{R}^+$	$\Psi_+(t,z;k) \propto e^{-i\omega_+ t} e^{ikz}\, u_+(k)$	$\Phi_+(t,z;k) \propto e^{-i\omega_+ t}\, e^{ikz}\, v_+(k)$
From right to left with momentum $-k,\ k \in \mathbb{R}^+$	$\Psi_-(t,z;-k) \propto$ $e^{-i\omega_+ t}\, e^{-ikz}\, \gamma^0\, u_+(k)$	$\Phi_-(t,z;-k) \propto$ $e^{-i\omega_+ t}\, e^{-ikz}\, \gamma^0\, v_+(k)$

TABLE 5.1: Positive energy electron spinors versus positron ones.

Notice that the $v_+(k)$ spinors are orthogonal to the positive energy ones $u_+(k)$ because $u_+^\dagger \gamma^0 v_+ = 0$. Furthermore, for both the free positrons and electrons spectral problems, one could see that spectra are not bounded from below and there is a gap $[-m, m]$ with no eigenvalues in between.

When the effect of an external static potential is included in the action, the only required modification to study the propagation of relativistic Fermi particles in this classical background is to replace $\boldsymbol{H}_D^{(0)}$ by the most general Hamiltonian [211]

$$\boldsymbol{H}_D = \boldsymbol{H}_D^{(0)} + V(z) = \boldsymbol{H}_D^{(0)} + \gamma^0[V_3(z)\mathbb{1} + V_\mu(z)\gamma^\mu + V_2(z)\gamma^2].$$

However, in 1+1 dimensions there is no magnetic field and hence, a gauge transformation can always be performed so that $V_1(z) = 0$ can be taken without loss of generality. Furthermore, it is convenient to choose $V_2(z) = 0$ because $\gamma^0\gamma^2 = \gamma^1$ is not Hermitic. Hence, the aforementioned background potential reduces to one term mimicking an electric potential and another one representing a mass term depending on the spatial coordinate z, i.e.:

$$V(z) = \xi(z)\,\mathbb{1} + M(z)\beta.$$

In addition, from now onwards only potentials with compact support are going to be studied:

$$V(z) = \begin{cases} 0, & \text{if} \quad |z| > L, \\ \xi(z)\,\mathbb{1} + M(z)\beta, & \text{if} \quad -L < z < L, \end{cases} \tag{5.9}$$

leading to the following Dirac spectral problem for electrons:

$$\boldsymbol{H}_D\Psi_\omega(z) = \omega\Psi_\omega(z) \;\Rightarrow\; [-i\gamma^2\partial_z + \gamma^0(m + M(z))]\Psi_\omega(z) = [\omega - \xi(z)]\Psi_\omega(z). \tag{5.10}$$

$\xi(z)$ and $M(z)$ can be chosen from a wide range of candidates: as Coulomb and quadratic *vector potentials* [212], along with linear or even confining potentials [213, 214]. In this chapter, however, external potentials localised at one point are going to be regarded to mimic the influence of a single

impurity on the propagation of fermions. Therefore:

$$V(z) = \Gamma(q,\lambda)\delta(z); \quad \Gamma(q,\lambda) = q\mathbb{1} + \lambda\beta. \tag{5.11}$$

$\Gamma(q,\lambda)$ is a 2×2 matrix depending on two dimensionless coupling constants. On the one hand, q physically represents an electric charge[4] and on the other hand, λ plays the role of a mass-like scalar or gravitational coupling to the Fermi field.

Early distributional definitions of the δ-point interaction for Dirac fields were proposed in [215, 216]. In these works, the purely electrostatic fermionic Dirac-δ potential was defined through a matching condition of the form

$$\Psi_\omega(0^+) = T_{E\delta}(q)\Psi_\omega(0^-); \quad T_{E\delta}(q) = \mathbb{1}\cos(q) - i\gamma^2\sin(q). \tag{5.12}$$

where the subindex ω means that the energy is fixed. Later, in [211] the matching condition (5.12) was extended for the general δ-potential (5.11) following the approach of [216], to be:

$$\begin{aligned} &\Psi_\omega(0^+) = T_\delta(q,\lambda)\Psi_\omega(0^-); \quad T_\delta(q,\lambda) = \exp\left(-i\gamma^2\Gamma(q,\lambda)\right), \\ &T_\delta(q,\lambda) = \mathbb{1}\cos\Omega - \frac{i}{2}\sin\Omega\left[\frac{\Omega}{q+\lambda}(\gamma^2+\gamma^1) + \frac{q+\lambda}{\Omega}(\gamma^2-\gamma^1)\right], \end{aligned} \tag{5.13}$$

being $\Omega = \sqrt{q^2-\lambda^2}$. Form $T_\delta(q,\lambda)$, it is straightforward to obtain the matrix that defines the mass-spike Dirac-δ potential:

$$T_{M\delta}(\lambda) = T_\delta(0,\lambda) = \mathbb{1}\cosh(\lambda) + i\gamma^1\sinh(\lambda). \tag{5.14}$$

This last particular case is studied in detail in [211], regarding the Casimir effect induced by vacuum fermionic quantum fluctuations.

For positrons, the spectral Dirac problem for the delta potential (5.9) is

$$\overline{\boldsymbol{H}}_D\Phi_\omega(z) = \omega\Phi_\omega(z) \;\Rightarrow\; [-i\gamma^2\partial_z - \gamma^0(m - M(z))]\Phi_\omega(z) = [\omega - \xi(z)]\Phi_\omega(z),$$

with the matching conditions

$$\Phi_\omega(0^+) = T_\delta(-q,\lambda)\Phi_\omega(0^-). \tag{5.15}$$

Solving the scattering problem involves knowing the matching condition matrices. The non-relativistic quantum mechanical problem in 1+1 dimensional theories is invariant under parity (i.e. $z\to -z$) and time-reversal ($t\to -t$ and $i\to -i$) transformations. Hence, in the following section it is going to be proved that under the matching conditions (5.13) and (5.15), the transmission and reflection coeffcients of *zurdo* (L) and *diestro* (R) scattering fulfil the relations $\sigma_R = \sigma_L$ and $\rho_R = \rho_L$. Consequently, under parity ($\mathcal{P}$) and time reversal ($\mathcal{T}$) transformations the matching matrices remain

[4]The coupling q will vary as an angle proportional to the fine structure constant. In a $1D$ space this constant can be written as $\alpha = |\frac{e^2}{m^2}|$ being e the electron charge and $1/m$ the wavelength of the Compton particle.

invariant, i.e. $T_\delta^{\mathcal{P}}(q,\lambda) = T_\delta(q,\lambda)$ and $T_\delta^{\mathcal{T}}(q,\lambda) = T_\delta(q,\lambda)$. The $\mathcal{PT}$ operator is antilinear as well as antiunitary. This guarantees real eigenvalues of $\hat{K}$ if $[\hat{K},\mathcal{PT}] = 0 \ \wedge \ \mathcal{PT}\phi = \phi$, for ϕ an eigenstate of $\mathcal{PT}$ [217].

It is relevant to point out that the problem of determining the spinor field fluctuations in static delta backgrounds will be adressed by solving at the same time the spectral problem of either the Dirac Hamiltonian $\boldsymbol{H}_D$ and its conjugate $\overline{\boldsymbol{H}}_D$ in one-dimensional relativistic quantum mechanics. The space of states is thus the tensor product of the eigenstate space of $\boldsymbol{H}_D$ by the eigenstate space of $\overline{\boldsymbol{H}}_D$. The eigenspinors of both Hamiltonians have been interpreted as the one particle states with positive energy to be occupied by electrons and positrons, after the fermionic second quantisation procedure be implemented in the last section of this chapter.

5.2. Spectrum for single δ potential

The spectral equations associated with the pair of Hamiltonians for electrons and positrons in the presence of a single δ potential:

$$\begin{aligned}
[-i\alpha\partial_z + \beta(m + q\delta(z))]\Psi_\omega(z) &= (\omega - \lambda\delta(z))\Psi_\omega(z), \\
[-i\alpha\partial_z - \beta(m - q\delta(z))]\Phi_\omega(z) &= (\omega - \lambda\delta(z))\Phi_\omega(z),
\end{aligned} \tag{5.16}$$

are equivalent to the Dirac systems of two first-order ODE's:

$$\left\{ \begin{array}{l} -i\frac{d\psi_2^\omega}{dz} = [\omega - m]\psi_1^\omega(z) \\ -i\frac{d\psi_1^\omega}{dz} = [\omega + m]\psi_2^\omega(z) \end{array} \right. , \qquad \left\{ \begin{array}{l} -i\frac{d\phi_2^\omega}{dz} = [\omega + m]\phi_1^\omega(z), \\ -i\frac{d\phi_1^\omega}{dz} = [\omega - m]\phi_2^\omega(z) \end{array} \right. . \tag{5.17}$$

The eigenspinors for the free Dirac Hamiltonian in zone I ($z < 0$) and those in zone II ($z > 0$), must be related across the singularity at $z = 0$ by the matching conditions (5.13):

$$\begin{pmatrix} \psi_1^\omega(0^+) \\ \psi_2^\omega(0^+) \end{pmatrix} = \begin{pmatrix} \cos\Omega & -i\frac{\Omega}{q+\lambda}\sin\Omega \\ -i\frac{q+\lambda}{\Omega}\sin\Omega & \cos\Omega \end{pmatrix} \begin{pmatrix} \psi_1^\omega(0^-) \\ \psi_2^\omega(0^-) \end{pmatrix}, \tag{5.18}$$

$$\begin{pmatrix} \phi_1^\omega(0^+) \\ \phi_2^\omega(0^+) \end{pmatrix} = \begin{pmatrix} \cos\Omega & -i\frac{\Omega}{-q+\lambda}\sin\Omega \\ -i\frac{-q+\lambda}{\Omega}\sin\Omega & \cos\Omega \end{pmatrix} \begin{pmatrix} \phi_1^\omega(0^-) \\ \phi_2^\omega(0^-) \end{pmatrix}. \tag{5.19}$$

Now the goal is to study the bound states (i.e. those with $|\omega| < |m|$) and scattering ones ($|\omega| > |m|$), both for the case of electrons and positrons.

Scattering states for a single δ-potential. As happens for the scalar case, there are two independent scattering spinors for a fixed energy $\omega(k) > m > 0$. One the one hand, the left-to-right ("*diestro*")

spinor for the electrons is

$$\Psi^R_\omega(z;k) = \begin{cases} u_+(k)e^{ikz} + \rho_R(k)\gamma^0 u_+(k)e^{-ikz}, & z<0, \\ \sigma_R(k)u_+(k)e^{ikz}, & z>0. \end{cases} \tag{5.20}$$

And on the other hand, the right-to-left ("*zurdo*") spinor for electrons takes the form

$$\Psi^L_\omega(z;k) = \begin{cases} \sigma_L(k)\gamma^0 u_+(k)e^{-ikz}, & z<0, \\ \gamma^0 u_+(k)e^{-ikz} + \rho_L(k)u_+(k)e^{ikz}, & z>0. \end{cases} \tag{5.21}$$

The scattering amplitudes $\{\sigma_R, \sigma_L, \rho_R, \rho_L\}$ can be obtained imposing the matching conditions (5.18) for these electron spinors. Solving the two arising linear systems, one gets the following scattering amplitudes for the electrons on the line interacting with a Dirac-δ:

$$\sigma_R = \sigma_L = \frac{k\Omega}{i(q\omega + m\lambda)\sin\Omega + k\Omega\cos\Omega}, \qquad \rho_R = \rho_L = \frac{-i\sin\Omega(\omega\lambda + mq)}{i(q\omega + m\lambda)\sin\Omega + k\Omega\cos\Omega}. \tag{5.22}$$

The "*diestro*" and "*zurdo*" scattering states for the positron spinors are

$$\Phi^R_\omega(z,k) = \begin{cases} v_+(k)\, e^{ikz} + \tilde\rho_R(k)\, \gamma^0 v_+(k)\, e^{-ikz}, & z<0, \\ \tilde\sigma_R(k)\, v_+(k)\, e^{ikz}, & z>0, \end{cases} \tag{5.23}$$

$$\Phi^L_\omega(z,k) = \begin{cases} \tilde\sigma_L(k)\, \gamma^0 v_+(k)\, e^{-ikz}, & z<0, \\ \tilde\rho_L(k)\, v_+(k)\, e^{ikz} + \gamma^0 v_+(k)\, e^{-ikz}, & z>0, \end{cases} \tag{5.24}$$

respectively. Forcing the positron scattering spinors to satisfy the associated matching condition (5.19), the following scattering amplitudes arise

$$\tilde\sigma_R = \tilde\sigma_L = \frac{k\Omega}{-i(q\omega + m\lambda)\sin\Omega + k\Omega\cos\Omega}, \qquad \tilde\rho_R = \tilde\rho_L = \frac{-i(\omega\lambda + mq)\sin\Omega}{-i(q\omega + m\lambda)\sin\Omega + k\Omega\cos\Omega}. \tag{5.25}$$

The S-matrices thus built either for electrons and positrons are unitary since it is easy to check that the conditions $\left|\sigma(k)\right|^2 + \left|\rho(k)\right|^2 = 1$ and $\sigma^*(k)\rho(k) + \rho^*(k)\sigma(k) = 0$ are fulfilled. Furthermore, as in the scalar case, the "*diestro*' and "*zurdo*' scattering amplitudes are equal for the electron (equivalently for the positron). This means that the Dirac-δ potential coupled to relativistic spin-1/2 particles is parity and time-reversal invariant.

Bound states for a single δ-potential. Spinor eigen-functions of $\boldsymbol{H}_\delta$ and $\overline{\boldsymbol{H}}_\delta$ may also arise if $k = i\kappa$ is purely imaginary, being $\kappa > 0$. In this case, $0 < \omega(i\kappa) < m$ and bound states emerge inside the gap. This means that fermions are somehow trapped at the δ-impurity. The ansatzs for the bound

state spinor wave functions are given by

$$\Psi^b_\omega(z;\kappa) = \begin{cases} A(\kappa)\gamma^0 u(i\kappa)e^{\kappa z} & z<0 \\ B(\kappa)u(i\kappa)e^{-\kappa z} & z>0 \end{cases}, \qquad \Phi^b_\omega(z;\kappa) = \begin{cases} C(\kappa)\gamma^0 v(i\kappa)e^{\kappa z} & z<0 \\ D(\kappa)v(i\kappa)e^{-\kappa z} & z>0 \end{cases}. \tag{5.26}$$

The exponentially decaying solutions of the systems in (5.17) (with $\omega^2 = m^2 - \kappa^2$) in the zone $z<0$ must be related to exponentially decaying solutions of the same systems for $z>0$ by implementing the electrostatic matching conditions (5.18) and (5.19) at $z=0$. Doing so yields the linear homogeneous systems:

$$\begin{pmatrix} -\cos\Omega + \frac{\Omega}{q+\lambda}\frac{\kappa\sin\Omega}{m+\omega(i\kappa)} & 1 \\ i\left(\frac{q+\lambda}{\Omega}\sin\Omega + \frac{\kappa\cos\Omega}{m+\omega(i\kappa)}\right) & \frac{i\kappa}{m+\omega(i\kappa)} \end{pmatrix}\begin{pmatrix} A \\ B \end{pmatrix} = 0 \quad \text{for electrons,} \tag{5.27}$$

$$\begin{pmatrix} i\left(\frac{\Omega}{q-\lambda}\sin\Omega - \frac{\kappa\cos\Omega}{m+\omega(i\kappa)}\right) & \frac{i\kappa}{m+\omega(i\kappa)} \\ \frac{(q-\lambda)}{\Omega}\frac{\kappa\sin\Omega}{m+\omega(i\kappa)} + \cos\Omega & 1 \end{pmatrix}\begin{pmatrix} C \\ D \end{pmatrix} = 0 \quad \text{for positrons.} \tag{5.28}$$

On the one hand, existence of non null solutions for A and B in (5.27) requires that the matrix in that algebraic system has vanishing determinant, i.e.:

$$\sin(\Omega)\left((m+\sqrt{m^2-\kappa^2})^2(\lambda+q)^2 - \kappa^2\Omega^2\right) + 2\kappa\Omega(m+\sqrt{m^2-\kappa^2})(\lambda+q)\cos(\Omega) = 0.$$

Its roots can be written as:

$$\kappa^{\pm}_{e^-} = \frac{m\left(\pm 2q\sqrt{\Omega^2(\lambda+q)^4\sin^2(\Omega)} + \lambda\Omega(\lambda+q)^2\sin(2\Omega)\right)}{(\lambda+q)^2\left(\lambda^2\cos(2\Omega) + \lambda^2 - 2q^2\right)}. \tag{5.29}$$

On the other hand, non null solutions for C and D in (5.28) requires:

$$\left(-\Omega^2\left(\sqrt{m^2-\kappa^2}+m\right)^2 + \kappa^2(q-\lambda)^2\right)\sin(\Omega) + 2\kappa\Omega\left(\sqrt{m^2-\kappa^2}+m\right)(q-\lambda)\cos(\Omega) = 0,$$

and its roots are given by:

$$\kappa^{\pm}_{e^+} = \frac{m\left(\pm 2q\sqrt{\Omega^2(q-\lambda)^4\sin^2(\Omega)} - \lambda\Omega(q-\lambda)^2\sin(2\Omega)\right)}{(q-\lambda)^2\left(\lambda^2\cos(2\Omega) + \lambda^2 - 2q^2\right)}. \tag{5.30}$$

The left graph of Figure 5.1 shows the dependence of κ/m with the parameters q, λ for a pure electric ($\lambda = 0$) delta potential and a pure massive one ($q = 0$). Remember that only in the domain of the q-λ plane where one of the κ is real and positive there exists one bound state and one fermion is trapped at the singularity. The results compiled in this section up to this point are original work, not yet published.

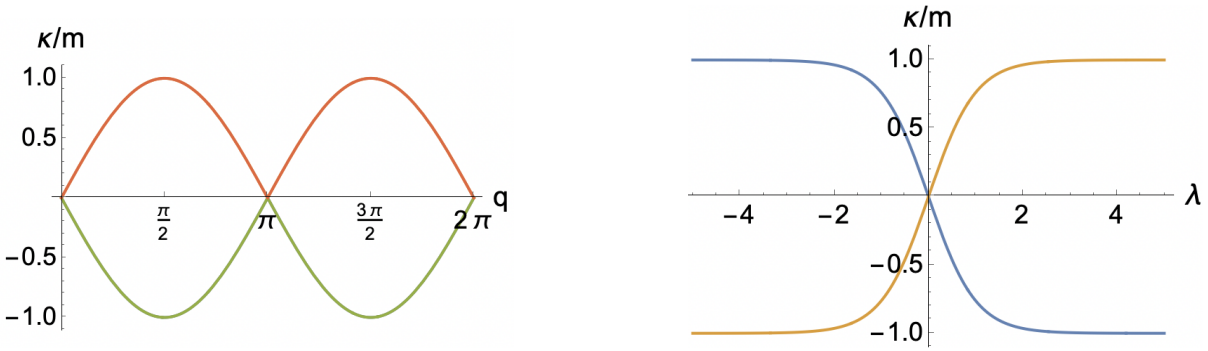

FIGURE 5.1: Left: Wave vector of bound states $\kappa^{+}_{e^-}/m$ and $\kappa^{+}_{e^+}/m$ (green) and $\kappa^{-}_{e^-}/m$ and $\kappa^{-}_{e^+}/m$ (red) in a pure electric δ potential. Right: Wave vector $\kappa^{\pm}/m$ of bound states for electrons (blue) and positrons (orange) in a pure massive δ potential.

The following two subsections go into the details of these two examples of purely electrical or fully massive delta potentials mentioned above.

5.2.1. Electrostatic contact interaction

Consider now a relativistic 1D fermion whose free propagation is disturbed by one impurity described by including solely an electric δ-potential at $z = 0$, rather than the general one previously described in (5.16). The one-dimensional Dirac Hamiltonians with a single electric Dirac δ-potential are:

$$\boldsymbol{H}^{E}_{\delta} = -i\sigma_1\frac{d}{dx} + m\sigma_3 + q\delta(x)\mathbb{1}, \qquad \overline{\boldsymbol{H}}^{E}_{\delta} = -i\sigma_1\frac{d}{dx} - m\sigma_3 + q\delta(x)\mathbb{1},$$

being $q = \nu e^2/m^2 \in \mathbb{S}^1$ with $\nu \in (0, 2\pi m^2/e^2)$. Recall that q is dimensionless.

Relativistic electron and positron bound states. The bound states and its momentum can be derived from the general formulae (5.26)-(5.30) just by taking $\lambda = 0$. From these equations as well as from (5.12), it is clear that all the dependence on the variable q is given by trigonometric functions. Hence, the parameter q can be interpreted as an angle. The signs of κ, ω change in every quadrant when q takes values from 0 to 2π. The outcome is that there exists one bound state in each quadrant, two for electrons and two for positrons, distributed as appears in Figure 5.2. These bound states correspond to positive energy levels within the gap $[0, m]$. The distribution of bound states is periodic in q. Table 5.2 shows the spinors of the bound states, arranged in quadrant order, according to the values that q takes from 0 to 2π.

It is worthwhile to mention that if $q = \frac{\pi}{2}$ or $q = \frac{3\pi}{2}$, zero modes do exist. For instance when $q = \frac{\pi}{2}$, then $\kappa_b = m$, $\omega_b = 0$ and the eigenspinor in Table 5.2 reads:

$$\Phi_{\omega}(z)\Big|_{\omega_b=0} = \sqrt{\frac{m}{2}}\begin{pmatrix} -i\,\mathrm{sign}(z) \\ -1 \end{pmatrix} e^{-m|z|}\,.$$

In both cases the normalisable wave functions have finite discontinuities at the origin (see Figure 5.3). Notice that the bound states just described in this section are closer to the bound states in the scalar case with the potential $V(z) = -a\delta(z) + b\delta'(z)$ (see [159]).

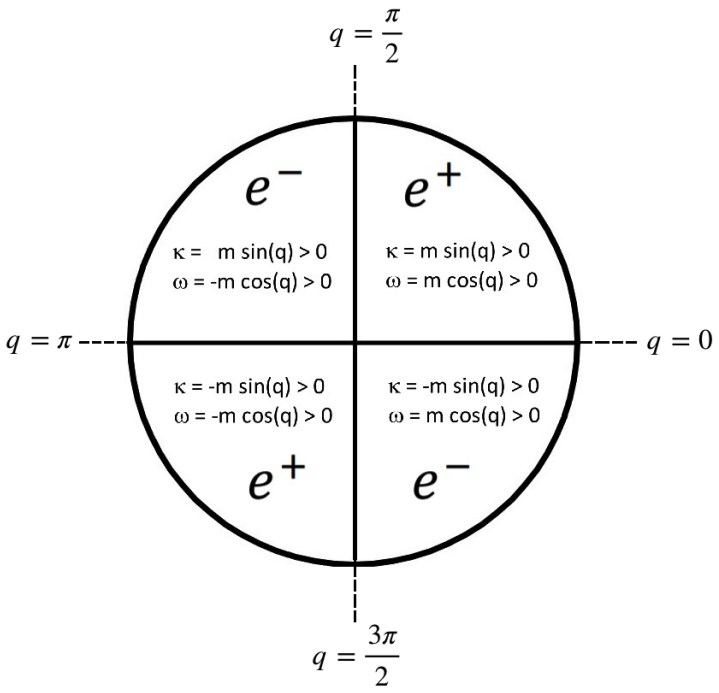

FIGURE 5.2: Distribution of bound states in an electric δ-potential arranged in quadrant order, according to the values that q takes from 0 to 2π.

Quadrant	**Bound state spinor**
$0 < q < \frac{\pi}{2}$	$\Phi_\omega(z) = \sqrt{m\lvert\sin q\rvert\cos^2\left(\frac{q}{2}\right)} \begin{pmatrix} -\text{sign}(z)\,\frac{i\sin q}{1+\cos q} \\ -1 \end{pmatrix} e^{-m\lvert z\rvert\sin q}$
$\frac{\pi}{2} < q < \pi$	$\Psi_\omega(z) = \sqrt{m\lvert\sin q\rvert\sin^2\left(\frac{q}{2}\right)} \begin{pmatrix} -\text{sign}(z) \\ \frac{-i\sin q}{1-\cos q} \end{pmatrix} e^{-m\lvert z\rvert\sin q}$
$\pi < q < \frac{3\pi}{2}$	$\Phi_\omega(z) = \sqrt{m\lvert\sin q\rvert\sin^2\left(\frac{q}{2}\right)} \begin{pmatrix} \frac{-i\sin q}{1-\cos q} \\ \text{sign}(z) \end{pmatrix} e^{m\lvert z\rvert\sin q}$
$\frac{3\pi}{2} < q < 2\pi$	$\Psi_\omega(z) = \sqrt{m\lvert\sin q\rvert\cos^2\left(\frac{q}{2}\right)} \begin{pmatrix} 1 \\ -\text{sign}(z)\,\frac{i\sin q}{1+\cos q} \end{pmatrix} e^{m\lvert z\rvert\sin q}$

TABLE 5.2: Bound state spinors for fermions in an electric δ-potential. The coefficients in the squared roots have been determined in the normalisation process $|\mathcal{N}|^2 \int_{\mathbb{R}} \Psi^\dagger(z)\Psi(z)dz = 1$. Notice that all the spinors in the table correspond to a fixed energy ω. The whole spinor can be obtained by means of $\Psi(t,z) = \int d\omega\, e^{-i\omega t}\,\Psi_\omega(z)$ and similarly for positrons.

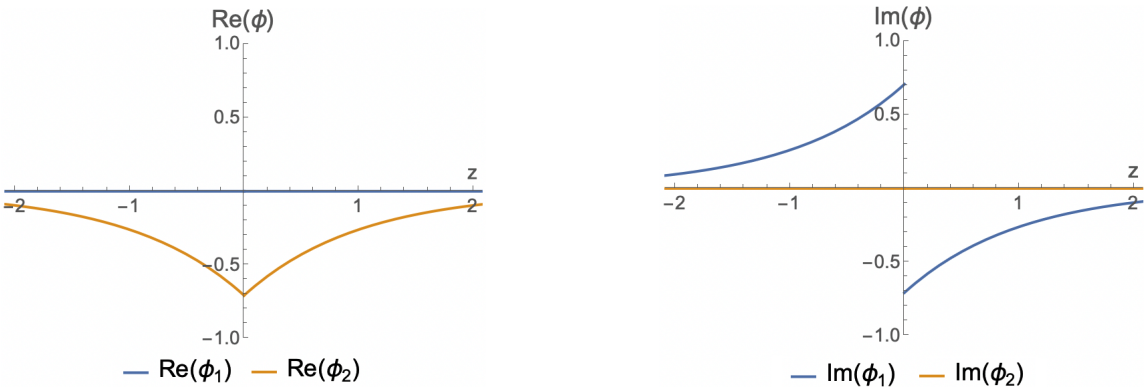

FIGURE 5.3: Bound state wave function $\Phi_\omega(z)$ for $q = \pi/2$ and $m = 1$ in a single electric delta interaction.

Charge density The charge density can be written as:

$$\begin{aligned} j^0(t,z) &= \pm Q\,\overline{\varphi}(t,z)\gamma^0\varphi(t,z) = \pm Q\,\varphi^\dagger(t,z)\varphi(t,z) \\ &= \pm Q\,\left(\varphi_1^*(t,z)\varphi_1(t,z) + \varphi_2^*(t,z)\varphi_2(t,z)\right), \end{aligned} \tag{5.31}$$

being Q a positive constant. It should be taken into account that the $+$ sign will be chosen in the case of electrons and $-$ for positrons. Substituting the bound states in Table 5.2 in (5.31) the charge density can be computed and expressed as

$$j_0(z) = m\,Q\,\sin q\cdot \begin{cases} \left(-e^{-2m|z|\sin q}\right) & \text{iff} \quad 0 < q < \frac{\pi}{2} \\ e^{-2m|z|\sin q} & \text{iff} \quad \frac{\pi}{2} < q < \pi \\ e^{2m|z|\sin q} & \text{iff} \quad \pi < q < \frac{3\pi}{2} \\ \left(-e^{2m|z|\sin q}\right) & \text{iff} \quad \frac{3\pi}{2} < q < 2\pi \end{cases}. \tag{5.32}$$

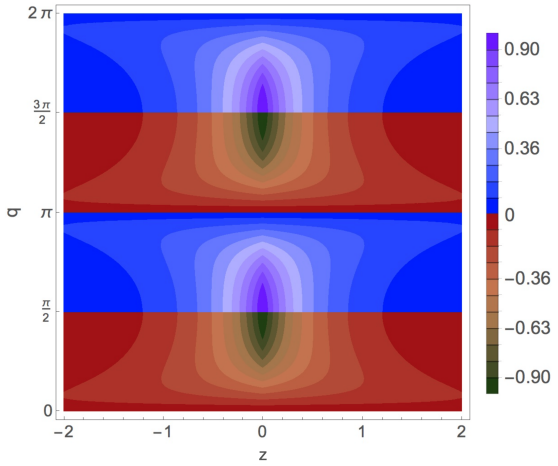

FIGURE 5.4: Charge density $j_0(z)$ in (5.32) as a function of x when $Q = m = 1$ for an electric δ-potential. For $0 < q < \pi/2$ and $\pi < q < 3\pi/2$ the charge densities of a positron bound state are plotted. For $\pi/2 < q < \pi$ and $3\pi/2 < q < 2\pi$ the charge densities of a electron bound state are plotted.

The results are shown in Figure 5.4. It is worth emphasising that the charge density is a continuous function. This implies that the continuity equation related to conservation of probability is fulfilled. Furthermore, $j_0(z)$ is symmetric about the origin, which is the point at which the charge density takes its maximum value.

Relativistic electron and positron scattering data. The transmission and reflection scattering amplitudes for electrons are obtained by setting $\lambda = 0$ in (5.22):

$$\sigma_R(k) = \sigma_L(k) = \frac{k}{k\cos q + i\sqrt{k^2+m^2}\sin q}, \qquad \rho_R(k) = \rho_L(k) = -\frac{i\ m\sin q}{k\cos q + i\sqrt{k^2+m^2}\sin q}. \tag{5.33}$$

Identically, for positrons the following scattering coefficients are obtained from (5.25):

$$\tilde{\sigma}_R(k) = \tilde{\sigma}_L(k) = \frac{k}{k\cos q - i\sqrt{k^2+m^2}\sin q}, \qquad \tilde{\rho}_R(k) = \tilde{\rho}_L(k) = -\frac{i\ m\sin q}{k\cos q - i\sqrt{k^2+m^2}\sin q}\ . \tag{5.34}$$

It is worth noting that

- Purely imaginary poles $k = i\kappa$ with $\kappa \in \mathbb{R}^+$ of the transmission amplitude σ are the bound states of the spectrum for electrons. From formula (5.33), it can be seen that poles of this type appear if the imaginary momentum satisfies

  $$\frac{\kappa_b}{\sqrt{m^2-\kappa_b^2}} = -\tan q,$$

  which admits positive solutions for κ only if $\tan q < 0$, i.e. if q lives in the second or fourth quadrant. For positrons, from $\tilde{\sigma}$ in equation (5.34) it is clear that bound states appear if the imaginary momentum satisfies the equation

  $$\frac{\kappa_b}{\sqrt{m^2-\kappa_b^2}} = \tan q,$$

  which admits positive solutions for κ_b only if $\tan q > 0$, i.e. if q lives in the first or third quadrant.

- Probability is conserved even in this relativistic quantum mechanical context, as long as the S-matrix is unitary.

- The relations between "*diestro*" and "*zurdo*" scattering amplitudes for electrons and positrons are as follows:

  $$\sigma_R(k) = \sigma_L(k) = \tilde{\sigma}_R^*(k) = \tilde{\sigma}_L^*(k), \qquad \rho_R(k) = \rho_L(k) = -\tilde{\rho}_R^*(k) = -\tilde{\rho}_L^*(k).$$

- The eigenvalues $\lambda_\pm$ of the unitary $\boldsymbol{S}$-matrix

$$\boldsymbol{S} = \begin{pmatrix} \sigma(k) & \rho(k) \\ \rho(k) & \sigma(k) \end{pmatrix} \quad , \quad \boldsymbol{S}^\dagger \cdot \boldsymbol{S} = \boldsymbol{I},$$

are the phase shifts, since $\lambda_\pm = \sigma \pm \rho = e^{2i\delta_\pm(k)}$. The phase shifts $\delta_\pm(k)$ in the even and odd channels are thus

$$\tan 2\delta_\pm(k) = \frac{\mathrm{Im}(\sigma(k) \pm \rho(k))}{\mathrm{Re}(\sigma(k) \pm \rho(k))},$$

whereas the total phase shift $\delta(k) = \delta_+(k) + \delta_-(k)$ for electrons can be written as:

$$\tan 2\delta(k) = \frac{\mathrm{Im}[\sigma^2(k) - \rho^2(k)]}{\mathrm{Re}[\sigma^2(k) - \rho^2(k)]} = \frac{2k\sqrt{k^2+m^2}\sin(2q)}{m^2 - (2k^2+m^2)\cos(2q)}.$$

For positrons $\tan 2\tilde{\delta}(k) = -\tan 2\delta(k)$ is satisfied.

One could write the corresponding spinors by replacing the scattering data just computed in (5.20) and (5.21) for electrons and in (5.23) and (5.24) for positrons.

5.2.2. Mass spike contact interaction

When considering $q = 0$ in (5.16), one obtains the one-dimensional Dirac Hamiltonian with a single Dirac δ-potential disturbing the mass term:

$$\boldsymbol{H}_\delta^M = -i\sigma_1 \frac{d}{dz} + (m + \lambda\delta(z))\sigma_3, \qquad \overline{\boldsymbol{H}}_\delta^M = -i\sigma_1 \frac{d}{dz} - (m - \lambda\delta(z))\sigma_3.$$

Relativistic bound states in mass-spike δ wells Particularising (5.29) to $q = 0$ yields the bound state momentum $\kappa_b = -m\tanh\lambda$, which provides a normalisable spinor only if $\lambda < 0$. The energy of the electron bound state is $\omega_b = m\,\mathrm{sech}\lambda$ and its spinor takes the form:

$$\Psi_\omega(z) = A \begin{pmatrix} 1 \\ -i\,\mathrm{sign}(z)\,\frac{\sinh\lambda}{1+\cosh\lambda} \end{pmatrix} e^{m|z|\tanh\lambda}, \qquad A = \sqrt{-m\cosh^2\left(\frac{\lambda}{2}\right)\tanh\lambda\,\mathrm{sech}\lambda}, \tag{5.35}$$

where A is obtained from the normalisation condition $\mathcal{N}^2\int_{\mathbb{R}}\Psi^\dagger(z)\Psi(z)dz = 1$. The charge density of this bound state is obtained by replacing the spinor (5.35) in the equation (5.31), yielding

$$j_0(z) = -m\,Q\tanh\lambda\,e^{2m|z|\tanh\lambda}, \tag{5.36}$$

which is represented in the left plot of Figure 5.5.

For positrons, setting $q = 0$ in (5.30) provides the solution $\kappa_b = m\tanh\lambda$. A spinor involving this imaginary momentum $k = im\tanh\lambda$ is normalisable only if $\lambda > 0$. The energy of this positron bound

state is $\omega_b = m \operatorname{sech}\lambda$ and its spinor can be written as:

$$\Phi_\omega(z) = D \begin{pmatrix} -\text{sign(z)}\, i\, \frac{\sinh\lambda}{1+\cosh\lambda} \\ -1 \end{pmatrix} e^{-m|z|\tanh\lambda}, \qquad D = \sqrt{m\cosh^2\left(\frac{\lambda}{2}\right)\tanh\lambda\,\operatorname{sech}\lambda}. \tag{5.37}$$

The charge density of this bound state is obtained by replacing the spinor (5.37) in the equation (5.31), arriving at the result

$$j_0(z) = -m\,Q\tanh\lambda\, e^{-2m|z|\tanh\lambda}, \tag{5.38}$$

which is represented in the right plot of Figure 5.5. Note that once again the continuity of $j_0(z)$ at every point guarantees the conservation of probability.

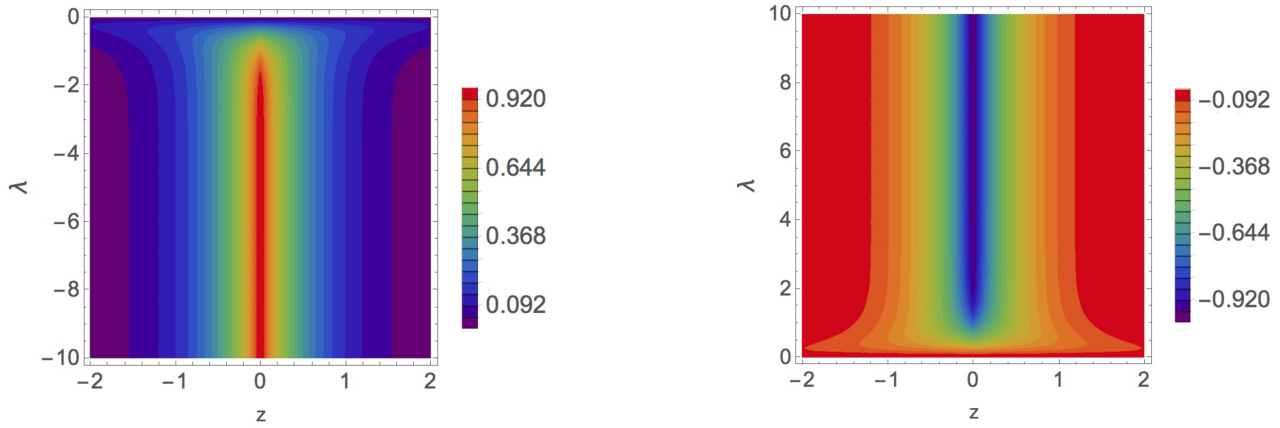

FIGURE 5.5: Charge density (5.36)-(5.38) as a function of z for electrons (left) and positrons (right) when $Q = m = 1$ and $q = 0$ ("massive"δ-potential).

Electron and positron scattering spinors The scattering amplitudes for electrons and positrons can be obtained form the generic ones (5.22) and (5.25) by putting $q = 0$:

$$\sigma_R(k) = \sigma_L(k) = \frac{k}{k\cosh\lambda + im\sinh\lambda}, \qquad \rho_R(k) = \rho_L(k) = \frac{-i\sqrt{k^2+m^2}\sinh\lambda}{k\cosh\lambda + im\sinh\lambda},$$

$$\tilde{\sigma}_R(k) = \tilde{\sigma}_L(k) = \frac{k}{k\cosh\lambda - im\sinh\lambda}, \qquad \tilde{\rho}_R(k) = \tilde{\rho}_L(k) = \frac{-i\sqrt{k^2+m^2}\sinh\lambda}{k\cosh\lambda - im\sinh\lambda}.$$

Notice that

- The S-matrix is unitary and the phase shifts appear as the exponents of its eigenvalues. The total phase shift is

$$\tan 2\delta(k) = \frac{\text{Im}[\sigma^2(k) - \rho^2(k)]}{\text{Re}[\sigma^2(k) - \rho^2(k)]} = \frac{-2km\sinh 2\lambda}{k^2 + m^2 + (k^2 - m^2)\cosh 2\lambda},$$

  for electrons and $\tan 2\tilde{\delta}(k) = -\tan 2\delta(k)$ for positrons.

- The purely imaginary poles of the transmission amplitude $\sigma(k)$ with positive imaginary part

are the bound states of the spectrum for electrons. This happens when $k_b = i\kappa_b = -im\tanh\lambda$, i.e., $\omega_b = m\,\mathrm{sech}\lambda$. It must be fulfilled that $\tanh\lambda < 0$. On the contrary, the purely imaginary poles of the transmission amplitude $\tilde{\sigma}(k)$ with positive imaginary part are the positron bound states of the spectrum. Now the condition is $k_b = i\kappa_b = im\tanh\lambda$, i.e., $\omega_b = m\,\mathrm{sech}\lambda$. It must be fulfilled that $\tanh\lambda > 0$.

- The relations between "*diestro*" and "*zurdo*" scattering amplitudes for electrons and positrons in a mass-spike δ-potential are as follows:

$$\sigma_R(k) = \sigma_L(k) = \tilde{\sigma}_R^*(k) = \tilde{\sigma}_L^*(k), \qquad \rho_R(k) = \rho_L(k) = -\tilde{\rho}_R^*(k) = -\tilde{\rho}_L^*(k).$$

It is relevant to note that I have published only part of the results presented in subsections 5.2.1 and 5.2.2 in [218]. The rest of the chapter is original work, not yet published under otherwise stated.

5.3. Scattering data and spectrum for double δ potentials

The more general static backgrounds that incorporate double δ potentials symmetrically placed around the origin can be expressed as (5.9) with:

$$M(z) = \lambda_1\delta(z+a) + \lambda_2\delta(z-a), \qquad \xi(z) = q_1\delta(z+a) + q_2\delta(z-a). \tag{5.39}$$

The dynamics induced in one fermionic particle and its antiparticle by this contact interaction are governed by the equations

$$i\partial_t\Psi_\omega(t,z) = \boldsymbol{H}_{\delta\delta}\Psi_\omega(t,z), \qquad i\partial_t\Phi_\omega(t,z) = \overline{\boldsymbol{H}}_{\delta\delta}\Phi_\omega(t,z),$$

with the Dirac operators

$$\boldsymbol{H}_{\delta\delta} = -i\alpha\frac{d}{dz} + \beta\left[m + \lambda_1\delta(z+a) + \lambda_2\delta(z-a)\right] + q_1\delta(z+a) + q_2\delta(z-a), \tag{5.40}$$

$$\overline{\boldsymbol{H}}_{\delta\delta} = -i\alpha\frac{d}{dz} - \beta[m - \lambda_1\delta(z+a) - \lambda_2\delta(z-a)] + q_1\delta(z+a) + q_2\delta(z-a). \tag{5.41}$$

Like for single delta potentials, the definition of this background through matching matrices at the singular points $z = \pm a$, is equivalent to provide a self-adjoint extension for $\mathbf{H}_{\delta\delta}$ and $\overline{\boldsymbol{H}}_{\delta\delta}$:

$$\begin{cases} \Psi_\omega(a^+) = T_\delta(q_2,\lambda_2)\Psi_\omega(a^-) \\ \Psi_\omega(-a^+) = T_\delta(q_1,\lambda_1)\Psi_\omega(-a^-) \end{cases}, \qquad \begin{cases} \Phi_\omega(a^+) = T_\delta(-q_2,\lambda_2)\Phi_\omega(a^-) \\ \Phi_\omega(-a^+) = T_\delta(-q_1,\lambda_1)\Phi_\omega(-a^-) \end{cases}. \tag{5.42}$$

$\Psi_\omega(\pm a^+)$ denotes the limit of the value of the spinor at $z = \pm a$ from the right, whereas $\Psi_\omega(\pm a^-)$ means the limit reached from the left. Two specific examples of double delta potentials will be presented below.

5.3.1. Double electric contact interaction

Next, only two electric Dirac-δ potentials centred in $z = \pm a$ are going to be considered (i.e. the choice $\lambda_1 = \lambda_2 = 0$ is going to be taken in (5.40)-(5.42)). Notice that the associated set of matching matrices $T_\delta(q) = \mathbb{1}\cos(q) - i\gamma^2 \sin(q)$ form a $U(1)$ abelian subgroup of $SU(2)$.

Electron and positron bound states: the discrete spectrum

- Electron bound states ($0 < \kappa < m$)

  The spinor takes the form

$$\Psi^b_\omega(z,k) = \begin{cases} A_1(\kappa)\, e^{\kappa z}\, \gamma^0\, u(i\kappa) & z < -a, \\ B_2(\kappa)\, e^{\kappa z}\, \gamma^0\, u(i\kappa) + C_2(\kappa)\, e^{-\kappa z}\, u(i\kappa) & -a < z < a, \\ D_3(\kappa)\, e^{-\kappa z}\, u(i\kappa) & z > a. \end{cases} \tag{5.43}$$

  where $u(k)$ is the positive energy electron spinor that solves the free static Dirac equation for plane waves moving along the real line (see (5.7)). The matching conditions (5.42) particularised to $\lambda_1 = \lambda_2 = 0$ are fulfilled if the following homogeneous linear system in the unknowns (A_1, B_2, C_2, D_3) is satisfied:

$$Q_1 \cdot (A_1, B_2, C_2, D_3)^T = 0,$$

  where Q_1 is given in Appendix C (C.9). Non null solutions of this homogeneous linear system exist if and only if $\det Q_1 = 0$, i.e. iff the following transcendent equation holds:

$$e^{-4a\kappa} = 1 + \frac{\kappa[\kappa\cos(q_1+q_2) + \sqrt{m^2-\kappa^2}\sin(q_1+q_2)]}{m^2 \sin q_1 \sin q_2}. \tag{5.44}$$

  Thus, bound states arise at the intersections between the exponential curve $e^{-4a\kappa}$ and the transcendent one:

$$Z_1(m,\kappa,q_1,q_2) = 1 + \frac{\kappa[\kappa\cos(q_1+q_2) + \sqrt{m^2-\kappa^2}\sin(q_1+q_2)]}{m^2 \sin q_1 \sin q_2},$$

  in the $\kappa \in (0, m)$ open interval, assuming $m > 0$. The number of bound states, i.e. the number of intersections between these two curves in the physical range of κ, depends on the values of the parameters $\{a, m, q_1, q_2\}$. By comparing the tangents of the exponential and the Z_1 curves at $\kappa = 0$, one can see that the identity between them occurs over the curve

$$\frac{\cot q_1 + \cot q_2}{m} = -4a, \qquad \rightarrow \qquad \cot q_1 + \cot q_2 = -\frac{4}{p}, \tag{5.45}$$

  being $p^{-1} = am$. This trigonometric transcendent equation describes in the q_1-q_2 plane an ordinary curve which is a frontier for the number of solutions of (5.44) to increase or decrease in one unit. Furthermore, making $\kappa = m$ in the transcendent spectral equation (5.44) yields the

condition of the existence of zero modes:

$$e^{-4am} = \cot q_1 \cot q_2 \qquad \rightarrow \qquad e^{-4/p} = \cot q_1 \cot q_2. \tag{5.46}$$

This equation represents another curve that divides the space between zones with one bound state and others with only continuous spectrum. This distribution of electron bound sates in the q_1-q_2 plane is displayed in Figure 5.6 (left).

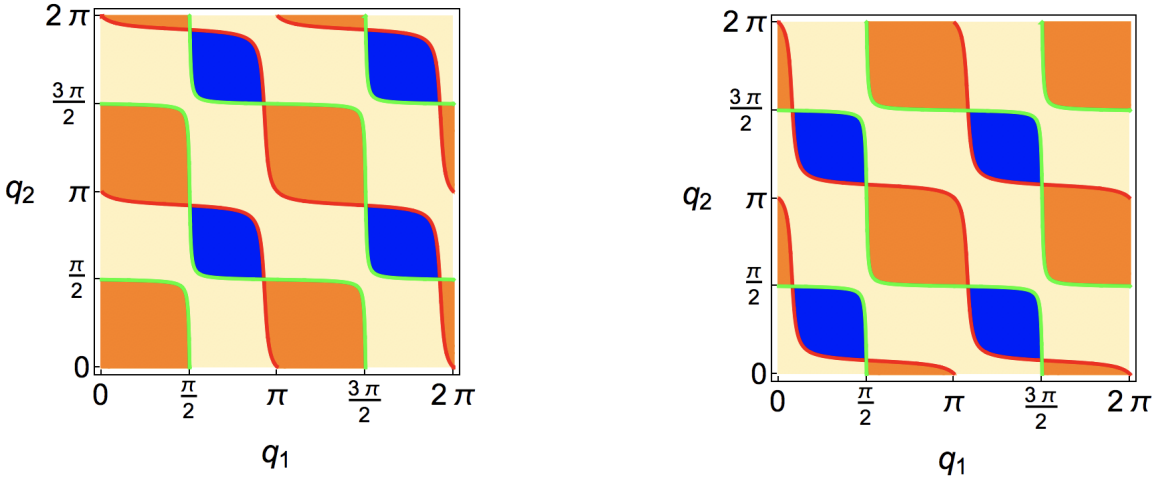

FIGURE 5.6: Bound state map in the q_1, q_2 space for electrons (left) or positrons (right) trapped by the double electric δ-potential. Blue area: two bound states. Yellow area: one bound state. Orange area: no bound states. The green line characterises the existence of zero modes (5.46). The red line is the trigonometric transcendent equation (5.45) in the left plot and (5.49) in the right plot. In these plots $a = 1, m = 1.2$.

It is worth stressing that once $\{q_1, q_2, a, m\}$ take a specific value, the spinor (5.43) should be normalised. It can be achieved by solving the transcendent equation (5.44) numerically for these values of $\{q_1, q_2, a, m\}$. Thereafter one replaces the specific numerical roots κ in the homogeneous linear system (C.9) to obtain the coefficients A_1, B_2, C_2, D_3. Finally, the normalisation condition $|\mathcal{N}|^2 \int_{\mathbb{R}} \Psi^\dagger(z)\Psi(z)dz = 1$ is applied to compute the value of the normalisation constant $\mathcal{N}$.

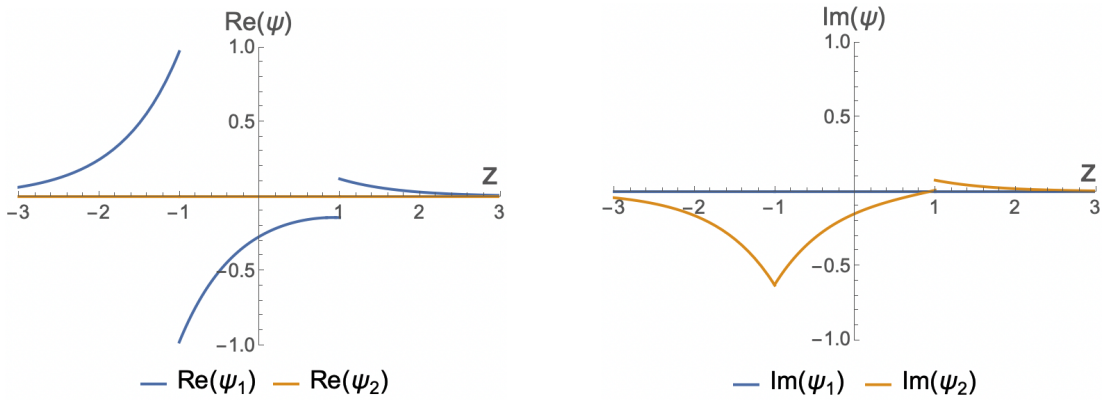

FIGURE 5.7: Ground bound state wave function $\Psi_{\omega_0}(z)$ for $m = 1.5, a = 1, q_1 = 2, q_2 = 2.5$. It corresponds to $\kappa_0 = 1.3669, \omega_0 = 0.6177$. Moreover, the numerical coefficients for this example are $A_1 = 1, B_2 = -0.0052, C_2 = -0.0648, D_3 = 0.1222$, $\mathcal{N} = \sqrt{14.587}$.

For instance, if one chooses $q_1 = 2$ and $q_2 = 2.5$ there will be two possible bound states within the gap $[0, m]$. Taken $a = 1, m = 1.5$, the momenta of the bound states is: $k_0 = i\kappa_0 = i1.3669$ and $k_1 = i\kappa_1 = i0.8552$. Their energy will be given by $\omega = \sqrt{m^2 - \kappa^2}$, i.e. $\omega_0 = 0.6177$ and $\omega_1 = 1.2323$. Notice that to the highest value of κ corresponds the lowest bound state energy. Consequently, k_0 characterises the ground state spinor plotted in Figure 5.7 and k_1 the excited bound state closer to the threshold of the continuous spectrum. The corresponding excited spinor is plotted in Figure 5.8.

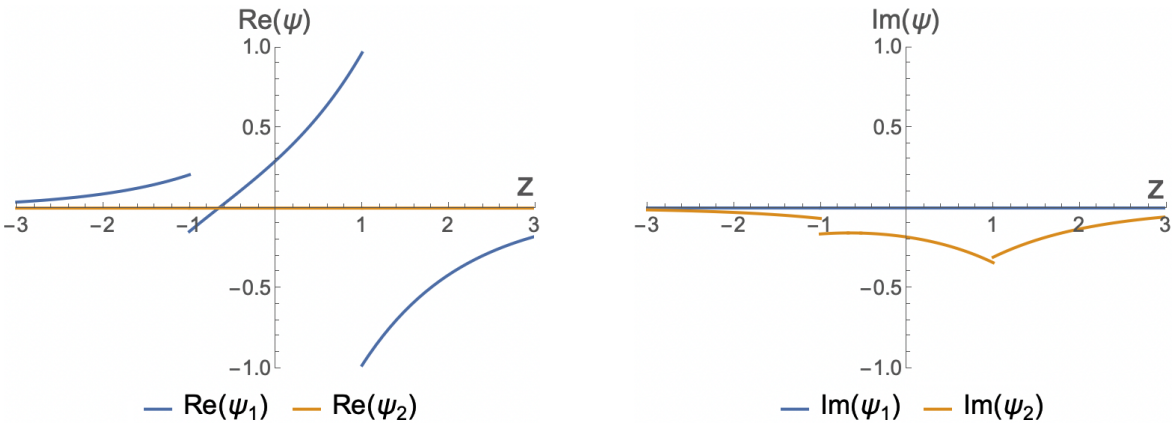

FIGURE 5.8: Excited bound state wave function $\Psi_{\omega_1}(z)$ for $m = 1.5, a = 1, q_1 = 2, q_2 = 2.5$. It corresponds to $\kappa_1 = 0.8552, \omega_1 = 1.2323$. Moreover, the numerical coefficients for this example are $A_1 = 1, B_2 = 0.8941, C_2 = -0.2883, D_3 = -4.7115, \mathcal{N} = \sqrt{0.2086}$.

- Positron bound state spinors, $0 < \kappa < m$

The spinor can be written as

$$\Phi^b_\omega(z,k) = \begin{cases} \tilde{A}_1(\kappa)\, e^{\kappa z}\, \gamma^0\, v(i\kappa) & z < -a, \\ \tilde{B}_2(\kappa)\, e^{\kappa z}\, \gamma^0\, v(i\kappa) + \tilde{C}_2(\kappa)\, e^{-\kappa z}\, v(i\kappa) & -a < z < a, \\ \tilde{D}_3(\kappa)\, e^{-\kappa z}\, v(i\kappa) & z > a. \end{cases} \tag{5.47}$$

where $v(k)$ is the positive energy positron spinor that solves the free static conjugate Dirac equation for plane waves moving along the real line (see (5.8)). An analogous computation that the one in the previous subsection but for positrons, yields the following homogeneous linear system

$$P_1 \cdot (\tilde{A}_1, \tilde{B}_2, \tilde{C}_2, \tilde{D}_3)^T = 0,$$

where P_1 is given in Appendix C (eq. C.10). The transcendent equation reads:

$$e^{-4a\kappa} = 1 + \frac{\kappa[\kappa \cos(q_1 + q_2) - \sqrt{m^2 - \kappa^2}\sin(q_1 + q_2)]}{m^2 \sin q_1 \sin q_2}. \tag{5.48}$$

Now, the trigonometric transcendent equation

$$-\frac{\cot q_1 + \cot q_2}{m} = -4a, \qquad \rightarrow \qquad \cot q_1 + \cot q_2 = \frac{4}{p} \tag{5.49}$$

is the one which describes in the q_1-q_2 plane an ordinary curve which is a frontier between areas admitting different numbers of positron bound states. If $\kappa = m$, the positron zero mode existence is also determined by (5.46). As in the case of electrons, these two curves (5.46) and (5.49) divide the space of parameters into different zones with zero, one or two bound sates. The distribution of bound states for positrons in the q_1-q_2 parameter space is depicted in Figure 5.6 (right).

Since there are two electric couplings given by angular coordinates $q_1, q_2 \in [0, 2\pi]$ in the model, the space of parameters is the Cartesian product $S^1 \times S^1$ of two circles in $\mathbb{R}^3$. This is a torus, from a topological point of view. Hence, in the natural system of units $\hbar = c = 1$, the maximum values of $\{q_1, q_2\}$ together with the mass of the particles and the distance between plates, can be understood as lengths related to the minor and major radius (r and R, respectively) of two tori:

$$T_1 \equiv \{R = a \cdot \max(q_1), r = \max(q_2)/m\}, \qquad T_2 \equiv \{r = a \cdot \max(q_1), R = \max(q_2)/m\}.$$

The transcendent equations (5.45), (5.46) and (5.49) describe curves which divide the parameter space into zones with different number of bound states. Furthermore, these curves do not depend on $\{a, m\}$ but on their product. Consequently, one could also represent them over the Riemann surface of the torus as shown in Figure 5.9.

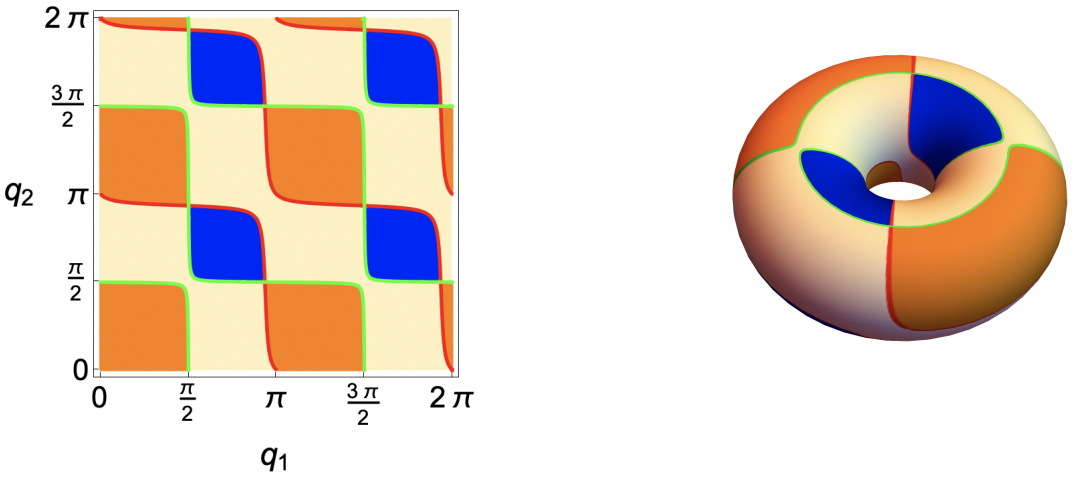

FIGURE 5.9: Bound state map for electrons interacting with a double electric delta potential and corresponding complex torus for $p^{-1} = 1.5$ with $a = 1, m = 1.5$.

The parameter $p^{-1} = a \cdot m$ and its inverse fix the complex structure[5] of the two tori associated to the family of theories characterised by $\{a, m\}$. Notice that here the torus is a connected complex manifold which is homeomorphic to the quotient $\mathbb{C}/L(a_1, a_2)$, being $L(a_1, a_2)$ the lattice generated by $a_1 = 2\pi a$, $a_2 = 2\pi/m \in \mathbb{C}$ [219, 220], as seen in Figure 5.10. Two lattices are equivalent if they

[5] Associating a complex structure means defining the ring of holomorphic and meromorphic functions. A torus may carry a number of different complex structures.

are related by the modular group[6] $PSL(2,\mathbb{Z}) \equiv SL(2,\mathbb{Z})/\mathbb{Z}_2$. The complex structure of a Lie group in the vector space $\mathbb{C}$ induces that of the torus. $\mathbb{C}$ is thus the universal covering space of the torus[7]. Hence, the choice of (a_1, a_2) or equivalently $(1, p = a_2/a_1)$, defines the complex structure of the torus, i.e. the specific way of identifying points in $\mathbb{C}$, modulo $PSL(2,\mathbb{Z})$.

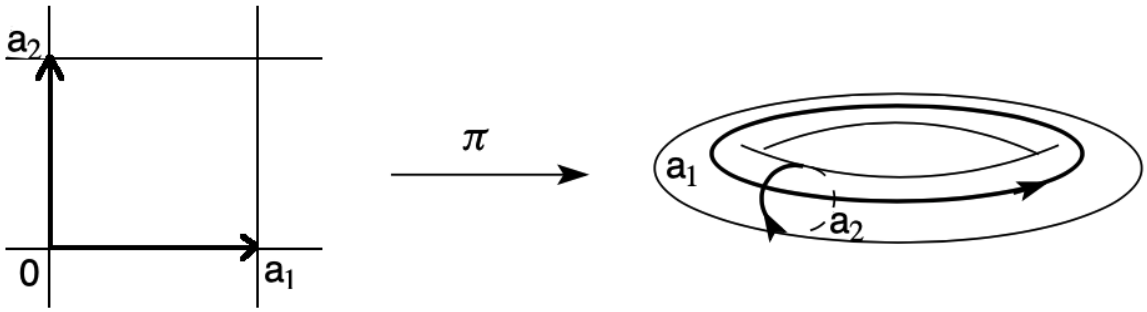

FIGURE 5.10: Universal covering map between the lattice generated by (a_1, a_2) and the corresponding torus. This picture has been created specifically to fit the case presented in this chapter. However, the general case por $p \in \mathbb{C}$ is collected in [220], from which the idea was taken to make this specific picture.

Consequently, when studying fermionic fields in a double electric delta potential, the naturally arising two-parametric family of theories are related to a subset of the moduli[8] of complex tori or genus one algebraic curves characterised by $ma \in \mathbb{R}$. In such a way, once $\{a, m\}$ are fixed, to each theory corresponds in principle only two tori associated to p and $1/p$. However, one could see that not all $p \in H$ are independent, but the equivalent ones are related by the modular group. Hence, the equivalence class under the modular group $H/PSL(2,\mathbb{Z})$ is the reason that only the torus such that $p^{-1} > 1$ (i.e. $a > 1/m$) must be taken into account.

Electron and positron scattering spinors: the continuous spectrum

- Electron scattering spinor waves: $k \in \mathbb{R}$.

  The scattering spinors for the electrons coming from the left towards the double delta potential ("*diestro*" scattering) are:

[6]The modular group [221] is the projective special linear group of 2×2 matrices with integer coefficients and determinant equal to one. Its action on the upper half plan of the complex plane H is the group of linear fractional transformations

$$z \to \frac{az + b}{cz + d},$$

with $a, b, c, d \in \mathbb{Z}$ and $ad - bc = 1$. The fundamental domain of the modular group can be completely defined as the set $D = \{z \in H | \ |\mathrm{Re}\, z| < 1/2 \cup |z| > 1\}$, whose closure includes at least one point from each equivalence class under the modular group.

[7]Identifying the opposite sides of the parallelogram gives the torus T. Furthermore, there is a universal covering map $\pi : \mathbb{C} \to T$ whose kernel can be identified with the first homology group $H_1(T,\mathbb{Z})$. Notice that the torus is locally isomorphic to $\mathbb{C}$.

[8]The moduli is the geometric space where each point represents an isomorphism class of smooth algebraic curves of a fixed genus.

$$\Psi^R_\omega(z,k) = \begin{cases} u_+(k)e^{ikz} + \rho_R(k)\ \gamma^0\, u_+(k)e^{-ikz} & z < -a, \\ A_R(k)\, u_+(k)e^{ikz} + B_R(k)\ \gamma^0\, u_+(k)e^{-ikz} & -a < z < a, \\ \sigma_R(k)\, u_+(k)e^{ikz} & z > a. \end{cases} \tag{5.50}$$

whereas scattering spinors for electrons coming from the right towards the double delta potential ("*zurdo*") scattering reads

$$\Psi^L_\omega(z,k) = \begin{cases} \sigma_L(k)\gamma^0\, u_+(k)e^{-ikz} & z < -a, \\ A_L(k)\, u_+(k)e^{ikz} + B_L(k)\ \gamma^0\, u_+(k)e^{-ikz} & -a < z < a, \\ \gamma^0\, u_+(k)e^{-ikz} + \rho_L(k)\, u_+(k)e^{ikz} & z > a. \end{cases} \tag{5.51}$$

These piecewise solutions must satisfy the matching conditions (5.42) for $\lambda_1 = \lambda_2 = 0$. Consequently, there are two algebraic lineal systems of four equations, one for the four unknowns of the "*diestro*" scattering $\{\sigma_R, A_R, B_R, \rho_R\}$ (eq. (C.11) in Appendix C) and other one for the four unknowns of the "*zurdo*" scattering $\{\sigma_L, A_L, B_L, \rho_L\}$ (C.12). Cramer's procedure offers the following solution for the scattering amplitudes:

$$\begin{aligned} \sigma_R(k;q_1,q_2) &= \sigma_L(k;q_1,q_2) = \frac{k^2}{\Lambda(k;q_1,q_2)} = \sigma(k;q_1,q_2), \\ \rho_R(k;q_1,q_2) &= -\frac{2im\sqrt{k^2+m^2}\sin q_1 \sin q_2\ \sin(2ak) + ikm\,\Theta(a,k,q_1,q_2)}{\Lambda(k;q_1,q_2)}, \\ \rho_L(k;q_1,q_2) &= -\frac{2im\sqrt{k^2+m^2}\sin q_1 \sin q_2\ \sin(2ak) + ikm\,\Theta^*(a,k,q_1,q_2)}{\Lambda(k;q_1,q_2)}, \\ \Lambda(k;q_1,q_2) &= k^2\cos(q_1+q_2) + ik\sqrt{k^2+m^2}\sin(q_1+q_2) + m^2\sin q_1 \sin q_2(e^{4iak}-1), \\ \Theta(a,k,q_1,q_2) &= e^{-2iak}\cos q_2 \sin q_1 + e^{2iak}\cos q_1 \sin q_2. \end{aligned} \tag{5.52}$$

Solving the systems also yields the coefficients $\{A_R, B_R, A_L, B_L\}$. They are collected in Appendix C (C.13) for completeness. It is important to highlight that when only a single delta potential is introduced in the system, the reflection coefficients for diestro and zurdo scattering are equal to each other due to the parity symmetry in the system. Now, when two delta potentials are considered, there could be other type of interactions between the plates due to the quantum vacuum fluctuations that did not arise in the previous case, and parity symmetry could be broken. This is reflected in the fact that now $\rho_L \neq \rho_R$.

Also, for $k = i\kappa$ and $0 < \kappa < m$, the zeroes of $\Lambda(i\kappa;q_1,q_2)$, i.e. the poles of $\sigma(k;q_1,q_2)$ in the positive imaginary axis of the k-complex plane, arise as the solutions of the transcendent equation

$$e^{-4a\kappa} = 1 + \frac{\kappa[\kappa\cos(q_1+q_2) + \sqrt{m^2-\kappa^2}\sin(q_1+q_2)]}{m^2\sin q_1 \sin q_2},$$

as it should be (see (5.44)).

- Positron scattering spinorial waves: $k \in \mathbb{R}$.

The procedure is totally analogous to the one for electrons. If the positrons come from the left towards the double delta singularity ("*diestro*" scattering), the spinorial waves in the regions where the positrons move freely are described in terms of scattering amplitudes following the ansatz:

$$\Phi^R_\omega(z,k) = \begin{cases} v_+(k)e^{ikz} + \tilde{\rho}_R(k)\,\gamma^0\,v_+(k)e^{-ikz} & z < -a, \\ \tilde{A}_R(k)\,v_+(k)e^{ikz} + \tilde{B}_R(k)\,\gamma^0\,v_+(k)e^{-ikz} & -a < z < a, \\ \tilde{\sigma}_R(k)\,v_+(k)e^{ikz} & z > a. \end{cases} \tag{5.53}$$

Scattering spinors for positrons coming from the right towards the double delta potential ("*zurdo*" scattering) are described by:

$$\Phi^L_\omega(z,k) = \begin{cases} \tilde{\sigma}_L(k)\gamma^0\,v_+(k)e^{-ikz} & z < -a, \\ \tilde{A}_L(k)\,v_+(k)e^{ikz} + \tilde{B}_L(k)\,\gamma^0\,v_+(k)e^{-ikz} & -a < z < a, \\ \gamma^0\,v_+(k)e^{-ikz} + \tilde{\rho}_L(k)\,v_+(k)e^{ikz} & z > a. \end{cases} \tag{5.54}$$

These solutions must be connected at the impurities placed at $z = \pm a$ through the matching conditions (5.42) for $\lambda_1 = \lambda_2 = 0$. The two algebraic lineal systems of four equations for the unknowns $\{\tilde{\sigma}_R, \tilde{A}_R, \tilde{B}_R, \tilde{\rho}_R\}$ (C.14) and $\{\tilde{\sigma}_L, \tilde{A}_L, \tilde{B}_L, \tilde{\rho}_L\}$ (C.15) give the following scattering amplitudes:

$$\begin{aligned}
&\tilde{\sigma}_R(k;q_1,q_2) = \tilde{\sigma}_L(k;q_1,q_2) = \frac{k^2}{\tilde{\Lambda}(k;q_1,q_2)} = \tilde{\sigma}(k;q_1,q_2), \\
&\tilde{\rho}_R(k;q_1,q_2) = \frac{2im\sqrt{k^2+m^2}\sin q_1 \sin q_2 \sin(2ak) - ikm\,\tilde{\Theta}(a,k,q_1,q_2)}{\tilde{\Lambda}(k;q_1,q_2)}, \\
&\tilde{\rho}_L(k;q_1,q_2) = \frac{2im\sqrt{k^2+m^2}\sin q_1 \sin q_2\ \sin(2ak) - ikm\,\tilde{\Theta}^*(a,k,q_1,q_2)}{\tilde{\Lambda}(k;q_1,q_2)}, \\
&\tilde{\Lambda}(k;q_1,q_2) = k^2\cos(q_1+q_2) - ik\sqrt{k^2+m^2}\sin(q_1+q_2) + m^2\sin q_1 \sin q_2(e^{4iak}-1), \\
&\tilde{\Theta}(a,k,q_1,q_2) = e^{-2iak}\cos q_2 \sin q_1 + e^{2iak}\cos q_1 \sin q_2.
\end{aligned} \tag{5.55}$$

The coefficients $\{\tilde{A}_R, \tilde{B}_R, \tilde{A}_L, \tilde{B}_L\}$ are given in the Appendix (C.16). For $k = i\kappa$ and $0 < \kappa < m$, the zeroes of $\tilde{\Lambda}(i\kappa;q_1,q_2)$, i.e. the poles of $\tilde{\sigma}(k;q_1,q_2)$ in the positive imaginary axis of the k-complex plane, arise as the solutions of the transcendent equation

$$e^{-4a\kappa} = 1 + \frac{\kappa[\kappa\cos(q_1+q_2) - \sqrt{m^2-\kappa^2}\sin(q_1+q_2)]}{m^2\sin q_1 \sin q_2},$$

in perfect agreement with the direct derivation of positron bound state energies from the bound state eigen-spinor ansatz (5.48).

5.3.2. Double mass spike contact interaction

Consider finally the one-dimensional Hamiltonians for the fermionic particle and antiparticle moving in the real line in the background of two mass-like Dirac-δ potentials centred at $z = \pm a$, i.e. (5.40) and (5.41) for $q_1 = q_2 = 0$. Now, the spectral problems for the Dirac Hamiltonian and its conjugate must be solved including the matching conditions defined in (5.42) for $q_1 = q_2 = 0$. Notice that the admissible matching matrices $T_\delta(\lambda) = \mathbb{1}\cosh(\lambda) + i\gamma^1 \sinh(\lambda)$, form the one-dimensional subgroup of $SU(1,1;\mathbb{C})$ of hyperbolic elements, those such that $\operatorname{tr} T_\delta(\lambda) > 2$.

Electron and positron bound states: the discrete spectrum

- Electron bound state spinors, $0 < \kappa < m$.

  Pugging the ansatz (5.43) in the matching conditions (5.42) for $q_1 = q_2 = 0$, defines the homogeneous linear system in the unknowns (A_1, B_2, C_2, D_3) given in equation (C.1) of Appendix C. The non trivial solutions exist if and only if the following transcendent equation holds:

$$e^{-4a\kappa} = \frac{(m + \kappa \coth \lambda_1)(m + \kappa \coth \lambda_2)}{m^2 - \kappa^2}. \tag{5.56}$$

  Thus, bound states can be obtained as an intersection between the exponential curve $e^{-4a\kappa}$ and the transcendent one:

$$Z(m, \kappa, \lambda_1, \lambda_2) = \frac{(m + \kappa \coth \lambda_1)(m + \kappa \coth \lambda_2)}{m^2 - \kappa^2}.$$

  The number of bound states, i.e. the number of intersections between these two curves in the physical range of κ, depends again on the parameters $\{m, \kappa, \lambda_1, \lambda_2\}$. Comparing the tangents of the exponential and the curve $Z(m, \kappa, \lambda_1, \lambda_2)$ at $\kappa = 0$ yields

$$\coth \lambda_1 + \coth \lambda_2 = -\frac{4}{p}, \qquad p^{-1} = am. \tag{5.57}$$

  The shape of the curve that this hyperbolic transcendent equation describes in the λ_1-λ_2 plane is similar to that of a hyperbola with two branches. One of the vertices is placed at the origin, the other at the point $(\lambda_1 = \lambda_2 = -\operatorname{arccoth} 2)$, and the axis is the $\lambda_1 = \lambda_2$ straight line. For points above the upper branch of the curve, no bound states are encountered. Points in between the two branches correspond to one bound state. Points in the zone below the lower branch give rise to two bound states. This distribution can be seen in Figure 5.11 (left).

  There is a very subtle question. One might think that when the minimum of the $Z(m, \kappa, \lambda_1, \lambda_2)$ function as a function of κ is placed at $\kappa = m$, the bound state at most lies at the threshold of the continuous spectrum. Since the critical points of $Z(m, \kappa, \lambda_1, \lambda_2)$ occurs when

$$\frac{dZ}{d\kappa}(m,\kappa,\lambda_1,\lambda_2)=0 \;\Rightarrow\; \begin{cases} \kappa_{m+} = -m\coth[\frac{\lambda_1+\lambda_2}{2}] \\ \kappa_{m-} = -m\tanh[\frac{\lambda_1+\lambda_2}{2}] \end{cases},$$

then $\kappa = m$ only is reached if $\lambda_1+\lambda_2 = -\infty$. Therefore, contrary to what happens in the case of the electric double delta potential, here there are no zero modes.

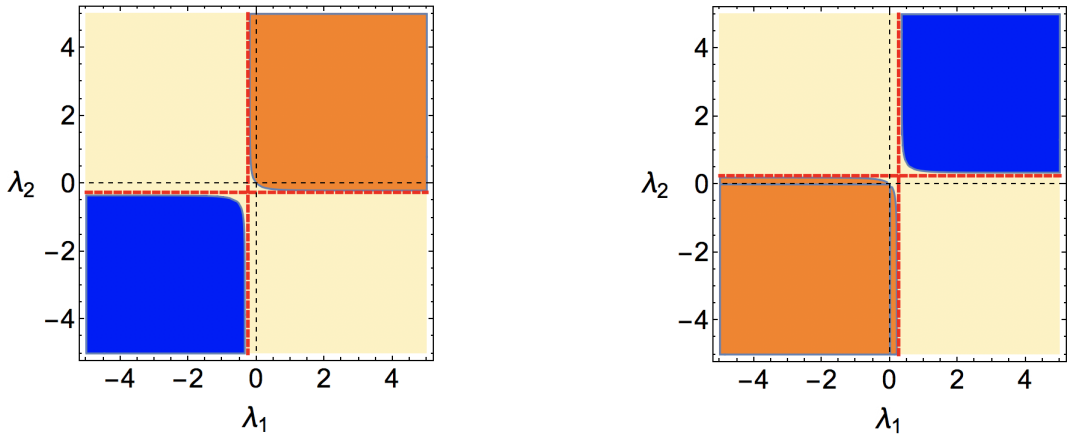

FIGURE 5.11: Electron (left) and positron (right) bound state map for a double mass-spike contact interaction. Blue area: 2 bound states. Yellow area: 1 bound state. Orange area: no bound states.

- Positron bound state spinors: $0 < \kappa < m$.

Plugging the spinor (5.47) into (5.42) for $q_1 = q_2 = 0$ yields an homogeneous linear system

$$P\cdot(\tilde{A}_1,\tilde{B}_2,\tilde{C}_2,\tilde{D}_3)^T = 0,$$

where P is given in (C.2). The transcendent equation now reads:

$$e^{-4a\kappa} = \frac{(m-\kappa\coth\lambda_1)(m-\kappa\coth\lambda_2)}{m^2-\kappa^2}. \tag{5.58}$$

Thus, the positron bound states correspond to the intersecting points of the exponential curve $e^{-4a\kappa}$ with the transcendent one:

$$R(m,\kappa,\lambda_1,\lambda_2) = \frac{(m-\kappa\coth\lambda_1)(m-\kappa\coth\lambda_2)}{m^2-\kappa^2},$$

in the $\kappa\in(0,m)$ open interval. The identity between tangents of the aforementioned functions occurs on the curve

$$\coth\lambda_1+\coth\lambda_2 = \frac{4}{p}. \tag{5.59}$$

This hyperbolic transcendent equation describes in the λ_1-λ_2 plane a curve with a similar shape to an ordinary hyperbola with two branches. One of the vertices is placed at the origin, the other at the point $(\lambda_1=\lambda_2=\operatorname{arccoth}2)$ in the first quadrant, and the axis is the $\lambda_1=\lambda_2$ straight line. For points above the upper branch of the curve, two bound states are encountered. Points in

between the two branches correspond to one bound state. Points in the zone below the lower branch correspond to no bound states, as it could be seen in Figure 5.11 (right). Once more, since the critical points of $R(m,\kappa,\lambda_1,\lambda_2)$ occurs when

$$\frac{dR}{d\kappa}(m,\kappa,\lambda_1,\lambda_2)=0 \;\Rightarrow\; \begin{cases} \kappa_{m+} = m\coth[\frac{\lambda_1+\lambda_2}{2}] \\ \kappa_{m-} = m\tanh[\frac{\lambda_1+\lambda_2}{2}] \end{cases},$$

then $\kappa = m$ only is reached if $\lambda_1+\lambda_2 = +\infty$ and there are no zero modes.

Electron and positron scattering spinors: the continuous spectrum

- Electron scattering spinorial waves: $k \in \mathbb{R}$.

Replacing (5.50) and (5.51) in (5.42) allows to obtain a pair of algebraic lineal systems of four equations for the four unknowns of the "*diestro*" scattering $\{\sigma_R, A_R, B_R, \rho_R\}$, and for the four unknowns of the "*zurdo*" scattering $\{\sigma_L, A_L, B_L, \rho_L\}$. Both systems are given in (C.3)-(C.4) respectively. The solution for the electron scattering amplitudes reads:

$$\begin{aligned}
\sigma_R(k;\lambda_1,\lambda_2) &= \sigma_L(k;\lambda_1,\lambda_2) = \frac{k^2}{\Delta(k;\lambda_1,\lambda_2)} = \sigma(k;\lambda_1,\lambda_2), \\
\rho_R(k;\lambda_1,\lambda_2) &= \frac{-2im\sqrt{k^2+m^2}\sinh\lambda_1\sinh\lambda_2\sin(2ak) - ik\sqrt{k^2+m^2}\Upsilon(k,\lambda_1,\lambda_2)}{\Delta(k;\lambda_1,\lambda_2)}, \\
\rho_L(k;\lambda_1,\lambda_2) &= \frac{-2im\sqrt{k^2+m^2}\sinh\lambda_1\sinh\lambda_2\sin(2ak) - ik\sqrt{k^2+m^2}\Upsilon^*(k,\lambda_1,\lambda_2)}{\Delta(k;\lambda_1,\lambda_2)}, \\
\Delta(k;\lambda_1,\lambda_2) &= k^2\cosh(\lambda_1+\lambda_2) + (k^2+m^2)(e^{4iak}-1)\sinh\lambda_1\sinh\lambda_2 \\
&\quad + ikm\sinh(\lambda_1+\lambda_2), \\
\Upsilon(k,\lambda_1,\lambda_2) &= e^{-2iak}\cosh\lambda_2\sinh\lambda_1 + e^{2iak}\cosh\lambda_1\sinh\lambda_2.
\end{aligned} \tag{5.60}$$

The coefficients $\{A_R, B_R, A_L, B_L\}$ are given in (C.5). Only if $\lambda_1 = \lambda_2$ the scattering process is parity invariant, because then $\rho_L(k;\lambda,\lambda) = \rho_R(k;\lambda,\lambda)$. If $k = i\kappa$ and $0 < \kappa < m$, the zeroes of $\Delta(i\kappa;\lambda_1,\lambda_2)$, i.e. the poles of $\sigma(k;\lambda_1,\lambda_2)$ in the positive imaginary axis of the k-complex plane, enable to recover the transcendent equation (5.56).

- Positron scattering spinorial waves: $k \in \mathbb{R}$.

Proceeding in a similar way for the analysis of the scattering of positrons by two δ-impurities (systems (C.6)-(C.7) in the Appendix C) provides the following scattering amplitudes for positrons:

$$\begin{aligned}
\tilde{\sigma}_R(k;\lambda_1,\lambda_2) &= \tilde{\sigma}_L(k;\lambda_1,\lambda_2) = \frac{k^2}{\tilde{\Delta}(k;\lambda_1,\lambda_2)} = \tilde{\sigma}(k;\lambda_1,\lambda_2), \\
\tilde{\rho}_R(k;\lambda_1,\lambda_2) &= \frac{i2m\sqrt{k^2+m^2}\sinh\lambda_1\sinh\lambda_2\sin(ak) - ik\sqrt{k^2+m^2}\tilde{\Upsilon}(k,\lambda_2,\lambda_1)}{\tilde{\Delta}(k;\lambda_1,\lambda_2)}, \\
\tilde{\rho}_L(k;\lambda_1,\lambda_2) &= \frac{i2m\sqrt{k^2+m^2}\sinh\lambda_1\sinh\lambda_2\sin(ak) - ik\sqrt{k^2+m^2}\tilde{\Upsilon}^*(k,\lambda_2,\lambda_1)}{\tilde{\Delta}(k;\lambda_1,\lambda_2)},
\end{aligned}$$

$$\begin{aligned}\tilde{\Delta}(k;\lambda_1,\lambda_2) &= k^2\cosh(\lambda_1+\lambda_2)+(k^2+m^2)(e^{4iak}-1)\sinh\lambda_1\sinh\lambda_2\\ &\quad -ikm\sinh(\lambda_1+\lambda_2),\\ \tilde{\Upsilon}(k,\lambda_1,\lambda_2) &= e^{-2iak}\cosh\lambda_2\sinh\lambda_1+e^{2iak}\cosh\lambda_1\sinh\lambda_2.\end{aligned} \tag{5.61}$$

The coefficients $\{\tilde{A}_R,\tilde{B}_R,\tilde{A}_L,\tilde{B}_L\}$ are gathered in (C.8). Again, only whether $\lambda_1=\lambda_2$ then $\tilde{\rho}_R(k;\lambda,\lambda)=\tilde{\rho}_L(k;\lambda,\lambda)$, and positron scattering through two δ-impurities is parity invariant. Besides, for $k=i\kappa$ and $0<\kappa<m$, the zeroes of $\tilde{\Delta}(i\kappa;\lambda_1,\lambda_2)$ arise as the solutions of the transcendent equation (5.58).

All the S-matrices defined in this section both for electrons and positrons are unitary ($S^\dagger S=\mathbb{I}$), since it can be checked that

$$|\sigma|^2+|\rho_R|^2=1,\qquad |\sigma|^2+|\rho_L|^2=1,\qquad \sigma\rho_L^*+\sigma^*\rho_R=0.$$

5.4. Second quantisation and vacuum energy at zero temperature

In order to build a relativistic QFT, one can postulate the operator

$$\hat{\Psi}(x)=\frac{1}{2\pi}\int\frac{d^2\boldsymbol{k}}{2\omega}\left[\hat{b}(k)u(k)e^{-ikx}+\hat{d}^\dagger(k)v(k)e^{ikx}\right],\qquad\text{with}\qquad \omega=+\sqrt{m^2+k^2},$$

which satisfies the Dirac equation, and interpret the coefficient $\hat{b}$ as a particle-annihilation operator upon second quantisation is performed. $\hat{d}$ would be an antiparticle- annihilation operator [97]. On the contrary, $\hat{b}^\dagger,\hat{d}^\dagger$ create nucleons and anti nucleons of momentum k, respectively. When dealing with fermions, the corresponding states should be antisymmetric to enforce Pauli's exclusion principle, and hence $\hat{b},\hat{d}$ fulfil the following anti commutation relations:

$$\begin{aligned}&\{\hat{b}(k),\hat{b}^\dagger(k')\}=2\omega\delta(k-k'),\quad \{\hat{d}(k),\hat{d}^\dagger(k')\}=2\omega\delta(k-k'),\\ &\{\hat{b},\hat{b}'\}=\{\hat{d},\hat{d}'\}=\{\hat{b},\hat{d}\}=\{\hat{b},\hat{d}'\}=\{\hat{b},(\hat{d}')^\dagger\}=0.\end{aligned}$$

One builds the "Fock" space acting with $\hat{b}^\dagger,\hat{d}^\dagger$ over the vacuum state, taking into account that $b(k)\,|0\rangle=d(k)\,|0\rangle=0$. The Hamiltonian and the charge operator would be

$$\begin{aligned}\boldsymbol{H}^{(0)} &= \int\frac{dk}{2}\left[\hat{b}^\dagger(k)\hat{b}(k)+\hat{d}^\dagger(k)\hat{d}(k)-\delta^{(3)}(0)\right],\\ \boldsymbol{Q} &= Q\int\frac{dk}{2\omega}\left[\hat{b}^\dagger(k)\hat{b}(k)-\hat{d}^\dagger(k)\hat{d}(k)\right].\end{aligned}$$

In this way, by the use of anti commutators, the energy is positive definite. Some caveats are worth stressing. Firstly, in this QFT there exist antiparticles with opposite charge to that of particles. Secondly, observables made from Fermi fields are products of a even number of fields so that they commute at spacelike intervals. Finally, preserving Heisenberg equations of motion and classical theory in the limit $\hbar\to 0$ for fermions, requires the use of anticonmmuting quantities or Grassmann variables.

Furthermore, the introduction of antiparticles enables to study the charge conjugation symmetry. For the specific choice of the Clifford algebra representation (5.4), the point supported potential defined by (5.13) has the following transformation properties under the symmetries $\mathcal{P},\mathcal{T},\mathcal{C}$:

- Under the parity transformation

$$\mathcal{P}\Psi(t,z)\mathcal{P}^{-1}=\eta_p\gamma^0\Psi(t,-z),\qquad |\eta_P|=1,$$

being η_p the instrinsic parity of the particle[9], the matching condition remains invariant since

$$\left.\begin{aligned}&\mathcal{P}\Psi(0^+)\mathcal{P}^{-1}=T_\delta^P(q,\lambda)\mathcal{P}\Psi(0^-)\mathcal{P}^{-1}=\eta_P T_\delta^P(q,\lambda)\gamma^0\Psi(0^+)\\&\mathcal{P}\Psi(0^+)\mathcal{P}^{-1}=\eta_P\gamma^0\Psi(0^-)=\eta_P\gamma^0T_\delta^{-1}(q,\lambda)\Psi(0^+)\end{aligned}\right\}\to T_\delta^P(q,\lambda)=\gamma^0T_\delta^{-1}(q,\lambda)(\gamma^0)^{-1}=T_\delta(q,\lambda).$$

Notice that parity is an intrinsic symmetry of both $\boldsymbol{H}_D^{(0)}$ and $\overline{\boldsymbol{H}}_D^{(0)}$. This is due to the fact that $\mathcal{P}\boldsymbol{H}_D^{(0)}\mathcal{P}^{-1}=\boldsymbol{H}_D^{(0)}$ and $\mathcal{P}\overline{\boldsymbol{H}}_D^{(0)}\mathcal{P}^{-1}=\overline{\boldsymbol{H}}_D^{(0)}$ independently of the specific choice of γ matrices, because $\gamma^0\gamma^2=-\gamma^2\gamma^0$ is always fulfilled.

- Under the time-reversal transformation

$$\mathcal{T}\Psi(t,z)\mathcal{T}^{-1}=U_T\Psi^*(t,z)U_T^\dagger=\eta_T\gamma^0\Psi(-t,z),\qquad U_TU_T^\dagger=1,\quad |\eta_T|=1,$$

the matching condition also remains invariant since

$$\left.\begin{aligned}&\mathcal{T}\Psi(0^+)\mathcal{T}^{-1}=T_\delta^T(q,\lambda)\mathcal{T}\Psi(0^-)\mathcal{T}^{-1}=\eta_T T_\delta^T(q,\lambda)\gamma^0\Psi(0^-)\\&\mathcal{T}\Psi(0^+)\mathcal{T}^{-1}=\eta_T\gamma^0\Psi(0^+)=\eta_T\gamma^0T_\delta(q,\lambda)\Psi(0^-)\end{aligned}\right\}\to T_\delta^T(q,\lambda)=\gamma^0T_\delta(q,\lambda)(\gamma^0)^{-1}=T_\delta(q,\lambda).$$

Time-reversal is an intrinsic symmetry of $\boldsymbol{H}_D^{(0)}$ and $\overline{\boldsymbol{H}}_D^{(0)}$ for any choice of the Clifford algebra, since $\gamma^0\gamma^2=-\gamma^2\gamma^0$ is always fulfilled. The equation $\mathcal{T}\boldsymbol{H}_D^{(0)}\mathcal{T}^{-1}=\boldsymbol{H}_D^{(0)}$ holds and similarly $\mathcal{T}\overline{\boldsymbol{H}}_D^{(0)}\mathcal{T}^{-1}=\overline{\boldsymbol{H}}_D^{(0)}$.

- However, under charge conjugation

$$\mathcal{C}\Psi(t,z)\mathcal{C}^{-1}=\eta_C\gamma^2\Psi^*(t,z),\qquad |\eta_C|=1,$$

the fermionic delta potential (5.13) is not invariant as long $q\neq 0$ because

$$\left.\begin{aligned}&\mathcal{C}\Psi(0^+)\mathcal{C}^{-1}=T_\delta^C(q,\lambda)\mathcal{C}\Psi(0^-)\mathcal{C}^{-1}=\eta_C T_\delta^C(q,\lambda)\gamma^2\Psi^*(0^-)\\&\mathcal{C}\Psi(0^+)\mathcal{C}^{-1}=\eta_C\gamma^2\Psi^*(0^+)=\eta_C\gamma^2T_\delta^*(q,\lambda)\Psi^*(0^-)\end{aligned}\right\}\to T_\delta^C(q,\lambda)=\gamma^2T_\delta^*(q,\lambda)(\gamma^2)^{-1}=T_\delta(-q,\lambda).$$

Charge conjugation is neither a symmetry of $\boldsymbol{H}^{(0)}$ nor $\overline{\boldsymbol{H}}^{(0)}$ since $\mathcal{C}\boldsymbol{H}^{(0)}\mathcal{C}^{-1}\neq\boldsymbol{H}^{(0)}$, due to the fact that $\gamma^2(\gamma^0)^*\neq\gamma^0\gamma^2$. Actually $\mathcal{C}\boldsymbol{H}^{(0)}\mathcal{C}^{-1}=\overline{\boldsymbol{H}}^{(0)}$.

[9] Space-reversal is represented by a parity operator which commutes with the orbital momentum and the spin operators, and anticommutes with the linear momentum operator. Furthermore, the free Dirac Hamiltonian should be parity invariant and $\mathcal{P}^2\equiv\mathbb{1}$ must be preserved. The only way to satisfy all these conditions is that $\mathcal{P}\Psi(t,z)=\eta_p\gamma^0\Psi(t,-z)$, being η_p a constant with unit modulus called intrinsic parity (see [222] for more details). It can be chosen such that $\eta_p=(-1)^p$. Particles and antiparticles have opposite intrinsic parity. In fact $\eta_p=+1$ for electrons and $\eta_p=-1$ for positrons.

On the other hand, the CPT theorem [223–225] ensures that every relativistic Quantum Field Theory is invariant under a simultaneous change of particles to antiparticles ($\mathcal{C}$), reflection about some arbitrary point in space ($\mathcal{P}$) and the reverse of the direction of time ($\mathcal{T}$). In this case it is clear that $\mathcal{CPT}\boldsymbol{H}^{(0)}(\mathcal{CPT})^{-1} = \overline{\boldsymbol{H}}^{(0)}$. Since the space of states has been defined as the tensor product of the space of eigenstates of $\boldsymbol{H}^{(0)}$ times that of $\overline{\boldsymbol{H}}^{(0)}$, the $\mathcal{CPT}$ symmetry only permutes the order of the components in the tensor product. This swap keeps the total space unchanged, as was also the case for the charge conjugation symmetry. Notice that one could only talk about charge conjugation symmetry once the second quantisation over the relativistic quantum mechanical problem has been perform to study the corresponding QFT, in which the concept of particle and antiparticle is introduced.

Another interesting question in QFT is the computation of the quantum vacuum energy. The problem of a Dirac field confined in a finite interval $[-L/2, L/2]$ has been studied in [45, 226, 227]. The main conclusions of these works are going to be summarised in the first part of this section for completeness. Then, an original discussion regarding the system of a Dirac field propagating in the real line under the influence of delta potentials will be presented.

The Dirac Hamiltonian is not self-adjoint while restricted to square-integrable spinors defined in a finite interval, since there is a non zero flux of charge density[10] through the boundaries:

$$\langle \Psi, \boldsymbol{H}_D \Phi\rangle - \langle \boldsymbol{H}_D \Psi, \Phi\rangle \propto \left[\Psi^\dagger\left(\frac{L}{2}\right)\Phi\left(\frac{L}{2}\right) + \Psi^\dagger\left(-\frac{L}{2}\right)\Phi\left(-\frac{L}{2}\right)\right], \qquad \forall \Psi, \Phi \in L^2\left(\left[-\frac{L}{2}, \frac{L}{2}\right]\right).$$

But $\boldsymbol{H}_D$ admits an infinite set of self-adjoint extensions in one-to-one correspondence with local unitary operators related to the boundary conditions. Hence, the domain of the self-adjoint extensions is the set of square-integrable spinors in $[-L/2, L/2]$ that satisfy the following boundary conditions for their two components:

$$\psi_1\left(-\frac{L}{2}\right) = (-1)^r e^{i(\alpha\pm\theta)}\psi_2\left(-\frac{L}{2}\right), \qquad \psi_1\left(\frac{L}{2}\right) = (-1)^r e^{i(\alpha\mp\theta)}\psi_2\left(\frac{L}{2}\right), \qquad r = 0, 1. \tag{5.62}$$

Here α, θ are the parameters of the unitary matrix U, written as in (1.25). These boundary conditions make the flow of charge density at the boundaries to vanish. So it is clear now that the unitarity of the QFT translates into a charge conservation for the Dirac field in the finite interval. It is interesting to note that the self-adjoint extension of the Dirac operator that represents the interaction of the quantum field with the boundary is given by the general M.I.T. bag boundary condition[11](see [230–232] and references therein).

[10]Notice that for fermions $\psi^\dagger\psi$ must be understood as a charge density distribution whereas for bosons $|\psi|^2$ is a probability density one. The physical meaning of the same quantity in both theories is completely different.

[11]The M.I.T. bag model was proposed by A. Chodos, R. L. Jaffe, K. Johnson, C.B. Thorn and V. Weisskopf [228] to study the confinement of quarks in the hadron model. This bag is a classical spherical cavity with quarks and gluons moving freely but confined inside it. There is no field outside the bag, i.e. there are no exterior modes. This confinement gives rise to the Casimir effect. Inside the bag $(\gamma\frac{1}{i}\partial)G(x,x') = \delta(x-x')$ is fulfilled. The bag b.c. satisfied on the surface of the spherical shell of radius a is given by $(1 + i\vec{r}\gamma)G(x,x')|_{r=a} = 0$. For planar configurations in which one considers fermion fields moving in one finite dimension between two parallel plates, the bag condition is expressed as $in^\mu\gamma_\mu\Psi = \Psi$ being $n^\mu = (0, \vec{n})$ the normal vector to the surfaces of the plates and directed to the interior of the slab configuration. For massive fermions, the planar chiral bag b.c. is obtained from (5.63) by setting $\alpha = -\pi/2$ and $\theta = 0$ [229].

The spectrum of normal modes can be obtained from (5.62) by assuming a linear combination of plane-wave spinors as a solution. Hence, in an analogous way to the one described in Chapter 2 for bosons, one reaches the spectral function:

$$h_U(k) = \left(\sqrt{m^2+k^2}\,\cos\alpha + m\cos\theta\right)\sin(kL) - k\sin\alpha\cos(kL). \tag{5.63}$$

The real zeroes of the spectral function correspond to propagating modes. Furthermore, for massive fermions, there are localised edge states[12] arising as solutions of $h(i\kappa) = 0$, $0 < \kappa < m$. But they do not contribute to the vacuum energy since $\omega = 0$ for all of them. In fact, the quantum vacuum energy can be computed by using the Cauchy's theorem of complex analysis as:

$$E_0 = -\sum_{k\in\mathbb{R}^+} 2\,\sqrt{m^2+k^2}\Big|_{h(k)=0} = \oint_C \frac{i\,dk}{\pi}\,\sqrt{m^2+k^2}\,\partial_k \log h_U(k), \tag{5.64}$$

where the minus sign in the first equality has been added due to the negative energy of the Dirac sea, and the factor 2 comes from the fact that positrons and electrons contributes in the same way to the summation over the spectrum. In [45] the contour C is chosen as a semiring of inner radius m and outer infinite radius with $Re(k) > m$, but E_0 can be also computed by using the contour described in Figure 3.8. Regarding the sign of the Casimir energy, only parity invariant self-adjoint extensions of the 1D Dirac operator, i.e. those that verify $U^\dagger = U$ and consequently $\alpha \pm \theta = \pi\mathbb{Z}$, produce changes in the sign of the quantum vacuum energy (for more details see [45]), as shown in Figure 5.12.

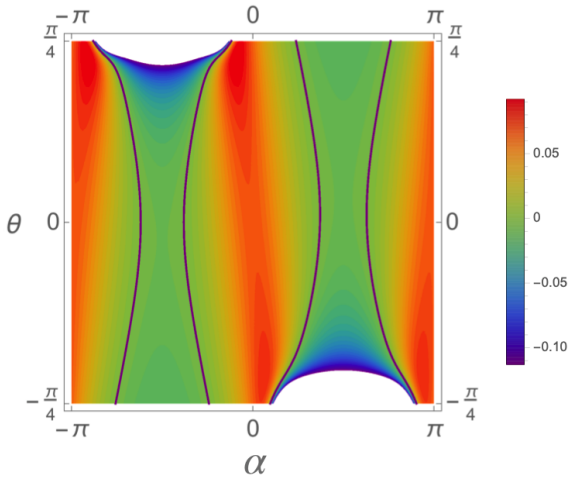

FIGURE 5.12: Plot from [45] that represents $2E_0/(me^{-2mL})$ for heavy fermions (with $mL = 20$) as a function of the self-adjoint parameters θ, α. The solid line corresponds to $E_0 = 0$.

Once presented the main bibliographic results, at this stage the new objective for future work is to extend this method to compute the Casimir force for a system of fermions under the influence of two general Dirac delta potentials. It can be understood as the fermionic version of Chapter 2, but for the specific potential given by (5.1). And whatsmore, once this system was studied, it would be straightforward to generalise it to fermions propagating in general Dirac delta-type lattices, in a analogous way to that described in Chapter 3.

[12] For massless fermions there are no localised states in the spectrum.

A review of the results of [45] for a fermionic field confined between plates mimicked by any unitary matrix such that $[U, \alpha] = 0$ (with α the matrix present in the free Dirac equation (5.2)), has been presented thus far. In [45] the authors only consider opaque plates placed at $z = 0, L$, so that fields live between them in the finite interval $[0, L]$. In that case, in order for the Hamiltonian to be self-adjoint, one has to impose boundary conditions at the extremal points of the interval that guarantee that the probability flux across the boundaries is zero. These boundary conditions are represented by unitary matrices. This is the fermionic version of what has been done in Chapter 2. However, the physical problem consider here in Chapter 5 is quite different, because the field also lives outside the finite interval $[0, L]$. The boundary condition matrix (5.13), introduced in this chapter to characterise the domain of the self-adjoint extension of the Dirac operator, is not unitary for any value of q and λ. In fact $T(q, \lambda)$ is only unitary in two cases providing $q > \lambda$:

1. If $\lambda = 0$ and $q = \pi$. It can be checked that $[T(\pi, 0), \sigma_1] = 0$. Hence, in this case T can be parametrised as (1.25) with $\alpha = \pi$, $n_1^2 + n_2^2 + n_3^2 = 1$ and $\theta = 0$. The formalism developed in [45] can be applied and one could obtain the following spectral function from (5.63):

$$h(k) = (-\sqrt{m^2 + k^2} + m)\sin(2ka).$$

   From this point one could compute E_0 by using the equation (5.64), and by subtracting the divergences in a similar way that the one explained in Chapter 2 . The numerical result is positive and it can be seen at the points $\alpha = \pi, \theta = 0$ in Figure 5.12 for heavy fermions such that $p^{-1} = ma = 10$.

2. If $q_r = \sqrt{\lambda^2 + \pi^2 r^2}$ being $r \in \mathbb{Z} - \{0\}$. It is easy to show that $[T(q_r, \lambda), \sigma_1] = 0$. Now the boundary condition parameters are $\alpha = \pi, \theta = n_1 = n_2 = 0, n_3 = 1$ if r is an odd number. If r is even, then $\alpha = \theta = n_1 = n_2 = 0, n_3 = 1$. The resulting spectral functions (5.63) for the two cases just mentioned now take the form:

$$h(k) = (\mp\sqrt{m^2 + k^2} + m)\sin(2ka).$$

   E_0 is positive as shown in Figure 5.12 for these specific values of α, θ for heavy fermions such that $p^{-1} = ma = 10$.

These two cases are essentially analogous to one presented for bosons in Chapter 2, when the boundary conditions mimicking the plates are Dirichlet ones. In that particular case, the plates became physically opaque and fluctuation propagation was restricted to the compact space between plates. Thus, the spectrum was discrete and E_0 could be computed by using complex integrals over contours which enclose the set of zeroes of the spectral function. This is also the key point used in [45]. However, when the boundary condition $T(q, \lambda)$ is not unitary, the method explained in Chapter 2 and used in [45] can no longer be applied. It would be necessary to approach the problem from other perspectives that go beyond the limits of this thesis.

The computation of the quantum vacuum energy can also be approached by the method of Green's functions. Either the relativistic free particle Green's function and the one for a fermion in the pure

electric background potential $V(z) = [-A\delta(z) - B\delta(z-b)]\mathbb{1}$ have been developed in [233, 234]. The Green's function solution of the equation

$$[-i\gamma^2\partial_z + m\gamma^0 + V(z) - \omega\mathbb{1}]G^\delta_\omega(z_1, z_2) = \delta(z_1 - z_2)\mathbb{1}$$

for the generic potential (5.11) is a 2×2 matrix which can be determined by means of

$$\begin{aligned} G^\delta_\omega(z_1,z_2) &= \frac{1}{W[\Psi^R_\omega, \Psi^L_\omega]}\left[\theta(z_1-z_2)\Psi^R_\omega(z_1)(\gamma^0\Psi^L_\omega(z_2))^t + \theta(z_2-z_1)\gamma^0\Psi^R_\omega(z_2)(\Psi^L_\omega(z_1))^t\right] \\ W[\Psi^R,\Psi^L] &= i\left(\Psi^R_1(z_1)\Psi^L_2(z_1) - \Psi^R_2(z_1)\Psi^L_1(z_1)\right) \neq W[\Psi^R,\Psi^L](z_1) \end{aligned} \tag{5.65}$$

by using the scattering solutions collected in Section 5.2. Notice that the subindex 1, 2 refers to the component of the spinor. This novel result and its application to the study of other magnitudes as the Casimir effect between two plates mimicked by the potential (5.39) in the fermionic context is work still in progress. Notice that, the solution of $\boldsymbol{H}_D\Psi_\omega(z) = \omega\Psi_\omega(z)$ can also be expressed from this point as

$$\Psi(z_1) = \int_{-\infty}^{\infty} V(z_2)G(z_1,z_2)\Psi(z_2)dz_2.$$

On the other hand, in [234] the relativistic Green's function has been used to compute the spinor solution of the Dirac equation in the background periodic potential $V(z) = U_0\sum_{n=-\infty}^{\infty}\delta(z-na)\mathbb{1}_2$ with $U_0 > 0$. This study is similar to the one performed for bosons in Chapter 3, and it will be the starting point for the generalisation of the results presented in this part of the thesis to the case of fermions propagating along lattices. It leaves further work to be done in this direction.

This chapter cannot end without briefly mentioning what happens when studying fermionic system similar to the ones presented so far but in higher dimensions. Firstly, in the presence of a magnetic field, the simplification $V_1(z) = 0$ done to define the potential (5.9) no longer applies. Secondly, Dimock [235] and Jackiw [236] stated that *three-dimensional δ interaction in Schrödinger theory are the formal non relativistic limit for the scalar field ϕ^4 self-interactions of relativistic QFT in (3+1) dimensions*. Jackiw also defined two and three dimensional δ interactions in Paper I.3 of [236] as the self-adjoint extension of a Hamiltonian over the space with a point removed. Remember that for scalar fields the Fourier transform of the eigenfunctions which are solutions of the corresponding spectral problem

$$\left[-\frac{d^2}{d(z^1)^2} - \frac{d^2}{d(z^2)^2} - \cdots - \frac{d^2}{d(z^n)^2} + m^2 + g\delta(z^1)\delta(z^2)\ldots\delta(z^n)\right]\psi_\omega(z^1,\ldots,z^n) = \omega^2\psi_\omega(z^1,\ldots,z^n)$$

involves ultraviolet divergent integrals [54, 236]. However they can be regularised by using a cut-off in the momentum, or by defining a coupling which includes this divergence and enables to solve the scattering problem. On the contrary, for fermionic systems the equation of motion are linear in the momentum rather than quadratic as in the scalar case. Then all the divergences are one order of magnitude smaller. Hence, the Fourier transform of the field might not be divergent but add a non-physical but finite quantity which would have to be renormalised. I would like to thank Prof. J. Mateos Guilarte for the stimulating discussions in this regard, in particular, for explaining to me his formulas (5.65), which are a result not previously found in the literature. There is still a lot of promising future work to be done regarding this analysis.

Chapter 6

CONCLUSIONS

In this last chapter the main conclusions regarding the results already explained in previous chapters would be summarised to present an overall view of the work carried out. The conclusions are arranged in chapter order.

- Concerning the study of a massless complex scalar field confined between $(D-1)$-dimensional plates mimicked by the most general type of lossless and frequently independent boundary conditions allowed by the unitarity of the QFT, some thermodynamic quantities (vacuum energy and total Helmholtz free energy, entropy, Casimir force) have been determined both in the cases of non zero and zero temperature. A new formula independent of the regularisation length for the quantum vacuum interaction energy between plates at zero temperature has been obtained. Furthermore this formula allows to classify the subdominant divergences of the theory as a function of the algebraic invariants of the unitary matrix that defines the self-adjoint extension of the Laplacian operator.

  One of the main conclusions of this analysis is that there exists a change in the sign of the Helmholtz free energy and the Casimir pressure between plates for non zero temperatures under different critical values $T_c^{\mathcal{F}}, T_c^{P}$. These critical values of the temperature enable to distinguish the regime in which the thermal fluctuations are the dominant ones in the system (for $T > T_c$) from the regime in which the quantum vacuum fluctuations are the leading contributions (for $T < T_c$). And furthermore, by analysing the Casimir pressure between plates, one can learn that the well-known theorem of *opposites attract* of Kenneth and Klich only holds for the boundary conditions that preserve $\mathbb{Z}_2$ symmetry within the quantum vacuum fluctuations dominated regime.

  Another relevant feature is that the one loop quantum correction to the entropy is positive definite for any boundary condition and any temperature, as expected. Consequently, the system is always thermodynamically stable.

  The third central outcome which is worth stressing is that if the boundary conditions are very close to the ones with zero mode $U \in \mathcal{M}_F^{(0)}$ at a given finite non zero temperature, the standard bibliographic result for the low temperature approximation of the Helmholtz free energy is not valid and needs to be refined. A logarithm correction to the dominant contribution of

the zero mode fits much better to the real data for the total Helmholtz free energy in this low temperature regime ($LT \ll 1$) for boundary conditions in $\mathcal{M}_F - \mathcal{M}_F^{(0)}$ but very close to $\mathcal{M}_F^{(0)}$, (i.e. when $k_0/T \ll 1$ being k_0 the lowest frequency of the field modes). This new scale k_0/T, not considered before in the specialised references, makes it possible to determine how low the temperature is at a fixed distance between plates and how close the spectrum is to that of zero-mode extensions.

On the contrary, the high temperature approximation of the Helmholtz free energy only depends on the high energy part of the one-particle states spectrum. The series expansion of $\mathcal{F}$ can thus be expressed in terms of a product of the heat kernel coefficients associated to the Laplacian operator in $\mathbb{R}^2$ without boundaries times the heat kernel coefficients for the Laplacian operator in $[0, L] \in \mathbb{R}$.

- The spectra of allowed energy bands and forbidden gaps for crystals, built as the superposition of individual potentials placed at the lattices nodes with compact support smaller than the lattice spacing, have been determined with complete generality. To this effect, the spectrum of modes for the phonons confined in the primitive cell interacting with the individual potential centred at the middle of this interval has been solved. The values of the coefficients of the Dirac δ potential and its first derivative establish whether there are or not negative energy bands in the spectrum of the generalised Dirac comb. On the contrary, the Pöschl-Teller chain always has a negative energy band for certain values of the quasi-momentum of the first Brillouin zone, independently of either the magnitude of the compact support of the individual potential and the value of the lattice spacing. In both types of lattices there are always bands of positive energies. Determining whether or not there are states with negative energy is fundamental when promoting the theory from non-relativistic quantum mechanics to Quantum Field Theory. For those lattices with negative energy bands, a mass must be introduced to ensure unitarity in the associated QFT.

  The comb can be interpreted as a piston whose middle membrane is a single individual potential seated at the center of the interval defined by the unit cell, and whose external walls correspond to a family of self-adjoint extensions of the Laplacian operator. This family is in one-to-one correspondence with a one-parameter family of Floquet-Bloch quasi periodic boundary conditions applied at the endpoints of the unit cell. Under this new interpretation, it is clear that the problem of phonons propagating along a squared two dimensional lattice with Bloch periodicity on its edges is essentially the same as the problem of a scalar field moving on the surface of a torus traversed by a magnetic flux (Aharonov-Bohm effect).

  The quantum vacuum energy E_0 of the comb has been computed by using the spectral zeta function regularisation method. As a result, one can realise that the zeta function of a comb is the continuous sum of zeta functions over the dual primitive cell of Bloch quasi-momenta. This is just the same as firstly summing over the discrete spectrum arising when considering

the field confined in the primitive cell and then, performing the summation over all the discrete spectra that build the whole allowed energy bands spectrum arising when the quasi momentum runs over the first Brillouin zone. The quantum vacuum energy at zero temperature thus calculated is the one loop quantum correction to the classical repulsive elastic forces produced by the quantum scalar field of the phonons. In the case of the generalised Dirac comb at zero temperature E_0 takes positive, negative and zero values depending on the parameters that characterise the lattice. Consequently, the quantum vacuum force can be attractive, repulsive or zero. This means that the lattice spacing can be decreased, increased or remain unchanged with respect to its classical analogue as a result of this quantum interaction. In contrast, E_0 is always positive for the Pöschl-Teller comb at zero temperature, so that the classical repulsive force between lattice nodes is enhanced.

The thermal correction to the quantum vacuum energy, the entropy and the Casimir force at finite non zero temperature has been derived in some convergent representations: the real frequencies one, the Matsubara representation of purely imaginary frequencies and another intermediate one. This last representation has not been developed so far. Its major advantage is that turning the integration contour towards the imaginary axis by a finite angle in the complex plane of frequencies avoids large oscillations of the Boltzmann factor. Positive corrections to the entropy appear for both the generalised Dirac comb and the Pöschl-Teller one at finite non zero temperature. This fact means that the classical analogue system is more stable than the quantum one. On the other hand, the Casimir force between the lattice nodes is always repulsive for both chains when non-trivial temperatures are considered, implying that the primitive cell increases its size due to the quantum interaction of the phonon field. These results have been generalised to three-dimensional lattices and qualitatively the same results have been obtained.

- In the fourth chapter, a quantum scalar field in a system of two parallel two dimensional plates mimicked by Dirac δ-potentials in a curved background of a topological Pöschl-Teller kink at zero temperature is presented. The quantum vacuum fluctuations around the kink solution could be interpreted as a scalar field in the spacetime of a domain wall. The main problem of working in curved spacetimes is that if it is not globally hyperbolic with a global Killing vector, it is not possible to foliate it in spatial Cauchy surfaces for each fixed temporal coordinate. Hence, it will not always be possible to give an interpretation of the spectra in terms of particles independently of the observer. Therefore T_{00}, the transfer operator T and the scattering data needed to compute E_0 will not be universal results, as happens in flat spacetimes. For general curved spacetimes, the quantum vacuum energy must be computed by using zeta regularisation and spectral functions of the Laplacian operator. However, it has been understood that for weak gravitational backgrounds in which the frequencies of the particles created by the gravitational background are much smaller than the Planck frequency, the perturbation theory can be used to treat this background classically so that the matter fields are the ones which will be quantised, and not the gravity itself. Furthermore, when the background potential is transparent, in the sense that the fields could be asymptotically interpreted as particles, it is possible

to define incoming and outgoing waves and the usual S-matrix as done in previous chapters for flat spacetimes. Under all these conditions, a generalisation of the *TGTG* formula for such a curved spacetime has been found.

One of the relevant characteristics of the configuration of the open system of two plates in a Pöschl-Teller background is that the translational symmetry is broken and the space is anisotropic. This translates into the fact that the scattering coefficients, as well as the Green's function, will depend on the position of the plates in a non-trivial way. The wave functions of the continuous spectrum of states with positive energy have been characterised by means of the scattering data. The bound states have also been studied, setting a threshold for the minimum negative energy in the system. The unitarity of the QFT requires this lower bound be fixed as the mass of the quantum vacuum fluctuations so that the total energy of the lowest energy state of the spectrum will be zero, making fluctuations absorption impossible.

The quantum vacuum interaction energy has been calculated using a generalisation of the *TGTG* formula, which only depends on the reflection coefficients associated to the scattering problem and the analogous of the plane waves in flat spacetimes but for the specific curved background potential chosen. The quantum vacuum energy thus depends on the parameters describing the potentials and on the distance from the plates to the centre of the kink. For obtaining the quantum vacuum energy, it has been necessary to compute the Green's functions from the scattering data. The transfer matrix has been determined with complete generality too, in terms of the Green's function. Although the *TGTG* formula has the advantage that it depends only on the scattering data of one of the plates and it is not necessary to solve the scattering problem of the whole system, the well-known DHN formula has also been derived.

It is worth highlighting that the quantum vacuum energy for this 3+1 dimensional problem is always negative, independently of the value of the coefficients of the delta potentials and its location in relation to the kink centre. This implies that the Casimir force between plates will always be attractive in this system. Furthermore, even in the case where there is only one plate in the system, the other plate feels the Casimir interaction because there is still a non zero quantum vacuum interaction energy in the system.

The thermodynamics of the system at finite non zero temperature have not been considered because when dealing with a weak gravitational field, the thermal fluctuations will be the dominant term, cancelling any characteristic trace of the curved space. As a consequence, the results of Chapter 2 as well as the conclusion drawn from them would be recovered.

- Finally, in the fifth chapter the spectrum of bound and scattering states of relativistic fermionic particles interacting with a double Dirac δ potential in 1+1 dimensions has been studied. The fermions propagating on the real line are interpreted as quanta emerging from the spinor fields. The objective is to study how the fluctuations of the spinor fields are distorted by a static background formed by two mass-spike and two electric Dirac δ potentials.

  The problem of determining the spinor field fluctuations in the static δ background has been

adressed by solving at the same time the spectral problem of either the Dirac Hamiltonian $\boldsymbol{H}_D$ and its conjugate $\tilde{\boldsymbol{H}}_D$ in one-dimensional relativistic quantum mechanics. The eigenspinors of both Hamiltonians have been interpreted as the one particle states with positive energy to be occupied by electrons and positrons after the fermionic second quantisation procedure be implemented. It has also been proved that the boundary condition matrix which represents the δ potential is parity and time-reversal invariant but it is not charge-conjugated invariant for the specific choice of the representation of the Clifford algebra $\{\gamma^0 = \sigma_3, \gamma^1 = i\sigma_2, \gamma^2 = \sigma_1\}$.

Concerning the background mimicked by a single δ potential, the spectral problems have been completely solved for the generic potential given by the expression $V(z) = (q\mathbb{1} + \lambda\sigma_3)\delta(z)$. This problem has not been solved so far. The S-matrices have been built from the zurdo (L) and diestro (R) scattering transmission and reflection coefficients. They verify that $\sigma_L = \sigma_R$ and $\rho_L = \rho_R$ either for electrons and positrons, as expected. The bound states inside the gap $[0, m]$ have been characterised by computing its momentum $k = i\kappa(q, \lambda, m)$, with $\kappa > 0$. As examples, the method has been particularised to one single electric delta potential $V(z) = q\mathbb{1}\delta(z)$ and one single mass-spike delta potential $V(z) = \lambda\sigma_3\delta(z)$. In the first case, due to the angular periodicity present in the problem, there is one bound state in each quadrant alternating between the electron ones (second and fourth quadrants) and the positron ones (first and third quadrants). On the contrary, in the case of a mass-spike delta potential there is only one bound state for electrons regarding $\kappa = -m\tanh\lambda$ with $\lambda < 0$ and one for positrons whenever $\kappa = m\tanh\lambda$ with $\lambda > 0$. Both for the electric and the massive cases the scattering coefficients for electrons (σ, ρ) and positrons $(\tilde{\sigma}, \tilde{\rho})$ are related by means of the conditions $\sigma = \tilde{\sigma}^*$ and $\rho = -\tilde{\rho}^*$. The spinor wave functions have been determined in both cases as well as the associated charge density. It should be noted that since the charge density is a continuous function, the continuity equation is satisfied and the probability amplitude is preserved in the system.

Regarding the background mimicked by a double δ potential, the spectral problems have been completely solved for two particular cases, namely a double electric δ potential completely described by $V(z) = q_1\mathbb{1}\delta(z-a) + q_2\mathbb{1}\delta(z+a)$ an a double mass-spike δ potential given by $V(z) = \lambda_1\sigma_3\delta(z-a) + \lambda_2\sigma_3\delta(z+a)$. In the electric case, the transcendent equations for computing the momenta of the bound states have been completely determined. It has been possible to elaborate a map of the number of bound states (two, one or zero) and zero modes present in the problem for a specific choice of $\{q_1, q_2, p^{-1} = am\}$. Notice that this map would be crucial to build the associated QFT in future works. As a result, it has been understood that the biparametric family of theories indexed by the coefficients of the δ in the electric potential is in one-to-one correspondence with a subset of the moduli of complex torus or genus one algebraic curves. The topology of the torus is determined by the two angular coordinates given by q_1, q_2. The complex structure of the torus is completely characterised by p^{-1}, i.e. by the mass of the particles and the distance between the two electric δ potentials. For the massive case, the map of the number of bound states has been obtained as well as the transcendent equations for the corresponding momenta. It is of note that in this case, there could be one, two or zero bound states depending of the value of λ_1, λ_2 and p^{-1}, but there are no zero modes. It is also worth

stressing that either in the electric and the massive case, the S-matrices and the scattering data have been computed. For the massive case it has been proved that only if $\lambda_1 = \lambda_2$ the scattering process is parity invariant.

Lastly, it has been understood that only if $\lambda = 0, q \neq 0$ or $q_r = \sqrt{\lambda^2 + \pi^2 r^2}, r \in \mathbb{Z} - \{0\}$ the boundary condition matrix $T_\delta(q, \lambda)$ which defines the self-adjoint extension of the Dirac Hamiltonian is unitary. In these cases, which represent totally opaque plates, the formalism developed in [45] can be applied to compute the spectral function and the quantum vacuum energy for fermions confined in a finite interval.

Furthermore, while studying all the topics set out in this thesis some open questions have appeared. They will be stated here for future investigations:

1. Regarding the second chapter, it would be interesting to find an explanation for the fact that the maximum and minimum values of the one loop quantum correction to the entropy are reached at the more unstable and stable fixed points of the boundary renormalisation group flow (i.e. Dirichlet and Neumann boundary conditions, respectively).

   Another intriguing open question is wheter there exists or not a relation between the one loop quantum correction to the entropy due to vacuum fluctuations and the entanglement entropy. During my predoctoral stay at City University of London under the supervision of Dr. Olalla Castro Alvaredo, the excess entropy resulting from exciting a finite number of quasiparticles above the ground state of an integrable both bosonic and fermionic Quantum Field Theory with an internal U(1) symmetry has been computed [46, 47]. Since the entanglement entropy has been a very active field of research within theoretical physics due to its applications to quantum computation, interacting integrable quantum field theories, out of equilibrium many body systems or holographic settings, among many other topics, this question could open new attractive lines of research.

   The reason that the sign of the Casimir energy and pressure changes depending on the boundary conditions and the temperature has not been found so far. In other words, it is not possible at this moment to guess the sign of the Casimir pressure between plates in advance before performing the computation. Achieving this goal would be a great advance. Finally, there is another aspect of this problem that is still outstanding: the characterisation of self-adjoint extensions which have negative energy states depending on the value of the distance between plates. How QFT would be built in these cases could be considered in future work.

2. Concerning the study of quantum scalar fields propagating along lattices, the computation of the Green's function is left for further investigations. From it one can obtain the vacuum expectation value of T_{00}, which provides much more information than computing the total quantum vacuum energy.

   It would be also an interesting new line of research to consider some type of smooth interactions between phonons and electrons in the lattices since the realistic material are made of electrons.

In this case the spin statistics properties must be taken into account.

Once more, there is not a general rule for guessing the sign of the one loop quantum corrections to the entropy in QFTs under the influence of classical backgrounds and much work in this direction is necessary. In addition, continuing the line of research to find out whether there is some kind of crystal built from compact support potentials for which quantum corrections to the classical entropy are negative could be engaging.

Moreover, the study of the one loop quantum corrections to the frequency of the phonons propagating along lattices can be used to discuss the stability of some hypothetical solutions regarding the vacuum state in quantum chromodynamics. Whenever theories which describe in a sufficiently rigorous way the coupling between the axion fluctuations and the QCD vacuum state can be found, the methods provided in this chapter could be useful.

3. Once the quantum vacuum interaction energy between plates in the curved background of a sine-Gordon kink has been computed by using the *TGTG* formula, it would be enlightening to obtain the same result but from the integration of the T_{00} component. In this way one could also study the spatial distribution of the energy density.

   On the other hand, determining a metric for a curved spacetime so that the equation describing the dynamics of the quantum vacuum fluctuations around the kink solution in flat spacetime be the equation of motion for a scalar field coupled to the gravitational background of a domain wall, will be a nice task to tackle in future works.

   The generalisation of the *TGTG* formula presented in this thesis to other type of configurations, either for another curved background potential and for other potentials that could properly mimic the plates, is straightforward. For instance, studying whether the introduction of two plates mimicked by $\delta\delta'$ potentials in the Pöschl-Teller background yields changes on the sign of the Casimir interaction between plates, is an intriguing and promising project in progress right now.

4. The quantum vacuum energy for fermionic fields either confined between plates mimicked by general δ-potentials and propagating in δ-lattices has not been studied so far. Taking into account the characterisation of the spectrum of modes for fermionic fields confined between plates presented in this thesis and the analysis of the self-adjoint extensions of the Dirac operator given in [45], the study of Dirac fields in the aforementioned QFTs can be pursued further. This is a relevant topic in Condensed Matter Physics due to the edge states which appear in meta materials that can be mimicked by these type of theories. It would be also enriching to solve the spectral problem for the completely generic potential given by the expression

$$V(z) = (q_1\delta(z-a) + q_2\delta(z-b))\mathbb{1} + (\lambda_1\delta(z-a) + \lambda_2\delta(z-b))\beta,$$

being $a, b \in \mathbb{R}$ and not only for the pure double electric δ or pure double massive δ potentials where the impurities are placed symmetrically with respect to the origin.

One could also calculate the Green's function for fermions confined between plates modelled by general delta potentials and try to redo the results for higher spatial dimensions.

5. The study of the quantum vacuum interaction energy between other extended objects such as monopoles and skyrmions in the *BPS limit* will be taken up later on. In this limit, the objects are sufficiently far apart and the waves of very low frequency will be the dominant contribution of the quantum fluctuations due to the interaction between objects. These waves have wavelengths of the order of the distance between the objects. If the bodies are far apart, the wavelength of the fluctuations is larger than the dimension of the objects and they can be considered as point-like, which makes it easier to study them.

6. Finally, some of the open problems aforementioned could also be studied in 2+1 dimensional systems. Therefore, structures such as graphene, whose treatment plays an important role nowadays in Condensed Matter Physics, could be modelled. Moreover, the conformal symmetry present in these two dimensional theories could play a relevant role, giving rise to novel results different from those obtained in QFTs in one and three spatial dimensions.

As a way to close this chapter, the ultimate conclusion that studying the spectrum of the quantum fluctuations of fields in the vacuum state interacting with other external classical fields is essential to obtain relevant parameters that characterise extended structures in 1+1 and 3+1 dimensional QFTs makes now more sense due to the strong analytical and numerical evidences shown, in spite of the open questions mentioned along this last chapter. Moreover, there is still a lot of promising work to be done regarding other extensions of this analysis, which is left for future investigations.

Appendix A

HEISENBERG GROUP

The Heisenberg group H [53, 237–240] can be defined as :

$$H \equiv \left\{ A \in GL(3,\mathbb{R}) \,|\, A = \begin{pmatrix} 1 & a & b \\ 0 & 1 & c \\ 0 & 0 & 1 \end{pmatrix}, \quad a,b,c \in \mathbb{R} \right\}.$$

Its Lie algebra $\mathfrak{h}$ is given by:

$$\mathfrak{h} \equiv \left\{ X \in \mathfrak{gl}(3,\mathbb{R}) \,|\, X = \begin{pmatrix} 0 & \alpha & \beta \\ 0 & 0 & \gamma \\ 0 & 0 & 0 \end{pmatrix}, \quad \alpha,\beta,\gamma \in \mathbb{R} \right\}. \tag{A.1}$$

Hence, $e^X \in H$ if X is strictly upper triangular. A basis of $\mathfrak{h}$ is built by the following matrices:

$$\left\{ X = \begin{pmatrix} 0 & 1 & 0 \\ 0 & 0 & 0 \\ 0 & 0 & 0 \end{pmatrix}, \quad Y = \begin{pmatrix} 0 & 0 & 0 \\ 0 & 0 & 1 \\ 0 & 0 & 0 \end{pmatrix}, \quad Z = \begin{pmatrix} 0 & 0 & 1 \\ 0 & 0 & 0 \\ 0 & 0 & 0 \end{pmatrix} \right\},$$

with commutation relations:

$$[X,Y] = Z, \quad [X,Z] = 0, \quad [Y,Z] = 0. \tag{A.2}$$

The above relations have the same form as the canonical commutation relations between the position and momentum operators in quantum mechanics[1]:

$$[\hat{X},\hat{P}] = i\mathbb{I}, \quad [\hat{X},i\mathbb{I}] = 0, \quad [\hat{P},i\mathbb{I}] = 0. \tag{A.3}$$

[1]Notice that the realisation (A.1), (A.2) for the Heisenberg algebra can be generalised to $2n+1$ dimensions for theories in classical mechanics in which there are n generalised coordinates and n generalised momenta, apart from the temporal coordinate.

Since H is a simply connected group, there is a natural one-to-one correspondence between the representations of H and the representations of its algebra $\mathfrak{h}$. The non trivial irreducible unitary representation of H is the group of unitary operators $U_H = \{\Pi_\hbar(A)|A \in H\}$ acting in $L^2(\mathbb{R})$ which are generated by translations in the space (described by the parameter a) and translations in the Fourier space (described by the parameter c), i.e.:

$$\Pi_\hbar(A)f(x) = e^{-ib}e^{icx}f(x-a), \quad \forall f \in L^2(\mathbb{R}). \tag{A.4}$$

The overall phase involving the parameter b is necessary to obtain a group of operators, since the translations in the position space and in the momentum space do not commute.

The Stone-von Neumann theorem [241] states that there is, up to isomorphism, a unique irreducible unitary representation of H in which its centre acts non-trivially:

Theorem A.0.1 (Stone-von Neumann's theorem) *Let $U(t)$ and $V(s)$ be two strongly continuous one-parameter groups on a Hilbert space $\mathscr{H}$ that satisfy*

$$U(t)V(s) = e^{its}V(s)U(t), \quad \forall t, s. \tag{A.5}$$

Then there is a Hilbert space $\mathscr{N}$ and a unitary map $\mathscr{R}$ from $\mathscr{H}$ onto $L^2(\mathbb{R}, \mathscr{N})$ so that $\mathscr{R}U(t)\mathscr{R}^{-1}$ is a translation to the right by t units and $\mathscr{R}V(s)\mathscr{R}^{-1}$ is a multiplication by $e^{-i\lambda s}$.

The relation (A.5) is called the Weyl form of the canonical commutation relations. The theorem ensures that, for a finite number of degrees of freedom, there is a one-to-one correspondence between two self-adjoint operators acting on separable Hilbert spaces and satisfying canonical commutation relations of the type (A.3) and the one-parameter unitary groups generated by means of e^{itX}, e^{isP}. Consequently, these two groups are unitarily equivalent and there is a unitary operator $W : L^2(\mathbb{R}) \to \mathscr{H}$ so that

$$W^*U(t)W = e^{it\hat{X}}, \qquad W^*V(s)W = e^{is\hat{P}}.$$

Thus, the elements of the algebra $\mathfrak{h}$ are equivalent to the position and momentum operators in quantum mechanics. This unique representation has several equivalent realisations: the Schrödinger model (if H acts on the space of square integrable functions as defined in (A.4)), the Heisenberg model or the theta representation, among others [242, 243].

The Schrödinger representation ρ_s is physically interesting because it is an infinite dimensional representation on functions of the complexified coordinates (or the momenta in the phase space) for which the Lie algebra is given by the usual $\{\hat{Q}, \hat{P}, \mathbb{1}\}$ operators of quantum mechanics. Notice that $\forall \psi(q) \in L^2(\mathbb{R})$:

$$\begin{aligned}
\rho_s(X)\psi(q) &= -iQ\psi(q) = -iq\psi(q), \\
\rho_s(Y)\psi(q) &= -iP\psi(q) = -i\frac{d}{dq}\psi(q), \\
\rho_s(Z)\psi(q) &= -i\mathbb{1}\psi(q) = -i\psi(q).
\end{aligned} \tag{A.6}$$

The Fourier transform of (A.6) yields an equivalent representation in the momentum space which will depend on p instead of q. Moreover, with the representation of the algebra given by (A.6) and the exponential map, one can obtain a representation for the Heisenberg group. Another extremely useful representation is the Bargmann–Fock or Weyl representation. It arises when defining

$$a = \frac{1}{\sqrt{2}}\left(q + \frac{d}{dq}\right), \qquad a^\dagger = \frac{1}{\sqrt{2}}\left(q - \frac{d}{dq}\right),$$

which after quantisation becomes the creation and annihilation operators with commutation relation $[\hat{a}, \hat{a}^\dagger] = \mathbb{1}$. The Weyl representation can be realised in terms of differential operators with polynomial coefficients in n complex variables $z_1, z_2 \dots z_n$ and generators given by

$$a_k^\dagger = z_k, \qquad a_k = \frac{\partial}{\partial z_k}.$$

The importance of this representation given in terms of $\{1, z, \bar{z}\}$ is that it diagonalizes the Hamiltonian operator for the quantum harmonic oscillator. The eigenvalues of the Hamiltonian will be interpreted as "quanta" of energy in the system. The operators on the state space (also called Fock space) of holomorphic functions could be expressed in terms of $a, a^\dagger$, which decrease or increase by one the number of quanta of energy of the harmonic oscillator. In contrast to the Schrödinger representation, the Weyl one has a distinguished state $|0\rangle$ corresponding to the constant function 1 and it can be thought of as the "vacuum" state.

Upon the second quantisation, when the concept of particle makes sense, the QFT can be interpreted as an infinite ensemble of non interacting harmonic oscillators. Thus the operators $a, a^\dagger$ destroy and create (respectively) particles of energy ω in each oscillator or canonical ensemble. For flat spacetime, one can build the Fock space of a quantum scalar field theory as the tensor product of infinite copies of the unitary representation of the Heisenberg group. The resulting reducible representation could be decomposed in the direct sum of the unique irreducible unitary representation

$$\otimes_{n=1}^{\infty} U_H = \oplus_{n=1}^{\infty} U_H,$$

since $[\hat{H}, \exp(\Pi_\hbar(A))] = 0$. Hence, each eigenspace of the Hamiltonian is an irreducible representation corresponding to a canonical set of particles. The quantum theory of a free particle uses the representation of the Heisenberg Lie algebra in terms of the operators $\hat{Q}, \hat{P}$ and the Hamiltonian $\hat{H} = \hat{P}^2/2m$. Due to the uniqueness of the representation of the Heisenberg group, several non trivial quantum systems will be characterised by using the same representation as the one for the free particle.

Appendix B

DERIVATION OF THE DHN FORMULA

The Dashen-Haslacher-Neveu formula [123] yields the contribution to the zero-point energy of the system of either the continuous and the discrete part of the spectrum of a Schrödinger operator $\hat{K}$. The Casimir energy between a pair of two-dimensional plates in the background of a kink is the summation over the frequencies $\omega = \sqrt{\vec{k}_{\parallel}^2 + k^2 + m^2}$ of the field modes spectrum:

$$\frac{E_0}{A} = \frac{1}{2} \sum\!\!\!\!\!\!\int_k \int_{\mathbb{R}^2} \frac{d\vec{k}_{\parallel}}{(2\pi)^2} \sqrt{m^2 + k^2 + \vec{k}_{\parallel}^2}.$$

This result is divergent due to the contribution of the energy density of the free theory in the bulk and the self-energy of the plates. As a consequence, it is necessary to introduce a regulator. For instance, one could introduce an exponentially decaying function and perform the integration over the parallel modes:

$$\begin{aligned} \frac{E_0}{A} &= \lim_{\epsilon \to 0} \frac{1}{2} \sum\!\!\!\!\!\!\int_k \int_{\mathbb{R}^2} \frac{d\vec{k}_{\parallel}}{(2\pi)^2} \sqrt{m^2 + k^2 + \vec{k}_{\parallel}^2}\, e^{-\epsilon \vec{k}_{\parallel}^2} = \lim_{\epsilon \to 0} \frac{1}{2} \sum\!\!\!\!\!\!\int_k \int_0^{\infty} \frac{dk_{\parallel}}{2\pi} k_{\parallel} \sqrt{m^2 + k^2 + k_{\parallel}^2}\, e^{-\epsilon k_{\parallel}^2} \\ &= \lim_{\epsilon \to 0} \frac{1}{2} \sum\!\!\!\!\!\!\int_k \frac{1}{2\pi} \left(\frac{\sqrt{\pi}}{4\epsilon^{3/2}} + \frac{\sqrt{\pi}(m^2 + k^2)}{4\sqrt{\epsilon}} - \frac{(m^2 + k^2)^{3/2}}{3} + o(\sqrt{\epsilon}) \right) = -\frac{1}{2} \sum\!\!\!\!\!\!\int_k \frac{(m^2 + k^2)^{3/2}}{6\pi}. \end{aligned}$$

Notice that in the final step, the terms proportional to $\epsilon^{-3/2}$ and $\epsilon^{-1/2}$ have been removed to eliminate the contribution of the parallel modes to the dominant and subdominant divergences, respectively. Now, it is necessary to proceed in the same way but for the modes in the orthogonal direction, where the one-dimensional kink lives. The divergences in the orthogonal direction would be different from the ones in the parallel directions, because now the space is not longer a free one. When putting the system in a very large box of length L with periodic boundary conditions (p.b.c.) on its edges, the spectrum becomes discrete. In the orthogonal direction one has to solve the problem:

$$\left[-\partial_z^2 - 2\,\mathrm{sech}^2(z) + v_0 \delta(z - a) + v_1 \delta(z - b) \right] \psi(z) = k^2 \psi(z),$$

with the boundary conditions:

$$\psi\left(-\frac{L}{2}\right) = \psi\left(\frac{L}{2}\right), \qquad \psi'\left(-\frac{L}{2}\right) = \psi'\left(\frac{L}{2}\right).$$

The ansatz is a linear combination of the scattering solutions (4.5), (4.6):

$$\psi(z) = B_1\psi_k^R(z) + B_2\psi_k^L(z).$$

When imposing the periodic boundary conditions over the above ansatz, a matrix system of equations arises:

$$\begin{pmatrix} -f_{-k}\left(\frac{L}{2}\right) - f_k\left(\frac{L}{2}\right)(t+r_R) & -f_{-k}\left(\frac{L}{2}\right) - f_k\left(\frac{L}{2}\right)(t+r_L) \\ f'_{-k}\left(\frac{L}{2}\right) + f'_k\left(\frac{L}{2}\right)(-t+r_R) & -f'_{-k}\left(\frac{L}{2}\right) + f'_k\left(\frac{L}{2}\right)(t-r_L) \end{pmatrix} \begin{pmatrix} B_1 \\ B_2 \end{pmatrix} = 0.$$

This system admits a solution whenever the determinant of the above matrix be zero, giving rise to a spectral equation:

$$\begin{aligned} h_{p.b.c.}(k,L) \equiv \; & (r_R + r_L)\left[f_{-k}\left(\frac{L}{2}\right) f'_k\left(\frac{L}{2}\right) + f_k\left(\frac{L}{2}\right) f'_{-k}\left(\frac{L}{2}\right)\right] + 2tW \\ & -2(t^2 - r_R r_L) f_k\left(\frac{L}{2}\right) f'_k\left(\frac{L}{2}\right) + 2f_{-k}\left(\frac{L}{2}\right) f'_{-k}\left(\frac{L}{2}\right) = 0. \end{aligned}$$

The zeroes of the secular function $h_{p.b.c.}(k,L)$ will be the frequencies of the modes over which one has to perform the summation to obtain the quantum vacuum interaction energy. Consequently, by using the residue theorem in complex analysis, as done in Chapter 2, one obtains:

$$-\frac{1}{2}\sum_{k\in Z(h_{p.b.c.})} \frac{(m^2+k^2)^{3/2}}{6\pi} = -\frac{1}{2}\oint_\Gamma \frac{dk}{2\pi i}\frac{(m^2+k^2)^{3/2}}{6\pi}\partial_k \log h_{p.b.c.}(k,L),$$

being Γ the contour represented in Figure 3.8, but in the case $\gamma = \pi/2$. Again, it is easy to prove that the integration over the circumference arc is zero in the limit $R \to \infty$. Hence, the integration over the whole contour Γ reduces to the integration over the straight lines $\xi_\pm = \pm i\xi + m$ with $\xi \in [0,R]$. Moreover, the dominant and subdominant divergent terms associated to the orthogonal modes must be subtracted as in (2.2):

$$\begin{aligned} -\frac{1}{2}\sum_{k\in Z(h_{p.b.c.})} \frac{(m^2+k^2)^{3/2}}{6\pi} = -\frac{1}{2}\lim_{L_0,R\to\infty}\int_0^R \frac{d\xi}{12\pi^2 i} \; & \left[(m^2+\xi_+^2)^{\frac{3}{2}}\left(L - L_0 - \partial_\xi \log\frac{h_{p.b.c.}(\xi_+,L)}{h_{p.b.c.}(\xi_+,L_0)}\right)\right. \\ & \left. -(m^2+\xi_-^2)^{\frac{3}{2}}\left(L - L_0 - \partial_\xi \log\frac{h_{p.b.c.}(\xi_-,L)}{h_{p.b.c.}(\xi_-,L_0)}\right)\right]. \end{aligned}$$

Performing the limits $L_0, R \to \infty$ yields the expression

$$\begin{aligned} & \frac{1}{2}\int_0^\infty \frac{d\xi}{12\pi^2 i}\left[-(m^2+\xi_+^2)^{\frac{3}{2}}\left(L - \partial_\xi \log h_{p.b.c.}(\xi_+,L) + \frac{1+3i\xi_+}{\xi_+(\xi_+ - i)}\right) + (m^2+\xi_-^2)^{\frac{3}{2}}\left(L - \partial_\xi \log h_{p.b.c.}(\xi_-,L) + \frac{1-3i\xi_-}{\xi_-(\xi_- + i)}\right)\right] \\ & + \frac{1}{2}\int_0^\infty \frac{d\xi}{12\pi^2 i}\left[(m^2+\xi_-^2)^{\frac{3}{2}} i2\frac{\partial\delta(\xi_-)}{\partial\xi}\right]. \end{aligned}$$

The results of the integration should not depend on the box size and consequently, one could study the limit $L \to \infty$. At this point and reversing the change of variable $\xi \to k$, the DHN formula (4.16) arises.

Appendix C

BOUND STATES AND SCATTERING FOR FERMIONS IN THE DOUBLE DELTA POTENTIAL

All along Chapter 5 the same pathway to solve the relativistic quantum mechanical problem has been followed, namely:

1. Imposing the matching conditions which define the self-adjoint extension of the Dirac operator over the ansatz of bound and scattering states either for electrons and positrons.
2. Obtaining the corresponding homogeneous linear systems where the unknowns are the coefficients of the ansatz for the spinor.
3. Computing the non trivial solutions of the systems. In the case of bound states, one also calculates the transcendent secular equation by equating the determinant of the associated matrix to zero.

Since the intermediate steps yield to cumbersome matrices, in order to lighten and simplify the reading, these systems are included in this appendix instead of in the main text.

C.1. Double mass spike contact interactions

In this section the following notation has been used:

$$f_{\pm}(\lambda_i,k)=\cosh(\lambda_i)\pm\frac{ik\sinh(\lambda_i)}{m+\sqrt{m^2+k^2}},\qquad g_{\pm}(\lambda_i,k)=\sinh(\lambda_i)\pm\frac{ik\cosh(\lambda_i)}{m+\sqrt{m^2+k^2}},\qquad i=1,2.$$

Electron bound states

$$Q=\begin{pmatrix} -e^{-a\kappa}f_-(\lambda_1,i\kappa) & e^{-a\kappa} & e^{a\kappa} & 0\\ i\,e^{-a\kappa}g_-(\lambda_1,i\kappa) & -\frac{i\kappa e^{-a\kappa}}{m+\sqrt{m^2-\kappa^2}} & \frac{i\kappa e^{a\kappa}}{m+\sqrt{m^2-\kappa^2}} & 0\\ 0 & -e^{a\kappa}f_-(\lambda_2,i\kappa) & -e^{-a\kappa}f_+(\lambda_2,i\kappa) & e^{-a\kappa}\\ 0 & ie^{a\kappa}g_-(\lambda_2,i\kappa) & ie^{-a\kappa}g_+(\lambda_2,i\kappa) & \frac{i\kappa e^{-a\kappa}}{m+\sqrt{m^2-\kappa^2}} \end{pmatrix}. \tag{C.1}$$

Positron bound states

$$P=\begin{pmatrix} e^{-a\kappa}f_+(\lambda_1,i\kappa) & -e^{-a\kappa} & e^{a\kappa} & 0\\ i\,e^{-a\kappa}g_+(\lambda_1,i\kappa) & \frac{i\kappa e^{-a\kappa}}{m+\sqrt{m^2-\kappa^2}} & \frac{i\kappa e^{a\kappa}}{m+\sqrt{m^2-\kappa^2}} & 0\\ 0 & e^{a\kappa}f_+(\lambda_2,i\kappa) & -e^{-a\kappa}f_-(\lambda_2,i\kappa) & e^{-a\kappa}\\ 0 & ie^{a\kappa}g_+(\lambda_2,i\kappa) & -ie^{-a\kappa}g_-(\lambda_2,i\kappa) & \frac{i\kappa e^{-a\kappa}}{m+\sqrt{m^2-\kappa^2}} \end{pmatrix}. \tag{C.2}$$

Electron scattering states

$$\begin{pmatrix} 0 & -e^{iak}f_-(\lambda_1,k) & e^{-iak} & e^{iak} \\ 0 & ie^{iak}g_-(\lambda_1,k) & \frac{e^{-iak}k}{m+\sqrt{m^2+k^2}} & -\frac{e^{iak}k}{m+\sqrt{m^2+k^2}} \\ e^{iak} & 0 & -e^{iak}f_+(\lambda_2,k) & -e^{-iak}f_-(\lambda_2,k) \\ \frac{e^{iak}k}{m+\sqrt{m^2+k^2}} & 0 & ie^{iak}g_+(\lambda_2,k) & ie^{-iak}g_-(\lambda_2,k) \end{pmatrix} \begin{pmatrix} \sigma_R^m \\ \rho_R^m \\ A_R^m \\ B_R^m \end{pmatrix} = \begin{pmatrix} e^{-iak}f_+(\lambda_1,k) \\ -ie^{-iak}g_+(\lambda_1,k) \\ 0 \\ 0 \end{pmatrix}, \tag{C.3}$$

$$\begin{pmatrix} ie^{iak}g_-(\lambda_1,k) & 0 & \frac{e^{-iak}k}{m+\sqrt{m^2+k^2}} & -\frac{e^{iak}k}{m+\sqrt{m^2+k^2}} \\ -e^{iak}f_-(\lambda_1,k) & 0 & e^{-iak} & e^{iak} \\ 0 & \frac{e^{iak}k}{m+\sqrt{m^2+k^2}} & ie^{iak}g_+(\lambda_2,k) & ie^{-iak}g_-(\lambda_2,k) \\ 0 & e^{iak} & -e^{iak}f_+(\lambda_2,k) & -e^{-iak}f_-(\lambda_2,k) \end{pmatrix} \begin{pmatrix} \sigma_L^m \\ \rho_L^m \\ A_L^m \\ B_L^m \end{pmatrix} = \begin{pmatrix} 0 \\ 0 \\ \frac{e^{-iak}k}{m+\sqrt{m^2+k^2}} \\ -e^{-iak} \end{pmatrix}. \tag{C.4}$$

The coefficients of the spinor in the region between plates fulfil the following relations:

$$\begin{aligned} &A_L^m(k,m,a,\lambda_1) = \frac{-ik\sqrt{k^2+m^2}e^{2iak}\sinh\lambda_1}{\Delta(k;\lambda_1,\lambda_2)}, \qquad B_L^m(k,m,a,\lambda_1) = \frac{k^2\cosh\lambda_1 + ikm\sinh\lambda_1}{\Delta(k;\lambda_1,\lambda_2)}, \\ &A_L^m(k,m,a,\lambda_1) = B_R^m(k,m,a,\lambda_2), \qquad A_R^m(k,m,a,\lambda_2) = B_L^m(k,m,a,\lambda_1), \\ &\Delta(k;\lambda_1,\lambda_2) = k^2\cosh(\lambda_1+\lambda_2) + (k^2+m^2)(e^{4iak}-1)\sinh\lambda_1\sinh\lambda_2 + ikm\sinh(\lambda_1+\lambda_2). \end{aligned} \tag{C.5}$$

Positron scattering states

$$\begin{pmatrix} 0 & e^{iak}f_+(\lambda_1,k) & e^{-iak} & -e^{iak} \\ 0 & ie^{iak}g_+(\lambda_1,k) & \frac{e^{-iak}k}{m+\sqrt{m^2+k^2}} & \frac{e^{iak}k}{m+\sqrt{m^2+k^2}} \\ e^{iak} & 0 & -e^{iak}f_-(\lambda_2,k) & e^{-iak}f_+(\lambda_2,k) \\ \frac{e^{iak}k}{m+\sqrt{m^2+k^2}} & 0 & -ie^{iak}g_-(\lambda_2,k) & ie^{-iak}g_+(\lambda_2,k) \end{pmatrix} \begin{pmatrix} \tilde{\sigma}_R^m \\ \tilde{\rho}_R^m \\ \tilde{A}_R^m \\ \tilde{B}_R^m \end{pmatrix} = \begin{pmatrix} e^{-iak}f_-(\lambda_1,k) \\ ie^{-iak}g_-(\lambda_1,k) \\ 0 \\ 0 \end{pmatrix}, \tag{C.6}$$

$$\begin{pmatrix} e^{iak}f_+(\lambda_1,k) & 0 & e^{-iak} & -e^{iak} \\ ie^{iak}g_+(\lambda_1,k) & 0 & \frac{e^{-iak}k}{m+\sqrt{m^2+k^2}} & \frac{e^{iak}k}{m+\sqrt{m^2+k^2}} \\ 0 & e^{iak} & -e^{iak}f_-(\lambda_2,k) & e^{-iak}f_+(\lambda_2,k) \\ 0 & \frac{e^{iak}k}{m+\sqrt{m^2+k^2}} & -ie^{iak}g_-(\lambda_2,k) & ie^{-iak}g_+(\lambda_2,k) \end{pmatrix} \begin{pmatrix} \tilde{\sigma}_L^m \\ \tilde{\rho}_L^m \\ \tilde{A}_L^m \\ \tilde{B}_L^m \end{pmatrix} = \begin{pmatrix} 0 \\ 0 \\ e^{-iak} \\ -\frac{e^{-iak}k}{m+\sqrt{m^2+k^2}} \end{pmatrix}. \tag{C.7}$$

The coefficients of the spinor in the region between plates fulfil the following relations:

$$\begin{aligned} &\tilde{A}_L^m(k,m,a,\lambda_1) = \frac{-i\,k\,\sqrt{k^2+m^2}e^{2iak}\sinh\lambda_1}{\tilde{\Delta}(k;\lambda_1,\lambda_2)}, \qquad \tilde{B}_L^m(k,m,a,\lambda_1) = \frac{k^2\cosh\lambda_1 - i\,k\,m\sinh\lambda_1}{\tilde{\Delta}(k;\lambda_1,\lambda_2)}, \\ &\tilde{A}_L^m(k,m,a,\lambda_1) = \tilde{B}_R^m(k,m,a,\lambda_2), \qquad \tilde{A}_R^m(k,m,a,\lambda_2) = \tilde{B}_L^m(k,m,a,\lambda_1), \\ &\tilde{\Delta}(k;\lambda_1,\lambda_2) = k^2\cosh(\lambda_1+\lambda_2) + (k^2+m^2)(e^{4iak}-1)\sinh\lambda_1\sinh\lambda_2 - ikm\sinh(\lambda_1+\lambda_2). \end{aligned} \tag{C.8}$$

C.2. Double electric contact interactions

In this section the following notation has been used:

$$h_{\pm}(q_i,k)=\cos(q_i)\pm\frac{ik\sin(q_i)}{m+\sqrt{m^2+k^2}},\qquad j_{\pm}(q_i,k)=i\sin(q_i)\pm\frac{k\cos(q_i)}{m+\sqrt{m^2+k^2}},\qquad i=1,2.$$

Electron bound states

$$Q_1=\begin{pmatrix} -e^{-a\kappa}h_+(q_1,i\kappa) & e^{-a\kappa} & e^{a\kappa} & 0\\ -e^{-a\kappa}j_-(q_1,i\kappa) & \frac{-ie^{-a\kappa}\kappa}{m+\sqrt{m^2-\kappa^2}} & \frac{ie^{-a\kappa}\kappa}{m+\sqrt{m^2-\kappa^2}} & 0\\ 0 & -e^{a\kappa}h_-(q_2,i\kappa) & -e^{-a\kappa}h_+(q_2,i\kappa) & e^{-a\kappa}\\ 0 & -e^{a\kappa}j_-(q_2,i\kappa) & -e^{-a\kappa}j_+(q_2,i\kappa) & \frac{ie^{-a\kappa}\kappa}{m+\sqrt{m^2-\kappa^2}} \end{pmatrix}. \tag{C.9}$$

Positron bound states

$$P_1=\begin{pmatrix} e^{-a\kappa}j_-(q_1,i\kappa) & \frac{ie^{-a\kappa}\kappa}{m+\sqrt{m^2-\kappa^2}} & \frac{ie^{a\kappa}\kappa}{m+\sqrt{m^2-\kappa^2}} & 0\\ e^{-a\kappa}h_-(q_1,i\kappa) & -e^{-a\kappa} & e^{a\kappa} & 0\\ 0 & e^{a\kappa}j_-(q_2,i\kappa) & -e^{-a\kappa}j_+(q_2,i\kappa) & \frac{ie^{-a\kappa}\kappa}{m+\sqrt{m^2-\kappa^2}}\\ 0 & e^{a\kappa}h_-(q_2,i\kappa) & -e^{-a\kappa}h_+(q_2,i\kappa) & e^{-a\kappa} \end{pmatrix}. \tag{C.10}$$

Electron scattering states

$$\begin{pmatrix} 0 & e^{iak}j_+(q_1,k) & \frac{e^{-iak}k}{m+\sqrt{m^2+k^2}} & -\frac{e^{iak}k}{m+\sqrt{m^2+k^2}} \\ 0 & -e^{iak}h_+(q_1,k) & e^{-iak} & e^{iak} \\ \frac{e^{iak}k}{m+\sqrt{m^2+k^2}} & 0 & e^{iak}j_-(q_2,k) & e^{-iak}j_+(q_2,k) \\ e^{iak} & 0 & -e^{iak}h_-(q_2,k) & -e^{-iak}h_+(q_2,k) \end{pmatrix} \begin{pmatrix} \sigma_R^e \\ \rho_R^e \\ A_R^e \\ B_R^e \end{pmatrix} = \begin{pmatrix} -e^{-iak}j_-(q_1,k) \\ e^{-iak}h_-(q_1,k) \\ 0 \\ 0 \end{pmatrix}, \tag{C.11}$$

$$\begin{pmatrix} e^{iak}j_+(q_1,k) & 0 & \frac{e^{-iak}k}{m+\sqrt{m^2+k^2}} & -\frac{e^{iak}k}{m+\sqrt{m^2+k^2}} \\ -e^{iak}h_+(q_1,k) & 0 & e^{-iak} & e^{iak} \\ 0 & \frac{e^{iak}k}{m+\sqrt{m^2+k^2}} & e^{iak}j_-(q_2,k) & e^{-iak}j_+(q_2,k) \\ 0 & e^{iak} & -e^{iak}h_-(q_2,k) & -e^{-iak}h_+(q_2,k) \end{pmatrix} \begin{pmatrix} \sigma_L^e \\ \rho_L^e \\ A_L^e \\ B_L^e \end{pmatrix} = \begin{pmatrix} 0 \\ 0 \\ \frac{e^{-iak}k}{m+\sqrt{m^2+k^2}} \\ -e^{-iak} \end{pmatrix}. \tag{C.12}$$

The coefficients of the spinor in the region between plates fulfil the following relations:

$$\begin{aligned} &A_L^e(k,m,a,q_1) = \frac{-i\,k\,m\,e^{2iak}\sin q_1}{\Lambda(k;q_1,q_2)}, \qquad B_L^e(k,m,a,q_1) = \frac{k^2\cos q_1 + ik\sqrt{k^2+m^2}\sin q_1}{\Lambda(k;q_1,q_2)}, \\ &A_L^e(k,m,a,q_1) = B_R^e(k,m,a,q_2), \qquad A_R^e(k,m,a,q_2) = B_L^e(k,m,a,q_1), \\ &\Lambda(k;q_1,q_2) = k^2\cos(q_1+q_2) + ik\sqrt{k^2+m^2}\sin(q_1+q_2) + m^2\sin q_1\sin q_2(e^{4iak}-1). \end{aligned} \tag{C.13}$$

Positron scattering states

$$\begin{pmatrix} 0 & e^{iak}j_-(q_1,k) & \frac{e^{-iak}k}{m+\sqrt{m^2+k^2}} & \frac{e^{iak}k}{m+\sqrt{m^2+k^2}} \\ 0 & e^{iak}h_-(q_1,k) & e^{-iak} & -e^{iak} \\ \frac{e^{iak}k}{m+\sqrt{m^2+k^2}} & 0 & -e^{iak}j_+(q_2,k) & e^{-iak}j_-(q_2,k) \\ e^{iak} & 0 & -e^{iak}h_+(q_2,k) & e^{-iak}h_-(q_2,k) \end{pmatrix} \begin{pmatrix} \tilde{\sigma}_R^e \\ \tilde{\rho}_R^e \\ \tilde{A}_R^e \\ \tilde{B}_R^e \end{pmatrix} = \begin{pmatrix} e^{-iak}j_+(q_1,k) \\ e^{-iak}h_+(q_1,k) \\ 0 \\ 0 \end{pmatrix}, \tag{C.14}$$

$$\begin{pmatrix} e^{iak}j_-(q_1,k) & 0 & \frac{e^{-iak}k}{m+\sqrt{m^2+k^2}} & \frac{e^{iak}k}{m+\sqrt{m^2+k^2}} \\ e^{iak}h_-(q_1,k) & 0 & e^{-iak} & -e^{iak} \\ 0 & \frac{e^{iak}k}{m+\sqrt{m^2+k^2}} & -e^{iak}j_+(q_2,k) & e^{-iak}j_-(q_2,k) \\ 0 & e^{iak} & -e^{iak}h_+(q_2,k) & e^{-iak}h_-(q_2,k) \end{pmatrix} \begin{pmatrix} \tilde{\sigma}_L^e \\ \tilde{\rho}_L^e \\ \tilde{A}_L^e \\ \tilde{B}_L^e \end{pmatrix} = \begin{pmatrix} 0 \\ 0 \\ \frac{-e^{-iak}k}{m+\sqrt{m^2+k^2}} \\ e^{-iak} \end{pmatrix}. \tag{C.15}$$

The coefficients of the spinor in the region between plates fulfil the following relations:

$$\begin{aligned} &\tilde{A}_L^e(k,m,a,q_1) = \frac{-i\,k\,m\,e^{2iak}\,\sin q_1}{\tilde{\Lambda}(k;q_1,q_2)}, \qquad \tilde{B}_L^e(k,m,a,q_1) = \frac{k^2\cos q_1 - ik\sqrt{k^2+m^2}\sin q_1}{\tilde{\Lambda}(k;q_1,q_2)}, \\ &\tilde{A}_R^e(k,m,a,q_2) = \tilde{B}_L^e(k,m,a,q_1), \qquad \tilde{B}_R^e(k,m,a,q_2) = \tilde{A}_L^e(k,m,a,q_1), \\ &\tilde{\Lambda}(k;q_1,q_2) = k^2\cos(q_1+q_2) - ik\sqrt{k^2+m^2}\sin(q_1+q_2) + m^2\sin q_1\sin q_2(e^{4iak}-1). \end{aligned} \tag{C.16}$$

Appendix D

PUBLICATION LIST

Part of the original work presented in this PhD thesis has been published during my candidature at the University of Valladolid in the following references:

1. M. Bordag, J.M. Muñoz-Castañeda and L. Santamaría-Sanz. *Vacuum Energy for Generalized Dirac Combs at $T = 0$*. Front. Phys. 7:38. (2019)

2. J.M. Guilarte, J.M. Muñoz-Castañeda, I. Pirozhenko and L. Santamaría-Sanz. *One- Dimensional Scattering of Fermions on δ-Impurities*. Front. Phys. 7:109. (2019)

3. M. Bordag, J.M. Muñoz-Castañeda and L. Santamaría-Sanz. *Revisiting the Casimir energy with general boundary conditions and applications in 1D crystals*. Mod. Phys. Lett. A, 35:3, 2040018 (2020)

4. M. Bordag, J.M. Muñoz-Castañeda and L. Santamaría-Sanz. *Free energy and entropy for finite temperature quantum field theory under the influence of periodic backgrounds*. Eur. Phys. J. C 80, 221 (2020)

5. J.M. Muñoz-Castañeda, L. Santamaría-Sanz, M. Donaire and M. Tello-Fraile. *Thermal Casimir effect with general boundary conditions*. Eur. Phys. J. C 80, 793 (2020)

6. M. Gadella, J.M. Guilarte, J.M. Muñoz-Castañeda, L.M. Nieto and L. Santamaría -Sanz. *Band spectra of periodic hybrid δ-δ' structures*. Eur. Phys. J. Plus 135, 786 (2020)

Moreover, the results developed during my stay at the City University of London are not presented in this thesis but they are collected in the following publications:

1. L. Capizzi, O. A. Castro-Alvaredo, C. De Fazio, M. Mazzoni, L. Santamaría-Sanz. *Symmetry Resolved Entanglement of Excited States in Quantum Field Theory I: Free Theories, Twist Fields and Qubits.* J. High Energ. Phys. 2022, 127 (2022)

2. L. Capizzi, C. De Fazio, M. Mazzoni, L. Santamaría-Sanz, O. A. Castro-Alvaredo. *Symmetry Resolved Entanglement of Excited States in Quantum Field Theory II: Numerics, Interacting Theories and Higher Dimensions.*J. High Energ. Phys. 2022, 128 (2022)

Bibliography

[1] W. Heisenberg and H. Euler. In: *Z. Phys.* 98 (1936), pp. 714–732. DOI: 10.48550/arXiv.physics/0605038.

[2] J. S. Schwinger. In: *Phys.Rev.* 82 (1951), 664–679. DOI: 10.1103/PhysRev.82.664.

[3] H. Gies, J. Jaeckel, and A. Ringwald. In: *Phys. Rev. Lett.* 97.14 (2006), p. 140402. DOI: 10.1103/PhysRevLett.97.140402.

[4] P. W. Milonni. *The Quantum Vacuum. An Introduction to Quantum Electrodynamics,* Academic Press, Inc., Boston, 1994.

[5] A. A. Grib, S. G. Mamayev, and V. M. Mostepanenko. *Vacuum quantum effects in strong fields*. Friedmann Laboratory Publishing, St. Petesburg, 1994.

[6] J. J. Sakurai. *Modern quantum mechanics. Third ed.* Cambridge University Press, 2020.

[7] B. R. Holstein and A. R. Swift. In: *Am. J. Phys.* 50 (1982), p. 829. DOI: 10.1119/1.12750.

[8] R. Rajaraman. *Solitons and Instantons: An Introduction to Solitons and Instantons in Quantum Field Theory*. Amsterdam: North-Holland, 1984.

[9] M. Veltman. *Path integrals, Feynman rules, Gauge theories*. Lectures given at the international school of elementary particle physics, Basko-Polje, 15-29 September 1974.

[10] R. L. Jaffe. In: *Phys.Rev. D* 72 (2005), p. 021301. DOI: 10.1103/PhysRevD.72.021301.

[11] M. Planck. In: *Verh.d.Deutsch.Phys.Ges.B* 13 (1911), pp. 138–148.

[12] W. Heisenberg. In: *Z.Phys.* 33 (1925), pp. 879–893. DOI: 10.1007/BF01328377.

[13] H. B. G. Casimir. In: *Proc. K. Ned. Akad. Wet.* 51.793 (1948). URL: https://inspirehep.net/literature/24990.

[14] M. J. Spaarnay. In: *Nature* 180.334 (1957). DOI: 10.1038/180334b0.

[15] M. Bordag et al. *Advances in the Casimir effect*. Oxford Sciences publications, 2009.

[16] J. N. Munday, F. Capasso, and V. A. Parsegian. In: *Nature* 457 (2009), pp. 170–173. DOI: 10.1038/nature07610.

[17] E. M. Lifshitz. In: *Sov. Phys. JETP* 2 (1956), pp. 73–83. URL: https://www.osti.gov/biblio/4359646.

[18] E. M. Lifshitz and M. Hamermesh. In: *Perspectives in Theoretical Physics, Pergamon* 2 (1992), pp. 329–349. DOI: 10.1016/C2009-0-14730-X.

[19] A. Romeo and A. A. Saharian. In: *J. Phys. A: Math. Gen.* 35 (2002), 1297– 1320. DOI: 10.1088/0305-4470/35/5/312.

[20] A. A. Saharian and G. Esposito. In: *J. Phys. A: Math. Gen.* 39 (2006), p. 5233. DOI: 10.1088/0305-4470/39/18/032.

[21] S. W. Lee and W. M. Sigmund. In: *Colloids Surf. A* 204 (2002), pp. 43–50. DOI: 10.1016/S0927-7757(01)01118-9.

[22] J. N. Munday, F. Capasso, and V. A. Parsegian. In: *Nature* 457 (2009), 170–3. DOI: 10.1038/nature07610.

[23] T. H. Boyer. In: *Phys. Rev. A* 9 (1974), 2078–84. DOI: 10.1103/PhysRevA.9.2078.

[24] V. M. Mostepanenko and N. N. Trunov. *The Casimir Effect and its applications*. Oxford Sciences Publications, 1997.

[25] F. Zhou and L. Spruch. In: *Phys. Rev. A* 52 (1995), pp. 297–310. DOI: 10.1103/PhysRevA.52.297.

[26] M. Bordag et al. In: *Phys. Rev. B* 74.205431-1–9 (2006). DOI: 10.1103/PhysRevB.74.205431.

[27] G. L. Klimchitskaya, E. V. Blagov, and V. M. Mostepanenko. In: *J. Phys. A: Math. Theor.* 41.164012-1–8 (2008). DOI: 10.1088/1751-8113/41/16/164012.

[28] S. G. Mamaev and V. M. Mostepanenko. *Casimir effect in space-times with non Euclidean topology. 3rd Seminar on Quantum Gravity*. 1984.

[29] V. P. Frolov and E. M. Serebriany. In: *Phys. Rev. D* 35 (1987), 3779–82. DOI: 10.1103/PhysRevD.35.3779.

[30] F. M. Serry, D. Walliser, and G. J. Maclay. In: *J. Microelectromech. Syst.* 4 (1995), 193–205. URL: https://www.quantumfields.com/IEEEJMEMSACO.pdf.

[31] F. M. Serry, D. Walliser, and G. J. Maclay. In: *J. Appl. Phys.* 84 (1998), 2501–6. DOI: 10.1063/1.368410.

[32] H. B. Chan et al. In: *Science* 291 (2001), 1941–4. DOI: 10.1126/science.1057984.

[33] J. J. Allen. *Micro Electro Mechanical System Design*. CRC Press, New York., 2005.

[34] M. Asorey and J.M. Muñoz-Castañeda. In: *Nucl. Phys. B* 874.3 (2013), pp. 852–876. DOI: 10.1016/j.nuclphysb.2013.06.014.

[35] L. J. Boya. In: *Riv. Nuovo Cim.* 31 (2008). DOI: 10.1393/ncr/i2008-10030-4.

[36] K. A. Milton. *Physical Manifestations of Zero-Point Energy. The Casimir Effect*. World Scientific, 2001.

[37] O. Kenneth and I. Klich. In: *Phys. Rev. Lett.* 97 (2006), p. 160401. DOI: 10.1103/PhysRevLett.97.160401.

[38] O. Kenneth and I. Klich. In: *Phys.Rev. B* 78 (2008), p. 014103. DOI: 10.1103/PhysRevB.78.014103.

[39] K. Kirsten. *Spectral Functions in Mathematics and Physics*. Chapman & Hall/CRC, 2001.

[40] D.V. Vassilevich. "Heat kernel expansion: User's manual." In: *Phys.Rept.* 388 (2003), pp. 279–360. DOI: 10.1088/1126-6708/2005/08/085.

[41] E. Elizalde. *Ten Physical Applications of Spectral Zeta Functions*. Springer, 2012.

[42] A. A. Bytsenko et al. *Zeta Regularization Techniques With Applications*. World Scientific Publishing Co Pte Ltd, 1994.

[43] J. M. Muñoz-Castañeda, K. Kirsten, and M. Bordag. In: *Lett. Math. Phys.* 105 (2015), pp. 523–549. DOI: 10.1007/s11005-015-0750-5.

[44] J. M. Muñoz-Castañeda. *Efectos de borde en teoría cuántica de campos*. Zaragoza University, 2009.

[45] M. Donaire et al. In: *Symmetry* 11.5 (2019), p. 643. DOI: 10.3390/sym11050643.

[46] L. Capizzi et al. In: *J. High Energ. Phys.* 2022.12 (2022), p. 127. DOI: 10.1007/JHEP12(2022)127.

[47] L. Capizzi et al. In: *J. High Energ. Phys.* 2022.12 (2022), p. 128. DOI: 10.1007/JHEP12(2022)128.

[48] E. Witten. In: *Nucl. Phys. B* 186 (1981), pp. 412–428. DOI: 10.1016/0550-3213(81)90021-3.

[49] L. Randall and R. Sundrum. In: *Phys. Rev. Lett.* 83 (1999), p. 3370. DOI: 10.1103/PhysRevLett.83.3370.

[50] L. Randall and R. Sundrum. In: *Phys. Rev. Lett.* 83 (1999), p. 4690. DOI: 10.1103/PhysRevLett.83.4690.

[51] D. Husemöller. *Fibre Bundles. Graduate Texts in Mathematics*. Springer, 1994.

[52] S. Coleman. *Aspects of symmetry*. Cambridge University Press, 1985.

[53] B. C. Hall. *Lie Groups, Lie Algebras and Representations. An Elementary Introduction*. Springer, 2003.

[54] J. M. Muñoz-Castañeda, J. M. Guilarte, and A. M. Mosquera. In: *Phys.Rev. D* 87.10 (2013), p. 105020. DOI: 10.1103/PhysRevD.87.105020.

[55] J. Q. Quach. In: *Phys. Rev. Lett.* 114 (2015), p. 081104. DOI: 10.1103/PhysRevLett.114.081104.

[56] G. V. Dunne. In: *Eur. Phys. J.* 55 (2009), p. 327. DOI: 10.1140/epjd/e2009-00022-0.

[57] K. Clausius. In: *Angewandte Chemie* 56 (1943), pp. 241 –247.

[58] L. H. Ford. In: *Phys.Rev. D* 11 (1975), pp. 3370–3377. DOI: 10.1103/PhysRevD.11.3370.

[59] G. Barton. In: *J. Phys. A: Math. Gen.* 38 (2005), p. 2997. DOI: 10.1088/0305-4470/38/13/013.

[60] G. Barton. In: *J. Phys. A: Math. Gen.*. 38 (2005), p. 3021. DOI: 10.1088/0305-4470/38/13/014.

[61] G. Barton. In: *J. Phys. C: Solid State Phys.* 19.7 (1986), p. 975. DOI: 10.1088/0022-3719/19/7/009.

[62] J. D. van der Waals. *Over de Continuïteit van der Gas-en Vloeistoftoestand*. PhD thesis, Leiden, 1873.

[63] F. London. In: *Z. Phys.* 63 (1930), p. 245. DOI: 10.1007/BF01341258.

[64] H. B. G. Casimir and D. Polder. In: *Phys. Rev.* 73 (1948), p. 360. DOI: 10.1103/PhysRev.73.360.

[65] M. J. Spaarnay. In: *Physica* 24 (1958), 751–64. DOI: 10.1016/S0031-8914(58)80090-7.

[66] T. H. Boyer. In: *Phys. Rev.* 174 (1968), 1764–76. DOI: 10.1103/PhysRev.174.1764.

[67] A. A. Grib and V. Yu. Dorofeev. In: *Int. J. Mod. Phys. D* 3.4 (1994), pp. 731–738. DOI: 10.1142/S0218271894000848.

[68] G. T. Moore. In: *Journal of Mathematical Physics* 11.2679 (1970). DOI: 10.1063/1.1665432.

[69] S. A. Fulling and P. C. W. Davies. In: *Proc. Roy. Soc. A* 348 (1976). DOI: 10.1098/rspa.1976.0045.

[70] S. W. Hawking. In: *Commun. Math. Phys.* 43 (1975), pp. 199–220. DOI: 10.1007/BF02345020.

[71] S. S. Bulanov et al. In: *Phys. Rev. Lett.* 104 (2010), p. 220404. DOI: 10.1103/PhysRevLett.104.220404.

[72] Luis Roso et al. In: *New J. Phys.* 24 (2022), p. 025010. DOI: 10.1088/1367-2630/ac51a7.

[73] R. Schützhold, H. Gies, and G. Dunne. In: *Phys. Rev. Lett.* 101 (2008), p. 130404. DOI: 10.1103/PhysRevLett.101.130404.

[74] W. Dittrich and H. Gies. *Probing the Quantum Vacuum:Perturbative Effective Action Approach in Quantum Electrodynamics and its Application*. Springer-Verlag Berlin Heidelberg, 2000.

[75] K. Kirsten and S. A. Fulling. In: *Phys. Rev. D* 79 (2009), p. 065019. DOI: 10.1103/PhysRevD.79.065019.

[76] E. Elizalde E, S. D. Odintsov, and A. A. Saharian. In: *Phys. Rev. D* 79 (2009), p. 065023. DOI: 10.1103/PhysRevD.79.065023.

[77] G. Fucci and I. G. Avramidi. *On the gravitationally induced Schwinger mechanism Quantum Field Theory Under the Influence of External Conditions ed K A Milton and M Bordag*. Singapore: World Scientific, 2010.

[78] G. Fucci. In: *J. Phys. A: Math. Theor* 51.21 (2018), p. 215202. DOI: 10.1088/1751-8121/aabe9b.

[79] T. Kaluza. In: *Sitz. Preuss. Akad. Wiss. Phys. Math.* K1 (1921), p. 966. DOI: 10.1142/S0218271818700017.

[80] O. Klein. In: *Zeits. Phys.* 37 (1926), p. 895. DOI: 10.1007/BF01397481.

[81] R. P. Feynman and A. R. Hibbs. *Quantum mechanics and path integrals*. McGraw-Hill, New York, 1965.

[82] R. F. Dashen, B. Hasslacher, and A. Neveu. In: *Phys. Rev. D* 10 (1974), p. 4114. DOI: 10.1103/PhysRevD.10.4114.

[83] S. Weinberg. *The Quantum Theory of Fields. Vol. 2. Modern Applications*. Cambridge University Press, 1995.

[84] L. S. Brown. *Quantum Fiel Theory*. Cambridge University Press, 1992.

[85] C. Itzykson and J. B. Zuber. *Quantum Field Theory*. Dover, 2006.

[86] M. E. Peskin and D. V. Schroeder. *An Introduction to Quantum Field Theory*. Addison- Wesley Publishing Company, 1995.

[87] N. S. Manton. In: *Annals Phys.* 159 (1985), p. 220. DOI: 10.1016/0003-4916(85)90199-X.

[88] M. Stone and P. A. Matthew. In: *Int. J. Mod. Phys. B* 8.2539 (1994). DOI: 10.1142/S0217979294001020.

[89] J. Polchinski. In: *Phys. Rev. Lett.* 75.4724 (1995). DOI: 10.1103/PhysRevLett.75.4724.

[90] G. 't Hooft. In: (2009). DOI: 10.48550/arXiv.gr-qc/9310026.

[91] N. M. R. Peres, A. H. Castro-Neto, and F. Guinea. In: *Phys. Rev.* 73 (2006), p. 241403. DOI: 10.1103/PhysRevB.73.239902.

[92] J. M. Muñoz-Castañeda and J. M. Guilarte. In: *Phys.Rev. D* 91.2 (2015), p. 025028. DOI: 10.1103/PhysRevD.91.025028.

[93] R. Balian and B. Duplantier. In: *Ann. Phys. (N.Y.)* 104.300 (1977). DOI: 10.1016/0003-4916(77)90334-7.

[94] R. Balian and B. Duplantier. In: *Ann. Phys. (N.Y.)* 112.165 (1978). DOI: 10.1016/0003-4916(78)90083-0.

[95] N. Graham et al. In: *Nucl. Phys. B* 645 (2002), p. 49. DOI: 10.1016/S0550-3213(02)00823-4.

[96] M. Bordag and J. M. Muñoz-Castañeda. In: *J. Phys. A: Math. Theor.* 45 (2012), p. 374012. DOI: 10.1088/1751-8113/45/37/374012.

[97] J. R. Taylor. *Scattering Theory. The Quantum Theory of Nonrelativistic Collisions*. Dover Publications, 2006.

[98] A. Galindo and P. Pascual. *Quantum Mechanincs (vols. I and II)*. Springer, 1991.

[99] C. Genet, A. Lambrecht, and S. Reynaud. In: *Phys. Rev. A* 67 (2003), p. 043811. DOI: 10.1103/PhysRevA.67.043811.

[100] I. Cavero-Peláez, J. M. Muñoz-Castañeda, and C. Romaniega. In: *Phys. Rev. D* 103 (2021), p. 045005. DOI: 10.1103/PhysRevD.103.045005.

[101] S. J. Rahi et al. In: *Phys. Rev. D* 80 (2009), p. 085021. DOI: 10.1103/PhysRevD.80.085021.

[102] S. Zaheer et al. In: *Phys. Rev. A* 82 (2010), p. 052507. DOI: 10.1103/PhysRevA.82.052507.

[103] T. Emig et al. In: *Phys. Rev. D* 77 (2008), p. 025005. DOI: 10.1103/PhysRevD.77.025005.

[104] T. Emig. In: *J. Stat. Mech.* P04007 (2008). DOI: 10.1088/1742-5468/2008/04/P04007.

[105] S. J. Rahi et al. In: *Phys.Rev. D* 80 (2009), p. 085021. DOI: 10.1103/PhysRevD.80.085021.

[106] V. V. Nesterenko and I. G. Pirozhenko. In: *Phys.Rev. D* 57.2 (1997), p. 1248. DOI: 10.1103/PhysRevD.57.1284.

[107] R. Jost and W. Kohn. In: *Phys. Rev.* 87 (1952), p. 979. DOI: 10.1103/PhysRev.87.977.

[108] R. Jost and W. Kohn. In: *Phys. Rev.* 88 (1952), p. 382. DOI: 10.1103/PhysRev.88.382.

[109] M. Asorey, A. Ibort, and G. Marmo. In: *Int. J. Mod. Phys. A* 20.5 (2005), p. 1001. DOI: 10.1142/S0217751X05019798.

[110] M. Reed and B. Simon. *Methods of Modern Mathematical Physics. Vol. I and II*. Academic Press, 1975.

[111] N. Manton and P. Sutcliffe. *Topological Solitons*. Cambridge University Press, 2004.

[112] T. Vachaspati. *Kinks and Domain Walls*. Cambridge University Press, 2006.

[113] Robert Wimmer. *Diploma thesis: quantization of supersymmetric solitons*. 2001.

[114] J. Scott Russell. In: *Report on Waves: Made to the Meetings of the British Association* (1842-43).

[115] D. J. Korteweg and F. de Vries. In: *Philosophical Magazine* 39 (1895). DOI: 10.1080/14786449508620739.

[116] N. J. Zabusky and M. D. Kruskal. In: *Phys. Rev. Lett.* 15.6 (1965), 240–243. DOI: 10.1103/PhysRevLett.15.240.

[117] P. Di Trapani et al. In: *Phys. Rev. Lett.* 81 (1998), p. 570. DOI: 10.1103/PhysRevLett.81.570.

[118] P. G. Kevrekidis, D. J. Frantzeskakis, and R. Carretero-González. *Emergent Nonlinear Phenomena in Bose-Einstein Condensates*. Springer, 2008.

[119] S. Coleman. In: *Nucl. Phys. B* 262.2 (1985), pp. 263–283. DOI: 10.1016/0550-3213(85)90286-X.

[120] A. A. Izquierdo et al. "Lectures on the mass of topological solitons". In: (2006). DOI: arXiv.hep-th/0611180.

[121] L. D. Faddeev and V. E. Korepin. In: *Phys. Rep.* 42.1 (1978). DOI: 10.1016/0370-1573(78)90058-3.

[122] I. Hernández Palmero. *La ecuación de sine-Gordon en Teoría Cuántica de Campos: Teoría de perturbaciones*. Universidad de Salamanca, 2014.

[123] R. F. Dashen, B. Hasslacher, and A. Neveu. In: *Phys. Rev. D* 10 (1974), p. 4130. DOI: 10.1103/PhysRevD.10.4130.

[124] R. F. Dashen, B. Hasslacher, and A. Neveu. In: *Phys. Rev. D* 11 (1975), p. 3424. DOI: 10.1103/PhysRevD.11.3424.

[125] R. D. Peccei and H. R. Quinn. In: *Phys. Rev. D* 16 (1977), p. 1791. DOI: 10.1103/PhysRevD.16.1791.

[126] S. Weinberg. In: *Phys. Rev. Lett.* 40 (1978), p. 223. DOI: 10.1103/PhysRevLett.40.223.

[127] Jr. C. G. Callan, R. F. Dashen, and D. J. Gross. In: *Phys. Lett. B* 63 (1976), p. 334. DOI: 10.1016/0370-2693(76)90277-X.

[128] Peter Thomas Jahn. "The Topological Susceptibility of QCD at High Temperatures". PhD thesis. Darmstadt, Tech. Hochsch., 2019. DOI: 10.25534/tuprints-00009485.

[129] A. A. Belavin et al. In: *Phys. Lett. B* 59 (1975), p. 85. DOI: 10.1016/0370-2693(75)90163-X.

[130] G. 't Hooft. In: *Phys. Rev. D* 18 (1978), p. 2199. DOI: 10.1103/PhysRevD.18.2199.3.

[131] Jr. C. G. Callan, R. F. Dashen, and D. J. Gross. In: *Phys. Rev. D* 17 (1978), p. 2717. DOI: 10.1103/PhysRevD.17.2717.

[132] I. V. Fialkovsky, V. N. Marachevsky, and D. V. Vassilevich. In: *Phys. Rev. B* 84 (2011), p. 035446. DOI: 10.1103/PhysRevB.84.035446.

[133] M. Bordag, J. M. Muñoz-Castañeda, and L. Santamaria-Sanz. In: *Mod. Phys. Lett. A* 35.3 (2020), p. 2040018. DOI: 10.1142/S0217732320400180.

[134] F. W. Olver et al. *NIST handbook of mathematical functions. 1st edn.* Cambridge University Press, 2010.

[135] M. Asorey and J.M. Muñoz-Castañeda. In: *Int. J. Geom. Methods Mod. Phys* 9.2 (2012), p. 1260017. DOI: 10.1142/S0219887812600171.

[136] B. Geyer, G. L. Klimchitskaya, and V. M. Mostepanenko. In: *Phys. Rev. A* 72 (2005), p. 022111. DOI: 10.1103/PhysRevA.72.022111.

[137] W. Thirring. In: *Z. Phys. A - Hadrons and nuclei* 235.4 (1970), pp. 339–352. DOI: 10.1007/BF01403177.

[138] M. Asorey and J. M. Muñoz-Castañeda. In: *J. Phys. A: Math. Theor.* 41 (2008), p. 304004. DOI: 10.1088/1751-8113/41/30/304004.

[139] M. Asorey et al. In: *J. Phys. A: Math. Theor.* 40 (2007), p. 6767. DOI: 10.1088/1751-8113/40/25/S21.

[140] J.M. Muñoz-Castañeda and L. Santamaria-Sanz et al. In: *Eur. Phys. J. C* 80 (2020), p. 793. DOI: 10.1140/epjc/s10052-020-8348-1.

[141] R. de L. Kronig and W. G. Penney. In: *Proc. R. Soc. Lond. Ser. A* 130 (1931), p. 449. DOI: 10.1098/rspa.1931.0019.

[142] J. M. Cerveró and A. Rodríguez. In: *Eur. Phys. J. B* 30 (2002), p. 239. DOI: 10.1140/epjb/e2002-00377-4.

[143] J. M. Cerveró and A. Rodríguez. In: *Eur. Phys. J. B* 32 (2003), p. 537. DOI: 10.1140/epjb/e2003-00132-5.

[144] J. M. Cerveró and A. Rodríguez. In: *Eur. Phys. J. B* 43 (2005), p. 543. DOI: 10.1140/epjb/e2005-00088-4.

[145] P. W. Anderson. In: *Phys. Rev.* 109.5 (1958), 1492–1505. DOI: 10.1103/PhysRev.109.1492.

[146] F. Bloch. In: *Z. Physik* 52 (1929), 555–600. DOI: 10.1007/BF01339455.

[147] N. W. Ashcroft and N. D. Mermin. *Solid State Physics*. Brooks/Cole, Boston, 1976.

[148] A. Zettl. *Carbon Nanotubes: Quantum Cylinders of Graphene*. Elsevier Science, 2008.

[149] G. Fucci. In: *Nucl. Phys. B* 891 (2015), pp. 676–699. DOI: 10.1016/j.nuclphysb.2014.12.023.

[150] G. Fucci, K. Kirsten, and J.M. Muñoz-Castañeda. In: *Anal. Math. Phys.* 11 (2021), p. 70. DOI: 10.1007/s13324-021-00507-2.

[151] M. Bordag. In: *J. Phys. A: Math. Theor.* 53 (2020), p. 015003. DOI: 10.1088/1751-8121/ab5b41.

[152] I. Alvarado-Rodríguez, P. Halevi, and J. J. Sánchez-Mondragón. In: *Phys. Rev. E* 59 (1999), p. 3624. DOI: 10.1103/PhysRevE.59.3624.

[153] M. Bordag, D. Hennig, and D. Robaschik. In: *J. Phys. A* 25 (1992), p. 4483. DOI: 10.1088/0305-4470/25/16/023.

[154] C. D. Fosco, F. C. Lombardo, and F. D. Mazzitelli. In: *Phys. Rev. D* 80 (2009), p. 085004. DOI: 10.1103/PhysRevD.80.085004.

[155] G. Barton. In: *J. Phys. A* 37 (2004), p. 1011. DOI: 10.1088/0305-4470/37/3/032.

[156] P. Parashar et al. In: *Phys. Rev. D* 86 (2012), p. 085021. DOI: 10.1103/PhysRevD.86.085021.

[157] M. Bordag. In: *Phys. Rev. D* 89 (2014), p. 125015. DOI: 10.1103/PhysRevD.89.125015.

[158] J. J. Alvarez et al. In: *Phys. Lett. A* 377 (2013), pp. 2510–2519. DOI: 10.1016/j.physleta.2013.07.045.

[159] M. Gadella, J. Negro, and L. M. Nieto. In: *Phys. Lett. A* 373 (2009), p. 1310. DOI: 10.1016/j.physleta.2009.02.025.

[160] M. Gadella et al. In: *Eur. Phys. J. Plus* 135 (2020), p. 786. DOI: 10.1140/epjp/s13360-020-00818-6.

[161] M. Bordag, J. M. Muñoz-Castañeda, and L. Santamaría-Sanz. In: *Eur. Phys. J. C* 80.3 (2020), p. 221. DOI: 10.1140/epjc/s10052-020-7783-3.

[162] M. Bordag et al. In: *Front. Phys.* 7.38 (2019). DOI: 10.3389/fphy.2019.00038.

[163] G. Pöschl and E. Teller. In: *Z. Phys. A* 83 (1933), 143–151. DOI: 10.1007/BF01331132.

[164] C. S. Park. In: *Phys.Rev.B* 92 (2015), p. 165422. DOI: 10.1103/PhysRevB.92.165422.

[165] R. R. Hartmann and M. E. Portnoi. In: *Sci. Rep.* 7 (2017), p. 11599. DOI: 10.1038/s41598-017-11411-w.

[166] H. Yıldırım and M. Tomak. In: *Phys. Rev. B* 72 (2005), p. 115340. DOI: 10.1103/PhysRevB.72.115340.

[167] H. Kroemer. In: *Proceedings of the IEEE* 51.12 (1963), pp. 1782–1783. DOI: 10.1109/PROC.1963.2706.

[168] Z. I. Alferov, R. F. Kazarinov, and I. Alferov et al. In: *Authors certificate 28448, U.S.S.R.Zh. Sov. Phys., Solid State* 9 (1963), p. 208.

[169] D. Çevik et al. In: *Phys. Lett. A* 380 (2016), 1600–1609. DOI: 10.1016/j.physleta.2016.03.003.

[170] J. M. Guilarte and J. M. Muñoz-Castañeda. In: *Int. J. Theor. Phys.* 50.7 (2011), pp. 2227–2241. DOI: 10.1007/s10773-011-0723-0.

[171] M. Asorey and J. M. Muñoz-Castañeda. In: *Int. J. Theor. Phys.* 50 (2011), pp. 2211–21. DOI: 10.1007/s10773-011-0720-3.

[172] M. Bordag, J. M. Muñoz-Castañeda, and L. Santamaría-Sanz. In: *Front. Phys.* 7 (2019), p. 38. DOI: 10.3389/fphy.2019.00038.

[173] I. S. Gradshteyn, A. Jeffrey, and I.M. Ryzhik. *Table of Integrals, Series and Products*. Academic Press, 1996.

[174] E. Elizalde and A. Romeo. In: *Phys. Rev. D* 40 (1989), pp. 436–443. DOI: 10.1103/PhysRevD.40.436.

[175] K. Milton. In: *J. Phys. A Math. Gen.* 37 (2004), p. 6391. DOI: 10.1088/0305-4470/37/24/014.

[176] T. W. Gamelin. *Complex Analysis*. Springer, 2001.

[177] M. Bordag. In: *arXiv* (2018). DOI: 10.48550/arXiv.1807.10354.

[178] M. Bordag. In: *J. Phys. A: Math. Gen.* 28 (1995), pp. 755–765. DOI: 10.1088/0305-4470/28/3/028.

[179] M. Bordag, E. Elizalde, and K. Kirsten. In: *J. Math. Phys* 37.2 (1996), p. 895. DOI: 10.1063/1.531418.

[180] K. V. Shajesh et al. In: *Phys. Rev. D* 94.6 (2016), p. 065003. DOI: 10.1103/PhysRevD.94.065003.

[181] S. Fulling. *Aspects of Quantum Field Theory in Curved Spacetime*. Cambridge University Press, 1989.

[182] N. Birrel and P. Davies. *Quantum Fields in Curved Space*. Cambridge University Press, 1982.

[183] R. M. Wald. *Quantum field theory in curved space-time and black hole thermodynamics.* University of Chicago Press, 1995.

[184] J. Leray. *Hyperbolic differential equations (mimeographed notes)*. Princeton Institute for Advanced Studies, 1952.

[185] R. Geroch. In: *J. Math. Phys.* 11 (1970), p. 437. DOI: 10.1063/1.1665157.

[186] J.M. Muñoz-Castañeda and M. Bordag. In: *Phys. Rev. D* 89.6 (2014), p. 065034. DOI: 10.1103/PhysRevD.89.065034.

[187] C. J. Fewster. In: *"Lectures on quantum field theory in curved spacetime". Lecture Note 39/2008 Max Planck Institute for Mathematics in the Natural Sciences* (2008).

[188] I. Khavkine and V. Moretti. *Algebraic QFT in Curved Spacetime and Quasifree Hadamard States: An Introduction*. Springer International Publishing, 2015.

[189] C. Bär and K. Fredenhagen. *Quantum Field Theory on Curved Spacetimes: Concepts and Mathematical Foundations*. Springer, 2009.

[190] B. S. Kay. *Quantum Field Theory in curved spacetime. Encyclopedia of Mathematical Physics*. Academic Press Elsevier, 2006.

[191] W. H. Press, B. S. Ryden, and D. N. Spergel. In: *Astrophys. J.* 347 (1989), pp. 590–604. DOI: 10.1086/168151.

[192] M. Santander, L. M. Nieto, and N. A. Cordero. In: *Am. J. Phys.* 65.12 (1997), pp. 1200–1209. DOI: 10.1119/1.18759.

[193] B. O'Neill. *Semi-Riemannian Geometry (with Applications to Relativity)*. Academic Press, 1983.

[194] R. P. Feynman, F. Morinigo, and W. Wagner. *Lectures on Gravitation*. Addison Wesley, 1995.

[195] I. Cavero-Peláez and J.M. Guilarte. In: *Quantum Field Theory Under the Influence of External Conditions (QFEXT09), World Scientific* (2010), pp. 457–464. DOI: 10.1142/9789814289931_0057.

[196] N. Levinson. In: *Kgl. Danske. Videnskab. Selskab., Mat.-Fys. Medd.* 25.9 (1949).

[197] S. A. Fulling. In: *Quantum Graphs and Their Applications, ed. by G. Berkolaiko et al., Contemp. Math.* 415 (2006), pp. 161–172. DOI: 10.48550/arXiv.math/0508335.

[198] M. R. Masir, P. Vasilopoulos, and F. M. Peeters. In: *New J. Phys.* 11 (2009), p. 095009. DOI: 10.1088/1367-2630/11/9/095009.

[199] K. Pankrashkin and S. Richard. In: *J. Math. Phys.* 55 (2014), p. 062305. DOI: 10.1063/1.4884417.

[200] C. L. Kane and E. J. Mele. In: *Phys. Rev. Lett*, 95.14 (2005), p. 146802. DOI: 10.1103/PhysRevLett.95.146802.

[201] B. A. Bernevig and Shou-Cheng Zhang. In: *Phys. Rev. Lett.* 96.10 (2006), p. 106802. DOI: 10.1103/PhysRevLett.96.106802.

[202] K. Klitzing, G. Dorda, and M. Pepper. In: *Phys. Rev. Lett*, 45.6 (1980). DOI: 10.1103/PhysRevLett.45.494.

[203] M. Asorey, A. P. Balachandran, and J. M. Pérez-Pardo. In: *Rev. Math. Phys.* 28 (2016), p. 1650020. DOI: 10.1142/S0129055X16500203.

[204] M. Veltmann. *Diagrammatica: The Path to Feynman Diagrams. Cambridge Lecture Notes in Physics, Series Number 4*. Cambridge University Press, 1994.

[205] T. Friedrich. *Dirac operators in Riemannian Geometry*. AMS, 2000.

[206] H. Blaine Lawson and ML Michelsohn. *Spin Geometry*. Princeton University Press, 1990.

[207] C. Chevalley. *The Algebraic Theory of Spinors and Clifford Algebras*. Springer, 1997.

[208] A. Haefliger. In: *C.R. Acad. Sci. Paris* 243 (1956), pp. 558–560.

[209] P. A. M. Dirac. In: *Proc. R. Soc. Lond. A.* 126.801 (1930), pp. 360–365. DOI: 10.1098/rspa.1930.0013.

[210] C. D. Anderson. In: *Phys. Rev.* 43.6 (1933), pp. 491–494. DOI: 10.1103/PhysRev.43.491.

[211] P. Sundberg and R. L. Jaffe. In: *Ann. Phys.* 309 (2004), pp. 442–458. DOI: 10.1016/j.aop.2003.08.015.

[212] H. Akcay. In: *Phys. Lett. A* 373 (2009), pp. 616–620. DOI: 10.1016/j.physleta.2008.12.029.

[213] J. R. Hiller. In: *Am. J. Phys.* 70 (2002), pp. 522–524. DOI: 10.1119/1.1456074.

[214] Y. Nogami, F. M. Toyama, and W. van Dijk. In: *Am. J. Phys.* 71 (2003), p. 950. DOI: 10.1119/1.1555891.

[215] I. R. Lapidus. In: *Am. J. Phys.* 51 (1983), pp. 1036–1038. DOI: 10.1119/1.13445.

[216] M. G. Calkin, D. Kiang, and Y. Nogami. In: *Am. J. Phys.* 55 (1987), pp. 737–739. DOI: 10.1119/1.15031.

[217] C. Bender. *PT Symmetry in Quantum and Classical Physics*. World Scientific, 2018.

[218] J. M. Guilarte et al. In: *Front. Phys.* 7.109 (2019). DOI: 10.3389/fphy.2019.00109.

[219] M. Nakahara. *Geometry, topology and physics*. IOP Publishing Ltd., 2003.

[220] C. Birkenhake and H. Lange. *Complex Tori. Progress in Mathematics, vol 177*. Birkhäuser, Boston, MA, 1999.

[221] R. C. Gunning. *Lectures on Modular Forms*. Princeton University Press, 1962.

[222] F. J. Ynduráin. *Relativistic Quantum Mechanics and Introduction to Field Theory*. Springer, 1996.

[223] J. Schwinger. In: *Phys. Rev.* 82 (1951), p. 914. DOI: 10.1103/PhysRev.82.914.

[224] G. Lüders. In: *Ann. Phys.* 2.1 (1957). DOI: 10.1016/0003-4916(57)90032-5.

[225] W. Pauli. In: *Nuovo Cim.* 6.1 (1957), p. 204. DOI: 10.1007/BF02827771.

[226] M. Asorey, D. García-Alvarez, and J. M. Muñoz-Castañeda. In: *Int. J. Geom. Methods Mod. Phys.* 12.6 (2015), p. 1560004. DOI: 10.1142/S021988781560004X.

[227] M. Asorey, A. Ibort, and G. Marmo. In: *Int. J. Geom. Methods Mod. Phys.* 12.6 (2015), p. 1561007. DOI: 10.1142/S0219887815610071.

[228] A. Chodos et al. In: *Phys. Rev. D* 9 (1974), p. 3471. DOI: 10.1103/PhysRevD.9.3471.

[229] S. G. Mamaev and N. N. Trunov. In: *Soviet Physics Journal* 23 (1980), 551–554. DOI: 10.1007/BF00891938.

[230] K. Johnson. In: *The M.I.T. Bag Model. Acta Phys. Pol. B* 6 (1975), p. 865. URL: https://www.actaphys.uj.edu.pl/R/6/11/865/pdf.

[231] K. A. Milton. In: *Ann. Phys.* 150 (1983), p. 432. DOI: 10.1016/0003-4916(83)90021-0.

[232] E. Elizalde, M. Bordag, and K. Kirsten. In: *J. Phys. A* 31 (1998), p. 1743. DOI: 10.1088/0305-4470/31/7/009.

[233] M. E. Charro, M. L. Glasser, and L.M. Nieto. In: *EPL* 120 (2017), p. 30006. DOI: 10.1209/0295-5075/120/30006.

[234] W. M. Fairbairn, M. L. Glasser, and M. Steslicka. In: *Surf. Sci.* 36.2 (1973), p. 462. DOI: 10.1016/0039-6028(73)90394-4.

[235] J. Dimock. In: *Commun. Math. Phys* 57 (1977), p. 51. DOI: 10.1007/BF01651693.

[236] R. Jackiw. *Diverse topics in theoretical and mathematical physics*. World Scientific, 1995.

[237] A. Kirillov Jr. *An Introduction to Lie Groups and Lie Algebras*. Cambridge University Press, 2008.

[238] R. Carter et al. *Lectures on Lie Groups and Lie Algebras (London Mathematical Society Student Texts)*. Cambridge University Press, 1995.

[239] D. Mumford. *Tata lectures on Theta. Vol. I*. Birkhäuser Boston, 1983.

[240] G. Lion and M. Vergne. *The Weil representation, Maslow index and Theta series*. Springer Science+Business Media New York, 1980.

[241] M. Reed and B. Simon. *Methods of Modern Mathematical Physics III: Scattering Theory*. Academic Press, 1979.

[242] P. Woit. *Quantum Theory, Groups and Representations. An Introduction*. Springer, 2017.

[243] A. A. Kirillov. *Lectures on the Orbit Method*. American Mathematical Society, 2004.